2nd RCM Report

Controlling of degradation effects in radiation processing of polymers

Second RCM of the CRP F2.20.39, held in Madrid, Spain from 11 to15 July 2005

INTERNATIONAL ATOMIC ENERGY AGENCY IAEA

The originating Section of this publication in the IAEA was:
Industrial Applications and Chemistry Section
International Atomic Energy Agency
Wagramer Strasse 5
P.O. Box 100
A-1400 Vienna, Austria

Controlling of degradation effects in radiation processing of polymers
IAEA-Report

Printed by the IAEA in Austria
August 2005

FOREWORD

The Coordinated Research Project (CRP) F2.20.39 on "Controlling of degradation effects in radiation processing of polymers" has objective to develop in participating laboratories reliable analytical methodologies concerning investigation of degradation effects of radiation on polymers. The second Research Co-ordination Meeting (RCM) of the CRP took place in Madrid, Spain, from 11 to 15 July 2005.

Polymers are generally classified as predominantly undergoing degradation and cross-linking when exposed to ionising radiation. The radiation-induced degradation of polymers is generally considered as an undesirable phenomenon from the point of view of industrial applications. However, radiation induced degradation of synthetic polymers is utilized for preparation of ion track membranes used in filtration techniques and Teflon powder being a component of inks, coatings and lubricants. Another important application of radiation-induced degradation is in lithographic patterning. By using X rays of electron beam it is possible to manufacture integrated circuits with radiation-patterned sub-micron dimensions.

Natural polymers like cellulose and other polysaccharides (chitosan, alginates, carrageenames etc) are predominantly chain-scissioning polymers, irradiation results in substantial decrease in molecular weight. This is accompanied with the formation of carboxyl group and reduction in crystallinity. The amorphic state is more soluble and reactive, therefore, has improved properties for applications in manufacturing of health-care products, cosmetics, plant growth promoters, fruit preserving coatings etc.

The meeting discussed the recent developments in the CRP, especially the new development in analytical techniques and understanding of radiation effects in polymers. The mechanisms leading to the degradation or crosslinking of polymers have been tried to be elucidated by the use of microscopic methods of instrumental analysis, which provide physico-chemical information as well as imaging of polymers, like Positron Annihilation Lifetime Spectroscopy, NMR-Isotopic Labelling, Raman microscopy and Atomic Force microscopy. Participants in the CRP reported their achievements and problems. An evident progress is done in many laboratories of developing member states. The network cooperation for next period of R&D in the framework of the CRP was outlined. The report reflects the major achievements of the CRP during two year of cooperation.

The IAEA wishes to thank all the participants in the CRP for their valuable contributions. The IAEA officer responsible for this CRP is A.G. Chmielewski of the Division of Physical and Chemical Sciences.

EDITORIAL NOTE

This publication has been prepared from the original material as submitted by the authors. The views expressed do not necessarily reflect those of the IAEA, the governments of the nominating Member States or the nominating organizations.

The use of particular designations of countries or territories does not imply any judgements by the publisher, the IAEA, as to the legal status of such countries or territories, of their authorities and institutions or of the delimitation of their boundaries.

The mention of names of specific companies or products (whether or not indicated as registered) does not imply any intention to infringe proprietary rights, nor should it be construed as an endorsement or recommendation on the part of the IAEA.

The authors are responsible for having obtained the necessary permission for the IAEA to reproduce, translate or use material from sources already protected by copyrights.

CONTENTS

EXECUTIVE SUMMARY

1. INTRODUCTION

Polymers are generally classified as predominantly undergoing degradation and cross-linking when exposed to ionising radiation. In degradation polymers, rapid recombination of broken chain ends is sterically hindered. Hence, because of disproportionate, polymer radicals are stabilized with the formation of two stable end groups resulting with reduced chain length, lower molecular weight polymers. The radiation-induced degradation of polymers is generally considered as an undesirable phenomenon from the point of view of industrial applications. However, radiation induced degradation of synthetic polymers is utilized for preparation of ion track membranes used in filtration techniques and Teflon powder being a component of inks, coatings and lubricants. Another important application of radiation-induced degradation is in lithographic patterning. By using x-rays of electron beam, it is possible to manufacture integrated circuits with radiation-patterned sub-micron dimensions.

Natural polymers like cellulose and other polysaccharides (chitosan, alginates, carrageenames etc) are predominantly chain-scissioning polymers, irradiation results in substantial decrease in molecular weight. This is accompanied with the formation of carboxyl group and reduction in crystallinity. The amorphic state is more soluble and reactive, therefore, has improved properties for applications in manufacturing of health-care products, cosmetics, plant growth promoters, fruit preserving coatings etc.

Recent developments in analytical techniques and the use of sensitive methods of analysis have provided better understanding of radiation effects in polymers. The mechanisms leading to the degradation or crosslinking of polymers have been tried to be elucidated by the use of microscopic methods of instrumental analysis, which provide physico-chemical information as well as imaging of polymers, like Positron Annihilation Lifetime Spectroscopy, NMR-Isotopic Labelling, Raman microscopy and Atomic Force microscopy

The CRP on “Controlling of degradation effects in radiation processing of polymers” has therefore been launched with the overall objective to develop in participating laboratories reliable analytical methodologies concerning investigation of degradation effects of radiation on polymers. Moreover, participants will develop procedures and chemical formulations enhancing or preventing degradation effects depending on the desired application of the process.

2. SUMMARY OF PARTICIPANTS REPORTS

2.1. Brasil

Packaging materials have been widely processed by ionizing radiation in order to improve their chemical and physical properties and also for sterilization purposes. The effects of different gamma radiation doses, up to 100 kGy, on the optical properties of various commercial pakaging films were studied. Polyethylene LDPE, polyamide 6 – polyamide 6.6 copolymer PA 6 – PA 6.6 and poly(ethylene terephthalate) PET as the packaging films were analyzed. A UV/VIS spectroscopy investigation on film samples before and after irradiation was also performed. The results observed on irradiated poly(ethylene terephthalate) samples emphasise no significant changes either in light absorption, or in transmittance. The tested films did not present any change in color or optical properties one week after irradiation. It is accepted that color changes of irradiated polymers can be reversible; therefore, our observations highlight that no modifications within one week occurred, or, they were reversible and the consequence of irradiation treatment has not brought detectable change for a week.

On the other hand, after the same post-irradiation period, the two other polyethylene and polyamide 6 – polyamide 6.6 copolymer films presented changes in optical properties that varied according to the increase in radiation dose. The results showed that, in the absorption spectra of irradiated LDPE and PA 6-PA 6.6 films, a red shift of the UV cutoff and a marked reduction in percentage transmittance (at low wavelengths) occurs as irradiation dose increases. Such changes are likely caused by the cross-linking and degradation processes that irradiated polymers underwent.

Future work
The topics of the future work plan will be:

- The study of mechanical and thermal properties of the packaging polyethylene (LDPE), amide 6 – amide 6.6 copolymer (PA 6 – PA 6.6) and poly(ethylene terephthalate) (PET) irradiated by gamma radiation and electron beam.
- The study of oxygen diffusion into these films that is affected by irradiation under the exposure to gamma radiation and electron beam.
- The study of the migration of oxygen-containing products into fatty food simulants during and after irradiation.
- The study on the evolution of gaseous oxidation products originated from the irradiated packaging films by chromatography.

Collaboration: Romania – for high dose rate irradiation in polymer degradation.

2.2. Bulgaria

1. The commercial isotactic PP, pristine and after ^{60}Co γ-irradiation in air, has been studied using microhardness and Positron annihilation methods. It was found that at irradiation dose D_γ = 100 kGy a clear inverse effect in iPP response to γ-radiation took place. The degree of crystallinity X_c, melting temperature T_m, as well the Vickers and total microhardnesses, all sharply change the trend of their variation at the same dose D_γ = 100 kGy.

The observed behaviour was explained by the different response of iPP to γ-radiation. At low doses the prevalent effect of γ-radiation is chain scission phenomena, while for higher doses the main effects are chain branching and/or crosslinking. At the same time, the appearance of a hexagonal polymorph at doses equal or greater than 50 kGy also contributes to the observed inverse effect in iPP response to γ-irradiation.

2. Synthetic biodegradable polymers have been increasingly used as medical, pharmaceutical, agricultural and tissue-engineering products. Among the different classes of synthetic biodegradable polymers, the thermoplastic aliphatic poly(esters) like PLA (polylactide), PGA (polyglycolide) and their copolymers (PLGA) have generated tremendous interest due to their favorable properties such as good biocompatibility, biodegradability, bioresorbability and mechanical strength. They possess processing facility, great variety, adaptability and reliability.

The properties of the PLA, PGA and their copolymers make them the preferred materials for a variety of medical devices and pharmaceutical applications like tissue fixation, tissue regeneration, wound dressing, anti-adhesion and drug delivery systems. The drug- release depends on many factors, including composition, sterilization and porosity. One of the methods for studying subnanometer pores is the Positron Annihilation lifetime (PAL) method. In the presented contribution the results of free volume hole (fvh) size evaluation in biodegradable PLA, PDLA, poly(L-lactide-co-DL-lactide), and poly(DL-lactide-co-glycolide), pure and doped with calcium sulphate or hydroxyapatite, are given.

The dependence between o-Ps lifetime and radius of the fvh, at which o-Ps is localized before annihilation, was used. The change of sizes after gamma-irradiation of the samples with a dose of 12.5 kGy are also presented.

3. Cooperation with the group of Czech Republic

High fluence implantation of ions into polymers is very interesting from the practical point of view. It is of interest for fundamental reasons and for potential applications of irradiated polymers in microelectronics, opto-electronics and medicine as well. The Bulgarian contribution in studies of degradation of PET, PEEK and PI polymers, induced by irradiation with 150 keV Ar^+ and 1760 keV ^4He ions is the determination of the free volume fraction in implanted polymers, by slow positron beam lifetime measurements.

4. Cooperation with the group of Turkey

Positron annihilation lifetime spectroscopy was used to analyze cavity size at the nano scale in some molecularly imprinted Hydroxyethyl Methacrylate based polymers.

5. Cooperation with the group of Spain

PAL and microhardness methods were applied to make more clear the prossesess underwent in iPP under gamma irradiation.

Future work

- Positron annihilation lifetime (PAL) measurements in Poly (ethylene-Norbornene) co-polymers, pristine and after irradiation with different doses of γ-radiation;
- PAL measurements in addition (to mentioned above) biodegradable polymers;
- PAL measurements for other participants in CRP "Controlling of degradation effects in radiation processing of polymers", if desirable.

2.3. Czech Republic

The performed research is consist of several subjects: 1) diffusion of Ag and Cu atoms in polyethyleneterephtalate (PET) and polyimide (PI); 2) degradation of PET, PI and poly(ether ether ketone) (PEEK) with Ar+ and 4He+ ion irradiation; 3) investigation of plasma polymers and their composites.

Rutherford Backscattering Spectroscopy (RBS) and Elastic Recoil Detection Analysis (ERDA) techniques are employed to study the elemental content and depth profile of different materials. The brief descriptions of these two methods are the follows:

- RBS is most commonly used non-destructive nuclear method for elemental depth analysis of nm-to-mm thick films. It involves measurement of the number and energy distribution of energetic ions (usually MeV light ions such He+) backscattered from atoms within the near-surface region of solid targets. From such measurement it is possible to determine, with some limitations, both the atomic mass and concentration of elemental target constituents as a function of depth below the surface
- ERDA uses high energy (~1MeV/amu) heavy-ion beams to cinematically recoil and depth profile low atomic number target atoms. The heavy ion projectile need only have a mass greater than the target atom, alpha particles are commonly used to obtain recoil spectrum for hydrogen and its isotopes.

Beside, the positron annihilation lifetime measurements were performed as well as UV-VIS spectroscopy, AFM and XPS(X-ray Photoelectron Spectroscopy).

XPS is a very frequently used technique for the composition study. But the limitations essential to these methods leave some information unrevealed. For example XPS does not detect hydrogen and the analysis depth is only several nanometers. Therefore for study of polymer composition RBS and ERDA are highly useful.

We also planning to do further research in a field of degradation of polymers by various methods, such as: light ion irradiation and ion implantation; discharge in Ar plasma and by irradiation using a UV-excimer lamp in reactive ammonia atmosphere. Study of plasma polymer composite thin films is another field of our interest. Plasma polymer not only with metal but with another plasma polymer, for instance – PTFE/PP or TiO_2/PP , is planned to be studied.

2.4. Egypt

Radiation induced degradation technology is a new and promising application of ionizing radiation to develop viscose, pulp, paper, food preservation, pharmaceutical production, and natural bioactive agents industries. Controlling the degree of degradation, uniform molecular weight distribution, savings achieved in the chemicals (used in conventional methods) on a cost basis, and environmentally friendly processes are the beneficial effects of using radiation technology in these industries.

In this respect, studies have been made on the controlling of degradation in radiation processing of natural polymers used for agricultural and industrial purposes such as CMC-Na, chitosan, alginate and starch. Trials were made to control and reduce the irradiation dose required for the CMC-Na degradation by the addition of some additives and controlling the irradiation conditions. The moistened CMC-Na showed a great influence on the degradation/ crosslinking ratio according to the content of water during EB irradiation. The possibility to crosslink CMC-Na/PAAm and starch/PAAm blends using electron beam irradiation to obtain good adsorbent materials of unique properties for possible practical uses was also investigated. Degraded Na-alginate was used as an additive during radiation crosslinking of PAAm for the use as soil conditioner in agriculture purposes. The growth and other responses of bean plant cultivated in soil treated with PAAm and PAAm /Na-alginate copolymer were investigated. The test field results showed that the mixing of small quantities of PAAm or PAAm /Na-alginate copolymer with sandy soil results in increasing its ability for water retention. The growth of the bean plant cultivated in the soil treated with PAAm/ Na- alginate is better than that one in PAAm alone. The most significant difference between the PAAm and PAAm- Na-alginate copolymer is that the latter is partially undergoing radiolytic and microbial degradation to produce oligo-alginate, which acts as plant growth promoter. The increase in bean plant performance by using PAAm/Na-alginate copolymer suggested its possible use in agriculture as a soil conditioner providing the plant with water as well as oligo-alginate growth promoter. The use of Controlled Degraded CMC-Na incorporated with PAAm was also investigated as a super -absorbent material for the use in diaper industry:

Future work

Detailed studies on controlling degradation effects on the irradiated natural polymers will be thoroughly investigated. Characterization and possible applications of the controlled degraded natural polymers will be also investigated for possible use as soil conditioners in agricultural uses and also in the diaper industry.

2.5. Korea, Rep. of

An ultra high molecular weight polyethylene(UHMWPE) was irradiated with the electron beam at dose levels ranging from 100kGy to 1MGy. The microstructures of the irradiated samples were characterized by FTIR, gel fraction measurement, DSC and small and wide angle X-ray scattering.

For the physical properties, a static tensile test and creep experiment as well as wear resistance were also performed. The cross-linking and the crystal morphology changes were the main microstructural changes to influence the mechanical properties. It was found that 250kGy appeared to be the optimal dose level to induce cross-links in the amorphous area and recrystalliztion in the crystal lamellae. At doses above 250 kGy, the electron beam penetrates into the crystal domains, resulting in cross-links in the crystal domains and reduction in the crystal size and crystallinity. The static mechanical properties (modulus, strength) and the creep resistance were enhanced by the electron beam irradiation. The stiffness rather correlated with the degree of cross-links, while the strength correlated with the crystal morphology. Irradiation of UHMWPE at its melting temperature induced a very high crosslinking, which led to an excellent wear resistance of UHMWPE.

Future work

- Gelatin is a useful biocompatible and biodegradable natural polymer. It is generally chemically crosslinked using toxic aldehyde which is to be removed after chemcal treatment. Radiation crossliking will be a good alternative to chemical crosslinking.
- Crosslinking of gelatin using radiation.
- Applications of crosslinked gelatin to tissue engineering.

2.6. Pakistan

Part A:

Gum Acacia has been known for many thousands of years and there are no artificial substitutes that match it for quality or cost of production. Several thousand tons of the gum are utilized for their thickening and stabilizing properties in different industries such as food, cosmetics, beverage and pharmaceutical.

In this study, gum acacia was irradiated by gamma rays at different dose levels from 5-25 kGy. The effect of irradiation on physiochemical properties of gum were analyzed by UV spectroscopy, viscometry etc. UV spectroscopic analysis of the gum samples irradiated without exclusion of air from 5-25 kGy demonstrated progressive increase in coloration at 220 nm, whereas the gum samples irradiated at the same doses under vacuum show stability in color. This shows that discoloration can be avoid if the samples were irradiated under vacuum. No significant change in viscosity was observed in gum samples irradiated even to a high dose of 25 kGy. This indicates the absence of any physical change detrimental to the viscosity of the gum.

Part B

Approximately 70 % of low density polyethylene (LDPE) is employed in film manufacturing. If these films are not properly stabilized, they develop extensive yellowing in the sunlight. In this study we have tried to investigate the photo-oxidation and yellowing of polyethylene film in the presence of different primary and secondary antioxidants. These samples were irradiated by electron beam as well as by gamma at dose levels from 10-50 kGy. The discoloration in the irradiated samples were monitored by a yellowness index tester. The results of yellowness index revealed that discoloration in LDPE can be controlled by the addition of appropriate antioxidants.

In the future, we will identify the compounds produced during irradiation by the use of thin layer chromatography or by HPLC. Effect of gamma irradiation on swelling of gum samples at different doses and their comparison with solid state. Study the synergist effect of antioxidants by using a different combination of primary and secondary antioxidants.

2.7. Poland

We studied the protection of polypropylene against effects of ionizing radiation by low molecular weight additives and the role of polypropylene in its blends with SBS in radiation induced radical processes. Assuming that the decomposition of polyolefines initiated by ionising radiation proceeds comparable to photodegradation, the amine light stabilizers were applied to reduce the level of damage induced by electron beam irradiation. It was found that some light stabilizers efficiently inhibit radical processes, however the effect is significant only in the amorphous phase of polypropylene. Simultaneous termination of radicals in the crystalline phase is limited what determine overall effect of protection. Furthermore some hindered amines initiate changes in morphology of polypropylene facilitating crystallization which results in an increase of the number and density of crystal nuclei. Except crystals of α structure a small fraction of β crystals was confirmed. Shorter crystallisation time and higher crystallisation temperature can prompt thermal processing. On the other hand, fast nucleation leading to lower crystal perfection, worsens the resistance of polypropylene towards irradiation. We conclude that due to two opposite tendencies, i.e. protection against free radicals and enhancement of sensitivity towards irradiation, the stabilization of polypropylene against radiodegradation by hindered amine light stabilizers is ambiguous contrary to their role in photodegradation.

The stabilizing effect with respect to electron beam irradiation in blends polypropylene-triblock copolymer was also investigated. We found that upon irradiation mechanical properties of bends are comparable to properties of SBS copolymer. Thus elastomer has a crucial influence on macroscopic effects in the resulting resin. The post-irradiation oxidation in polypropylene proceed faster in blends than in neat material; in consequence the degradation of polypropylene is terminated in a shorter period of time. Polypropylene is much cheaper than thermoplastic elastomers therefore it can be used as cheap component to thermoplastic diene elastomers.

Future work

Application of polymers as a scaffold for tissue engineering increases every year. As the whole volume of the material must be free from bioburden, their sterilization by ionizing irradiation is necessary. The degradation of macromolecules, formation of polar groups and changes in morphology induced by radiation can influence the changes in biocompatibility and adhesion of cells on the surface of scaffolds. Therefore we plan to investigate the above effects in urethane based copolymers and estimate both desired and unwanted modifications initiated by electron beam irradiation.

2.8. Romania

The improvement in the thermal resistance of irradiated elastomers was promored by the superficial action of hydrocarbon absorbed into polymer samples. Different pressures of environmental gas were applied to emphasise the optimal effect of this treatment. The increase in gel content by about 10 % ensures good protection for long term application of this kind of materials. In addition, the radiation treatment promote crosslinking of the substrarte, that offers suitable behaviour for application of these products in the radiation action areas. This type of investigation can be extended to other polymeric materials, which can be crosslinked under ionizind radiation.

The radiation processing of polymers followed two main directions. The compatibilisation of polymer blends for new formulations will be applied in the production of electrical insulations. Several mixtures were investigated starting from ethylene-propylene elastomers and ethylene vinylacetate copolymer. The optimisation of irradiation conditions and the testing of final product are considered as the main goals of this kind of activity. Simutaneously, durability checking on the polymeric items produced by irradiation with accelerated electrons (energy of 1.8-2.0 MeV) are performed for the characterisation of life time.

The protection efficiency of antioxidants, which are added to different polymeric substrates destined for food packaging and medical wear, was tested. The derivatives of rosin, abietic acid and carnosic acid were studied. Their compatibility to human biology is taken into consideration, because healthy products must be manufactured. These additives are foreseen to be used for the increase in radiation stability during radiosterilisation. The thermal resistance improvement of elastomer, EPDM, by the radiation treatment in hydrocarbon environment was studied.

The next activity will be devoted to the recycling of polymer wastes. Various mixtures of commodity polyethylene and polypropylene will be incorporated in the EPDM matrix for the reusing of partially degraded polyolefins. In the same time, PET bottle material will be radiochemically processed to hydrolise them in aggresive salt solutions. The polymer decomposition will be considered in the direction of the reduction of pollution and energy consumption.

Another area that will be covered is the study on nanocomposites used in the production of dielectrics. Various nanofillers will be added into elastomers subjected to ionizing radiation to assess the modifications induced in material properties under hard service conditions.

Some co-operation actions are foreseen:

- with Brasil – for high dose rate irradiation in polymer degradation.
- with Bulgaria – for the assessment of surface behaviour by anihilation investigations,
- with Spain – for the optimisation of recycling formulations and for studying antioxidant efficiency.

2.9. Spain

The government research center: CIEMAT (Center for Energy, Environment and Technological Researches) in Madrid has the following irradiation facilities:

- 48 Co-60 gamma sources with a total of 3750 Curies.
- Van de Graaff accelerator (2 MeV)

The main R&D activities are:

- High dose rate for accelerated aging of materials and equipment for nuclear industry.
- Low dose rates for simulation of cosmic radiation for components in the space industry.
- Other: sterilization, special coloration in gems, etc.

The industrial installation: IONMED (Tarancón, 70 km east of Madrid) has as radiation source a 10 MeV Rhodotron accelerator (Beam current variable from 0.5 to 5 mA; beam power from 5 to 80 kW; belt speed variable from 0.5 to 5 m/min; dose per turn: 1 kGy to 100 kGy).

The major industrial applications are:

- Sterilization of surgical and medical equipment, laboratory items and pharmaceutical, hygiene and cosmetic articles.
- Hygienization of food (dairy products, cereals, spices, wine bottle corks, etc.).
- Reticulation of polymer materials (wires, cables and pipes, automobile parts, etc.).

There is another industrial installation in Aragogamma (Barcelona), which has a radiation source of Co-60 (130 000 Curies). The main application is dedicated to sutures (own production).

A new industrial installation is under construction at Electron Service Line, S.L., in Sevilla, which will be operative in June 2006.

This industrial facility will have electron sources (4 Mevex accelerators of 10 MeV and 30 kW each). Two bunkers with two accelerators in each, for double-side irradiation will be used. High speed, up to 20 m/min, and high capacity of irradiation will be applied. The main applications will be all kinds of products: medical, pharmaceutical, cosmetics, cork, packaging, food, industrial goods (automotive, aeronautical, electrical, textiles, etc.) for either sterilization, hygienization or cross-linking.

Prepared for X-ray installation and specially designed for R&D applications.

Irradiation considerably affects the structure of either amorphous ethylene-norbornene copolymers and semicrystalline syndiotactic polypropylene. Both of these polymeric systems synthesized witt mettallocenic polymers. In the former ones, the glass transition, the unique existing characteristic transition, is moved to lower temperatures independently of the norbornerne content, although the greater effect has been found for the copolymer with the highest norbornene incorporation, the calorimetric results being in a complete agreement to those found by dynamic mechanical thermal analysis. On the other hand, the thermal transitions in irradiated sPP specimens vary a little during the first heating up to a dose of 210 kGy. However, the irradiation effect is striking for the subsequent crystallization and second melting. The crystallization rate of sPP is significantly slowed down, decreasing the already small dimensional stability of this polymer. Determination of mechanical parameters has been quite difficult in irradiated specimens because they become more fragile and the preparation of suitable strips are really complicated.

Future work:

a) Further analysis of the final properties of irradiated amorphous ethylene-norbornene copolymers and semicrystalline syndiotactic polypropylene.

b) Evaluation of the effects of irradiation on sPP-based nanocomposites.

c) Irradiation and evaluation of iPP-based nanocomposites.

2.10. Turkey

Radiation-induced degradation has been considered for controlling the molecular weights of polysaccharides as well as enhancing the conductivity of polyaniline blends. Polysaccharides such as alginates, carrageenans and chitosans find extensive uses in food processing, health-care applications, paper and textile industries as well as in environmental applications. In most of these applications however their average molecular weights are needed to be below 10^4. Although chemical and enzymatic methods are being used for controlled degradation of these materials, the use of ionising radiation seems to provide unique advantages for the same purpose. Radiation has been shown to be very effective in degrading these polysaccharides irradiated either in solid form or in aqueous solutions. Literature data on the chain scission efficiency of these polymers vary considerably however, hence justifying our work on evaluating the environmental effects on radiation-induced degradation of polysaccharides.

Kappa- and iota-carrageenan and sodium alginate were the polysaccharides used in the study. The commercial samples were kept at well-defined humidity conditions (0, 50, 75 and 90%RH) until they reached their equilibrium water uptake values and then irradiated with gamma rays up to 100kGy dose. Although the overall effect of radiation has always been chain scission, the presence of the small amount of absorbed water (5-20%) caused a significant lowering in the chain scission yields G(S). At higher water contents G(S) values increased again. This behavior was attributed to plastifying effect of water at low concentrations facilitating the mobility of polymer chains to increase the probability of encounter of macroradicals thus leading to lower chain scission yields. These results have shown that one has to consider the important effect of humidity of irradiation environments when irradiating solid polysaccharide powders under actual radiation processing conditions.

In the second part of this work the radiation-induced conductivity in polyaniline/poly(vinyl chloride) (PANI/PVC) blends was studied.

Blend films were cast from non-conducting PANI and PVC solutions and gamma irradiated in air up to 800 kGy doses. The controlled release of HCl from irradiated PVC provided the necessary acid doping for PANI to turn it into conducting form. The initial conductivity of blends (10^{-9} S/cm) were found to be increased up to (10^{-4} S/cm) upon irradiation. The maximum conductivity was achieved for PANI/PVC blends with equal repeating unit compositions.

Future work

Studies will be continued on controlling of molecular weights of polysaccharides by radiation and enhancing the conductivities of PANI blends. Collaboration with Bulgari wil be pursued on the use of PALS in determining the fre-volumes generated inpolymers by irradiation.

2.11. USA

Oxygen plays a major role in determining the effects of radiation on polymeric materials, and for many polymers it can have a controlling influence on the ratio of chain scission versus crosslinking. Radiation-oxidation mechanisms are extremely complex, and only partially understood. We have undertaken experiments to identify radiation-oxidation products and reaction mechanisms utilizing samples of polypropylene having C-13 isotopic labelling at each of the 3 positions within the macromolecular chain using NMR for analysis. PP is a useful polymer for studies, as commercial applications exist for which control of radiation oxidation is critical: namely ¨vis-breaking¨(partial degradation to improve melt flow properties for material processing), and also the minimization of degradation in applications of radiation sterilization (e.g., syringes).

Unstabilized thin films of C-13 labeled PP have been subjected to γ-irradiation and to post-irradiation thermal oxidation, and then analyzed with solid-state ^{13}C NMR spectroscopy. It was found that the vast majority of oxidation-induced functional groups formed either during irradiation or upon post-irradiation treatment occurred on the tertiary (CH) carbons of the polypropylene. Of these products, tertiary hydroperoxides and/or dialkyl peroxides, which share the same ^{13}C resonance, were the most abundant, with tertiary alcohols as the second most abundant product. We detected no peroxides or alcohols originating from the secondary (CH_2) or the methyl positions of the PP; indeed we found no evidence of any chemistry occurring at the methyl side chain carbon. Carboxylate products were observed from both the secondary and tertiary carbon atoms (likely a mixture of acids, esters, and peresters). Other oxidation products included methyl ketones (for which the carbonyl carbon originated from the tertiary PP carbon), in-chain ketones (from the secondary PP carbon), and ketals (from both the tertiary and secondary PP carbons).

Oxidation product distributions for irradiated materials were substantially different for room temperature versus elevated temperature exposure. Samples irradiated at 24^{o}C in air exhibited exceptionally high concentrations of peroxidic species, whereas irradiation at 80^{o}C gave rise to higher yields of oxidation products attributable to the decomposition of peroxides, such as tertiary alcohols and carboxylic acids, and particularly large amounts of methyl ketones, indicative of a high yield of chain scission for a combined environment of radiation and temperature. Overall similar temperature-dependent trends were found in the case of samples exposed to irradiation under inert atmosphere, followed by exposure to air at varying temperatures. For example, in pre-irradiated samples exposed to air at room temperature for over a year, peroxides accounted for about 70% of the total oxidation products. This ratio decreased when higher temperature post-irradiation exposures were used, for example amounting to about 54% peroxides when 109^{o}C was chosen for the post-irradiation treatment. With increasing post-irradiation temperature, the proportion of products attributable to peroxide decomposition increased, with methyl ketones more than doubling and alcohols rising by about 75% upon going from room temperature to 109^{o}C. For samples irradiated in air, and then exposed to elevated temperature in air, important products such as ketones and alcohols that had formed during the irradiation were seen to further increase in concentration at first, and then reach a plateau, while peroxide concentrations changed little throughout the post-irradiation exposure.

The results gained in this study allow polypropylene to be compared to polyethylene, which we have studied recently using a fully isotopically-labeled sample, together with NMR analysis. Quite different radiation-oxidation chemistry trends are apparent. The relative rank ordering of oxidation product yields in polypropylene tends to remain the same throughout a given irradiation or post-irradiation exposure. As described above, peroxides dominate the products, and show remarkable thermal stability. In polyethylene, the peroxides are of low stability, and disappear rapidly when irradiated samples are subjected to elevated temperature. The dominant products in polyethylene are also different (either acids/esters, or ketones, dependent upon the extent of degradation).

Future work

Future studies will make use of additional analytical techniques to understand radiation degradation products in C-13 labeled PP, including FTIR and mass spec (for gaseous oxidation products). Isotopic labeling studies using other polymer types are also envisioned.

2.12. Vietnam

Chitin and chitosan have been used in variety of applications such as in food processing, water treatment, cosmetics, medicine, agriculture. However, in some fields, the application of this polysaccharide is limited by its high molecular weight (MW) so that the degradation of chitosan to prepare low MW of chitosan or oligochitosan has been considered.

At present, three methods for degradation of chitosan including chemical treament, enzymatic hydrolysis and radiation technology can be applied. Enzymatic hydrolysis involves mild process conditions and lead to the production of low MW with high yields but the enzymes are too expensive to be commercialised. Besides, several oxidative reagents have been studied for degradation of chitosan to obtain low MW but most of them are toxic reagents that are not desirable for application in cosmetics, pharmaceutics and food. Nevertheless, some reagents were used for degradation such as sodium nitrite, sodium hypochlorite and hydrogen peroxide. Especially, hydrogen peroxide has been chosen in this work because the productions of chitosan achieve preselected size, low cost of production, simple procedure and capability of being a nontoxic reagent. Exceptionally, further degradation by H_2O_2 led to ring-opening oxidation, the formation of carboxyl groups and deamination. For those reasons, radiation and oxidative reagent were combined to enhance the scission of chitosan. Recently, radiation was used as a tool for degradation of different polymers, namely, natural polymers such as alginate, chitosan, carrageenan, cellulose, pectin have been investigated for recycling these bioresources and reducing the environmental pollution.

An understanding of chemical structure and molecular weight of resulting product is essential to the successful application. Therefore, we investigated features of the modified chitosan by H_2O_2 combined with radiation treatment.

Optimal conditions of concentration, temperature, pH were also determined. Characteristics of chitosan products were investigated by measurements of proton nuclear magnetic resonance spectroscopy (^{1}HNMR), infrared spectroscopy (IR), viscosity average molecular weight (MW), ultraviolet spectrophotometry (UV), thermogravimetry analysis (TGA) and X-ray diffraction (XRD).

Future work

- Testing in the field of oligochitosan products for application of disease resistance on the plant.
- Perfection of this product for commercialization.

3. SUMMARY AND CONCLUSIONS

The results of the research and development works carried out by the participants of the CRP can be evaluated under three subtitles: i) Natural Polymers, ii) Synthetic Polymers and iii) New techniques for better understanding of radiation degradation of polymers.

Research activity within the RCM group includes progress in radiation degradation of polysaccharides from agricultural products (including sodium alginate, carrageenans, chitosan and gum acacia); use of radiation-degradation for doping of conductive polymers; controlling degradation processes in artificial joint implants, surface treatment of materials and food packaging; stabilizer additives for radiation environments; surface treatment of materials; and application of specialized analytical techniques (positron annihilation spectroscopy, ESR, RBS, ERDA, NMR/isotopic-labeling) to gain improved understanding of radiation degradation effects and mechanisms. Projects within the RCM group span the spectrum from fundamental studies through specific technological applications. Participants from Czech Republic, Spain and Turkey benefited from scientific collaboration with Bulgaria on PAS.

3.1. Natural polymers

Radiation-induced degradation of carboxy-methyl cellulose (CMC) has been considered with the purpose of finding some additives to enhance degradation hence lowering of irradiation dose. For soil conditioning in agricultural applications sodium alginate was degraded for use as an additive in poly(acryl amide) gels. The radiation degraded CMC-Na incorporated into PAAm gels has been investigated as a super adsorbent material to be used in personal health-care applications.

Gum accacia was irradiated up to 25 kGy and the effect of radiation has been investigated by spectroscopic, viscometric and optical methods. Up to a sterilization dose of 25kGy no adverse effect of radiation has been observed.

Radiation-induced degradation of kappa-, and iota-carrageenan and sodium alginate has been investigated in detail by GPC for controlling of the molecular weight of polysaccharides. It has been shown that the environmental humidity has a strong effect in the chain scission yields of these polymers. The presence of small amounts of absorbed water (5-20%) caused significant decrease in the chain scission yield. It has been shown that a target molecular weight can be reached at a significantly lower dose (sometimes two-fold) if the irradiation of solid polysaccharides were carried out in more dry environments. The combination of chemical oxidation and irradiation has been shown to result in enhanced degradation of chitosan leading to increased water solubility.

3.2. Synthetic Polymers

Controlling of synthetic polymer degradation induced by ionizing radiation still remains an important problem as it was demonstrated by ten of twelve contributions. Commercial implementation of radiation-processing in polymeric materials ought to be reviewed in some aspect due to more restrictive regulations. In the same time it was revealed that imperfections in quality of final products in many applications (packaging, joint prostheses, medical devices, etc) should be mitigated. To fulfill new criteria of radiation treatment some difficulties were identified and resolved:

New mechanisms of degradation in polyolefines were proposed and confirmed. The role of oxygen access in degradation of polymeric materials was elaborated, both during irradiation and post-irradiation aging.

Newly formulated radiation-resistant materials were proposed. The protective influence of some stabilizers and other organic small molecular weight additives incorporated into polymers was elucidated. Approaches to improve radiation stability of polymers were proposed via precisely controlled radiation treatment conditions, particularly by inhibition of degradation processes by thermal annealing or using of a hydrocarbon environment. It was demonstrated that radiation-induced conductivity in composites seems to be a promising method to obtain a new class of conducting polymers.

These findings confirm progress in comprehension and controlling of degradation effects in radiation processing of polymeric materials and provide a contribution to develop a fundamental basis of technological applications. On the other hand presented contributions confirm that the phenomena involved in radiation degradation of synthetic polymers and their physicochemical background are far from complete understanding.

3.3. Advanced analytical techniques for understanding radiation-degradation

A number of specialized analytical techniques are being developed and/or profitably applied for studies of the fundamental nature of radiation degradation effects in polymers. The goal of these investigations is to develop a deeper scientific understanding of processes underlying radiation-induced effects in order to provide a basis for better controlling (enhancing or reducing) degradation. The use of positron annihilation spectroscopy, combined with microhardness measurements, is providing understanding of complex mixes of chain branching and crosslinking in irradiated polymers. Information on the influence of irradiation on nanometer pore size in a variety of different polymers, including filled polymers, is being obtained. The use of isotopic labeling of polymers with C-13 allows NMR identification of radiation-oxidation products in solid polymer samples at room temperature. Studies of polypropylene samples separately labeled in the three carbon positions along the chain backbone, is providing insights into the detailed chemistry of degradation reactions that occur in samples exposed to irradiation at different temperatures, and also in samples exposed to post-irradiation degradation under varying conditions. Electron spin resonance spectroscopy (ESR) is continuing to provide a detailed understanding of the type of reactive free radical species that are intermediates of radiation-degradation processes. A number of radicals having extremely long lifetimes (months) have been investigated in irradiated polymers. Rutherford Backscattering Spectroscopy (RBS) is being employed as a non-destructive technique which provides the atomic mass and concentration of constituents as a function of depth below a polymer surface, up to several microns. Elastic Recoil Detection Analysis (ERDA) allows the determination of hydrogen concentration and depth profile. Applying these two techniques (RBS and ERDA) together gives information about the complete atomic composition.

4. RECOMMENDATIONS

The participants of the CRP all agreed on the importance and timeliness of the subject of radiation-induced degradation of natural and synthetic polymers both from scientific and technical points of view.

One of the objectives of this CRP in terms of establishing cooperations and collaboration among the participants has been fullfilled to a certain extent, it is therefore highly recommended to benefit from the individual expertise of the participants in establishing new collaborations to complement their works.

The subject of radiation processing of polymers has been covered in a number of international symposia. The coordination of CRP activities with these type of international meetings is recommended in the selection of venue and dates of future meetings.

A number of radiation-induced degradation applications have already been identified during the presentations and discussions at the RCM. The participants of the CRP are recommended and encouraged to prepare TC project proposals to be submitted to the IAEA for the next cycle.

The participants of the CRP are recommended to promote the results of the CRP to end-users in order to help implement radiation processing into new industrial applications.

The participants recommended to have the next RCM in November 2006 in Korea.

REPORTS BY PARTICIPANTS IN THE RCM

EFFECTS OF GAMMA RADIATION ON COMMERCIAL FOOD PACKAGINGTITLE OF PAPER

E.A.B. MOURA, A.V. ORTIZ, H. WIEBECK, A.B.A. PAULA, A.O. CAMARGO, L.G.A.SILVA
Brazilian Nuclear Energy Commission
Institute for Energetic and Nuclear Researches - IPEN
Radiation Technology Centre, Sao Paulo – SP, Brazi

Abstract

Packaging materials have been widely processed by ionizing radiation in order to improve their chemical and physical properties and also for sterilization purposes. The effects of gamma radiation doses up to 100 kGy on the optical properties of different commercial pakaging films were studied. Polyethylene (LDPE), polyamide 6 - polyamide 6.6 copolymer (PA 6 - PA 6.6) and poly(ethylene terephthalate) (PET) as the packaging films were analyzed. A UV/VIS spectroscopy investigation on film samples before and after irradiation was also performed. The results showed that, in the absorption spectra of irradiated *LDPE* and *PA 6-PA 6.6* films, a red shift of the UV cutoff and a marked reduction in percentage transmittance (at low wavelengths) occurs as irradiation dose increases. The results observed on irradiated poly(ethylene terephthalate) samples emphasise no significant changes either in light absorption, or in transmittance.

1. INTRODUCTION

The use of ionizing irradiation in foodstuff pasteurization has shown to be effective and reliable in controlling foodborne pathogens and in extending the shelf life of the final products. In 1997, the US Food and Drug Administration approved irradiation of fresh and frozen red meat. Since then, the interest in radiation processing of foodstuffs has been renewed[1].

Foodstuffs are prepackaged prior to irradiation to prevent subsequent recontamination by microorganisms. On the other hand, ionizing irradiation can affect the polymeric food packaging materials itself. Irradiation of polymers generally leads to formation of free radicals and ions, with effects such as simultaneous scission and cross-linking of the polymeric chains. If irradiation is carried out in the presence of oxygen, formation of gases and low molecular weight radiolysis products may occur. Also, polymers used in food packaging often contain additives that could potentially undergo degradation upon irradiation and the degradations products formed might migrate into the foodstuff and affect its organoleptic properties and toxicological safety. The mechanical and optical properties of a polymeric packaging material can be affected by both cross-linking and degradation processes[2]. Optimal cross-linking of polymeric chains causes the formation of a macroscopic network and results in a desirable lower permeability and improved mechanical properties of flexible packaging material. On the other hand, irradiated packaging materials may acquire undesirable optical properties as a consequence of unacceptable color formation or increased light transmittance in the near UV range, which in turn, might reduce the foodstuff's shelf life[3]. In this study, we have examined the effects of gamma radiation on optical properties of some commercial plastic packaging films that are widely used by the meat industry in Brazil.

2. MATERIALS AND METHODS

The experiments were carried out using monolayer plastic packaging films obtained from commercial film manufacturers (Table I).

TABLE I. MAIN CHARACTERISTICS OF PACKAGING MATERIALS USED FOR THE IRRADIATION TESTS

Film Names[(a)]	Extruded Film Materials	Thickness (μm)	Manufacturers
Unipac-PE-60	Low density polyethylene – LDPE	60	Unipac Embalagens Ltda.
Unipac-PA-30	Amide 6-amide 6.6 copolymer – PA 6-PA 6.6	30	Unipac Embalagens Ltda.
Unipac-PET-12	Bi-oriented poly(ethylene terephthalate) – PET	12	Du Pont

(a) Reference to flexible packaging manufacturer Unipac Embalagens Ltda.

The nylon and polyethylene films are air-cooled blown extruded films and neither was subjected to IBC (internal bubble cooling). The PET film is a standard bi-oriented film used by the food packaging industry for printing and lamination. Pieces of each packaging material (14 x 14 cm^2) were cut from commercially available sheets and irradiated individually. Industrially, these films do not undergo any complementary treatment (sterilization or similar decontamination procedure) because they are produced under strict GMP (Good Manufacturing Practices). Hence, irradiation was carried out without any further intervention on the samples. Prior to irradiation, fifteen samples were placed in a cylindrical device made of 304 stainless steel and then irradiated at different doses within the 0-100 kGy range. Irradiation was carried out at room temperature, in air, and at dose rates of 5.35 - 5.78 kGy/h using a ^{60}Co source of the "GammaCell 220" type (Atomic Energy of Canada Limited). Irradiation doses were measured with cellulose tri-acetate "CTA-FTR-125"dosimeters from Fuji Film. The films were tested one week after irradiation. In order to avoid any effect of either natural or artificial light on the samples prior to testing, they were placed in a black plastic bag and stored in a drawer in the laboratory. UV/VIS spectra were obtained using a Shimadzu UV1601PC spectrophotometer.

3. RESULTS AND DISCUSSION

Each final spectrum represents the average of 4 samples of equal size and thickness obtained randomly from non-irradiated and irradiated PE, PA or PET film.

3.1. Unipac-PE-60 film

Upon visual examination, Unipac-PE-60 samples presented a yellowish coloration and also emitted unpleasant off-odor after irradiation above 15 kGy. The intensity of such alterations increased with radiation dose. Figure 1 shows the changes in absorption spectra of Unipac-PE-60 upon exposure to a dose range of 0-100 kGy. As can be seen, irradiated samples tend to exhibit a red-shift in the wavelength of the UV cutoff and the formation of an absorption tail. It is worth noting that, for these polyethylene samples, absorbance does not increase at 10 kGy; increases with very slight differences between spectra for doses of 40 and 50 kGy, and also of 80 and 100 kGy, but increases displaying an inconsistent behavior at doses of 20, 30 and 65 kGy. Also, absorbance is apparently more affected by irradiation at wavelengths 210-250 nm. The changes observed could be due to unsaturations and the presence of carbonyl and hydroxyl compounds.

Irradiation of LDPE gives a combination of degradation and cross-linking, accompanied by the formation of unsaturated products. If the irradiation is carried out in the presence of air, in most cases carbonyl and hydroxyl compounds are formed[4]. At present, we have no explanation for the observed behavior at 20, 30 and 65 kGy.

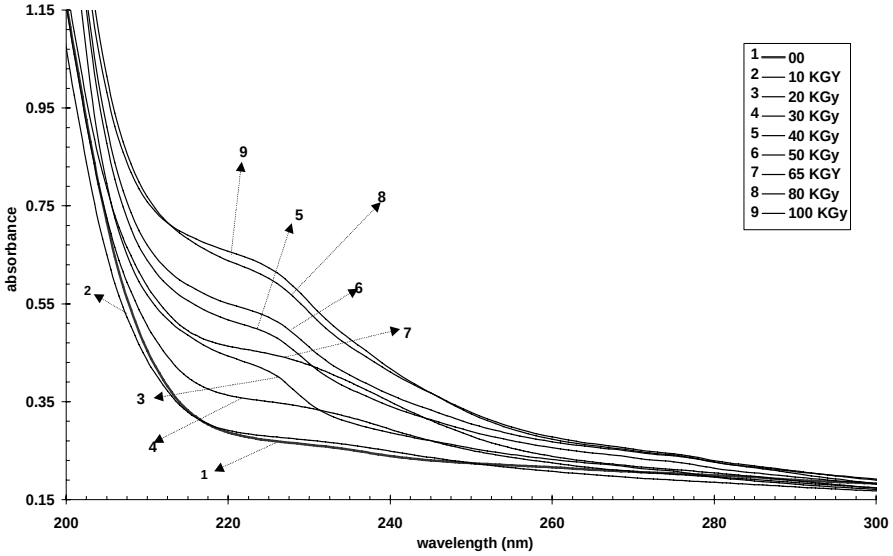

FIG. 1. Absorption spectra of Unipac-PE-60 samples before and after gamma radiation doses up to100 kGy

Figure 2 shows the variation in transmittance percentage of Unipac-PE-60 samples with increasing radiation dose at some wavelengths. It is possible to see that gamma irradiation leads to a decrease in transmittance percentage at low wavelengths and to a slight increase at higher wavelengths. It is clear that, at wavelengths within the UV range, there is a reduction in light transmission with increasing gamma radiation dose that is very marked in the spectral region between 195 and 240nm; interestingly this suggests that UV barrier has improved in the irradiated material.

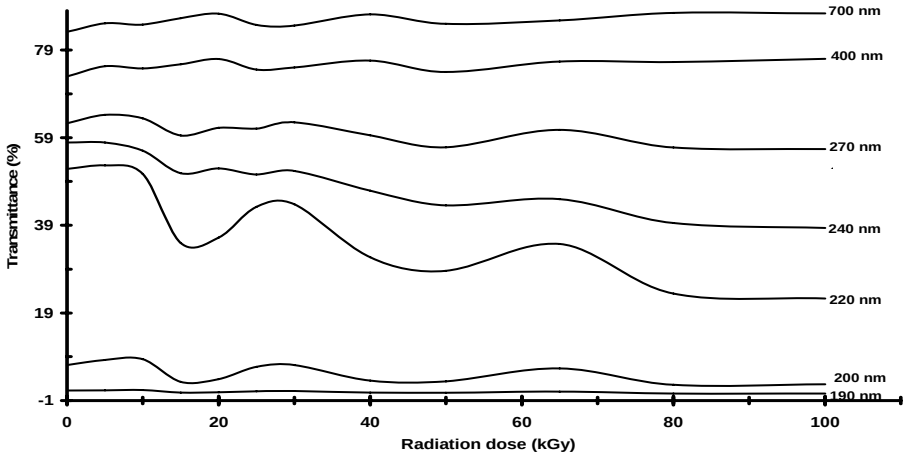

FIG. 2. Variation in transmittance percentage with radiation dose of Unipac-PE-60 samples gamma radiation doses up to 100 kGy

3.2. Unipac-PA-30 film

After irradiation, Unipac-PA-30 samples become brittle and give off strong and unpleasant odor, whose intensity increases with radiation dose. Figure 3 shows the variation in absorption spectra for samples of Unipac-PA-30, after exposure to a dose range of 0-100 kGy. As can be seen, the irradiated samples exhibit a red-shift in the wavelength of the UV cutoff and the formation of an absorption tail, except in the 15-25 kGy dose range, where light absorption is similar to the non-irradiated material. Note that the absorbance intensity of Unipac-PA-30 samples increases displaying an inconsistent behavior at doses of 5, 10 and 65 kGy.

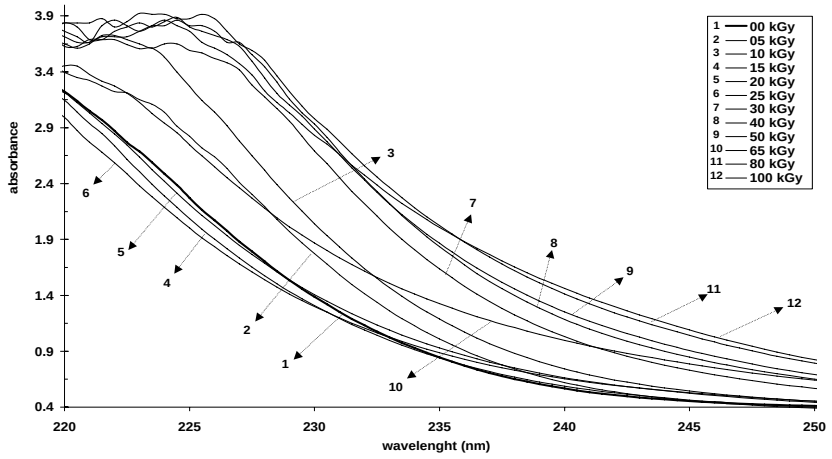

FIG. 3. Absorption spectra of Unipac-PA-30 samples before and after gamma radiation doses up to100 kGy

As shown in Figure 4, the transmittance percentage reduced with increasing radiation dose at low wavelengths, except for Unipac-PA-30 in the 15-25 kGy dose range. These changes could be due to the formation of imide groups, unsaturations and carbonyl and hydroxyl compounds.

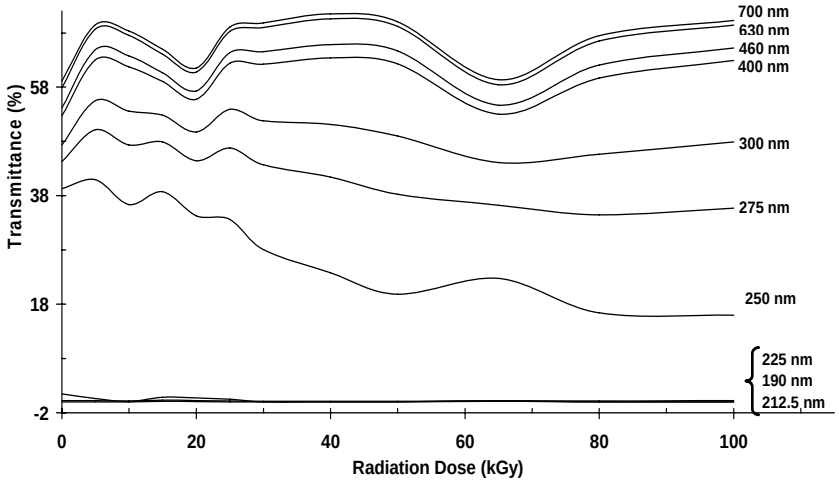

FIG. 4. Variation in transmittance percentage with radiation dose of Unipac-PA-30 samples gamma radiation doses up to 100 kGy

3.3. Unipac-PET-12 film

After irradiation, Unipac-PET-12 samples emphasise no significant changes either in light absorption or transmission at the doses tested (Figure 5). On the other hand, the optical properties of the Unipac-PE-60 and Unipac-PA-30 samples present changes are likely caused by cross-linking and degradation process with increasing radiation dose.

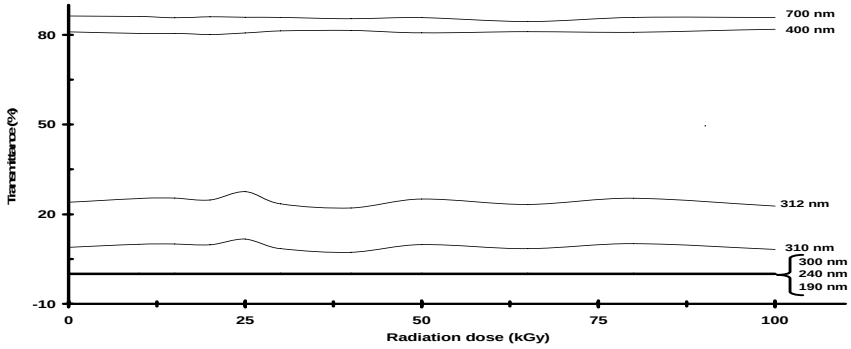

FIG. 5. Variation in transmittance percentage with radiation dose of Unipac-PET-12 samples gamma radiation doses up to 100 kGy

4. CONCLUSION

The results observed on irradiated poly(ethylene terephthalate) samples emphasise no significant changes either in light absorption, or in transmittance. The tested films did not present any change in color or optical properties one week after irradiation. It is accepted that color changes of irradiated polymers can be reversible; therefore, our observations highlight that no modifications within 1 week occurred, or, they were reversible and the consequence of irradiation treatment has not brought detectable change for a week. On the other hand, after the same post-irradiation period, the two polyethylene and polyamide 6 – polyamide 6.6 copolymer films presented changes in optical properties that varied according to the increase in radiation dose. The results showed that, in the absorption spectra of irradiated LDPE and PA 6-PA 6.6 films, a red shift of the UV cutoff and a marked reduction in percentage transmittance (at low wavelengths) occurs as irradiation dose increases. Such changes are likely caused by the cross-linking and degradation processes that irradiated polymers underwent.

REFERENCES

[1] ROSS R.T., ENGELJOHN, D., "Food Irradiation in the United States: Irradiation as a Phytosanitary Treatment for Fresh Fruits and Vegetables and for the Control of Microorganisms in Meat and Poultry", Radiat. Phys. Chem. 57 (2000), 211-214.

[2] KILLORAN, J.J., "Packaging Irradiated Food in: Preservation of Food by Ionizing Radiation", vol.II, ed. E. Josephson, M. Peterson, CRC, Florida (1983) 317-326.

[3] CLOUGH R.L., GILLEN K.T., MALONE G.M., WALLACE J.S., "Color Formation in Irradiated Polymers", Radiat. Phys. Chem. 48 (1996) 583-594.

[4] SPINKS J.W.T., WOODS R.J., "Introduction to Radiation Chemistry", 3rd edition, Wiley, New York, (1990) 468 pp.

GAMMA IRRADIATION EFFECT ON ISOTACTIC POLY(PROPYLENE) STUDIED BY MICROHARDNESS AND POSITRON ANNIHILATION LIFETIME METHODS

M. MISHEVA[1], G. ZAMFIROVA [2], V. GAYDAROV [2], J.M. PEREÑA[3], M.L. CERRADA[3], E. PÉREZ[3], R. BENAVENTE[3]
[1]Sofia University "Kl. Ohridsky", Faculty of Physics, Sofia. Bulgaria
[2] Higher School of Transport "T. Kableshkov", Sofia, Bulgaria
[3]Instituto de Ciencia y Tecnología de Polímeros (CSIC), Madrid, Spain

Abstract

The commercial isotactec PP, pristine and after ^{60}Co γ-irradiation in air, has been studied using microhardness and Positron annihilation methods. It was found that at irradiation dose D_γ = 100 kGy a clear inverse effect in iPP response to γ-radiation took place. The degree of crystallinity X_c, melting temperature T_m, as well the Vickers and total microhardnesses, all sharply change the trend of their variation at the same dose D_γ = 100 kGy. The observed behavior was explained by the different response of iPP to γ-radiation. At low doses the prevalent effect of γ-radiation is chain scission phenomena, while for higher doses the main effect are chain branching and/or crosslinking. The complicated dependence of the relative o-Ps intensity on degree of crystallinity was ascribed to the supposition that γ-irradiation of PP with doses up to 100 kGy influences mainly the lamella surface. The explanation of changes is based on the idea of pushing the irradiation defects out of the crystalline areas into the intermediate layers that leads to improvement of both lamellae and their fold surface perfectness.

1. INTRODUCTION

Poly(propylene) is a widely used polymer due to its relatively cheap production and good mechanical properties. In some cases, e.g. when it is used for food packing or for medical tools production, the PP has to be subjected to gamma (γ) irradiation purposely for sterilization. So, the response of PP to γ-radiation is of considerable interest.

Isotacted PP is considered to be capable of crystallizing into several isomorphic modifications, abbreviated as α-iPP(monoclinic), β-iPP(hexagonal)and γ-iPP (orthorhombic) [1]. Beta lamellae possess lower density, higher rates of crystallization and metastability in comparison to the α-form [2, 3]. The crystal structure of the γ-iPP has remained a puzzle for a long time. This phase can be obtained under a high pressure or from small molecular fractions called “short chains”. It was proved that the thickness of the crystalline layer decrease in the gamma phase. Also the long period in γ-phase is bigger than that in the α-phase.

Regardless of exact interaction mechanism of a γ-photon with matter (e.g. polymer), the final result is the creation of a highly energetic electron. In the course of slowing down, this primary electron produces ionized and exited species that finally lead to creation of free radicals. If the radicals are in the amorphous parts, they can react resulting in chain cross-linking or chain scissions, which influences the mechanical properties of polymers.

If the radicals are formed in the crystalline areas, then a recombination process is most probable, due to the “cage effect”. Part of gamma quanta energy is trapped by the crystal as an exciton. Excitons migrate along the chain to the surfaces of the lamellae, and form a defective layer on crystal-amorphous boundaries.

Substantial modifications in the crystal structure can occur at higher radiation doses (thousands of Grays).

One of the simplest ways to judge the mechanical properties is to carry out the micro indentation studies [4]. Using different loads P, see equations (1) and (3) for determination of microhardness, the method can give an idea for the microhardness change in the depth of the studied samples.

Many of the polymer properties depend also on the presence of subnanometer local free-volume holes (pores) in the macromolecular matrix. In the recent years the positron annihilation lifetime (PAL) spectroscopy is widely used to probe free-volume holes (fvh) in different materials, including polymers [5]. In this contribution the results of microhardness and PAL measurements of iPP, unirradiated and irradiated with 60Co γ-rays up to dose Dγ = 103 kGy, are presented and discussed.

2. EXPERIMENTAL

2.1. Materials

Isotactic PP ([−CH2−CH(CH3) −]n) is commercial product of Repsol YPF. The samples represent about 0.3 mm thick plates. Gamma irradiation was carried out using 60Co γ-rays up to dose 103 kGy (Table I) at a rate of 6.63 kGy/h on air. Before measurement specimens were kept at room temperature about 2 months in order to eliminate short-lived radicals.

TABLE I. IRRADIATION DOSES D_γ, THE VOLUMES V_P OF FREE-VOLUME HOLES, DSC DEGREE OF CRYSTALLINITY X_C, AND MELTING TEMPERATURE T_M OF THE STUDIED IPP MATERIALS.

No	D_γ, kGy	V_p, Å^3	X_c, %	T_m, K
1	0	120.0(1.2)	45.3	437
2	20	115.4(1.1)	46.7	435
3	50	118.8(3.5)	48.6	431
4	100	120.0(3.5)	53.3	426
5	400	112.0(1.1)	51.7	421
6	1000	112.0(1.1)	48.2	414

From DSC data the degree of crystallinity, Xc, have been determined using a value of 209 J/g [6] for an ideal purely crystalline iPP. The respective values are given in Table 1.

2.2. Microhardness measurements

The measurements were carried out on a standard Vickers microhardness device mph-160 fitted to a NU-2 light microscope (Germany). The indentor is a square-shaped diamond pyramid with top angle 136o. The projected diagonal lengths of indentation d μm were measured after removing the load P. The values of Vickers microhardness MHV were calculated by the expression

$$MHV = kP / d^2 ,$$

where k is a geometrical factor equal to 18544 for this type of the indentor. When measuring MHV as function of irradiation dose we used the constant loading P=40 g. Eight different values of P (from 1.25 to 160 g) were used to study the microhardness change in the depth of the samples.

Total microhardness MHT is calculated by the expression

$$MHT = kP / D^2 ,$$

where D is the diagonal of the indentation made by the pyramidal indentor under load P.

2.3. Positron annihilation lifetime spectroscopy

The lifetime spectrometer was a standard fast-fast coincidence apparatus. It provides a time resolution ~ 280 ps FWHM. A positron source, 22NaCl sealed with Kapton foils, was sandwiched between two samples. Corrections for positrons annihilating in the source were made according to Djourelov et al. [7]. The statistics of positron annihilating only in the samples studied was of the order of 1x106 counts for each spectrum. At least 8 spectra during two days of measurements were recorded for each sample.

The experimental spectra were fitted with the program POSITRONFIT-EXTENDED [8]. The program CONTIN (PALS-2) [9, 10] was also used. In the latter case the lifetime spectrum of Indium (In) samples with τ =194 ps (>99%) was used as a reference spectrum. All measurements were made at room temperature in an air-conditioned laboratory.

The PALS method is based on the interaction of an energetic positron (e+), emitted from a radioactive source (e.g. 22Na), and condensed matter. When such e+ enters into matter, it losses its energy and become thermalized in about 10-12 s. The thermalized e+ can annihilate as a free particle, or can form a bound state, positronium atom, Ps, with a medium electron. One quarter of Ps atoms are in singlet state, para-Ps (p-Ps, with anti parallel spins of the e- and e+). The rest ¾ of the Ps atoms are in triplet state, ortho-Ps (o-Ps, with e- and e+ parallel spins). The lifetime of the p-Ps self-annihilation is ca 120 ps. In vacuum the lifetime of the o-Ps self-annihilation is much longer – about 140 ns. In condensed matter e+ from o-Ps may annihilate with a medium electron, the so-called pick-off annihilation. In this case, o-Ps lifetime, τo-Ps, shortens to a few ns.

In polymers o-Ps atoms tend to be trapped in free-volume holes or pores, localized mainly in amorphous parts of polymers, and τo-Ps depends on fvh size. The so-called Tao-Eldrup model [11, 12] in which a spherical-shaped pore of radius R has been assumed, gives the following dependence between R and τo-Ps

$$\tau_{o-Ps} = 0.5\left[1 - \frac{R}{R_0} + \frac{1}{2\pi}\sin\left(\frac{2\pi R}{R_0}\right)\right]^{-1}.$$

In this equation

$$R_0 = R + \Delta R$$

The thickness ΔR of the electron layer on the pore walls ΔR =0.1656 nm was empirically determined in ref.[13]. The equation (3) will be used to extract the sizes of the free volume holes in the studied polymers.

3. RESULTS AND DISCUSSION

The degree of crystallinity, Xc, as a function of irradiation dose, Dγ, is depicted in fig.1. Xc depends linearly on Dγ. At that it increases (8%) till dose of 100 kGy, and after that decreases at higher doses, i.e. a clear inverse effect in iPP response to γ-irradiation is observed. Such inverse reaction has been ascribed to different response of iPP to γ-radiation [14]. At low doses the prevalent effect of γ-radiation is chain scission phenomena, while for high doses the main effect is chain branching and/or crosslinking. The increase in the degree of crystallinity up to a dose of 100 kGy is partially ascribed to so called “radiation annealing” [15].

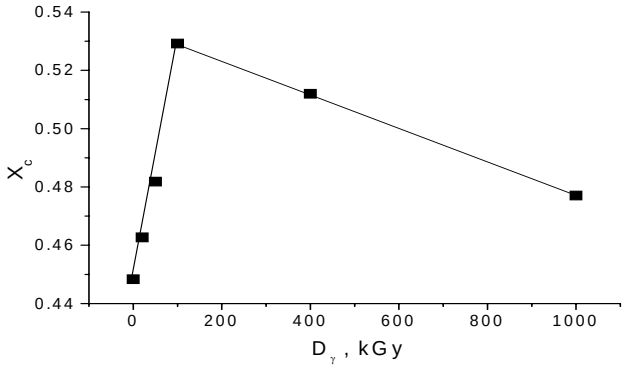

FIG. 1. Degree of crystallinity Xc versus irradiation dose Dγ

When the free radicals are formed in the crystalline areas, then a recombination process is most probable, due to the "cage effect". Part of the gamma quanta energy is trapped by a crystallite as an exciton. The excitons migrate along the chains to the surfaces of the lamellae, forming a defective layer on crystal-amorphous boundaries. This radiation annealing results in a better perfectness of both crystallites and fold surfaces. At higher radiation doses up to 1000 kGy, the processes provoke by γ-irradiation lead to creation of many damages in both crystalline and amorphous parts of iPP. The values of the crystalline and amorphous densities get closer and the process is similar to the partial radiation melting [16]. This leads to Xc decreasing.

Besides that, the result of WAXS experiments [17] on iPP showed that β–polymorph appears for doses of 50 kGy and higher. The coexistence of both α and β crystal lattices was ascribed to the rupture of some macromolecullar chains and subsequent organizing into β crystalline lattice. The latter is hexagonal and thinner lamelae. So, the dependence of Xc on irradiation dose is due to combined influence of radiation annealing (Dγ ≤ 100 kGy), radiation melting, accompanied by the creation of damages into the material (Dγ > 100 kGy), and α-β polymorphic transition (Dγ ≥ 50 kGy).

The dependence of the melting temperature Tm on irradiation dose is shown in fig.2. Again, this dependence could be fitted with two lines with different slopes. The change of trend is due to "radiation annealing", supervened of the appearance of the β polymorph and "radiation melting" at higher doses.

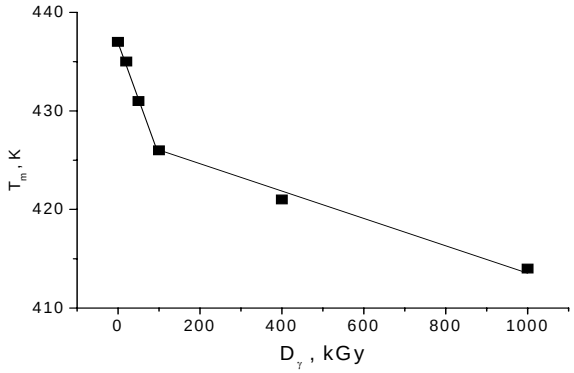

FIG. 2. Melting temperature T_m versus irradiation dose D_γ

As defined by eq. (1), MHV is connected with the plastic properties. According to so-called additive model [18], MHV for a semicrystalline polymer can be presented as

$$MHV = X_c MHV^{cr} + (1 - X_c) MHV^{am},$$

where MHVcr and MHVam are the hardness of the crystalline and amorphous phases respectively. As MHVcr >> MHVam , the above equation implies that MHV is related to the quality and quantity of the crystal phase. The equation (4) could be transformed as follows:

$$MHV \approx X_c MHV^{cr}$$

In fig.3a the MHV is presented against Xc. A good (R=0.98006) linear dependence is observed, especially when MHV of pristine sample is excluded (R=0.99063). From the equation (4a) the MHVcr values were calculated and plotted vs. irradiation dose (Fig 3b). At low doses, the radiation annealing leads to less defective crystalline phase of the studied iPP and MHVcr increases. The following decrease is connected with the creation of many defects in crystallites at higher doses, and as well as with the α–β polymorphic transition.

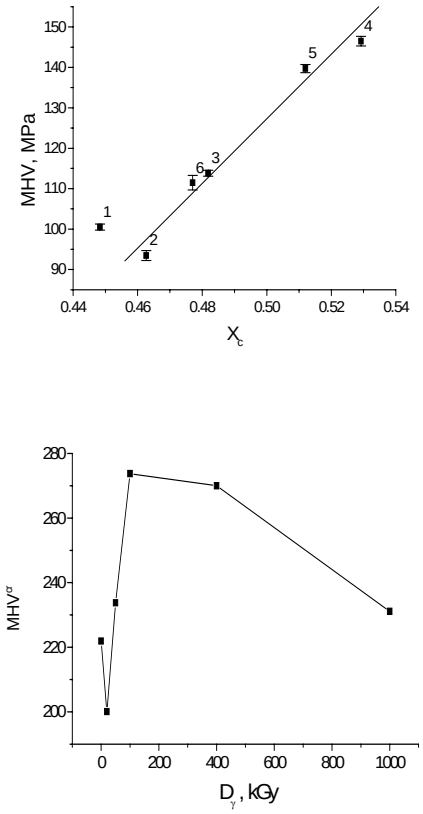

FIG. 3. Standard Vickers microhardness as a function of degree of crystallinity X_c. The labels correspond to the number of studied samples in Table 1 (a); MHV^{cr} part of Vickers microhardness as function of irradiation dose D_γ(b).

The MHV and MHT dependencies on irradiation dose are presented in fig.4.

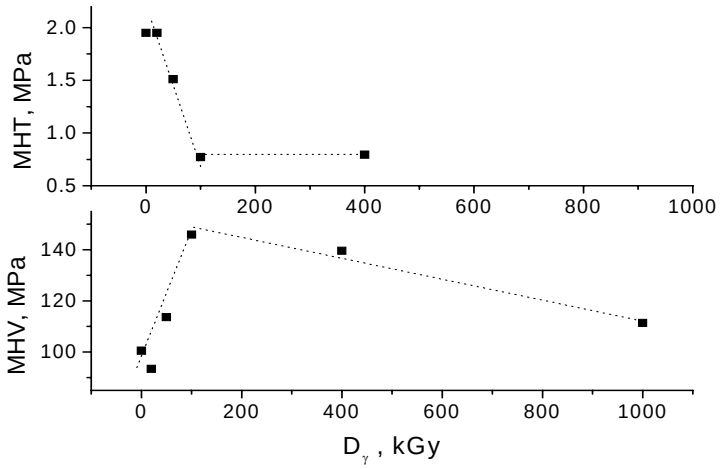

FIG. 4. Total microhardness MHT, and standard Vickers microhardness MHV versus irradiation dose Dγ

It is obvious (as MHV~Xc) that the variation of MHV with dose is simply a reflection of the degree of crystallinity change with dose. As can be seen from the figure, MHV and MHT vary in an opposite manner for low doses. From the microhardness point of view this implies that the resistance against the reversible deformation decreases, i.e. the material becomes more elastic. At doses higher than 100 kGy, as already discussed, both the crystalline and amorphous parts of iPP become more defective, and MHV and MHT decrease. In order to follow the microhardness changes in the depth of the samples, MHV and MHT were determined by using different loads P (from 1.25 to 160 g). The results for Dγ =0 kGy and Dγ =100 kGy are presented in fig.5. MHV for Dγ =100 kGy has its lowest value near the surface. At first it continuously increases with depth, and after that it levels off. This behavior of MHV is a consequence of the sample irradiation in air. Near the surface, where oxidation took place, the material underwent predominately chain scission and became softer. In the depth of the samples in the absence of oxygen the cross-linking prevail over the scissions and MHV became larger. As known [19] PP pertains to polymers that show improvement in their mechanical properties under the formation of cross-link sites.

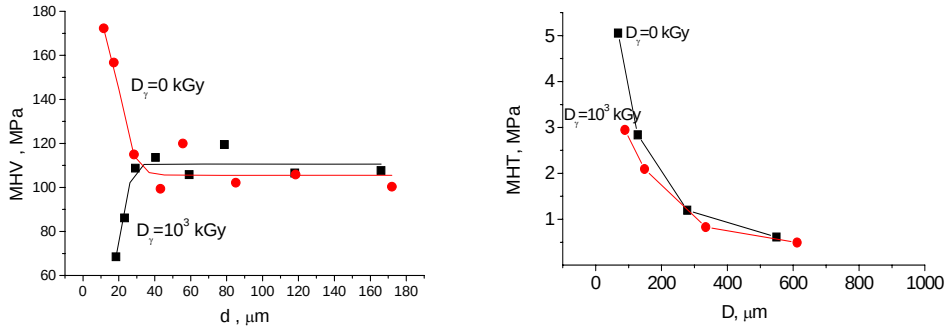

FIG. 5. Vickers microhardness MHV as function of the projected diagonal lengths of indentation d (a). Total microhardness MHT versus D, the diagonal of the indentation created by the pyramidal indentor under load P (b).

The behavior of MHV for unirradiated samples- decreasing from surface to the bulk is not clear. The total microhardness MHT comprises plastic, elastic and viscoelastic resistance against the deformation of the samples and the depth of penetration D under load (see equation 2) depends on the elasticity of the material, increasing with it. So, the values of MHT diminish when the elasticity goes up. In this context, the MHT behavior shown in fig.5b implies, somewhat unexpectedly, that the elasticity increases with depth under the sample surface for the studied iPP. Due to limited thickness of the studied samples, the largest load P used for these measurements was P=20 g, because of the influence of the sample support.

Ussually positron spectra for polymers are fitted into three lifetime components [20]. The first one τ1 is interpreted as a weighted average of two contributions: $\tau 1' = 125$ ps due to self-annihilation of p-Ps, and $\tau 1'' > \tau 1'$, due to annihilation of free positrons in the bulk of the sample [21]. The second lifetime τ2 is attributed to annihilation of positrons trapped before annihilation at low electron density sites in more ordered part of the matrix. As usually, the third lifetime component, τ3, is associated with o-Ps pick-off annihilation at fvh sites, localized in amorphous regions. In the present case $\tau 1 \approx$ 220-250 ps, $\tau 2 \approx$ 450-500 ps and $\tau 3 \approx$ 2160-2260 ps. The pore volumes are shown in Table I above. Some authors consider that in semicrystalline polymers, see for example [22], a certain contribution to the o-Ps component comes from the Ps atoms, formed at defects in crystalline phase and consequently four lifetime components are used to fit the spectra. This view is consistent with the results, obtained by CONTIN-PALS2 code in the present case. The chosen solutions show two o-Ps lifetimes, as seen in fig.6.

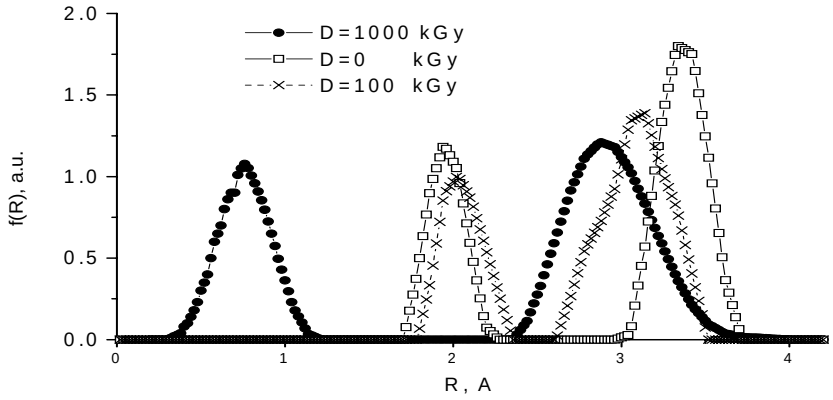

FIG. 6. Free-volume hole radius distribution functions for some of the studied samples. The smaller radii refer to free-volume holes, localized in the crystalline phase, while the larger radii refer to holes, localized in the amorphous phase of the corresponding material

According to radius distributions, we tried to analyze the lifetime spectra with four free components. In such case however, due to too many fitting parameters, the obtained results are not stable, resulting in large uncertainties, and some additional constrains during spectra processing have to be used. In the present case, positron spectra decomposition with fixed $\tau 1 = 125$ ps (p-Ps self-annihilation lifetime) and $3I1 = I3' + I4$, gave for the relative intensity of the longest lifetime component I4 value, which is only about 3% lower than I3 and both have the same variation with Dγ. Due to that the results for three-component decomposition of lifetime spectra will be discussed further. As it is known, [23] and references therein, the o-Ps intensity I3 in non-polar polymers changes during the lifetime measurements. This is ascribed to the creation and disappearing of such species, produced by the injecting positrons themselves, which can inhibit the Ps formation. In the present study we did not observed any systematic variation of I3 during two days of measurements of a given sample. The average values of τ3 and I3 as functions of irradiation dose Dγ are presented in fig.7.

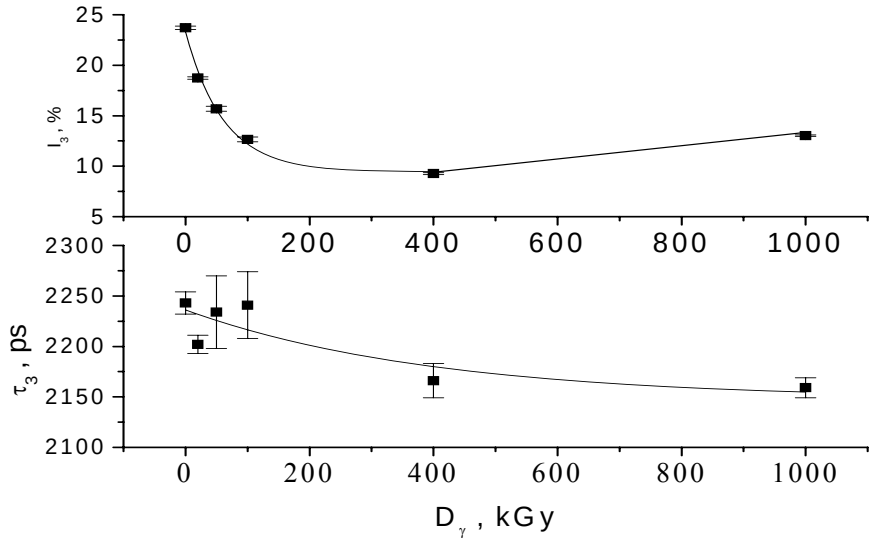

FIG. 7. O-Ps lifetimes τ3 and their relative intensities I3 versus irradiation dose Dγ

The o-Ps lifetimes τ3, and as a consequence the fvh volumes, change in very narrow limits (~5-6 %). At doses Dγ≤100 kGy the o-Ps lifetime is almost unchanged and after that decreases with the increase of the irradiation dose.

The temperature of measurement, RT, is above the glass transition temperature Tg, of iPP. So, the free-volume holes in the present case are not only of static but also mainly of dynamic nature type [4]. The fvh sizes above Tg depend on mobility of polymer macromolecules. In principle, the two major processes – chain scission and cross-linking, going into polymers upon γ-irradiation influences the molecular mobility. The scission facilitated mobility, while the action of cross-linking is twofold. From one side cross-linking hinder the molecular mobility, but on the other side, connecting two adjacent macromolecules in some fixed points, some additional static room may be created.

Having in mind the discussion connected with microhardness, we consider that the τ3 decreasing for Dγ >100 kGy is due to not very strong γ-induced cross-linking.

The o-Ps intensity also decreases with dose increase and its variation is considerable (relative change ca 60%). The o-Ps intensity may be considered as a measure of fvh concentration if polymer does not contain Ps-quenching functional groups. The decrease of I3 is ascribed to the crosslinking in the depth of the irradiated samples. Due to their considerable mean energy, positrons do not probe the nearest undersurface area. This interpretation of the I3 behavior with dose increasing is consistent with the MHV change in the depth of samples (fig.5a) and the o-Ps lifetime decrease (fig.7).

As fvh are localized mainly in amorphous phase, I3 should be inversely dependent on the degree of crystallinity, i.e. will decrease when Xc increases. Such linear dependence has been observed many times (see for instance ref. [24]). In the present case o-Ps intensity I3 as function of (1-Xc) is presented in fig.8.

It is clearly seen that although I3 increases with the increase of the amount of the amorphous phase, there is an inverse response of I3 to (1- Xc) at Dγ =100 kGy. Besides, for doses Dγ=4.102 and 103 kGy, although I3 increases with (1-Xc) increase, its values are lower than those following as consequence from I3 =f (1-Xc) for Dγ≤100 kGy.

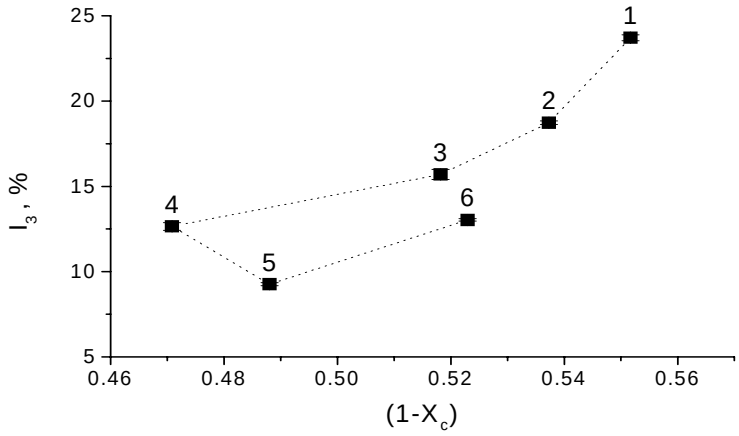

FIG. 8. O-Ps relative intensity I_3 versus $(1-X_c)$

It is interesting to compare the behavior of $I_3 = f(1-X_c)$, MHV variation with X_c (fig.3a) and X_c dependence on D_γ (fig.1). The o-Ps intensity I_3 depends on fvh concentration. In polymers the fvh are localized mainly in amorphous phase. According to [25] a two phase model (crystalline and amorphous phases) of semicrystalline polymers is a too big simplification. A three-phase model, which includes the crystal/amorphous interface is more reliable. So, I_3 variation follows the change of both- full amount of amorphous phase and the quality and quantity of the crystal-amorphous interface. According to [26] the γ-irradiation of poly(ethylene oxide) with doses up to 100 kGy influences mainly the lamellae surface. The explanation of changes, as mentioned, is based on the idea of pushing the irradiation defects out of the crystalline areas into the intermediate layers leading to an improvement of lamellae perfection. We suppose that such "radiation annealing" takes place also for iPP samples studied here, that show a prominent crystalline-amorphous boundary near to the fold area. So, the higher values of I_3 for $D_\gamma \leq 100$ kGy in comparison of those for $D_\gamma = 400$ and 1000 kGy is due to very "bushy" lamellae surfaces, abundant of free volume holes.

On the other hand, the values of MHV are determined from the integral amount of crystalline phase and do not depend on the structure of amorphous phase. Because of this, independently of the complex variation of X_c with D_γ all values of MHV (excluding $D_\gamma = 0$) lie on the same line.

4. CONCLUSIONS

The commercial isotactic PP, pristine and after 60Co γ-irradiation in air, has been studied using microhardness and Positron annihilation methods.

It was found that at irradiation dose Dγ = 100 kGy a clear inverse effect in iPP response to γ-radiation took place. The degree of crystallinity Xc, melting temperature Tm, as well the Vickers and total microhardnesses, all sharply change the trends of their variations at the same dose Dγ = 100 kGy.

The observed behavior was explained by the different response of iPP to low and high doses of γ-radiation. At low doses (Dγ ≤ 100 kGy) the prevalent effect of γ-radiation is "radiation annealing" of crystallites and formation of a prominent crystalline-amorphous boundary near to the fold area. At higher doses the main effect is "radiation melting", accompanied by the creation of a lot of damages into the material (Dγ > 100 kGy), and α-β polymorphic transition (Dγ ≥ 50 kGy).

The complicated dependence of the relative o-Ps intensity on degree of crystallinity was ascribed to the supposition that γ-irradiation of PP with doses up to 100 kGy influences mainly the lamella perfection and surface. The explanation of changes is based on the idea of pushing the irradiation defects out of the crystalline areas into the intermediate layers that leads to improvement of both lamellae and their fold surface perfectness.

REFERENCES

[1] B. LOTZ, J. WITTMANN, A. LOVINGER, Polymer 37 (1996) 4979
[2] S.MEILLE, D.FERRO, S.BRÜCKNER, A.LOVINGER, F.PADDEN, Macromolecules 27 (1994) 2615
[3] J.VARGA, J Macromol Sci B41 (2002) 1121
[4] F.J.BALTA-CALLEJA, Principals of polymer structure and morphology, NATO ASImeeting "Structure Development in Processing for Polymer Property Enhancement", Caminha, Portugal, (May,1999)
[5] Y.C.JEAN, Materials Science Forum 175-178 (1995) 59
[6] W. WANG, M. KONTOPOULOU in: Advances in Materials and Processes in Rotomolding, SPE/RETEC, Cleveland OH June 2002, Rotational molding of TPOs containing polyolefin plastomers
[7] N.DJOURELOV, M.MISHEVA, J. Phys. Cond. Matter, 8 (1996) 2081
[8] P.KIRKEGAARD, M.ELDRUP, O.E.MOGENSEN AND N.J.PEDERSEN, Comp. Phys.Comm., 23 (1981) 307
[9] R.GREGORY , J. Appl. Phys., 70 (1991) 4665,
[10] R.GREGORY,Y.ZHU, Nucl. Instr. Methods A, 290(1990)172
[11] M. ELDRUP, D. LIGHTBODY, J. N. SHERWOOD, Chem. Phys. 63 (1981) 51
[12] S. J. TAO, J. Chem. Phys. 56 (1972) 5499
[13] H. NAKANISHI, S. J. WANG, Y. C. JEAN, in: "Positron Annihilation studies of fluids",S. C. Sharma, Ed., World Scientific, Singapore 1988, p. 292
[14] A.VALENZA, S.PICCAROLO, G.SPADARO, Polymer 40 (1999) 835
[15] S.TSVETKOVA, E.NEDKOV, Radiat Phys Chem 43 (1994) 397
[16] A.KELLER, G.UNGAR, P.GRABB, Rad Phys Chem 22 (1983) 849
[17] M.L.SERRADA, E.PEREZ, C.ALVAREZ, A.BELLO, R.BENAVENTE, J.M.PERENA, in:Controlling of degradation effects in radiation processing of polymers, internal report of the 1st RCM of the CRPF2.20.39 held in Vienna, 8-11 December 2003, p.137
[18] F.J.BALTA-CALLEJA, J.MARTINEZ-SALAZAR AND D.R.RUEDA, Encyclopedia of Polymer Sciences and Engineering, vol 7 (1978) p 614
[19] Encyclopedia of polymer science and engineering, vol.4, 1986, Lohn Willey & Sons
[20] Y.C.JEAN, Macrochemical Journal 42 (1990) 72
[21] H.A.HRISTOV, B.BOLAN, A.F.YEE, L.XIE, D.W.GIDLEY, Macromoleculs 29 (1996) 8507
[22] L.XIE, D.W.GIDLEY, H.A.HRISTOV, A.F.YEE, Polymer 35 (1994) 14
[23] T.SUZUKI, K. KONDO, E.HAMADA , Y.ITO, Acta Physica Polonica A99 (2001) 515
[24] L.BRAMILLA, G.CONSOLATI, R.GALLO, F.QUASSO, F.SEVERINI, Polymer 44 (2003) 1041
[25] G.DLUBEK, J.STEJNY, T.H.LUPKE, D.BAMFORD, K.PETTERS, C.H.HUBNER, M.A.ALAM, M.J.HILL, J.Pol.Sci. B40 (2002) 65
[26] E.NEDKOV , S.TSVETKOVA, Rad.Phys.Chem. 44 (1994) 251]

POSITRON ANNIHILATION LIFETIME STUDY OF BIODEGRADABLE POLY(L-LACTIDE), POLY(DL-LACTIDE), POLY(L-LACTIDE-CO-DL-LACTIDE), AND POLY(DL-LACTIDE-CO-GLYCOLIDE), BEFORE AND AFTER GAMMA IRRADIATION

M.MISHEVA[1], N.DJOURELOV[2]
[1]Faculty of Physics, Sofia University, 5 J. Bourchier Boulevard, Sofia, Bulgaria
[2]Institute for Nuclear Research and Nuclear Energy, Bulgarian Academy of Sciences, Sofia, Bulgaria

Abstract

The sizes of subnanopores in biodegradable poly(L-lactide), poly(DL-lactide), poly(L-lactide-co-DL-lactide), and poly(DL-lactide-co-glycolide), pure and doped with calcium sulphate or hydroxyapatite were evaluated by measuring the positron lifetimes. The dependence between o-Ps lifetime and radius of the fvh, at which o-Ps is localized before annihilation was used. The change of sizes after gamma-irradiation of the samples with a dose of 12.5 kGy was observed. As could be expected, the doping lead to decreasing of pore sizes due to filling up of polymer largest pores with the small particles of the additives. The gamma-irradiation of the studied materials leads as a rule to increasing of the pore sizes through scissions and crosslinking of the polymer macromolecules.

1. INTRODUCTION

In the modern world the use, and hence the production of polymeric materials is expending continuously. Simultaneously, the amount of polymer wastes is increasing and the problem of its environmentally friendly destroying becomes very important.

One of partial solution of the problem is to produce and use, where it is possible, biodegradable polymers. Synthetic biodegradable polymers have been increasingly used as medical, pharmaceutical, agricultural and tissue-engineering products [1]. Among the different classes of synthetic biodegradable polymers, the thermoplastic aliphatic poly(esters) like PLA (polylactide), PGA (polyglycolide) and their copolymers (PLGA) have generated tremendous interest due to their favorable properties such as good biocompatibility, biodegradability, bioresorbability and mechanical strength. They possess processing facility, great variety, adaptability and reliability [2, 3].

The properties of the PLA, PGA and their copolymers make them the preferred materials for a variety of medical devices and pharmaceutical applications like tissue fixation, tissue regeneration, wound dressing, anti-adhesion and drug delivery systems. The drug- release depends on many factors [4], and among these composition, sterilization and porosity. One of the methods for studying subnanometer pores is Positron Annihilation lifetime (PAL) method.

The question of sterilization arises when the bio-erodable polymers are used as implants. The sterilization can be done by irradiation of materials with gamma-rays from a radioactive ^{60}Co source. Although for the bio sterilization a dose of 25 kGy has to be used, because of the danger to destroy the studied samples, we started with a smaller dose of 12.5 kGy.

In this contribution are presented the preliminary results about sizes of local subnanometre free-volume holes (fvh) in biodegradable poly(L-lactide), poly(DL-lactide), poly(L-lactide-co-DL-lactide), and poly(DL-lactide-co-glycolide), pure and doped with calcium sulphate or hydroxyapatite. The change of pore sizes due to gamma irradiation of these materials was also studied. The Positron Annihilation Lifetime (PAL) Spectroscopy has been applied for this study.

2. EXPERIMENTAL

2.1. Materials and methods

PLA is prepared from cyclic diester of lactic acid (lactide) by ring opening polymerization as shown in Figure 1A.

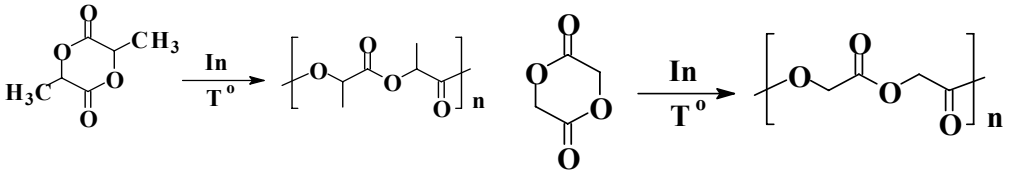

A. Lactide – Poly(lactide) B. Glycolide – Poly(glycolide)

*FIG. 1. Production of poly(lactide) (**A**) and poly(gycolide) (**B**).*

Lactic acid exists in two stereoisomeric forms that give rise to four morphologically distinct polymers. D-PLA and L-PLA are the two-stereoregular polymers, DL-PLA is the racemic polymer obtained from a mixture of D-PLA and L-PLA, and meso-PLA can be obtained from DL-lactide. PGA is prepared from the cyclic diester of glycolic acid (glycolide) by ring opening polymerization as shown in Figure 1B. Of this family of linear aliphatic polyesters, PGA has the simplest structure. Because PGA is highly crystalline, it has a high melting point (225-230 ºC) and low solubility in organic solvents. PGA has the strongest initially mechanical strength amongst PLA and their copolymers.

In order to adapt the materials properties of PGA to a wider range of possible applications, researchers undertook an intensive investigation of copolymers of PGA with more hydrophobic materials PLA.

For the formation of polymer implants one- and two socket metal forms were made. The compositions of polymer implants are presented in Table 1 and they are composed either from pure polymers or from polymers with additives. All used polymer products and additives are trade products. Polymer implants were formed through a mechanical mixing of the components, followed by placing the polymer mixture in the hollow square cross-section of the form and pressing with heating of the press plates. The used temperature of heating was little higher than the melting point of polymers and doxycycline in order to gain a homogeneous mixture by melting the components. The duration of pressing for all samples was 20 min and the used presser - 150 Bar. After cooling to room temperature, the formed implant was taken from the pressform and was placed in a sterile vessel.

The compositions of the studied polymer implants, their abbreviations and the temperature of pressing are given in Table 1.

Polymer implants from polyesters without and with additives were formed. The antibiotic – doxycycline was added in order to bring forward the healing and to reduce the risk of infections. The two other additives were used because they resemble the constructive elements of bones.

TABLE I. THE COMPOSITION OF THE STUDIED POLYMER IMPLANTS, THEIR USED ABBREVIATIONS, USED TEMPERATURE OF PRESSING AND FVH VOLUMES, V_P, CALCULATED THROUGH EQUATION (1).

No	Sample	Composition	Pressing temperature	V_p, Å^3 unirradiated
1	M1	Poly(L-lactide)	200°	81.5(9); 84.3(5)
2	M1CS	Poly(L-lactide) + $CaSO_4$	200°	87.1(5); 92.9(5)
3	M1HA	Poly(L-lactide) + $Ca_{10}(PO_4)_6(OH)_2$	200°	81.5(9); 84.3(9)
4	M2	Poly(DL-lactide)	100°	80.6(9); 91(1)
5	M2CS	Poly(DL-lactide) + $CaSO_4$	100°	82.4(9); 90(2)
6	M2HA	Poly(DL-lactide)+ $Ca_{10}(PO_4)_6(OH)_2$	100°	77.9(9); 88(1)
7	M3	Poly(L-lactide-*co*-DL-lactide) 70:30	210-215°	92.9(5); 87.1(9)
8	M3CS	Poly(L-lactide-*co*- DL-lactide) 70:30 + $CaSO_4$	210-215°	82.4(9); 90(2)
9	M3HA	Poly(L-lactide-*co*- DL-lactide) 70:30+ $Ca_{10}(PO_4)_6(OH)_2$	210-215°	79.7(9); 86.1(9)
10	M4D	Poly(DL-lactide-*co*-glycolide) 50:50+ Doxycycline	90-95°	67.8(8); 74.4(9)
11	M4CS	Poly(DL-lactide-*co*-glycolide) 50:50+ $CaSO_4$	90-95°	65.4(8); 75.3(9)
12	M4HA	Poly(DL-lactide-*co*-glycolide) 50:50 + $Ca_{10}(PO_4)_6(OH)_2$	90-95°	55.7(4);

2.2. Positron annihilation lifetime spectroscopy (PALS)

PALS is widely used for direct evaluation of the radii of free-volume holes (fvh) in different materials, including polymers [5]. The range of fvh volume probed by PALS is 0.2-2 nm. As pointed out by P.E.Mallon [6] PAL is the only method to probe small fvh with R ≈ 2 – 5 Å, where other techniques for examination of defects and voids in materials are not workable. PAL can probed both static and dynamic holes (longer than 10^{-10} s) in polymers.

The method is based on the behavior of a positron emitted from a radioactive source and ejected into some kind of matter. The mean energy of positrons emitted from the most often used source ^{22}Na is about 0.21 MeV. Soon after entering in condensed matter, the energetic positron spent its energy for ionization and excitation of the matrix atoms and in ca 10^{-12} s becomes thermalized (E_k ≈0.025 eV). The thermalized positron can annihilate as a free particle with a matrix electron with opposite spin within 120-300 ps. In result two 511 keV γ–rays, propagating in opposite directions were born;

It can be trapped in an open volume before annihilation. Obviously, the mean electron density there is lower than in the bulk that leads to a longer positron lifetime of the order of 300-500 ps, depending of the hole size. In molecular solids positron can catch an electron from its surroundings and to form a hydrogen-like atom called positronium (Ps). One quarter of the Ps atoms are in singlet state, para-positronium (p-Ps) with antiparallel spins of the electron and positron. The rest three quarters of Ps atoms are in triplet state, ortho-positronium (o-Ps) with parallel electron-positron spins. The self-annihilation lifetime of para-, and ortho-Ps in vacuum are 0.12 and 140 ns, respectively. In matter positron from o-Ps atom may annihilate with a medium electron instead of with its own partner, the so-called pick-off process. In polymers o-Ps tends to be trapped in fvh, localized in amorphous parts. The lifetime, $\tau_{o\text{-}Ps}$, of o-Ps there depends on the size of the hole.

If the fvh is approximated with an infinite spherical potential of radius R with an electron layer of thickness ΔR [7, 8] the relationship between R and $\tau_{o\text{-}Ps}$ is given by

$$\tau_{o-Ps} = 0.5\left[1 - \frac{R}{R_0} + \frac{1}{2\pi}\sin\left(\frac{2\pi R}{R_0}\right)\right]^{-1};$$

Where: [R]= Å; [$\tau_{o\text{-}Ps}$]=ns.

In this equation $R_0 = R + \Delta R$, and ΔR=1.656 Å is empirically found by measuring the $\tau_{o\text{-}Ps}$ in samples containing fvh with known radii [8]. So, the essence of the PAL method for evaluation of fvh volume is the following: measurement of o-Ps lifetime $\tau_{o\text{-}Ps}$, calculation by equation (1) of the pore radius R and volume $V_P = \frac{4}{3}\pi R^3$. Obviously, as the pore shape may not be spherical and hole sizes have always some extend distribution, the so obtained values of volume V_p are average ones.

Below the glass-transition temperature T_g, i.e. in the glass state of a polymer, for an o-Ps atom the polymer structure appears as "frozen-in" and o-Ps lifetime reflects the geometrical size of the local fvh at the moment of annihilation. This is the present case, as the room temperature of measurements is below T_g of the studied materials.

The lifetime spectrometer was a standard fast-fast coincidence system. It provides a time resolution ~ 280 ps Full Width at Half Maximum (FWHM). The polymer samples represent plates of 1.6-1.9 mm thickness. The positron source prepared by ^{22}NaCl solution evaporated on and covered by 1 mg/cm^2 Kapton foils was sandwiched between the studied sample and an Indium (In) plate. As a rule four lifetime spectra were recorded for each sample. Corrections for positrons annihilating in the source and in In plate were made according to [9]. The experimental spectra were fitted with a model, assuming the existence of a few discrete positron lifetimes in the samples with the program PATFIT [10]. The presented values for lifetimes τ_i and their relative intensities I_i represent weighted-mean values over four measured spectra. All measurements were made at room temperature in an air-conditioned laboratory.

3. RESULTS AND DISCUSSION

Usually the positron lifetime spectra of polymers, including semicrystalline ones, are fitted into three components. The first one τ_1 is interpreted as a weighted average of two contributions: $\tau_1' = 125$ ps due to self-annihilation of p-Ps, and $\tau_1'' > \tau_1'$, due to annihilation of free positrons in the bulk of the sample [11]. The second lifetime, τ_2 is attributed to annihilation of positrons trapped before annihilation at low electron density sites in more ordered parts of the matrix. As usually, the third lifetime component, τ_3, is associated with o-Ps pick-off annihilation at f.v.h. sites, localized in amorphous regions. In the present case the 3-term decomposition of the four lifetime spectra, collected for every one studied material, gave for positron annihilation parameters values, which scatter in a fairly large interval. This means that the studied samples are not very homogeneous ones. For this reason, and taking into account that only the longest lifetime $\tau_{o\text{-}Ps}$ is sensitive to the structural changes [12], we made two-component decomposition of the spectra. The mean lifetimes $\tau_m = \sum_{i=1}^{N} \tau_i I_i$, for N=2 and 3 are the same in error limits. The lifetime $\tau_2 \equiv \tau_{o\text{-}Ps}$ is used further.

The volumes of pores, calculated through o-Ps lifetimes τ_2 are shown in Table I. As it is known, the o-Ps intensity $I_{o\text{-}Ps} \equiv I_2$ in a unpolar polymer changes during the lifetime measurements [13], and references there in, because of the creation and disappearing of such species, produced by the injecting positrons themselves, which can inhibit the Ps formation.

In the present study we did not observed any systematic variation of I_2 (or of I_3) during measurements of a given sample. In some cases [6] the o-Ps intensity may be considered as a measure of fvh concentration if polymer does not contain Ps-quenching functional groups. In the present case however, surfaces of some of the samples are not sufficiently large to cover in excess the spot of dry ^{22}NaCl, and some of positrons might annihilate in Indium plates. So, while the values of lifetimes are reliable, there exists some uncertainty about I_2. Because of this we will comment only the size but not the concentration of fvh. The obtained o-Ps lifetimes and their relative intensities are presented in different combinations in figures from 1 to 3.

The fvh radii, R, for pure samples M1 and M2 are the same in error limits, while R for M3 is about 10 % higher. The M4D can't be considered as pure Poly(DL-lactide-*co*-glycolide) (PDLLG), as it is doped with doxycycline. The content of latter is about 29 wt %. The mean pore radius in M4D is about 10% lower than in M1. The reason is that M4D is a real solution between PDLLG and the drug and doxycycline particles fill in the largest pores.

Gamma-rays leads to structural changes such as chain scissions and crosslinking in irradiated polymers. The former process creates new macromolecular ends and therefore new and/or larger fvh. The crosslinking, connecting two adjacent macromolecules in some fixed points, may create some additional static room in the amorphous parts. So, irrespective of which process took place, it should be expected that the size of fvh will increases after gamma irradiation of the studied materials. As seen from fig.2 this is the present case for all polymers but M3. It is not clear the reason for this deviation.

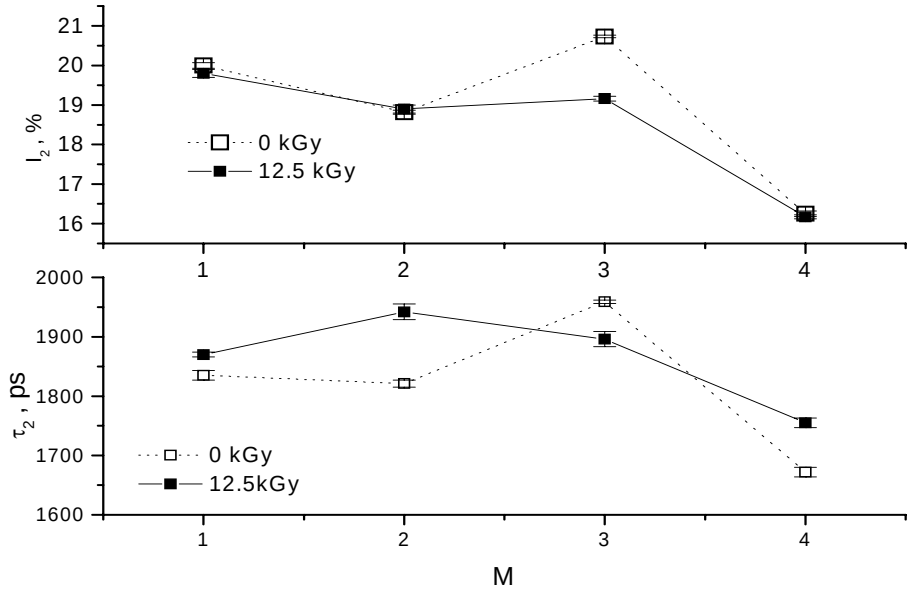

FIG. 2. Ortho-positronium lifetimes τ2, a measure of fvh size, and their relative intensities I2 for pure samples before and after gamma irradiation. The lines are only to guide the eyes.

The introducing of $CaSO_4$ into the studied polymers influence the fvh sizes in a various way – fig.3. The size of fvh for M1 increases, while the opposite is observed for M3. The pore radii for pure and doped M2 and M4 samples underwent a little change. The gamma irradiation of all studied materials, doped with $CaSO_4$ leads to expected increase of pore sizes.

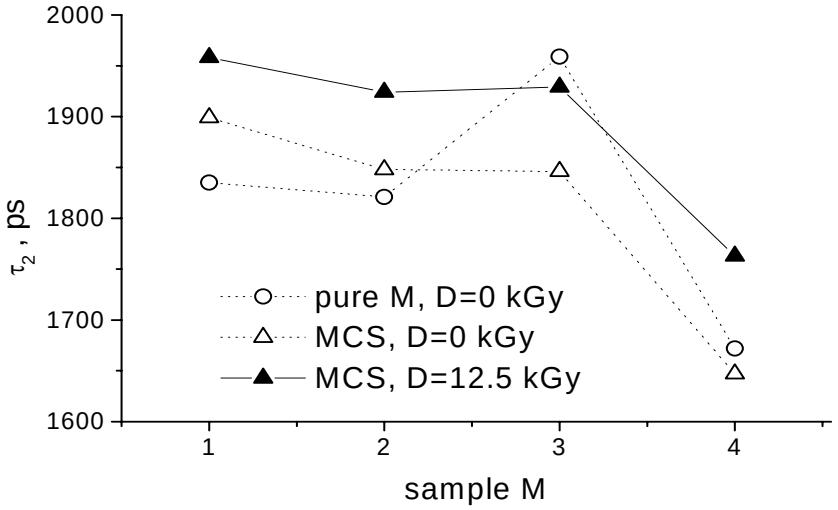

FIG. 3. The same as in figure 1 for pure samples and samples, doted by $CaSO_4$, before and after gamma-irradiation.

The influence of polymer doping with $Ca_{10}(PO_4)_6(OH)_2$ can be seen in fig.4. The doping of the studied polymers with $Ca_{10}(PO_4)_6(OH)_2$ leads to pore size decreasing. This can be explaind if supposing that the small particles of the hydroxyapatide filled up the largest pores in the polymer matrix. The change of R is smallest for M1HA polymer, and the largest for M3HA and M4HA samples. The gamma irradiation increases the pore sizes in all the doped samples. At that, the increasing is highest for M4HA.

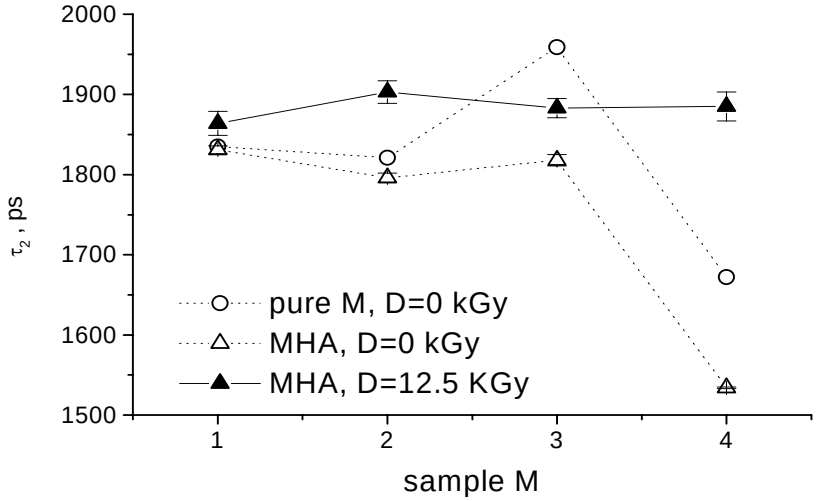

FIG. 4. The same as in figure 1 for pure samples and samples, doted by hydroxyapatide, before and after gamma-irradiation.

4. CONCLUSIONS

The sizes of subnanopores in biodegradable poly(L-lactide), poly(DL-lactide), poly(L-lactide-co-DL-lactide), and poly(DL-lactide-co-glycolide), pure and doped with calcium sulphate or hydroxyapatite were evaluated by measuring the positron lifetimes. The dependence between o-Ps lifetime and radius of the fvh, at which o-Ps is localized before annihilation was used. The change of sizes after gamma-irradiation of the samples with a dose of 12.5 kGy was observed.

As could be expected, the doping lead to decreasing of pore sizes due to filling up of polymer largest pores with the small particles of the additives. The gamma-irradiation of the studied materials leads as a rule to increasing of the pore sizes through scissions and crosslinking of the polymer macromolecules.

More general conclusions of the presented preliminary results are not possible. It should be interesting to compare the obtained results from the present study with other characteristics of the same materials, and/or the rate of drug release from them.

REFERENCES

[1] T. HAYASHI, Prog. Polym. Sci., 19 (1994) 663

[2] K-U. LEWANDROWSKI, D.L. WISE, D.J. TRANTOLO, J.D. GRESSER, M.J. YASZEMSKI, D.E. ALTOBELLI, eds., Marcel Dekker, Inc., N.Y. 2002. Chapter 6, p.111

[3] L. LU, S.J. PETER, M.D. LYMAN, H. LAI, S.M. LEITE, J.A. TAMADA, J.P. VACANTI, R. LANGER, A.G. MIKOS, Biomaterials 21 (2000) 1595

[4] F.ALEXIS, Pol.Int. 54, no1 (2005) 36

[5] Y.C.JEAN, Material Sci.Forum 175-178 (1995) 59-

[6] P.E.MALLON, In: Principles and Applications of Positron & Positronium Chemistry, Eds.:Y.C.Jean, P.E.Mallon and D.M.Schrader, World Sci.Press, Singapore, 2003, p.253

[7] M.ELDRUP, D.LIGHTBODY, J.N.SHEROOD, Chem.Phys. 63 (1981) 51;

[8] H.NAKANISHI, S.J.WANG AND Y.C.JEAN, In: Positron Annihilation Study of Fluids, Ed S.C.Sharma (Singapore:World Scientific), 1987, p 292

[9] N.DJOURELOV, M.MISHEVA, *J.Phys.: Cond.Matter* **8 (**1996) 2081

[10] P.KIRKEGAARD, N.J.PEDERSEN, M.ELDRUP 1989 *PATFIT-88, Riso-M-2740*

[11] H.A.HRISTOV, B.BOLAN, A.F.YEE, L.XIE, D.W.GIDLEY, Macromoleculs 29 (1996) 8507

[12] T.GOWOREK, K.CIESIELSKI, B.JANINSKA, J.WAWRYSZCZUK, Chem.Phys. 230 (1998) 305

[13] T.SUZUKI, K. KONDO, E.HAMADA , Y.Ito, Acta Physica Polonica A99 (2001) 515

ANALYSIS OF PLASMA POLYMERS AND CONVENTIONAL POLYMERS MODIFIED BY VARIOUS TECHNIQUES.

H. BOLDYRYEVA, A. MACKOVA
Nuclear Physics Institute AS CR, Rez, Czech Republic

Abstract

In this paper the summery of the most recent research activities of our laboratory are presented. The research is performed at Nuclear Physics Institute of Academy of Science of the Czech Republic. There are three topics will be discussed: 1) diffusion of Ag and Cu atoms in polyethyleneterephtalate (PET) and polyimide (PI); 2) implantation of PET, PI and poly(ether ether ketone) (PEEK) with Ar^+ and $^4He^+$ ions; 3) investigation of plasma polymers and their composites. To determine the composition and elements depth distribution of studied samples Rutherford Backscattering Spectroscopy (RBS) and Elastic Recoil Detection Analysis (ERDA) were employed. X ray Photoelectron Spectroscopy (XPS) was used for determination of metal-polymer interaction and chemical state of atoms.

1. INTRODUCTION

The diffusion of Cu and Ag in PET and PI is examined using different methods with the aim to shed more light onto the diffusion mechanism. Wide range of applications of metallized polymers [1] in microelectronics has stimulated research of metal-polymer interaction. Polyimide encompassing low dielectric constant, high temperature and radiation stability, therefore it is candidate for fabrication of multilayer metallization structures on the chip level and for packaging. It has been observed that the microstructure and hence the mechanical and dielectric properties of the metal-polymer interface is strongly affected by the degree of metal-polymer diffusion and intermixing [2]. Thus there is a basic need to understand the mechanism of metal diffusion in polymers and its effects on the structure and formation of metal-polymer interface. The diffusion depends on physical and chemical properties of metal and structure of the polymer as well. Cu and Ag for example exhibit higher mobility in polymers in comparison with Cr or Ti [3]. The samples were prepared by deposition of Ag and Cu thin layers on polymer surface using CVD and diode sputtering techniques, and then samples were annealed at temperatures up to 240°C.

High fluence ion implantation of polymers is of interest for fundamental reasons and for potential applications of irradiated polymers in microelectronics, opto-electronics and medicine as well. However, ion irradiation of polymers is accompanied by radiation-induced effects changing drastically structure and properties of irradiated material [4]. In this topic of investigation, PET was implanted with 150 keV Ar^+ ions to the fluences of 10^{12}-10^{15} ions/cm^{-2}, PET, PEEK and PI with 1,76 MeV $^4He^+$ ions to the fluences 10^{13}-10^{14} ions/cm^{-2}. Structural and compositional alterations of the implanted polymers were studied. The ion irradiation leads to degradation of polymeric chains, chemical bond cleavage, creation of free radicals and release of gaseous degradation products [5]. Subsequent chemical reactions of transient highly reactive species results in creation of excessive double bonds [6], production of low mass stable degradation products, large cross-linked structures [7] and eventually oxidized structures [8].

Composite Ag/CH coatings and amine rich plasma polymer films were investigated. Polymers containing silver are known for their antibacterial properties [9] and amine plasma polymers are applied for the development of acoustic wave sensors [10], microfiltration membranes [11] or enzyme electrodes. Several techniques can be applied for the composition study of thin polymer films, among them XPS is most frequently used. But because limitations essential to these methods leave some information unrevealed, the application of such non-destructive techniques as RBS and ERDA for the estimation of the element composition and depth profiling in plasma polymers is very favourable.

2. EXPERIMENTAL

2.1.Diffusion of Ag and Cu atoms in PET and PI

The samples were prepared by deposition of thin Cu and Ag layers on polypyromellitimide (PI, $C_{22}H_{10}N_2O_5$, ρ=1,43g.cm^{-3}) and PET is the polyethylenetereftalate (PET, $C_{10}H_8O_4$, ρ=1,397 g.cm^{-3}.). Cu and Ag layers with typical thickness less than 10 nm were deposited using CVD or diode sputtering (BAL-TEC, SCD 050 system) techniques on polymer substrates. The deposition was performed at room temperature and temperatures close to polymer glassy transition temperatures (T_g= 360°C and 76°C for PI and PET, respectively). In the case of diode sputtering (RT, total argon pressure about 4 Pa, the electrode distance 50 mm and current 20 mA), deposition times were 50 and 80 s. Annealing conditions are summarized in the Table I. The annealing was performed on air atmosphere in small annealing furnace.

TABLE I. DEPOSITION AND ANNEALING CONDITIONS FOR CVD AND DIODE SPUTTERING AG AND CU FILMS DEPOSITED ON PI AND PET SUBSTRATES.

Polymer substrate—deposition-metal	Deposition temperature, [ºC]	Annealing temperature, [ºC]
PI-CVD-Ag	250	80
		160
		240
PI-Sputtering-Ag	RT	80
		160
		240
PET-CVD-Ag/PET-Sputtering-Ag (50s, 80s)	RT/RT	60/50
		80/70
		120/80
PI-CVD-Cu	230	80
		160
		240

Metal concentration depth profiles we obtained from RBS spectra (2.2 MeV He ions, 170° laboratory scattering angle). ERDA measurement was performed with 2.7 MeV He ions and the protons recoiled under the angle of 30^0 were registered. Measurements of photoelectron spectra were carried out on an angular-resolved X-ray induced photoelectron spectrometer ADES-400 (VG Scientific) using Mg Kα radiation (1253.6 eV) and a rotable hemispherical energy analyser. The spectra were recorded at normal emission angle except those recorded for quantitative analysis where both normal and 60° emission angles were used. The energy positions were referenced to the Cu 2p peak at 932.6 eV and Au 4f peak at 84.0 eV binding energy. Atomic concentrations were determined from XPS peak areas corrected for photoelectron cross-sections, the inelastic mean free paths, and experimentally determined transmission function of the energy analyzer. In a control experiment the Ag continuous surface layer was removed by 96% ethylalcohole solution and, after this treatment, the XPS measurement was performed again.

2.2.Degradation of PET, PEEK and PI induced by implantation with Ar^+ and $^4He^+$ ions

Three kinds of polymers were studied: polyimide (PI), poly(ethylene teraphthalate) (PET), and poly(ether ether ketone) (PEEK). All of the pristine materials were in the form of 12-μm-thick foils. A series of samples includes PET films implanted by 150 keV Ar^+ ions to different fluences as given in Table II. Another series of samples include PET, PEEK, and PI irradiated by 1.76-MeV $^4He^+$ ions (see Table II).

The projection ranges were calculated by the TRIM computer code, being R_p = 200 nm, as well as the range straggling, ΔR_p = 37 nm, and R_p ~ 7500 nm, ΔR_p ~ 260 nm, for the implanted Ar^+ ions and for He^+ ions, respectively.

TABLE II. SAMPLE'S LABELS, TYPE OF IMPLANTATION, AND FLUENCE.

Fluence (ions/cm^2)	Series 1: implanted by 150-keV Ar^+ ions	Series 2: implanted by 1.76-MeV He^+		
pristine	PET^0	PET^0	$PEEK^0$	PI^0
1×10^{12}	PET_1			
1×10^{13}	PET_2	PET^2	$PEEK^2$	
3×10^{13}	PET_3	PET^3	$PEEK^3$	
1×10^{14}	PET_4	PET^4	$PEEK^4$	PI^4
1×10^{15}	PET_5			

The implantation of 12μm thick PET foil was performed at Van de Graaff accelerator in NPI Rez by the 1.76MeV He^+ ions in vacuum chamber. The Ni-foil monitor was removed during this measurement and the implanted dose was controlled by the RBS spectra signal height. RBS and ERDA analyses were used to determine the H, C and O amount changes after degradation procedure. The RBS spectra were evaluated using the computer code GISA 3 [12]. The RBS measurements were performed under 170° laboratory scattering angle. The glancing geometry ERDA measurement with 2.68 MeV alpha particle beam was performed to obtain hydrogen depth profile, recoiled protons were registered under the angle of 30^0 with a surface barrier detector covered with 12 μm thick Mylar stopping foil.

The concentration of conjugated double bonds, created on polymer molecular chain by ion irradiation, was determined by UV-VIS spectroscopy in a 150-800 nm wave interval using a Perkin-Elmer device [13]. A pulsed slow-positron beam [14], with a FWHM of about 600 ps, was used. Short-gated (25 ns) positron annihilation lifetime (PAL) spectra were collected for different incident positron energies up to 9 keV. Each spectrum was measured for 1 hour with the total counts being ~ $1.5x10^6$. POSITRONFIT program was used to analyse the PAL spectra. The analysis was performed by two components, because the two short-lived components (~ 0.15 ns and ~ 0.4 ns) of a three-component analysis, usually seen by conventional PAL spectroscopy, cannot be separated for the PAL spectra measured by the beam technique because of the poor time-resolution. The long-lived component is due to pick-off annihilation of orto-positronium (o-Ps) and o-Ps lifetime is correlated with the size of the free-volume holes, while the corresponding intensity has been found to be influenced by many factors, such as the temperature, irradiation, electric field, and polar groups and cannot be used directly as a quantity expressing the concentration of the free-volume holes [15].

2.3. Plasma polymers and their composites

Two sets of the samples were investigated. The first one - plasma polymerized diaminocyclohexanelayers (DACH) and the second one - Ag:C:H composite layers on the silicon substrate. Amine containing plasma polymers were deposited by Plasma Enhanced Chemical Vapour Deposition (PECVD) of diaminocyclohexane (DACH, 5 Pa, 0.85 cm3/min) in a tubular reactor with capacitively coupled ring electrodes (13.56 MHz). The experiments were performed in continuous wave (CW) and pulse mode (duty cycle 0.1). The average power was varied between 2 and 30 W. Composite Ag/CH films were prepared by DC magnetron sputtering of silver target in a mixture of Ar and n-hexane. The flow rate of the gases was varied independently to achieve different Ar/n-hexane ratios, but the total flow rate (7.7 cm3/min) and the pressure of gas mixture (2 Pa) were held constant. The deposition was performed at 0.1 A current; the deposition time was 5 min for each sample. The variation of Ar/n-hexane ratio allows to control the film composition: the lower values result in low concentration of Ag in C:H matrix, while the higher ones lead to nearly metallic silver coatings.

The RBS and ERDA analyses of prepared samples were performed in vacuum target chamber using the 2.745 MeV alpha particle beam and 2.4 MeV proton beam. The ion beam was provided by electrostatic accelerator. The RBS and ERDA techniques, based on elastic scattering of charged particles, enabled us to determine the content and depth profiles of C, H, N and Ag elements with the sensitivity from 10^{11} - 10^{15} atoms/cm^2. The RBS measurement with 2.745 MeV alpha particles gives us more accurate information about Ag depth profile in the deposited layers. We can distinguish non-homogeneous distribution of Ag within the deposited layer due to the better depth resolution in the backscattered alpha particle spectra. Also we obtain the information about the thickness of the deposited layers. The accuracy of RBS amount determination is in the range of 2 atomic %. Hydrogen depth profiles could be determined non-destructively to the depth of 5μm with a typical depth resolution of 50 nm by ERDA. Spectra were evaluated by SIMNRA5.0 [16]. The accuracy of the H determination is in case of the samples deposited on silicon substrates in the range of 5 atomic %.

3. RESULTS AND DISCUSSION

3.1.Diffusion of Ag and Cu atoms in PET and PI

Annealing at higher temperatures may leads to degradation of the polymer substrate accompanied with emission of volatile, hydrogen or oxygen rich degradation products. This effect was examined by RBS and ERDA techniques and no compositional changes were observed. Concentration depth profiles of diffusing metal atoms were determined from RBS spectra. On PET-Ag samples surface concentration decrease and deeper Ag penetration with increasing annealing temperature is observed. Diffusion coefficients for deposition times 50s and 80s were determined using standard procedure from the plot of ln (concentration) vs. depth [3]. Arrhenius plot for diffusion of Ag deposited by two deposition techniques and for different times are shown in Figs. 1a and 1b. Diffusion coefficients of Ag atoms on Ag-PET samples prepared using diode sputtering are by one order of magnitude higher than those on the samples prepared using CVD technique. Diode sputtering enables one to prepare metal layers with low thickness facilitating high inward mobility of metal atoms. Higher diffusion coefficients are also observed for Ag layers deposited for 50 s in comparison with those deposited for 80s (see Fig. 1a).

In the XPS spectra (Fig. 2) the main part of C1s peak C-C doesn't change its position; small uncertainty is connected with corrections on sample charging during XPS measurement. Most significant reduction of the C=O peak is observed for annealing temperature 70°C for both deposition times 50s and 80s (see Fig. 2). The data indicate that at the temperature 70°C a perturbation of C=O bond takes place . On the samples prepared by diode sputtering for 50 s, Ag fraction measured by XPS after removing a continuous Ag surface layer decreases significantly with annealing temperature. It indicates the higher depth incorporation of Ag atoms as is referred in [17]. Low difference between Ag fraction XPS measured under the angles 0° and 60° indicates higher compactness of Ag layer deposited for 80 s, in comparison with the layer deposited for 50s. The fact that XPS spectra of above mentioned Ag/PET samples showed the shift of the Ag binding energy of 0.5 eV relatively to the bulk Ag layer (368,4 eV) is another evidence of the presence of Ag clusters see Fig. 2. Most significant shift of Ag binding energy is observed for annealing at the temperature of 70°C. Arrhenius plots of Ag and Cu in PI deposited by CVD at RT and 250°C are presented in the Figs. 3a, b. Diffusion coefficients of Ag CVD deposited at RT on PET (Fig. 1b) are , at comparable annealing temperature, about twice higher than those for Ag deposited under the same conditions on PI (Fig. 3b). This is in accordance with expectation because of higher density of PI. Increase of the deposition temperature from RT to 250°C leads to significant decline of Ag diffusion coefficient in PI (Fig.3b). Under the similar deposition conditions, diffusion coefficients of Cu in PI are nearly one order of magnitude higher than those of Ag. This can be due to a smaller diameter of Cu atoms and in turn to their higher mobility in comparison with Ag atoms. Present diffusion coefficients for Ag in PET and PI are comparable with those reported for Ag in BPA-PC (bisfenol-A-polycarbonate) in [18] or Ag in photoresist AZ1350-J (C6,17H6O1N0,14S0,063) [19].

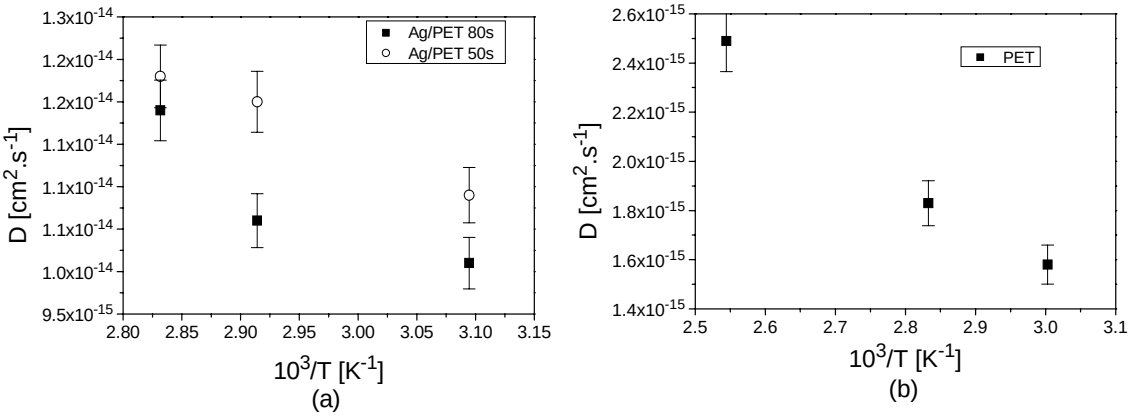

FIG. 1. a) Arrhenius plot of Ag deposited by diode sputtering at RT on PET substrate – deposition time 50 s and 80 s . b) Arrhenius plot of Ag deposited by CVD at RT on PET substrate.

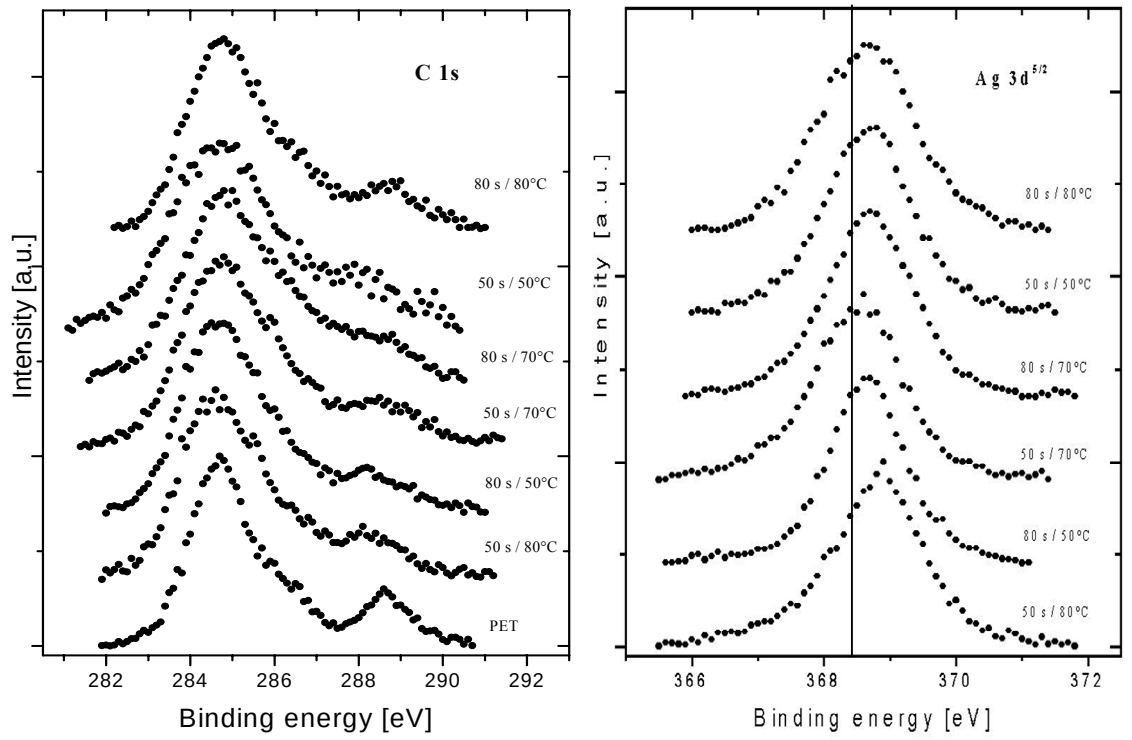

FIG. 2. XPS C1s and Ag 3d $^{5/2}$ spectrum recorded from Ag deposited by diode sputtering for 50s and 80s at RT on PET substrate. The vertical line follows binding energy of bulk Ag layer (368,4 eV).

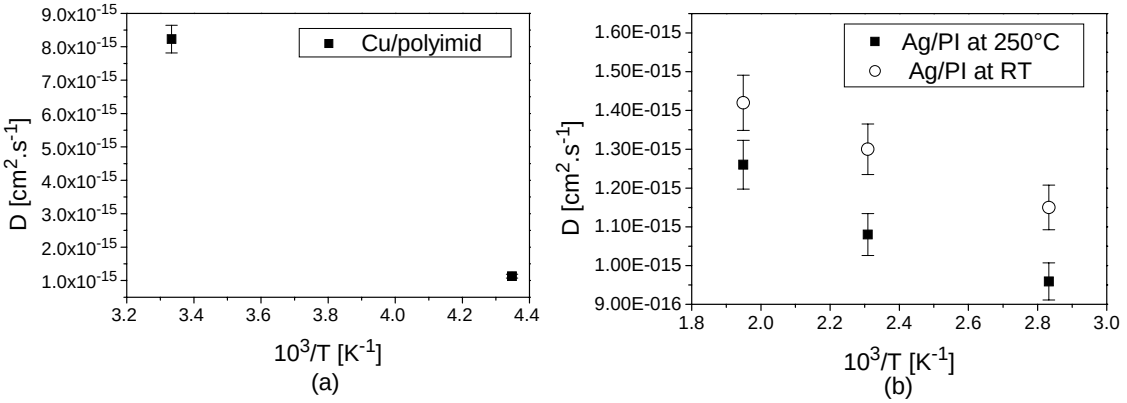

FIG. 3. a) Arrhenius plot of Cu deposited by CVD on PI substrate at 230°C b) Arrhenius plot of Ag deposited by CVD on PI substrate at RT and 250°C.

3.2.Degradation of PET, PEEK and PI induced by implantation with Ar+ and 4He+ ions

Length and concentration of conjugated double bonds, which are products of polymer degradation, can qualitatively be determined by UV-VIS spectroscopy. UV-VIS spectra from pristine PEEK and PET and irradiated polymers with ^{4}He+ ions are shown in Fig. 4 a,b. It is evident that with increasing ion fluence the concentration of free radicals, broken/exited bonds on polymer or even and length of the double bonds increases and absorbency is increased dramatically in the case of highest dose irradiated PET (the sample PET4 - $1x10^{14}$ ions/cm^2). For better understanding probably further measurements, such as FTIR spectroscopy, are needed. PET exhibits higher irradiation sensitivity in comparison with PEEK. Polymer foils irradiated by Ar^+ ions exhibit the increasing UV-VIS absorbency in dependence on increasing ion dose too (see Fig. 5b). Positron annihilation analysis (not presented here) showed that the set of samples irradiated by 1,76 MeV $^4He^+$ ions does not exhibit any changes in the free-volume holes (size or concentration) in the subsurface 1 micron layer, which is the detectable range for the 9-keV positrons in PET, PEEK and PI. Thus, for the layer probed by positrons the interaction between the alpha particles and the constituent atoms is negligible.

Fig. 5a shows the o-Ps (type of positron state) lifetime and intensity as a function of the incident positron energy for the Ar^+ ions implanted PET. It is clearly seen that the o-Ps lifetime decrease slightly from the surface to the bulk. This effect is observed in many polymers and is explained by the enhanced polymer chain mobility near to the surface. The change in the o-Ps intensity with the fluence is clear seen (Fig. 5a), however it is very difficult to extract any conclusion for possible change in the free-volume hole concentration. First, it may be explained by filling of the fraction of the free-volume holes by Ar-ion, and, second, effect of increased concentration of free radicals and ions formed in the damaged layer due to the irradiation. We also see decrease of positronium lifetime in the depth appropriate Ar^+ ions range, which could be explained by the escape of H,O and light chain fragments from polymer during ion-implantation. RBS and ERDA measurement show the depletion of hydrogen and oxygen in the case of the highest used doses, in case of sample implanted with Ar^+ ions $10x10^{15}$ ions/cm^2 we observed depletion of hydrogen and oxygen corresponding with Ar^+ ions depth profile (projected range) see Fig. 6. For the lower Ar^+ ions dose $1x10^{14}$ ions/cm^2 only hydrogen depletion was observed, the surface layer with 31 atomic % of hydrogen was created after implantation to the range appropriate Ar^+ ions depth profile about 200 nm (pristine PET hydrogen amount – 36%). On the other hand no changes in oxygen, carbon and hydrogen elemental profiles appear in case of PEEK and PI irradiated by $^4He^+$ ions. PI polymer has high resistance against ion irradiation as was concluded from all types of analyses.

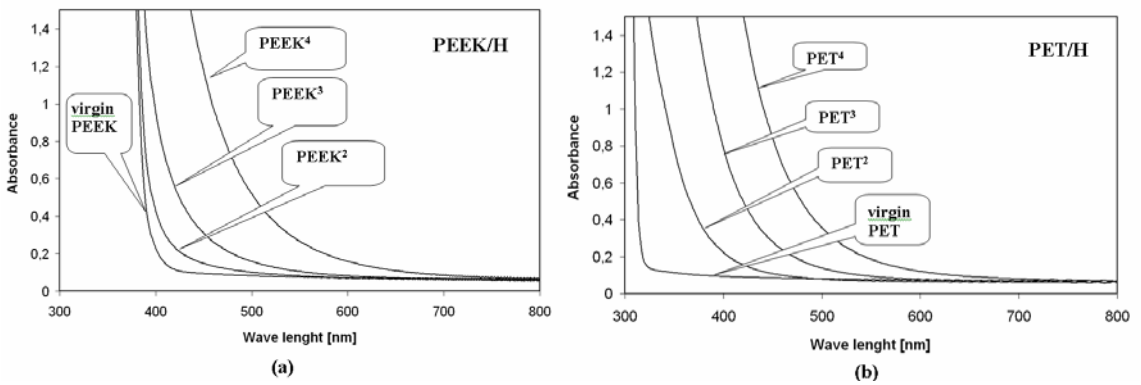

FIG. 4. Figure 1 UV-VIS spectra from He^+ 1.76 MeV implanted a) PEEK and b) PET polymers

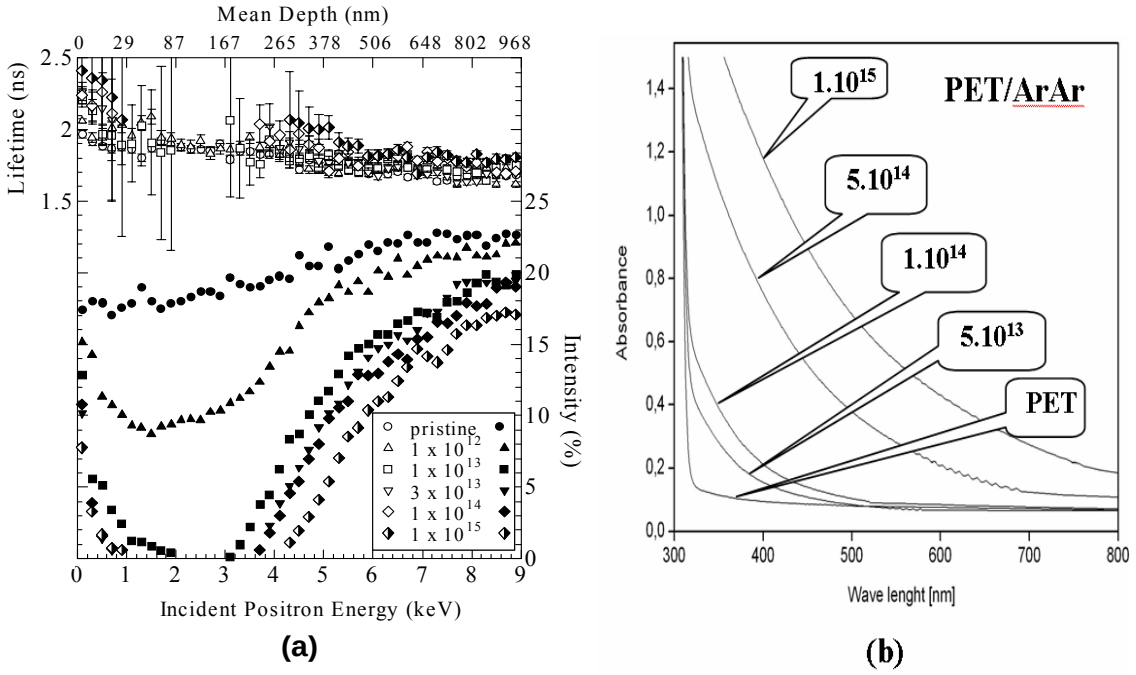

FIG. 5. a) o-Ps lifetime and intensity as a function of the incident positron energy for pristine and implanted with 150 keV Ar^+ ions at different fluences - PET b) UV-VIS spectra of pristine PET and PET implanted with Ar^+ ions.

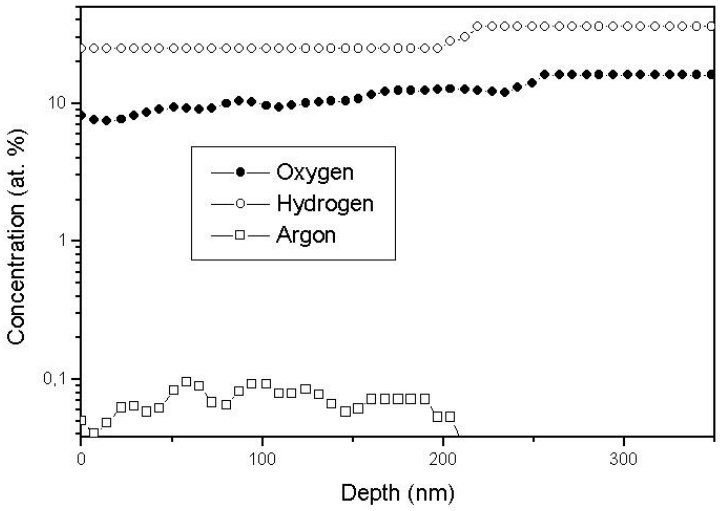

FIG. 6. RBS and ERDA measured O, H and Ar depth profiles (Ar^+ dose $10x10^{15}$ ions/cm^2) in PET.

3.3.Plasma polymers and their composites

Two sets of the samples were measured and the composition was obtained from RBS and ERDA spectra evaluation. The composition is evaluated in atomic % and the thickness of the layer in atoms/cm^2. Typical taken spectra see in Fig 7. The deposition of amine containing plasma polymers was performed in a flow of DACH monomer. The dynamic equilibrium establishes fast after the ignition of the discharge, provided that all external parameters of the discharge are held constant. This means that the concentration of various species is constant and various processes run with the constant rates. The film grows uniformly and the element profiles are constant (Fig. 8a, b). The samples prepared in CW mode at 2 and 5 W power have the same composition (Fig. 8b). The C/N ratio is 4.56 for the samples 6R, 5R. The pulse mode yields the films with a little lower hydrogen content (Fig. 8a). The C/N ratio is 4.0 and 4.89 for 1M(30 W) and 6M (2 W) samples, respectively. The surface layers of amine plasma polymers have the lower N concentration, caused during aging, on the one hand, by hydrolysis of amines by atmospheric H_2O with elimination of NH_3 or by surface restructuring, on the other hand. The pulse DACH seems to be more susceptible to these changes than CW one.

The depth profiles of different elements in Ag/CH composite films are shown in the Fig. 9 a, b. The Ag profile is not homogeneous, the Ag surface concentration is lower than concentration deeper within the deposited layer. We ascribe it to the known 'target poisoning' effect [20]. At the beginning of the deposition the positive ions collide with the pure silver target, efficiently sputtering Ag atoms, and the first deposited layers have the high Ag content (40-50%). The various species of n-hexane molecules produced by the discharge take part in the formation of hydrocarbon polymer on adjacent surfaces as well as on the silver target. The lower n-hexane concentration in the gas mixture (Fig. 9a) gives the lower polymerization rate and the resulted films contain more silver (48% for Ar/n-hexane 7/0.7 cm_3/min sample 22.5 and 43% for Ar/n-hexane 6.4/0.9 cm^3/min sample 23.5). As the process is going on, the target gets covered by non-conductive CH coating. The efficiency of Ag sputtering decreases and the Ag concentration in the films falls down, while the concentration of C and H increases. In our case, the Ag content in the surface layers is two times lower than within the film.

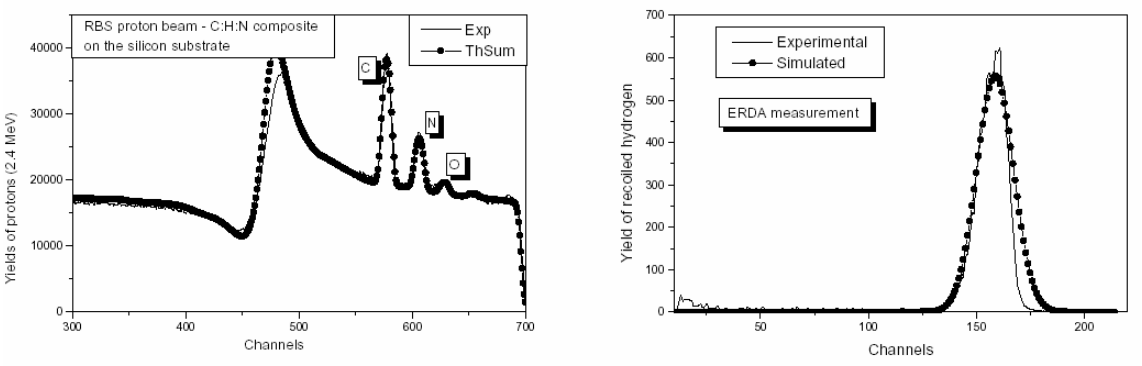

FIG. 7. a) The RBS (2.4 MeV protons) spectrum of amine polymer layers on silicon (C 39%, N 8%, H 50%, O 3% thickness 7800 E15 atoms/cm2) , b) ERDA measurement of the Ag:CH layer deposited on the silicon using alpha particles 2.745MeV.)

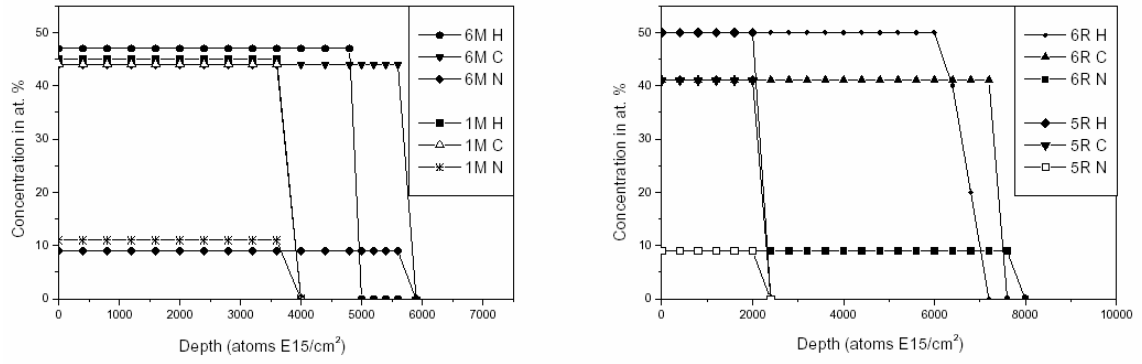

FIG. 8. Concentration depth profile of C, H, N elements in amine plasma polymers. Samples a) 6M (30W), 1M (2W) and b) 5R (2W), 6R (5W).

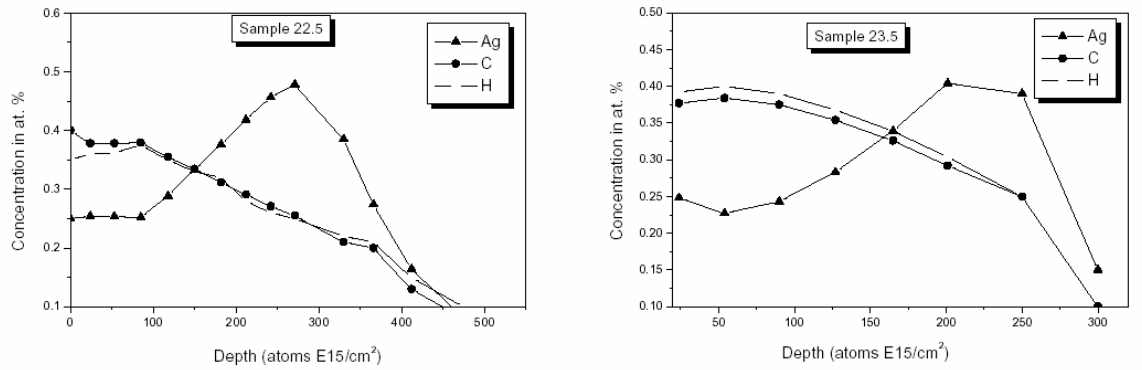

FIG. 9. Concentration depth profile of Ag, C, H elements in Ag/C:H composite thin films. Samples a) Ar/n-hexane 7/0.7 cm3/min sample 22.5 b) Ar/n-hexane 6.4/0.9 cm3/min sample 23.5

CONCLUSIONS

1) The study on diffusion activity of Ag and Cu atoms in PI, PET was done. The samples were prepared by CVD and diode-sputtering techniques on polymer substrate and the diffusion was initiated by annealing to temperatures below polymer glassy transition temperatures. The diffusion coefficients of the order of 10^{-15} - 10^{-14} $cm^2 .s^{-1}$ were found in accord with the results reported earlier for other polymers. Under similar deposition and annealing conditions the higher diffusion coefficients are observed for Ag atoms in PET in comparison with those in PI. Faster diffusion of Ag atoms was observed on the samples prepared by diode-sputtering technique. This may be due to the fact that CVD technique produces thicker and more compact Ag films. In comparison with Ag the Cu atoms exhibit much higher diffusion coefficients in PI.

2) PET implanted with 150 keV Ar+ ions to the fluences of 10^{12}-10^{15} ions/cm^2, PET, PEEK and PI implanted 1,76 MeV $^4He^+$ ions to the fluences $1x10^{13}$-$1x10^{14}$ ions/cm^2 were studied. UV-VIS spectroscopy shows that PET exhibits higher irradiation sensitivity in comparison with PEEK. The increasing UV-VIS absorbency in dependence on increasing ion dose was observed. PAL measurement indicates slightly decrease of free-volume hole concentration in Ar^+ ions implanted PET. RBS and ERDA analyses determined a decline in hydrogen and oxygen content for higher Ar^+ ion doses in the depth corresponding to the projected range of Ar^+ ions.

3) The main goal of the RBS and ERDA measurement was to characterize the composition and to determine the depth profiles of the elements in the deposited layers. RBS/ERDA techniques are shown to be useful in understanding and optimizing the dynamics of plasma deposited films growth.

REFERENCES

[1] K. L. Mittal, Metallized Plastics: Fundamentals and Applications, (Marcel Dekker, NY, 1998).
[2] P.S. Ho, R. Haight, R. C. White, B. D. Silverman and F. Faupel, in : Fundamental of Adhesion, ed. L. H. Lee (Plenum Press, New York, 1991), p. 383.
[3] F. Faupel, R. Willecke, A. Thran, M. Kiene, C. V. Bechtolsheim, T. Strunskus, Defect and Diffusion Forum, 143-147 (1997) 887.
[4] V. Švorčík, P. Tomášová, B. Dvořánková, V. Hnatowicz, R. Ochsner, H. Ryssel, Nucl. Instr. Meth B 215 (2004) 366.
[5] J. Červená, J. Vacík, V. Hnatowicz, A. Macková, V. Peřina, Surf. Coat. Tech. 158 (2002) 391.
[6] F.Grinnell, M.K.Feld, J.Biol. Chem. 257 (1982) 4893.
[7] L.Calcagno, G.Compagnini, G.Foti, Nucl. Instr. Meth. B 65 (1992) 413.
[8] V.Švorčík, V.Rybka, V.Hnatowicz, K.Smetana, J. Mater. Sci. Mat. Med. 8 (1997) 435.
[9] D. P. Dowling, K. Donnelly, N. L. McConnell, R. Eloy, M. N. Arnaud: Thin Solid Films 398-399 (2001) 602
[10] J. J. Chance, W. C. Purdy: Thin Solid Films, 335 (1998) 237
[11] M. Muller, C. Oehr: Surface and Coatings Technology 116-119 (1999) 802
[12] J. Saarilahti, E. Rauhala, Nucl. Instr. Meth. B 64 (1992) 734.
[13] V.Švorčík, K.Ročková, B.Dvořánková, L.Brož, V.Hnatowicz, R.Öchsner, H.Ryssel, J. Mater. Sci. 37 (2002) 1183.
[14] Ch. He, E. Hamada, N.Djourelov, T. Suzuki, H. Kobayashi, K. Kondo, Y. Ito, Nucl. Instr. Meth. B 211 (2003) 571.
[15] H. Frans, J. Maurer, Marcus Schmidt, Rad. Phys. Chem. 58 (2000) 509-512.
[16] M. Mayer, SIMNRA User‘s Guide, Inst. fuer Plasmaphysik, Forschunscentrum Julich , 1998
[17] A. V. Walker, T. B. Tighe, M. D. Reinard, B. C. Haynie, D. L. Allara, N. Winograd, Chemical Physics Letters 369 (2003) 615-620.
[18] R. Willecke, F. Faupel, Macromolecules, 30 (1997) 567.
[19] M.R.F. Soares, L. Amaral, M. Behar, D. Fink, Nucl. Instr. Meth. B 191 (2002) 690.
[20] P.V. Brande, S.Lucas, R.Winand, L.Renard, A.Weymeersch, Surf. Coat. Tech. 61 1-3(1993)151

CONTROLLING OF DEGRADATION EFFECTS IN RADIATION PROCESSING OF POLYMERS

EL-SAYED A. HEGAZY, H. ABDEL-REHIM, D. A. DIAA, AND A. EL-BARBARY
National Center for Radiation Research and Technology
Atomic Energy Authority, Cairo, Egypt

Abstract

Radiation induced degradation technology is a new and promising application of ionizing radiation to develop viscose, pulp, paper, food preservation, pharmaceutical production, and natural bioactive agents industries. Controlling the degree of degradation, uniform molecular weight distribution, saving achieved in the chemicals (used in conventional methods) on a cost basis, and environmentally friendly process are the beneficial effects of using radiation technology in these industries. However, for some development countries such technology is not economic. Therefore, a great effort should be done to reduce the cost required for such technologies. One of the principle factors for reducing the cost is achieving the degradation at low irradiation doses. This not only reduces the cost of radiation but also improve the quality of the end use products. The end product of irradiated natural products such as carboxy-methylcellulose and chitosan alginate may be used as food additive or benefited in agricultural purposes.

1. INTRODUCTION

When organic materials are irradiated by ionizing radiation, they are divided into two types, degradation (chain scission) and chain link (crosslinking). Interest in radiation degradation chemistry of natural and synthetic polymers has increased tremendously as the potential was recognized for using radiation to improve industrial process such as pulping, viscose, cosmetics and food preservation and new natural active agents. Possibilities for using radiation in degradation include; Natural polysaccharides with high molecular weight like alginate and chitosan, which are found in seaweed and crustaceans and are widely utilized in food, pharmaceutical and bioengineering industries. A new class of biologically active compounds of polymer type, as well as the technology for overall protection of food products, has been developed. Recently, oligosaccharides derived from the depolymerization of polysaccharides by enzyme reaction were shown to have novel features such as the enhancement of antibiosis, promotion of germination and root elongation of plants. Radiation-induced depolymerization caused by chain scission was successfully used for such purposes and has been tested and implemented in the industry. Moreover, new food protection technology has been proposed, using active polymer coatings and packages (prepared by radiation method) with improved barrier and bactericidal properties.

Degradation is a very important reaction in the chemistry of high-molecular-weight compounds. It is used for determining the structure of polymeric compounds, and obtaining valuable low molecular weight substances from natural polymers. Sometimes degradation is used to lower the molecular weight of polymers partially to facilitate fabrication. The splitting of polymeric macromolecules to form free radicals is employed for synthesizing modified polymers. At the same time polymer degradation may often be considered as an undesirable side reaction occurring during the chemical transformation, fabrication and usage of polymers.

Polysaccharides and their derivatives exposed to ionizing radiation had been long recognized as degradable type of polymers [1,2]. First event observed during the irradiation of polysaccharides leads to breakdown of the ordered system of intermolecular as well as intramolecular hydrogen bonds. Consequently, the rigidity of chains is influenced by intramolecular hydrogen bonding and the degree of crystallinity of the material decreases[i]. Polysaccharides irradiated in solid state and in diluted aqueous solutions suffer scission of acetal linkages in main chains. Radiation chemistry of cellulose, and its derivatives, has long been investigated with special attention.

Random cleavage of glycoside bonds in the main chain, initialized by radicals placed on macromolecules was found to be a leading reaction [3, 4]. In this respect, the present work is dealing with studying the effect of ionizing radiations on the crosslinking and degradation of some natural polymers such as CMC-Na and starch.Trials were made to control and reduce the irradiation dose required for the CMC-Na degradation by the addition of some additives and controlling the irradiation conditions. The possibility to crosslink CMC-Na/PAAm and starch/PAAm blends using electron beam irradiation to obtain good adsorbent materials of unique properties for possible practical uses was also investigated.

2. RESULTS AND DISCUSSION

The work in this research project is dealing with controlling of degradation in radiation processing of natural polymers used for agricultural and industrial purposes.

2.1.Radiation effects on cellulose

Cellulose exposed to high-energy radiation in dry state undergoes ionization, then most of kicked out electrons are thermalized and eventually recombined with their parent ions. As a result, excited fragments of the polymer are formed. They decompose with cleavage of chemical links, mostly splitting of carbon-bonded hydrogen. This leads to the formation of free radicals on polymer chains and hydrogen atoms. The localization of the energy initiates degradation and dehydrogenation reactions. Several studies revealed that in the case of cellulose derivatives, as CMC, Nitrocellulose Chitosan and Alginate significant part of the free radicals are generated at the substituted side chains. Thus, these free radicals were reported to be responsible for such reactions as grafting or intermolecular crosslinking [5, 6].

In this sense; radiation effect on CMC, using high energy radiation, was investigated under different conditions. The irradiation process of CMC was taken place in a solid state or in a water-soluble form of different concentrations. The effect of some additive, such as KCl and H_2O_2, on the degradation process during irradiation was also discussed. To elucidate the effect of irradiation on CMC; an aqueous solutions of different concentrations of CMC were exposed to electron beam irradiation. It was found that, the irradiation underwent degradation at high and low concentrations, however, the crosslinking of these polymer occurs when the polymer irradiated at concentrations ranged between (40-70 wt / wt %) as shown in Figure (1).

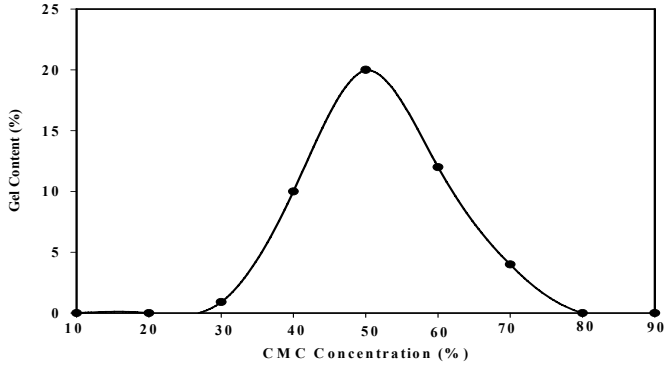

FIG. 1. Effect of different CMC concentrations on its gel content at 20 kGy using EB irradiation in air atmosphere.

It can be assumed that, water contributes in the crosslinking process of CMC in two ways. First, it enhances the mobility of the rigid molecules of CMC, allowing the diffusion of macro radicals to close the distance between each others and consequently allow their recombination. Second, it induces an increase of radical concentration such as, hydrogen atoms and hydroxyl radicals, which resulted from water radiolysis. These radicals can create CMC macro radicals by abstracting H-atom from the polymer chain. Hence, the presence of water enhances the yield of macro radicals; crosslinking of CMC was achieved from a direct effect of irradiation when radiation interacts directly with polymer chains and from an indirect effect when it interacts with the products of water radiolysis.

2.2.Radiation degradation of CMC in solid state

Dry CMC was irradiated at different doses (Fig.2). It can be seen that there is an extreme reduction in intrinsic viscosity at the early doses and thereafter, a gradual decrease is observed with increasing the dose. The viscosity sharply decreased from 17 to 2 when CMC was irradiated at 20kGy. Thereafter, as the irradiation dose increased, the intrinsic viscosity gradually decreased. Meanwhile, as shown in Fig.3, the addition of 10% water enhanced the degradation process at 20 kGy. The intrinsic viscosity of dry CMC is higher than that of moistened CMC at low irradiation doses. However, at 50 kGy irradiation, the intrinsic viscosity of moistened CMC is higher than that of dry CMC. In the presence of water, beside the CMC chain scission, the CMC have the ability to crosslink at high doses. Generally CMC degrade by scission of the glycoside bond.

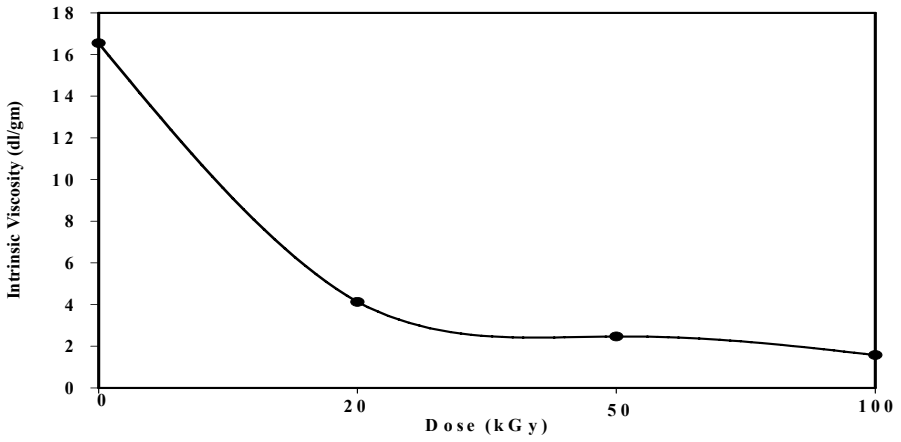

FIG. 2. Effect of irradiation dose on intrinsic viscosity of dry CMC-Na; in 0.01M NaCl, measured in 0.01M NaCl.

The effects of Moistened CMC-Na concentration and salt additive on the intrinsic viscosity at 20 kGy irradiation dose are shown in Fig. 4. It was found that the intrinsic viscosity decreases as the water content increases compared with that irradiated in dry form. However, in the presence of 1% KCl, the intrinsic viscosity is higher than that of moistened CMC, it enhances the crosslinking process and controlling the degradation effects during radiation processing.

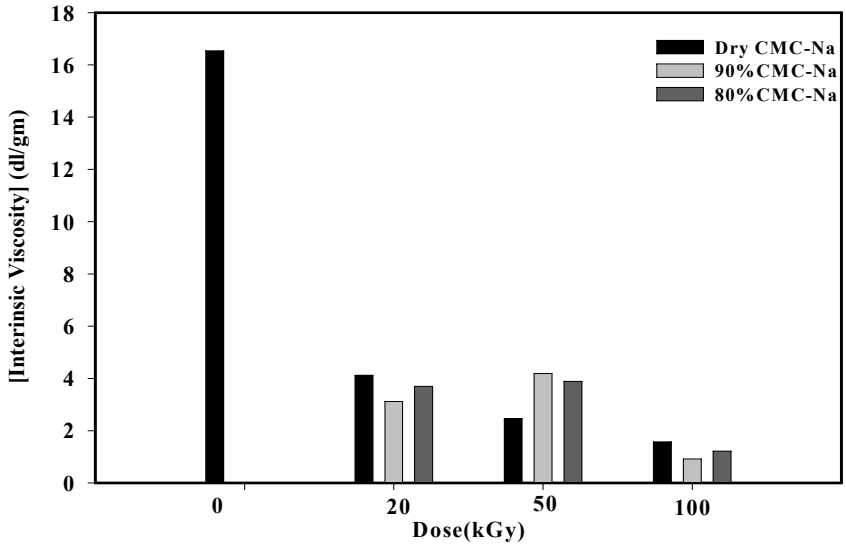

FIG. 3. Effect of irradiation dose on the degradation processes of different aqueous CMC-Na concentrations in terms of intrinsic viscosity, measured in 0.01M NaCl.

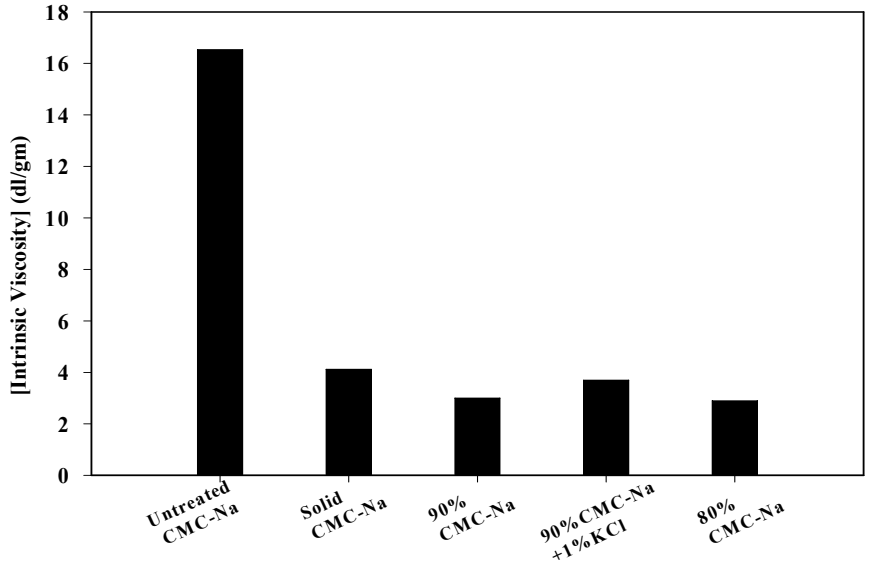

FIG. 4. Effect of different CMC-Na concentrations on the intrinsic viscosity; measured in 0.01M NaCl and irradiated at 20kGy.

2.3.Thermo gravimetric analysis (TGA)

The occurrence of chain scission is clearly demonstrated by TGA. If the polymer undergoes degradation, its weight will decrease. Thermo-gravimetric TG curves of irradiated and un-irradiated CMC-Na is investigated and shown in Figure (5). It is clear that the % weight loss of un-irradiated and irradiated 50% CMC-Na appeared at 300 and 280^{o}C, respectively, indicating that the irradiated CMC-Na decomposed at lower temperature than that the un-irradiated one by 20 °C which corresponds to the reduction of its molecular weight. The same behavior was observed when the samples of CMC-Na were irradiated in the dry and moistened form. The thermal stability of dried irradiated CMC-Na is higher than that of moistened one.

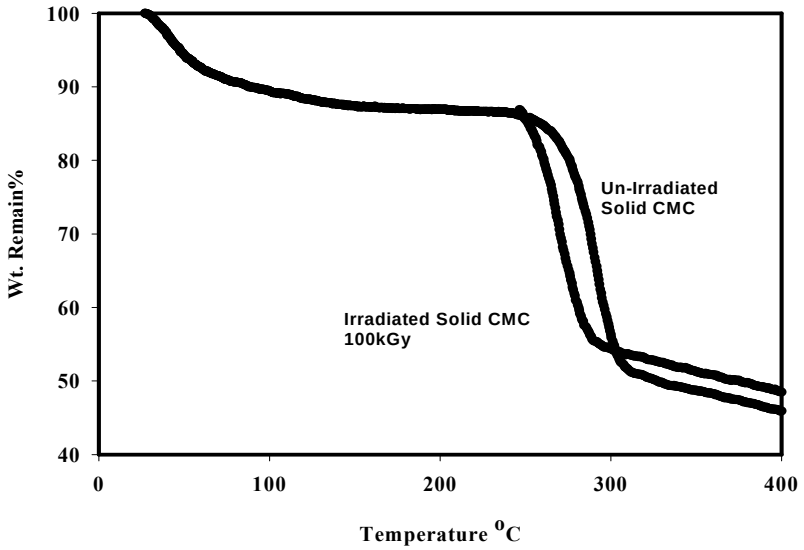

FIG. 5. TGA Thermal Diagram of un-irradiated and irradiated CMC-Na at 100 kGy.

2.4.FTIR studies on the radiation degradation of CMC at different doses

FTIR was performed to follow up the effect of different irradiation doses on structural changes in the CMC-Na. Figure (6) shows that the intensity of the carboxylate groups at 1625 cm^{-1} decreases with increasing the irradiation dose. Also, the aliphatic stretch band at 2890 cm^{-1} and C-O band at 1065 cm^{-1} decrease as the irradiation dose increases. This means that the cleavage not only occurred in the main chain of CMC-Na but also in carboxy methylated groups on the cellulose ring.

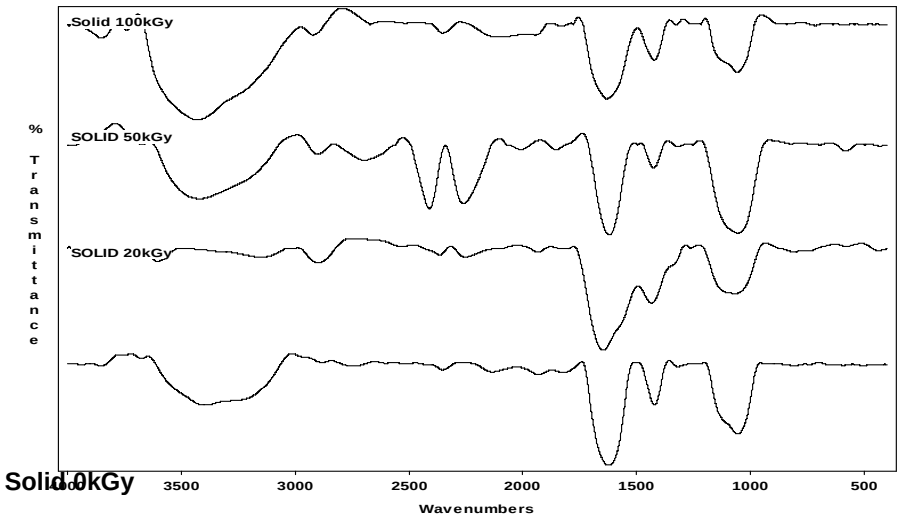

FIG. 6. FTIR spectra of solid CMC-Na irradiated at different doses.

2.5.Effect of radiation on the thermal parameters of CMC-Na

The capability of gamma irradiation on the CMC-Na to cause changes in some of its measurable physical and chemical properties can be detected by thermal analysis. To determine the morphological and structural changes in the polymers, the change in thermal parameters, such as melting temperature (Tm) and heat of fusion (ΔH) of irradiated CMC-Na at different doses under various conditions, were investigated using DSC as shown in Figure (7) and Table I. From the DSC thermal diagrams, it can be seen that there is a significant change in the (Tm) of the original CMC-Na exposed to gamma irradiation at different doses. A decrease in (Tm) was observed with increasing the exposure dose to certain limit. Thereafter, the increase in radiation dose leads to an increase in (Tm). The same behavior was observed for heat of fusion (ΔH). The apparent decrease in (Tm) and (ΔH) of CMC-Na irradiated with low doses indicated that the irradiation caused structural changes in the CMC-Na chains and consequently, in the crystallinity. However, the apparent increases in the (Tm) and (ΔH) of CMC-Na irradiated with high doses can be attributed to the increase in its crystallinity. The degradation by high dose gamma irradiation results in fragments have a capability to reorient again in crystal form, therefore, there is no significant change in (ΔH) of un-irradiated and high dose irradiated CMC-Na.

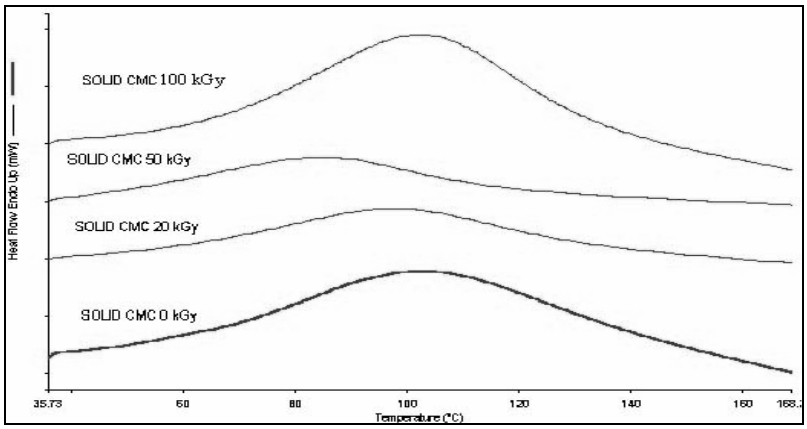

FIG. 7. DSC diagram of solid CMC under the effect of different irradiation doses.

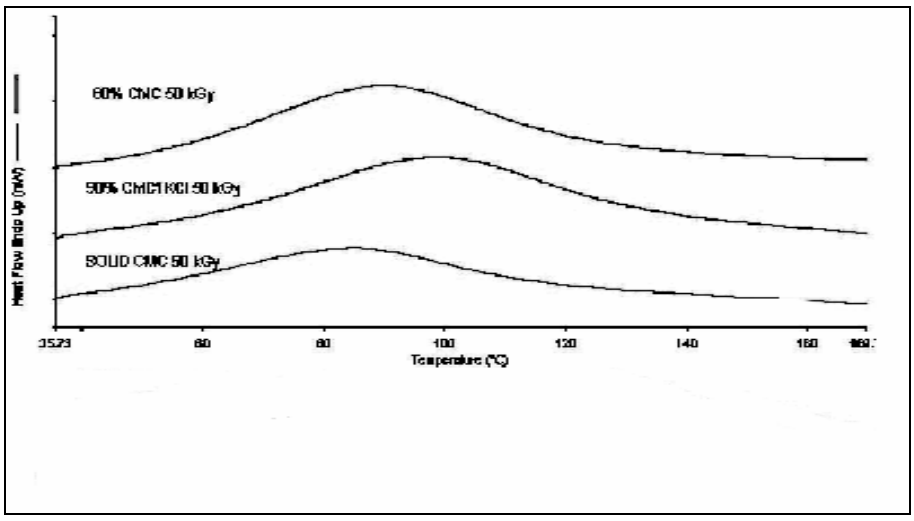

FIG. 8. DSC diagram of different CMC concn.; irradiated at 50kGy

Change in Tm and ΔHm of CMC-Na irradiated at same dose under different conditions was investigated as shown in Figure (8) and Table (2). It was observed that (Tm) and (ΔHm) changed depending on irradiation condition, in solid or wet state and in presence of additives such as KCl. The Tm is remarkably decreased for 80% CMC-Na and in presence of KCl compared to the solid CMC-Na.

TABLE I. EFFECT OF IRRADIATION DOSE ON MELTING TEMPERATURE (TM) AND HEAT OF FUSION (ΔH) FOR SOLID CMC.

Dose (kGy)	Tm (^{o}C)	Δ H (J/G)
0	102.5	359
20	91.03	214.9
50	85.6	217.7
100	102.6	442.3

TABLE II. EFFECT OF CONCENTRATION ON THE MELTING TEMPERATURE(TM) AND HEAT OF FUSION (ΔH) FOR CMC-NA AT 100KGY:

Sample	Tm (^{o}C)	Δ H (J/G)
Solid CMC	102.3	442.3
90% CMC +1%KCl	92.0	424.9
80% CMC	90.0	329.6

2.6.Synergistic effect of combining ionizing radiation and oxidizing agents on controlling degradation of some natural products:

Studying the effect of hydrogen peroxide and/or Gamma irradiation on the degradation process of Soduin alginate was investigated and shown in Figure (9). It was found that the molecular weight of the polymer decreases by using gamma radiation or H_2O_2. However, combining both gamma radiation and H_2O_2 accelerates the degradation rate of alginate and reduces dose required to degrading alginate.

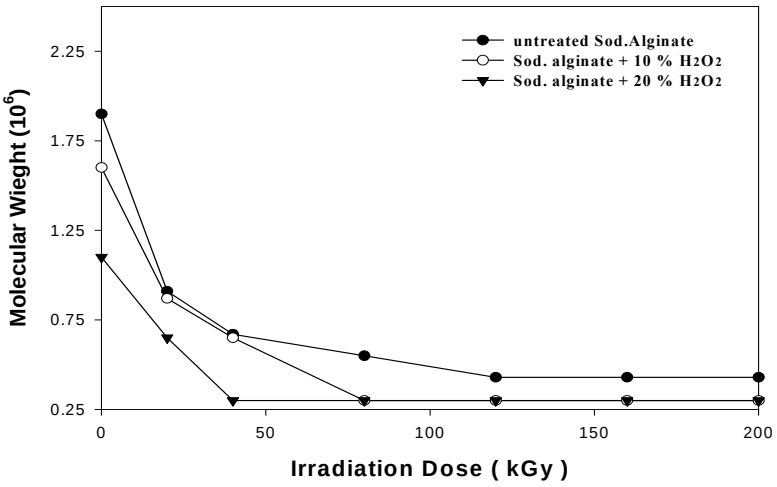

FIG. 9. Effect of H_2O_2 % and different irradiation dose on molecular weight of Na- alginate.

The dose required to reduce the molecular weight of Na-alginate from $1.9x10^6$ to about $3\text{-}4x10^5$ is 120 kGy. Meanwhile, the higher the H_2O_2 concentration the more pronounced the degradation of Na- alginate. Similar behavior is observed for Chitosan and CMC-Na as shown in Figs. 10 and 11, respectively.

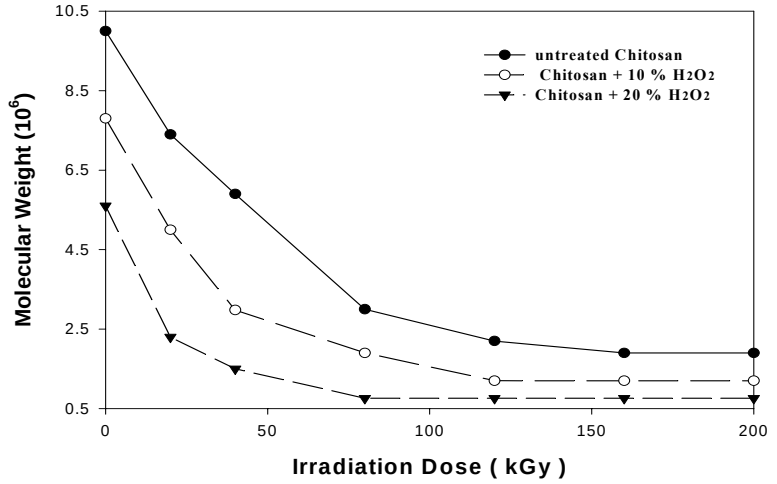

FIG. 10. Effect of irradiation dose on the change in molecular weight of chitosan (high molecular weight) in H_2O_2.

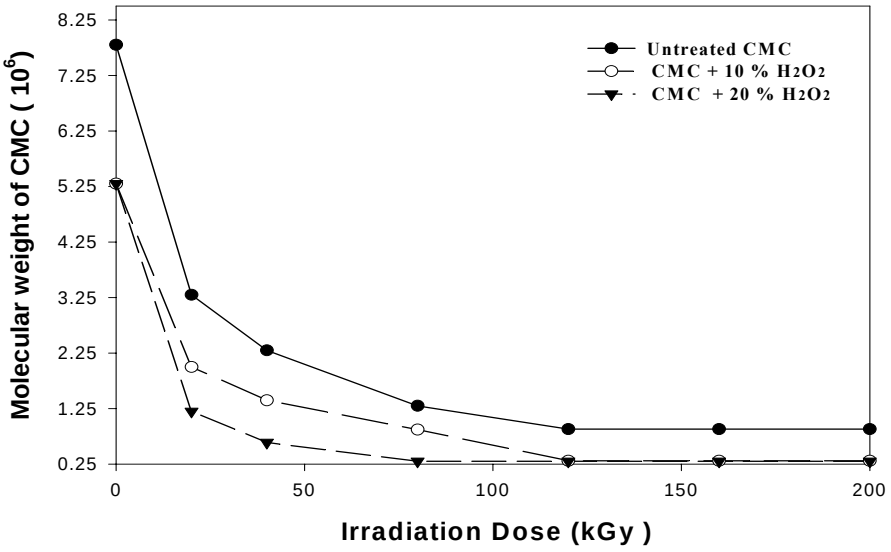

FIG. 11. Effect of irradiation dose on the change in molecular weight of CMC in H_2O_2.

2.7. Application of degraded Na-alginate in agriculture

Degraded Na-alginate could be used as additives during radiation crosslinking of PAAm for the use as soil conditioner in agriculture purposes. The growth and other responses of bean plant cultivated in the soil that treated with PAAm and PAAm /Na-alginate copolymer were investigated. The test field results showed that the mixing of small quantities of PAAm or PAAm /Na-alginate copolymer with sandy soil results in increasing its ability to water retention. The growth of the bean plant cultivated in the soil treated with PAAm/ Na- alginate is better than that one in PAAm alone. The most significant difference between the PAAm and PAAm- Na-alginate copolymer is that the latter is partially undergoing radiolytic and microbial degradation to produce oligo-alginate, which acts as plant growth promoter. The increase in bean plant performance by using PAAm/Na-alginate copolymer suggested its possible use in agriculture uses as a soil conditioner providing the plant with water as well as oligo-alginate growth promoter. Therefore, it could be concluded that the efficiency of PAAm as soil conditioner increases by the addition of Na-alginate.

FIG. 12. Bean plant cultivated in soil after 9 weeks:(A)Untreated (control), (B) Treated with PAAm and (C) treated with PAAm/Na-alginate.

2.8.The use of controlled degraded CMC incorporated with PAAm in diaper industry

The radiation crosslinking of PAAm is affected by the presence of CMC-Na due to the degradability of the latter one which could be controlled according to its concentration in the bulk medium and irradiation dose. Accordingly, the gel content and swelling properties of PAAm-Na-CMC could be controlled. Figure 13 shows that the degree of swelling increases with dose and showing a maximum swelling at 30 kGy and thereafter it deceases at higher dose (40 kGy). This is due to the degradation processes at relatively medium doses up to 30 kGy and the partial crosslinking may occur at 40 kGy. So, this is a matter of degradation/ crosslinking ratio depending on the dose and concentration of CMC-Na in the mixture.

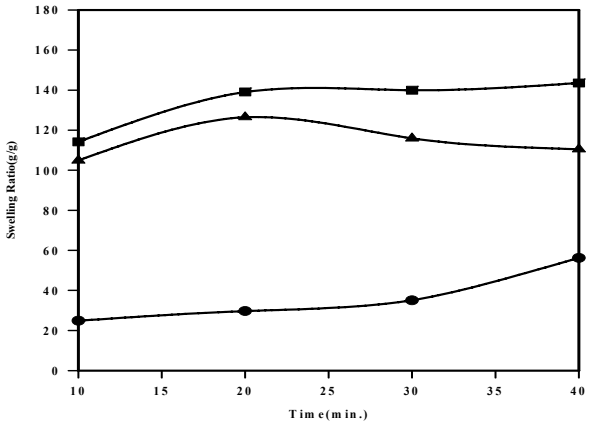

FIG. 13. The swelling ratio for CMC-Na in distilled water, irradiation dose; (■) 30kGy, (▼) 40kGy and (●) 20kGy.

The swelling of the prepared hydrogel was investigated for its possible use in personal care articles particularly diapers. Thus, its degree of swelling was measured in simulating urine solution, and compared with commercial super-porous hydrogels based on acrylate polymers, Figure (13). It is clear that there is a slight difference between the swelling of the prepared CMC-Na /PAAm hydrogel and the commercialized one in the simulated urine solution. The prepared crosslinked copolymers possess high and fast swelling properties in simulated urine media. An acceptable swelling capacity for super-absorbent is approximately 20-40 g of urine per gram of hydrogel. Therefore, the swelling ratios of CMC-Na /PAAm gels in urine are acceptable for diaper application.

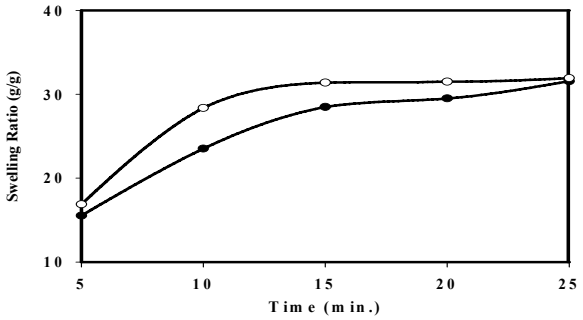

FIG. 14. The swelling ratio of (●) CMC-Na /PAAm super-absorbent hydrogel, (o) commercial diaper; in simulated urine solution.

3. CONCLUSION

It can be concluded that radiation is a very effective tool for controlling the degradation and cross-linking of natural occurring polymers and the synthesis of relative economic, environmentally friendly super-absorbent hydrogels which may potentially be used in personal care products industry and in agricultural purposes.

REFERENCES

[1] C.G. Delides, C.Z. Panagiotalidis and O.C. Lega-Panagiotalisdis, The degradation of cotton by ionizing radiation. *Textile Res. J.* 51 311(1981).

[2] Fumio Yoshii, Long Zhao, Radoslaw A. Wach, Naotsugu Nagasawa, Hiroshi Mitomo, Tamikazu Kume Hydrogels of polysaccharide derivatives crosslinked with irradiation at paste-like condition Nuclear Instruments and Methods in Physics Research B: 208, 320(2003).

[3] Von Sonntag, Free-radical reactions of carbohydrates as studied by radiation techniques. *Adv. Carbohydr. Chem. Biochem.* 37, 7 (1980.

[4] Von Sonntag and H.P. Schuchmann, Carbohydrates. In: C.D. Jonah and B.S.M. Rao, Editors, *Radiation Chemistry. Present Status and Future Trends*, Elsevier Science, Amsterdam (2001), pp. 481–511.

[5] D.N.S. Hon and H.C. Chan, Photoinduced grafting reactions in cellulose and cellulose derivatives. *ACS Symp. Ser.* 187, 101(1982).

[6] B.G. Ershov, Radiation-chemical degradation of cellulose and other polysaccharides. *Russ. Chem. Rev.* 67, 315(1998).

MODIFICATION OF MICROSTRUCTURES AND PHYSICAL PROPERTIES OF ULTRA HIGH MOLECULAR WEIGHT POLYETHYLENE BY ELECTRON BEAM IRRADIATION

Y. C. Nho
Radiation Application Div. Korean Atomic Energy Research Institute, Daejeon, S. Korea
S. M. Lee, H. H. Song
Department of Polymer Science and Engineering, Hannam University, Daejeon, S. Korea

Abstract

An ultra high molecular weight polyethylene was irradiated with the electron beam at dose levels ranging from 100kGY to 1MGy. The microstructures of the irradiated samples were characterized by FTIR, gel fraction measurement, DSC and small and wide angle X-ray scattering. For the mechanical properties, a static tensile test and creep experiment were also performed. The cross-linking and the crystal morphology changes were the main microstructural changes to influence the mechanical properties. It was found that 250kGy appeared to the optimal dose level to induce cross-links in the amorphous area and recrystalliztion in the crystal lamellae. At doses above 250 kGy, the electron beam penetrates into the crystal domains, resulting in cross-links in the crystal domains and reduction in the crystal size and crystallinity. The static mechanical properties (modulus, strength) and the creep resistance were enhanced by the electron beam irradiation. The stiffness rather correlated with the degree of cross-links, while the strength with the crystal morphology.

1. INTRODUCTION

Ultra high molecular weight polyethylene (UHMWPE) is named from the unusually high molecular weight (higher than 3 x 10^6 g/mol) which is about 10-20 times longer than the ordinary linear high density polyethylene. Because the ultra high molecular weight polymer exhibits superior wear and fatigue properties as well as biocompatibility, it has been utilized for the replacement of damaged or diseased articulating cartilage in joint replacement surgery [1-4]. However, one of the major problem for UHMWPE utilizing as the biomaterials is the long term wear or fatigue of the polymer to produce debris particles or shape deformation which cause loosening the joint prostheses and foreign body reaction problem [1,4,5]. Several studies to improve the wear resistance have been attempted [6-8]. Oonish et al. [6] have revealed for the first time that the UHMWPE irradiated with gamma rays had shown high wear resistance. The radiation technique of gamma ray has been the most popular technique to achieve both sterilization and improving mechanical properties as required for the biomaterials. Recent advances in electron beam technology, however, have made the electron beam irradiation technique as a strong competitor to the gamma radiation process [10]. Although the interactions with the polymeric material are basically the same for gamma radiation and high energy electron beam, some differences between the two techniques are observed in their outcome [11,12].

It is well known that the high density cross-linking is induced by the high energy radiation, which is considered as one of the major factors to improve mechanical properties of irradiated polymers [1, 14]. The cross-linking reaction is effected by the irradiation environment and the initial polymer morphology such as degree of crystallinity, crystal size distribution, molecular weight, so on [10, 15-19]. It is then highly expected that fine structural changes (other than the cross-linking) are induced during the irradiation process and they must play an important role in modifying the physical properties. Nevertheless, systematic studies on the microstructures and their changes by the irradiation and their correlations with the physical properties are very rare.

The objective of this work is to elucidate the microstructural modifications and related physical property changes of the UHMWPE by the electron beam irradiation with doses ranging from 100KGy to 1MGy. We employed the small and wide angle X-ray scattering, FTIR, and DSC for the detailed structural investigation and examined the structure-property correlations of irradiated UHMWPE.

2. EXPERIMENTAL

2.1.Materials and sample preparation

An ultra high molecular weight polyethylene (UHMWPE) was received as a compression molded sheet of 1.2 cm thickness. The molecular weight is about $4.5x10^6$ g/mol. For the tensile test the sample was initially milled into a rectangular sheet of 5 mm thickness and was compression molded at 190 ^oC in a home made mold designed after the ASTM D68 standard. Sufficient time was allowed before releasing the pressure in order not to induce any orientation in the sample during the compression molding.

2.2.Electron beam irradiation

Electron beam irradiation was carried out in air utilizing the accelerator (ELV-4) at EB-tech, Daejeon, S. Korea. The electron energy operated was 1 Mev. The heat generated during the irradiation was cooled using an aluminum cold plate in order to prevent any thermal effect on the samples during the irradiation. The irradiation doses were chosen at 100, 250, 500, 750, 1000kGy and conveyer speed was 1m/min (100kGy) and 2m/min (250kGy~1MGy).

2.3.Characterization

Thermal properties of the electron beam irradiated samples were studied using a differential scanning calorimeter (TA DSC2910). Samples of ~4 mg were measured in a nitrogen gas atmosphere and the heating rate was at 10 ^oC/min. The percent crystallinity of the samples were derived based on the heat of fusion measurement,

$$x_c = \frac{\Delta H_{sample}}{\Delta H_{PE}} \times 100\,(\%) \qquad (1)$$

where ΔH_{sample} represents the heat of fusion of irradiated sample and ΔH_{PE} for the heat of fusion of 100% crystallinity [20].

Two main reactions associated with the high energy irradiation are the chain scission and cross-linking reaction [4, 21]. To examine the two reactions, FTIR spectroscopy experiments were performed utilizing a Perkin-Elmer 1000PC spectrometer. For the efficient measurements, the irradiated samples were microtomed into a 25 □m thickness.

Gel content and swelling ratio were determined based on the ASTM D2765-95 method. However, the specimen size (5mm x 5mm x 2.5mm, 49±1 g) was chosen somewhat larger than suggested for the accuracy of the data. The samples in a 25 μm metal mesh were kept in xylene at 120 ^oC for 48 hrs. The weight was measured (W_g) after the solvent on the specimen surface being evaporated. The specimen, then, was dried in a vacuum oven at 120 ^oC for 72 hrs and the weight (W_d) was measured. The percent extract and swelling ratio are derived as follows;

- extract % = $[(W_0 - W_d)/W_0] \times 100$ (2)
- swelling ratio = $[(W_g - W_d)/W_d]\, K + 1$ (3)

Where W_0 is the original weight of specimen tested, W_d the weight of dried gel, W_g the weight of swollen gel after immersion period, K the density of solvent at the immersion temperature (approx. 1.08) [21, 22]. Low percent extract represents the high gel fraction and low swelling ratio the high cross-linking density.

Wide and small angle X-ray scattering were performed at the 4C1 and 4C2 X-ray beamlines in Pohang Accelerator Laboratory. X-ray beam from the synchrotron radiation was utilized. The X-ray wave length was 1.608 A and the beam size at the sample position was 0.4 x 0.4 mm. Two dimensional position sensitive area detector was utilized to collect the scattered data. The sample to detector distance was 9.03 cm for the wide angle X-ray scattering and 310 cm for the small angle X-ray scattering.

For the mechanical properties, both static tensile test and creep test were performed. The tensile properties were measured using a tensile tester (Shimadzu AG-5000G). The specimen size was 5.3 x 2.5 x 54 mm and test was made at the speed of 3mm/min in the atmosphere. A laboratory built creep tester was utilized for the creep test. The load was controlled by using the high pressure N_2 gas and a digitial pressure gage. A 4-step load method was utilized to achieve a long term creep behavior with the short term experimental data. The applied loads were 2.94, 4.90, 6.86, 8.82 MPa and each step load was applied when the creep deformation reaches a plateau. The entire time span for the creep test of each sample was for about 80 hrs.

2.4.X-ray data analysis

The collected X-ray scattered intensities at wide angles and those of small angles contain structural information of different length scale in real space. The analysis of the wide angle X-ray intensities is rather straight forward. The raw intensity curves were analyzed using a conventional 'Curve Fit' program to decompose the individual peaks from the intensity curves. The crystallinity index (x_c) and crystal thicknesses (t) were then estimated by the following equations;

$$x_c = \frac{I_c}{I_t} \qquad (4)$$

where I_c is the integrated intensities of crystal peaks and I_t the total scattered intensities.

$$t = \frac{0.9\lambda}{B\cos\theta_B} \qquad (5)$$

where B is the full width at half maximum of the diffraction peak in radian, θ_B the diffraction angle of the individual peak, and □ the wavelength of the X-ray.

The analysis of small angle intensities, on the other hand, is not straight forward but requires mathematical manipulation to gain some useful structural information, in this case, the lamellar structure. The polymer lamellar stacks are composed of alternating crystalline and amorphous layers. One lamellar stack then can be considered as a one-dimensional array and the perdioc length ranges from several nanometers to tens of nanometers. The Lorentz corrected X-ray scattered intensities at appropriate small angles reveal the periodic length scale between the individual lamellar layers. However, a correlation function derived from the raw X-ray scattered intensities at small angles provides the lamellar layer or the amorphous layer thickness. In an isotropic situation, the correlation function [23] is given as

$$\gamma(r) = \frac{\int I(s)\times\cos 2\pi rsds}{\int I(s)ds} \qquad (5)$$

where s is the scattering vector defined as $\frac{2\sin\theta}{\lambda}$ and r is the correlation length in real space. In Figure 1, one example of correlation function is depicted and the curve reveals the lamellar long spacing, lamellar thickness, and amorphous layer thickness.

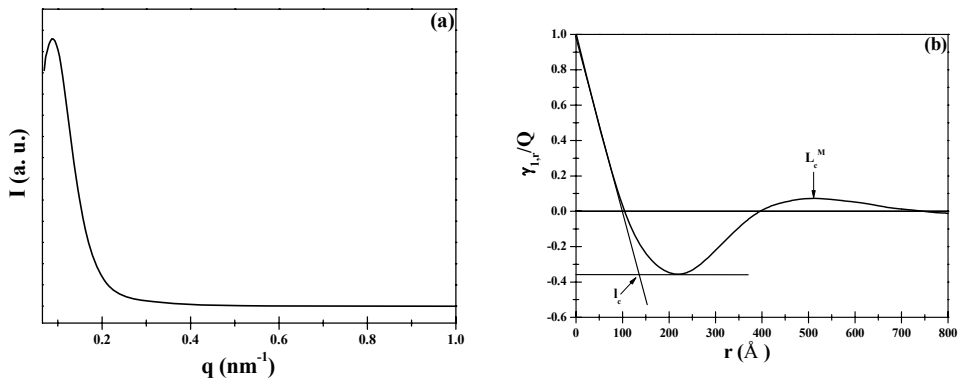

FIG. 1. An example of small angle X-ray scattering pattern from lamellar structure (a) and derived correlation function (b). L_c^M denotes the lamellar long spacing and l_c the crystal lamellar or amorphous layer thickness.

3. RESULTS AND DISCUSSION

3.1.Chain scission and cross-linking

When the polymer is exposed to the electron beam irradiation, two major chemical reactions, i.e., chain scission and chain cross-linking, are anticipated [13]. The chain scission is through C-C bond breakage by the high energy bombardment (Figure 2-(a)) and the cross-linking between the neighboring chains is induced by the free radicals produced by the breakage of C-H bond (Figure 2-(b)) [22]. The cross-linking and chain scission reaction are not independent but influencing one another. They both take place competitively and the chain scission, in general, accompanies cross-linking reaction. The mechanism is highly influenced by many factors including the average molecular weight, degree of crystallinity, concentration of free radicals, oxidation and etc. [24]. In Figure 3, FTIR spectra of the electron beam irradiated samples are plotted. As the irradiation dose is increased, a new absorption band at 1712 cm^{-1} becomes marked and intensifies with the increase of irradiation dose. The peak at 1712 cm^{-1} can be related to the ketonic carbonyl group which is produced by oxidation reaction associated with either the chain scission or cross-link. The integrated intensities of the absorption peak at 1712 cm^{-1} are derived and plotted in Figure 4. The amount of carbonyl group, thus the chemical reaction, increases with the irradiation dose but the increment slows down when approaching the dose level of 500 kGy.

Degree of cross-linking can also be by measuring the gel fraction from the polymer solution. As the irradiation dose increases, the production of free radical increases, resulting in the increase of cross-linking density and the 3-dimensional network which becomes insoluble in an ordinary solvent. In Figure 5, the gel fractions and swelling ratio estimated by equation (2) and (3), respectively, are plotted against the irradiation dose. Amount of gel fraction increases rapidly in the beginning and reaches a plateau near the irradiation dose of 250 kGy. As the cross-linking density increases with the irradiation dose, the spaces between the chains become very limited, thus resulting in a reduction of chain swelling. The plot in Figure 6 reveals a good correlation between the gel fraction (cross-linking) and the swelling ratio. Our results of FTIR and gel fraction measurement suggest that the cross-linking can be achieve more effectively up to the irradiation dose of 250 ~ 500 kGy. The gain appears to be minimal beyond this irradiation dose level.

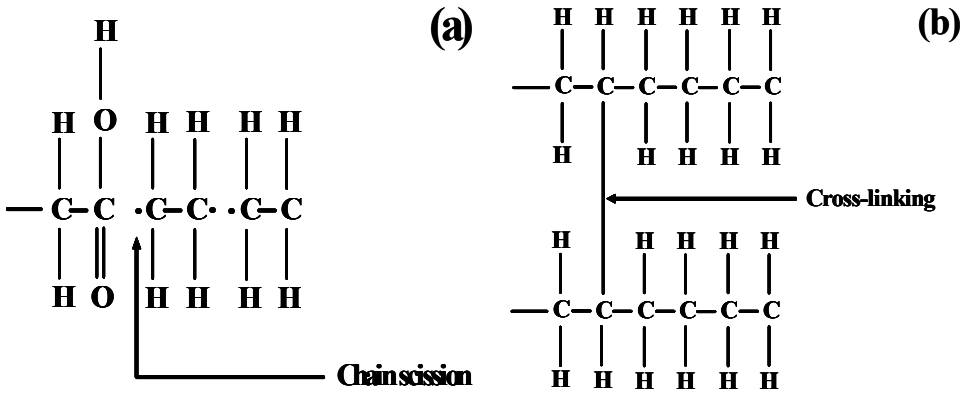

FIG. 2. Suggested chain scission (a) and cross-linking (b) reaction in UHMWPE by high energy irradiation.

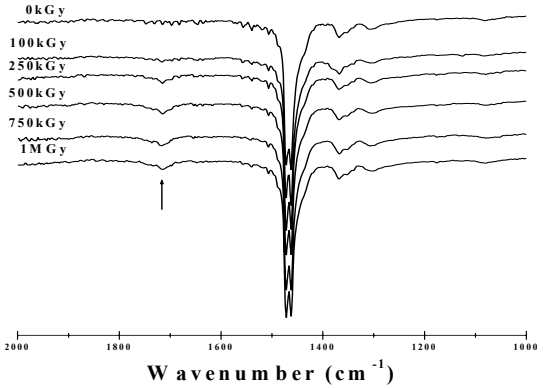

FIG. 3. FTIR spectra of electron beam irradiated UHMWPE.

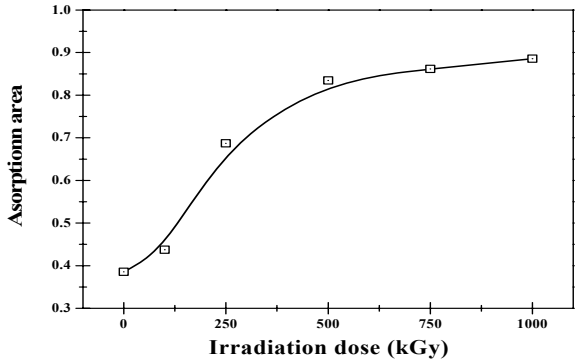

FIG. 4. Plot of integrated intensities of absorption bands at 1712 cm^{-1} vs. irradiation dose.

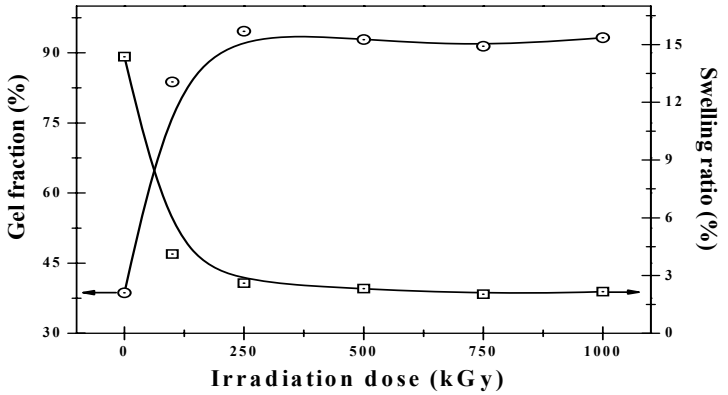

FIG. 5. Plot of gel fraction and swelling ratio vs. irradiation dose.

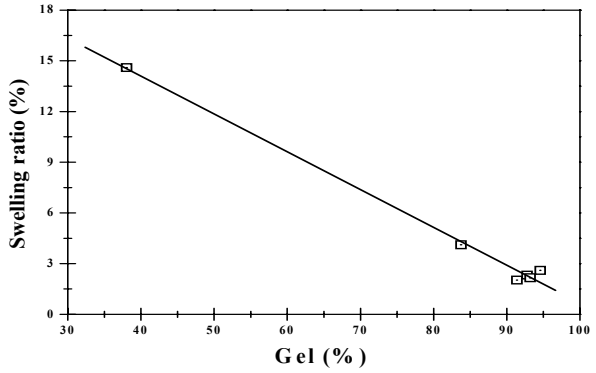

FIG. 6. Correlation between the degree of gel fraction(cross-linking) and swelling ratio.

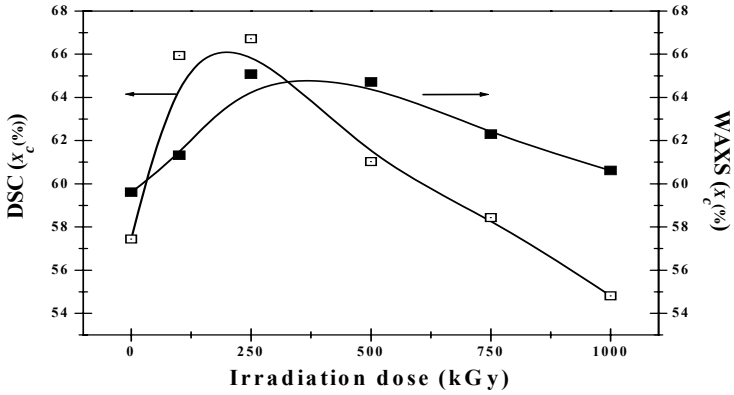

FIG. 7. Crystallinity of electron beam irradiated UHMWPE estimated by DSC and wide angle X-ray scattering experiments.

3.2.Morphological changes

Any changes of internal microstructures of the polymers upon electron beam irradiation are also examined by the X ray scattering and DSC. In Figure 7, the crystallinities of the samples as determined by the DSC and X ray scattering are plotted as a function of the irradiation dose. Both curves exhibit that the crystallinity increases and reaches a maximum at the irradiation dose of 250 kGy. But the crystallinity decreases on further increase of irradiation dose. Similar behaviors can also be observed in the studies of □-radiation or the UV-radiation [25, 26]. In Figure 8, the crystal thicknesses of (110) and (200) planes are also plotted against the irradiation dose. The plot depicts the similar behavior to that of crystallinity shown in the Figure 7. The penetration of electron beam shall be more effective in the loosely packed amorphous area. Furthermore, the oxygen content required for the chain scission is higher in the amorphous region as well. The chain scission and cross-link, therefore, take place predominantly in the amorphous area first. When the polymer chains undergo chain scission in the amorphous region, the increased chain ends provide the mobilities of the entangled chains, leading to the recrystallization of the less ordered crystals or the super-cooled chains. However, when the irradiation dose increases and reaches a certain energy level, the electron beam can penetrate into the crystalline domains. Our results indicates that 250 kGy is sufficient enough to induce chain scission or cross-linking in the crystalline area, resulting in reducing the crystal thickness or the crystallinity.

The crystal thicknesses of (110) and (200) crystal planes estimates the lateral size of the lamellar stacks, while the lamellar thickness provides the perpendicular dimension of the lamellae. In order to gain structural information associated with the lamellae thickness, small angle X-ray scattering (SAXS) study was performed and the results are shown in Figure 9. The curves in Figure 9 are Lorentz corrected SAXS intensities (Iq^2). The peak position shown in the figure represents the long spacing of the lamellar structure, i.e., an average repeating distance between the lamellar units in the stack. But this distance only gives the combined information of lamellar layer thickness and the inter-lamellar amorphous layer thickness. In order to obtain the crystal lamellar thickness (l_c) or the amorphous layer thickness (l_a) individually, a correlation function was derived from the raw scattered intensities, as discussed previously. In Figure 10, the lamellar long-spacing (a), lamellar and amorphous layer thickness (b) are plotted. The long-spacing (Figure 10-(a)) decreases with the irradiation dose and levels off at 500kGy. The lamellar thickness (l_c) increases with the dose increase and reaches a maximum at about 250kGy followed by the reduction on further increase of the dose. The amorphous layer thickness (l_a), on the other hand, continuously decreases with the dose and the decrement slows down and shows slight upturn at the high dose. The initial increase of lamellar thickness is probably due to the recrystallization associated with the chain scission at the inter-lamellar amorphous gap, as described earlier. The initial rapid decrease of amorphous layer can be attributed to the recrystallization consuming the inter-lamellar amorphous region. The decrease of the lamellar thickness at the higher dose is also associated with the reaction in the crystal domain, most likely near the interfacial region between the crystalline and amorphous area. Our results of crystal thickness and lamellar thickness illustrate that the recrystallization takes place three dimensionally, not only at the fold planes but also at the inter-lamellar surfaces.

In general, the crystallinity and melting temperature show a good correlation that the higher crystallinity or larger crystal domains show higher melting point. In Figure 11, melting temperatures of the irradiated samples from the DSC thermograms are plotted. The melting points increase with the irradiation dose and show a similar saturation behavior at the high doses to those of cross-links (Figure 4 and 5). The initial high increase can be attributed to the increase of crystal domains as discussed earlier. However, the increase noted beyond 250 kGy, where the crystallinity or the crytstal domain size decreases (Figure 7 and 8), is somewhat unusual. We suggest that cross-links in the crystal domains may play some role in enhancing the melting temperature above 250 kGy. The cross-linking points in the crystal domains would hold the chains, reducing the mobility gain from the thermal energy, thus enhancing the thermal stability and requiring higher thermal energy to be melted [27].

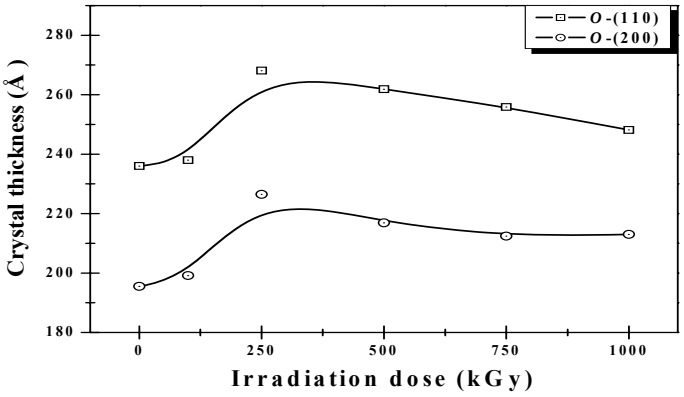

FIG. 8. Plot of crystal thickness ((010) & (200) plane) of electron beam irradiated UHMWPE vs. irradiation dose.

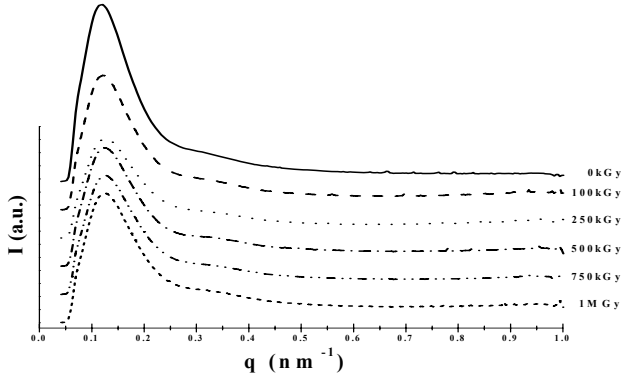

FIG. 9. Lorentz corrected small angle X-ray intensities of irradiated UHMWPE.

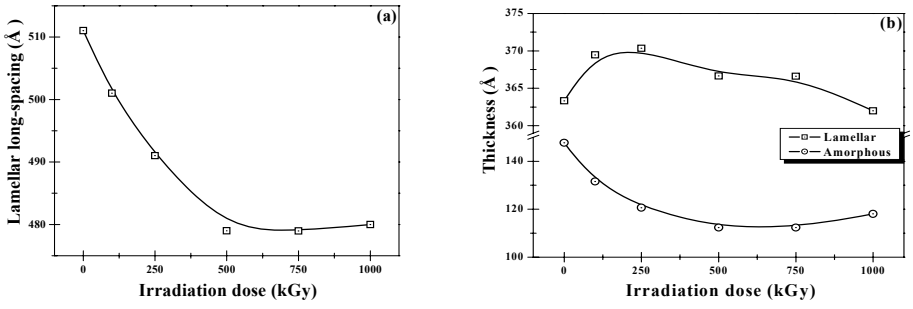

FIG. 10. Lamellar long spacing (a) and lamellar and amorphous layer thickness (b) of the irradiated UHMWPE.

3.3.Mechanical properties

Our results on structural modification suggest effective changes in mechanical properties of the irradiated specimens. For the mechanical properties, we performed a static uniaxial tensile experiment and a creep test. The creep test was carried out using a 4-step load method, which allows one to obtain long term creep effects by the short term test utilizing the Boltzman's superposition principle. Stress-strain curves (Figure 12) of the irradiated samples and mechanical parameters (Figure 13) such as modulus (a), fracture strain (b), and fracture stress (strength) (c) derived from the stress-strain curves are plotted. The modulus is increasing with the irradiation dose, but the fracture strain decreases. The results indicate that the polymer becomes stiffer by the electron beam irradiation. The initial stiffening at the low irradiation dose might be attributed to the crystal morphological changes, i.e. increase of crystallinity and the crystal domain size as well as the cross-linking. However, further increase in stiffness of the irradiated samples even at the high irradiation dose, where the crystallinity and domain size decay, do not correlate with the crystal morphological modifications (see Figure 7, 8 and 10). In Figure 14, the tensile moduli of the irradiated samples are plotted against the degree of cross-linking (gel fraction). The plot shows a good correlation between the two parameters throughout the entire irradiation dose range, suggesting that the increase of cross-linking plays the major role in enhancing the stiffness of the polymer chains by the electron beam irradiation. Fracture stresses (strength) of the samples shown in Figure 13-(c) reveal somewhat different pattern compared to the other mechanical parameters discussed above. The plot shows a maximum strength at 250 kGy and decays on further increase of the dose. The result suggests that the strength is rather related to the crystal morphology than the degree of cross-linking.

Results of creep test (4-step load at 2.94, 4.90, 6.86, 8.82 MPa) and creep strain taken at 5000 min for the load 8.82 MPa, are depicted in Figure 15-(a) and (b), respectively. The prestine sample (0 kGy) shows the highest deformation rate, while the irradiated samples show reduced deformation and the one of 1 MGy shows the lowest value. We also note that the creep resistance (Figure 15-(b)) increases rapidly with the irradiation up to 250kGy and only a minimal gain is observed with the further increase of irradiation dose. We recall that chain scission and cross-linking take place mainly in the amorphous area in this irradiation dose range and cause recrystallization. The increased creep resistance can be attributed to both crystal morphological change and cross-linking induced by the electron beam irradiation.

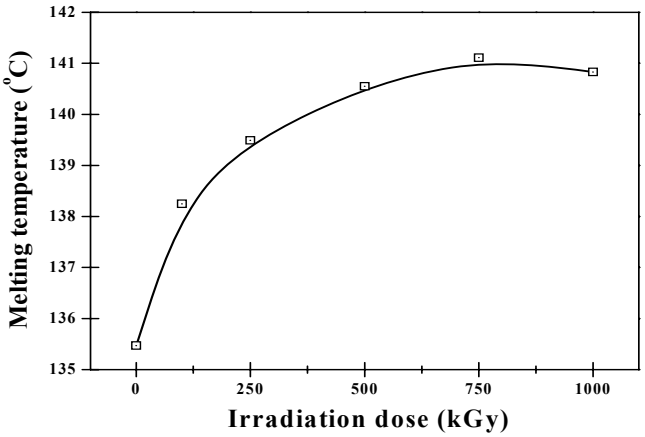

FIG. 11. Plot of melting point of irradiated UHMWPE vs. irradiation dose.

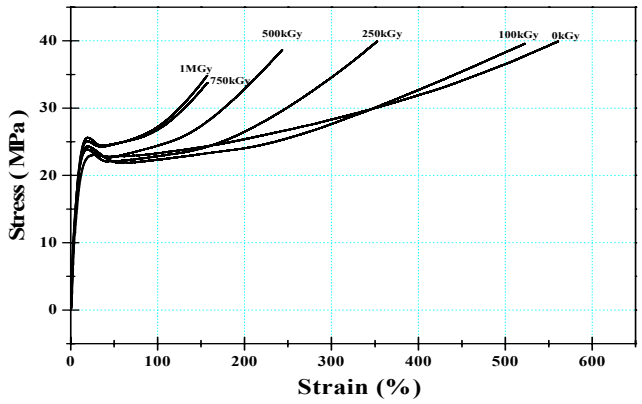

FIG. 12. Stress-strain curves of electron beam irradiated UHMWPE.

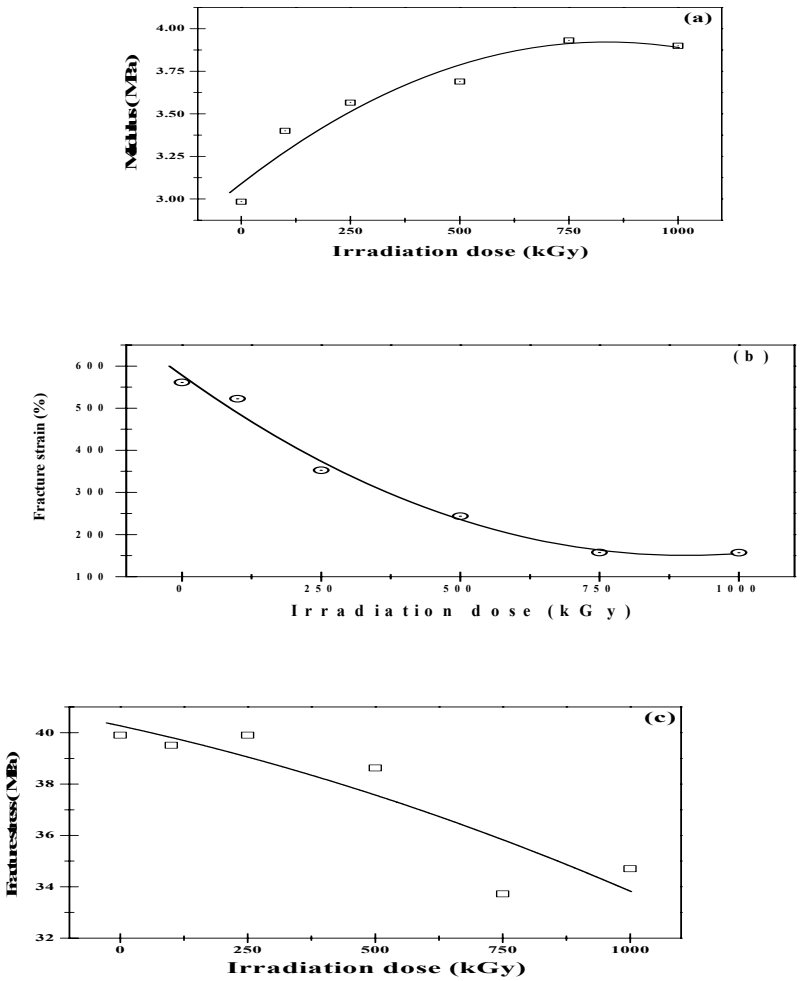

FIG. 13. Modulus (a), fracture strain (b), and fracture stress (strength) (c) vs. irradiation dose

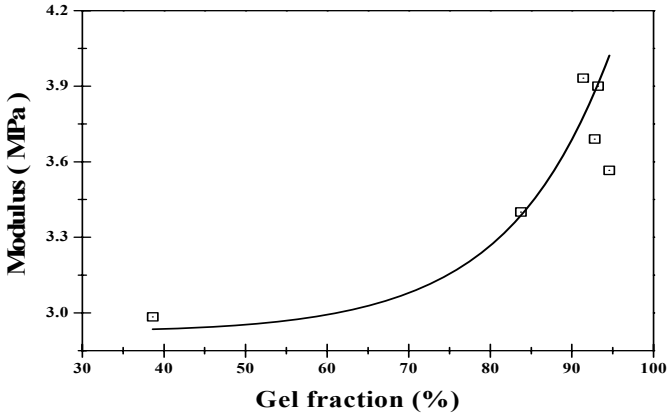

FIG. 14. Correlation between tensile modulus and gel fraction of irradiated UHMWPE.

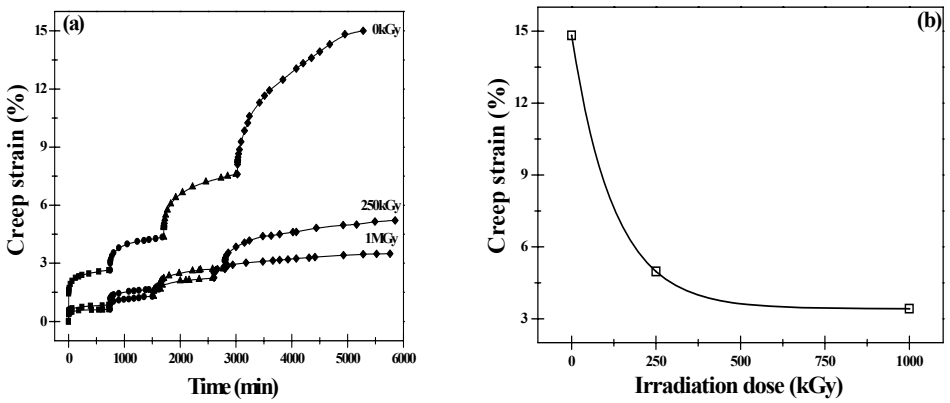

FIG. 15. Creep curves of irradiated UHMWPE by the step loads (a) and plot of creep deformations at 5000 min (b) vs. irradiation dose.

4. CONCLUSIONS

Structural modifications and related physical property changes in electron beam irradiated UHMWPE were studied. The cross-linking and crystal morphology changes were the main structural modifications induced by the irradiation. It appeared that 250 kGy is the optimum dose level to induce cross-linking very effectively in the amorphous region and recrystallization in the crystal domains. Above this dose level, the crystal domains are affected by the irradiation to result in cross-links in the crystal domains and reduction in crystal size and crystallinity. The stiffness (modulus and fracture strain) of the polymer chains was mainly dependent on the degree of cross-linking, while the fracture strength was more related to the crystal morphology. The creep resistance was also enhanced very effectively by the electron beam irradiation up to 250kGy and only minimal gain is observed above the optimum dose level.

REFERENCES

[1] Stein, H., UHMWPE; Engineered Materials Handbook; Vol.2: Eng. Plastics, ASM International (1992) 167-171.
[2] Lee, K. Y. J., KSTLE **14**(1998), 3, 46-50.
[3] McDonald, M.D., Bloebaum, R.D., J Biomed Mater Res **29** (1995), 1.
[4] Goldman, M, Gronsky, R.; Long, G..G..; Pruitt, L., Polym Degradation & Stability **62** (1998), 97.
[5] Harris, W.H., Clin Orthop **311** (1995), 46.
[6] Ikada, Y., Nakamura, K., Ogata, S., Makino, K., Tajima, K., Endoh, E., Hayashi, T., Fujita, S., Fujisawa, A., Mastlda, S., Oonishi, H., J. Po1ym Sci Part A **37** (1999), 159.
[7] Kang, P. H., Nho, Y. C., Radiation Physics and Chemistry **60** (2001), 79.
[8] Makhlis, F.A., Radiation physics and chemistry of polymers, New York: Wiley, (1975).
[9] Pruitt. L., Ranganatann, R., Mater Sci & Eng **C3** (1995), 91.
[10] Woo, L., Sandford, C. L., Radiation Physics and Chemistry **63** (2002), 845.
[11] Premnath, V., Bellare, A., Merrill, E.W., Jasty, M., Harris, W.H., Polymer **40** (1999), 2215.
[12] Auslender, V.L.et al., Rdiation Physics and Chemistry **63** (2002), 613.
[13] Dole, M.(Ed.), Radiation Chemistry of Macromolecules, Academic Press, New York (1972).
[14] Goldman, M., Gronsky, R., Ranganathan, R., Pruitt, L., Polymer **37** (1996), 2909.
[15] Elzubair, A., Suarez, J. C. M, Bonelli, C. M. C, Mano, E. B., Polymer Testing **22** (2003), 647.
[16] Mandelkern, L., In: Dole M, editor, The radiation chemistry of macromolecules. New York: Academic Press (1972), 287.
[17] Keller, A., In: Bassett DC, editor, Developments in crystalline polymers, London: Appl Sci **1**(1982), 37.
[18] Bhateja, S.K., Polymer **23** (1982), 654.
[19] Bhateja, S.K., J Appl Polym Sci **28** (1983), 861.
[20] Wang , Y.Q., Li, J., Mater Sci & Eng **A266** (1999), 155.
[21] Lewis, G.., Biomaterials **22** (2001), 371.
[22] Lu, S., Buchanan, F.J., Orr, J.F., Polym. Testing **21** (2002), 623.
[23] Roe, R.J., Methods of X-ray and Neutron Scattering in polymer science, New York: Oxford University Press (2000), 201.
[24] Stark, N.M., Matuana, L.M., Polym Degradation & Stability **86** (2004), 1.
[25] Sen, M., Basfar, A.A., Radia. Phys. Chem. **52** (1998), 247.
[26] Benson, R.S., NIM B **191** (2002), 752.
[27] Deanin, R.D. Polymer Structure, Properties and Applications, Cahners Publishing Company, Inc., Boston, Massachusetts (1972).

INFLUENCE OF RADIATION ON SOME PHYSICO-CHEMCIAL PROPERTIES OF GUM ACACIA. MITIGATION OF DEGRADATION BY DIFFERENT CLASS OF ANTIOXIDANTS IN LDPE EXPOSE TO IONIZING RADIATIONS

T. YASIN, S.AHMED
Polymer Processing and Radiation Technology LabACL, PINSTECH, IslamabadPakistan

Abstract

Controlling of degradation in polysaccharide is also gaining impetus from commercial point of view. Comprehensive studies on the influence of ionizing radiation on the physico-chemical properties of polysaccharides are very important for their applications in different industries. The effect of gamma radiation on gum acacia has been studied and its effect on some physico-chemical properties, as measured by UV spectroscopy and viscometry has been discussed. The gum samples are irradiated in the range of 5 kGy to 25 kGy both in air and vacuum. Samples irradiated under vacuum shows colour stability while viscosity remain unaffected.

1. INTRODUCTION

Gum Acacia has been known for many years and there are no artificial substitutes that match it for quality or cost of the production. There are more than 500 botanically known species of Acacias, distributed through out the tropical and subtropical areas of the world. The most common and commercial gum is derived from Acacia Senegal. Acacia Senegal gum is a natural gummy exudates obtained by tapping the branches of Acacia Senegal tree [1]. The trees are tapped during the dry season approximately from October to May or June of the following year. Gum exudation is favored by the dry hot weather while cold weather may completely stop the process.

Chemically gum acacia consists mainly of high-molecular weight polysaccharides made up of rhamanose, arabinose, and galactose, glucuronic and 4-o-methylglucuronic acid, calcium, magnesium, potassium, and sodium [1, 2]. The percentage of different sugar residues present in the gum molecule are 41-53 % D-galactose, 25-27 % L-arabinose, 10-14 % L-rhamnose and 12-18 % D-glucuronic acid [3]. Gum Acacia forms viscous solutions up to 60 % either by dissolving in water or absorbing their own volume of water [4]. Therefore, it can be regarded as 95% soluble fiber according to some recently available test methods. This is due to higher galactose content of gum acacia, which leads to a greater solubility, and hence the solution is possible even at low temperature. The relevance of studies on influence of gamma irradiation on gum originate from the fact that several thousands tons of the gums are utilized in different industry such as food, cosmetics, beverage and pharmaceutical applications [5]. Moreover the use of ionizing radiation as method of increasing shelf-life of food products is becoming increasingly acceptable and gamma irradiation has been suggested as a possible alternate to ethylene oxide for sterilization of gum. However, polysaccharides generally show a decrease in functional properties on irradiation due to attack by the free radicals generated during irradiation processing [6].

The aims of the study are to:

- Determine physicochemical properties of irradiated gum to assess the effect of irradiation on physicochemical and functional properties of gum Acacia and to see whether these changes add to the structure of gum acacia which make it more useful especially in the food industry; and
- Examine if there are any degradation changes in gum structure and to determine which parameters of gum Acacia are affected by irradiation.

2. EXPERIMENTAL

Commercially available gum Acacia was obtained from local market and used as such. Samples in solid state were irradiated to simulate the actual condition prevalent during sterilization of bulk quantities for industrial purpose.

2.1. Moisture content

500 mg of the same gum sample was heated at 110 ^{o}C for 10 minutes to achieve constant weight in an Infrared Moisture Determinator (Sartorius). Five determinations were carried out to calculate the moisture content.

Moisture content was calculated as percentage by using the following formula

$$\text{Moisture content (\%)} = 100 \times (W_1 - W_2)/W_1$$

Where W_1 is the original weight of the sample W_2 is the weight of sample after changing.

2.2. Viscosity measurement

Viscosity was measured using U-tube viscometer (type BS/IP/U, serial No. 2948) with the flow time for 1% aqueous solution of sample at room temperature (25 ^{o}C). The relative viscosity (η_r) was then calculated using the following equation:

$$\eta_r = (T - T_o)/T_0$$

Where T is the travel time of solution and T_o is the travel time of pure solvent.

2.3. Ultraviolet absorption spectra

Absorption spectra of 1% gum solution were determined using a Perkin Elmer spectrophotometer at 220 nm.

3. RESULTS AND DISCUSSION

Polysaccharides are degraded when exposed to ionizing radiation either in dry form or in solution [7, 8]. A number of factors (such as moisture, temperature, presence of oxygen etc) control the chemistry of chemical processes during irradiation. These factors affect the results and are very important for reproducible results.

The moisture content of the gum samples before and after irradiation is presented in Table I. This table shows that the percentage of moisture contents is almost constant in different gum samples ranging from 4.39 % to 5.34 %. This consistency in moisture content indicate that any difference in behavior of the polymers on irradiation is not due to differences in the amount of water available for free radical formation.

TABLE I. MOISTURE CONTENTS OF GUM ACACIA

Sample	Dose of Irradiation (kGy)	Moisture Contents (%)
A	Control	5.19
A`	5 kGy	4.39
B	Control	4.47
B`	10 kGy	5.15
C	Control	5.23
C`	15 kGy	5.34
D	Control	5.03
D`	20 kGy	5.17

The ultraviolet absorption spectrum of the gum samples shows two absorption peaks, one at 220 nm and second at 263 nm. Maximum absorbance was observed at 220 nm as compared to 263 nm and 220 nm wavelength is selected to calculate the absorption results. The effect of gamma irradiation on absorbance of Gum Acacia at 220 nm is presented in table II.

TABLE II. EFFECT OF GAMMA IRRADIATION ON ABSORBANCE OF GUM ACACIA AT 220 NM

Sample	Dose of irradiation (kGy)	Absorption (in air)	Absorption (in vacuum)
A	5	2.406	2.229
B	10	2.418	2.205
C	15	2.574	2.238
D	20	2.691	2.247
E	25	2.731	2.228

It can be seen from the table that the gum samples on irradiation without exclusion of air from 5 to 25 kGy demonstrated a progressive increase in coloration. A degree of linearity was observed on increasing the dose of irradiations. This change in absorption spectra may originate from transformation of an organic compound into more conjugated structure in the presence of air, which needs to be avoided. Color change is also an organoleptic property, which is considered unfavorable by consumer, and thus a disincentive. The gum samples irradiated with exclusion of air shows consistency in absorption.

Generally, polysaccharides either in dry form or in solution degrade under irradiation that results in the decrease in the molecular weight. This decrease in molecular weight can be monitored by viscometry or by gel permeation chromatography. The results of relative viscosities of the control as well as samples irradiated at different doses are summarized in table III. It can be seen from the table that no significant change in viscosity was observed in solid gum samples irradiated even to the high dose of 20 kGy. Table IV shows the results of viscosity of these samples irradiated at different doses in the presence and absence of air. Lack of pronounced change indicates absence of any physical change detrimental to the viscosity of the gum. It may be important to remark here that a decrease in viscosity with increasing irradiation doses in the ranging of 2 to 10 kGy has been reported for guar gum and locust bean gum [5].

TABLE III. EFFECT OF GAMMA IRRADIATION ON VISCOSITY OF GUM ACACIA

Sample	Dose of Irradiation (kGy)	Viscosity
A	Control	1.18
A`	5 kGy	1.18
B	Control	1.13
B`	10 kGy	1.12
C	Control	1.17
C`	15 kGy	1.16
D	Control	1.16
D`	20 kGy	1.17

TABLE IV. EFFECT OF GAMMA IRRADIATION ON VISCOSITY OF GUM ACACIA

Sample	Dose of irradiation (kGy)	Viscosity (in air)	Viscosity (in vacuum)
A	5	1.18	1.14
B	10	1.12	1.09
C	15	1.16	1.14
D	20	1.17	1.15
E	25	1.14	1.07

As mentioned earlier that dilute aqueous solution of polysaccharide degrades more under irradiation. Aqueous solution with polymer concentration 1 % is irradiated at different irradiation doses to see its effect on viscosity. The results are tabulated in table V. The results show a slight decrease in viscosity and nearly constant at higher doses. Little is known about this specific behavior but it can be concluded from the table that specific polysaccharide amongst different polysaccharides present in gum will degrade into lower molecular weight fragments and lower viscosity. No effect on viscosity is observed as irradiation dose is increased as the quantity of this polysaccharide is constant in all samples and the effect is consistent.

TABLE V. EFFECT OF GAMMA IRRADIATION ON VISCOSITY OF GUM ACACIA IN 1 % SOLUTION

Sample	Dose of irradiation (kGy)	Viscosity
S1	5 kGy	1.07
S2	10 kGy	1.06
S3	15 kGy	1.06
S4	20 kGy	1.07
S5	25 kGy	1.08

4. CONCLUSIONS

UV spectroscopic analysis of the gum samples irradiated without exclusion of air from 5-25 kGy demonstrated progressive increase in coloration at 220 nm, whereas the gum samples irradiated at the same doses under vacuum show stability in colour. This shows that discoloration can be avoided if the samples irradiated under vacuum. No significant change in viscosity was observed in gum samples irradiated even at a high dose of 25 kGy. This indicates the absence of any physical change detrimental to the viscosity of the gum.

REFERENCE

[1] GABB, S. (1997). Gum Production in Sudan: A brief introduction. The Sudan Foundation, London.

[2] GOLDSTEIN, A.M, ATLER, E.N., SEAMAN, J.K., In Industrial Gum (Whistler, R.L., BeMiller, J.N., ed.) Academic Press, New York, (1973) 303-321.

[3] ANDERSON, D.M.W. BRIDGEMAN, M.M.E.; FARGUHAR, J.G., MCNAB, C.G.A. (1983). Int. Tree Crops J., Edinburgh Univ., 2: 245-254.

[4] GAC Gum Arabic Company (1993). Gum Arabic: A product of nature. The Gum Arabic Company Ltd. Khartoum.

[5] KING, K., GRAY, R, Food Hydrocolloids, 6/6 (1993) 554-569.

[6] DAUPHIN,J,F. SAINT-LOBE,L.R., In Radiation Chemistry of Carbohydrates. (Elias, P.S., And Cohan, A.J. eds), Elsevier Scientific, Amsterdam, (1977) 131-172

[7] CHOI, W.S., AHN, K.J., LEE, D.W., BYUN, M.W, PARK, H.J., J Polymer Deg. Stab., 78 (2002) 533-538

[8] WASIKIEWICZ, J.M., YOSHII, F., NAGASAWA, N., WACH, R.A., MITOMO, H., Rad. Phys. Chem., 73 (2005) 287-297

MITIGATION OF DEGRADATION BY DIFFERENT CLASS OF ANTIOXIDANTS IN LDPE EXPOSE TO IONIZING RADIATIONS

T. YASIN, S. AHMED
Polymer Processing and Radiation Technology LabACL, PINSTECH, IslamabadPakistan

Abstract

Low density polyethylene develops extensive yellowing in the sunlight. The photo-oxidation and yellowing of polyethylene film in the presence of different antioxidants upon a radiation was monitored by yellowness index tester in order to study the stabilization mechanism of different groups of antioxidants.

1. INTRODUCTION

Approximately 70 % of LDPE are employed in film manufacturing. These films are used for various purposes, e.g. packaging and as covers [1]. For sterilization applications, the polymer must be capable of withstanding sterilization procedures, which are used to destroy pathogens. In present practices, that is usually means withstanding 10-50 kGy of gamma or EB radiation. During the irradiation process, oxidative degradation takes place with potential loss of mechanical properties and discoloration [2]. Appropriate stabilizing additives are necessary for stabilization of properties and to avoid discoloration during irradiation and storage.

Antioxidants are of great importance in the manufacture of various plastic but primarily in their stabilization/clarity according to the application of the final product. They are divided into two large groups with respect to the mechanism of their action. The first include those which terminate the oxidative chain by reacting with free radicals at the stage of their formation e.g. the amine and phenol types, the second group includes substances either preventing the decomposition of hydroperoxides by a radical mechanism or decomposition hydroperoxide into products that are inactive for development of an oxidizing chain. These are sulphides, thiosulphates and salts of dialkyl dithiocarbamic acid.

In our lab Irganox 1010 has been incorporated in a formulation containing LDPE/EVA, flame retardant and crosslinking agent TMPTMA, crosslinked by gamma radiation to produce flame retardant cable and wire insulation [3-5]. Extension to produce sheets, films, of the product prompted us to look into the colour development characteristics of other well known antioxidants in comparison with Iragnox 1010.

The present paper concerns the efforts directed towards the rectification of the problems of discoloration and instability observed in the case of LDPE irradiated by gamma and electron beam irradiation. The colour contributions of several model antioxidants to LDPE were measured and the structural feature which likely responsible for colour development were identified.

2. EXPERIMENTAL

LDPE was from Nippon Unicar Company Ltd. The antioxidants used are listed in Table I and were obtained from Sumitomo Chemical Co. Ltd. Japan and Nocceler, Japan. All the chemicals/reagents were used as such without further purification.

TABLE I. TYPES OF ANTIOXIDANTS

Type	Commercial name	Chemical structure
AO1	NOC EZ	(Diethyl-dithio-carbamate) Zinc
AO2	NOC BZ	(Di-n-butyl-dithio-carbamate) Zinc
AO3	NOC S	(Dimethyl-dithio-carbamate) Sodium
AO4	NOC SDC	(Diethyl-dithio-carbamate) Sodium
AO5	Sumilizer TPS	Distearyl 3,3'-thiodipropionate
AO6	NOC TT	Bis(dimethylthiocarbamoyl)disulphide
AO7	NOC NS-6	2,2'-methylene-bis(4-methyl-6-tert-butylphenol)
AO8	NOC NS-5	2,2'-methylene-bis(4-ethyl-6-tert-butylphenol)
AO9	Antage DAH	2,5-di-tert-amylhydroquinone
AO10	Sumilizer BP-101	Tetrakis[methylene-3-(3,5-di-tert-butyl-4-hydroxyphenyl)propionate]methane
AO11	Sumilizer Ga-80	3,9-bis{2-{3-(3-tert-butyl-4-hydroxy-5-methylphenyl)-propionyloxy}-1,1-dimethyl]-2,4,8,10-tetraoxasipiro[5.5]undecane

2.1.Preparation of samples and irradiation

Antioxidants were added by blending with LDPE at 130 ºC using laboplastomill (Toyoseiki Co. Ltd. Japan) for three minute. The concentration of antioxidants used was 0.2 %. The admixture samples were pressed at 150 kgf/cm^2 by using hot press (Toyoseiki Co. Ltd.) for three minutes using a spacer of 0.5 mm. Then immediatly cooled between the two plates of a cold press at 25 ºC for five minute at the same pressure.

2.2.Irradiations

Irradiation with gamma rays was carried out using a dose rate of 10 kGy/h. Irradiation by electron beam was carried out by a Cockrofit- Walton type accelerator (2 MeV, 30 mA) operated at 1 mA current and acceleration energy of 1 MeV by repeating 10 kGy/pass (143 kGy/s) to prevent heating resulting from thermal accumulation.

2.3.Yellowness index measurement

Three round-shaped specimens were used for measurement of yellowness index. The YI measurement was carried out on GARDNER XI-10 Colorimeter according to ASTM D1925-70.

3. RESULTS AND DISCUSSION

Table II and III shows the effective of thiocarbamate and Sulfide type antioxidants on color development during gamma and EB radiation exposure. It can be seen from the table II that yellowness index (YI) of polyethylene without any antioxidants is around 29.08. By adding AO1 in PE the YI value increase from 29.08 to 45.37 at 10 kGy, show that colour stability is greatly effect by the antioxidant and very slight change, further showing colour stability up to 50 kGy. Same trend is observed when subjected to EB irradiation. By comparing the YI values of AO1 and AO2, shows decrease from 45.37 to 28.19 at 10 kGy.

This difference in YI value may be attributed to the change in electron density resulted from ethyl to butyl group. As electron donating ability of butyl is greater than ethyl, therefore colour stability in AO2 is higher than AO1. Slight difference in YI is observed in case of AO3 and AO4. In AO3 and AO4, ethyl group of the AO4 is responsible for contributing more stability to the antioxidant and YI is slightly lower. The role of metal component in antioxidant is also very important and this can be seen by comparing the results of AO1 with AO4. In theses antioxidants the organic moiety is same and only the metal is changed from zinc to sodium, which resulted a decrease in YI from 45.37 to 25.70. Generally, an increasing trend is observed with the increase of dose rate from 10 to 50 kGy. This increase shows that the amount of antioxidants consumes with the increase of irradiation dose from 10 to 50 kGy. The brightness follows similar trends like YI (Table III)

TABLE II. EFFECT OF THIOCARBAMATE AND SULFIDE TYPE ANTIOXIDANTS ON COLOR DEVELOPMENT DURING GAMMA AND EB RADIATION EXPOSURE

Antioxidant	Gamma-Irradiation			EB-irradiation		
	10 kGy	25 kGy	50 kGy	10 kGy	25 kGy	50 kGy
Control	29.08	29.52	28.43	28.85	28.01	29.54
AO1	45.37	38.80	40.43	41.13	44.61	40.00
AO2	28.19	29.55	25.53	27.03	27.33	30.20
AO3	26.57	34.91	32.13	35.83	34.73	33.85
AO4	25.70	28.33	25.29	30.39	27.50	27.72
AO5	28.87	26.12	25.67	30.46	30.14	28.03
AO6	33.30	33.44	33.89	38.10	38.60	38.85

In sulfide type antioxidants, the YI shows a slight increase with the increase of gamma radiation as observed in AO5 and AO6. Slightly higher values of YI in case of AO5 and AO6 are due to their complete organic nature. Heat stability is also one of the major characteristic for the choice of antioxidant to colour plastic materials. In general, organic antioxidants/additives are relatively more sensitive to heat than inorganic ones. So, the chances of degradation of organic antioxidants are greater. Inorganic antioxidants are relatively more stables and the stability is higher for those having less reactive group. The stability of colour depends also on the stability of the polymer and of further additives present in the plastic materials. Sulfur containing antioxidant function by catalytically decomposing hydroperoxide.

TABLE III. EFFECT OF THIOCARBAMATE AND SULFIDE TYPE ANTIOXIDANTS ON BRIGHTNESS DURING GAMMA AND EB RADIATION EXPOSURE

Antioxidant	Gamma-Irradiation			EB-irradiation		
	10 kGy	25 kGy	50 kGy	10 kGy	25 kGy	50 kGy
Control	33.85	34.58	29.39	32.58	31.04	34.63
AO1	44.05	49.31	44.90	45.24	46.94	51.14
AO2	32.93	34.98	30.48	33.32	34.24	35.47
AO3	35.61	38.13	36.16	40.90	38.38	40.01
AO4	28.74	33.71	32.84	32.46	30.79	30.24
AO5	36.72	31.44	30.09	40.62	36.45	32.23
AO6	35.29	42.74	41.07	44.07	47.12	42.97

Hindered phenolic antioxidants have been shown to be effective in protecting polymer against the degrading effects of irradiation. In this work five structurally different phenolic antioxidants were tried and their effect on yellowness index and brightness is shown in table IV and V respectively.

TABLE IV. EFFECT OF PHENOLIC ANTIOXIDANTS ON COLOR DEVELOPMENT DURING GAMMA AND EB RADIATION EXPOSURE

Antioxidant	Gamma-Irradiation			EB-irradiation		
	10 kGy	25 kGy	50 kGy	10 kGy	25 kGy	50 kGy
AO5	39.48	39.87	51.77	24.70	27.87	30.25
AO6	29.10	25.92	27.78	28.09	26.40	28.08
AO7	27.67	28.84	26.21	25.90	27.50	28.47
AO8	28.89	25.63	27.35	28.14	27.38	26.75
AO9	26.83	26.12	26.92	24.18	26.83	26.88

TABLE V. EFFECT OF PHENOLIC ANTIOXIDANTS ON BRIGHTNESS DURING GAMMA AND EB RADIATION EXPOSURE

Antioxidant	Gamma-Irradiation			EB-irradiation		
	10 kGy	25 kGy	50 kGy	10 kGy	25 kGy	50 kGy
AO5	39.08	34.48	36.42	33.28	30.33	32.34
AO6	36.53	32.57	31.28	30.86	32.87	31.86
AO7	36.16	38.89	34.38	31.24	35.61	33.33
AO8	37.04	33.88	36.19	34.83	34.15	30.66
AO9	36.44	31.44	36.58	34.31	31.01	30.88

The colour data in table IV attribute color development during gamma/EB irradiation to be a property of the incorporated additives. Antioxidant AO7 and AO8 are identical structure except at para position i.e., AO8 has ethyl group instead of methyl in AO7. The oxidative transformation products are identical in both the case but the significant colour development in AO7 can be explained by the stabilization of the oxidative transformational products by methyl group by hyperconjugation. AO9, AO10 and AO11 have almost same colour data, which show that their oxidative transformation products is stable and electron cannot be delocalized due to their non planar structure.

4. FUTURE PLAN

- Identify the compounds produced during irradiation by the use of thin layer chromatography or by HPLC
- Effect of gamma irradiation on swelling of gum samples at different doses and their comparison with solid state.
- Study the synergist effect of antioxidants by using a different combination of primary and secondary antioxid

REFERENCES

[1] GUGUMUS F., In Plastic Additives Handbook, (Gächter R., Müller H., Ed.), (1990) 1-100

[2] CLOUGH R.L., GILLEN K.T., MALONE G.M., WALLACE J.S., "Color Formation in Irradiated Polymers", Radiat. Phys. Chem. **48** (1996) 583-594.

[3] SHAMSHAD A, FUZAIL, M., YASIN, T., "Protection of LDPE Wire Insulation by Hindered Phenol (Irganox 1010) And Hindered Amine Tinuvin 770 Blend With Irgafos 168 Against Damage From Ionizing Radiation", technical paper published internal report of the 1st RCM of the CRPF 2.20.39 held in Vienna, Austria 8-11 Dec 2003.

[4] SHAMSHAD A, YASIN, T., GHAFFAR, A., "Radiation effects on hindered phenols in paraffin oil, wax and LDPE" Radiation Physics and Chemistry, 68, 925-931, 2003

[5] SHAMSHAD A, FUZAIL, M., YASIN, T., "Development of Polyolefin Based Radiation Crosslinked Flame-retardant Formulations for Wire Insulations" Congress ICRR 2003, 17-22 August, Brisbane (Australia).

DEGRADATION OF POLYPROPYLENE BY IONIZING RADIATION

G. PRZYBYTNIAK, Z. ZIMEK, A. RAFALSKI, K. MIRKOWSKI
Institute of Nuclear Chemistry and Technology, Warszawa, Poland

Abstract

Protection of polypropylene against effects of ionizing radiation requires effective additives that inhibit radical processes. Hindered amine light stabilizers are considered as the agents fulfilling such demands. We found that they scavenge radicals in amorphous phase of isotactic polypropylene, decrease radiation damage determined on a basis of apparent viscosity reduction and facilitate nucleation. Other aspect of polypropylene degradation was studied in its blends with elastomer styrene-butadiene-styrene (SBS). The phase separation results in independent and parallel radiolysis of both components. The post-irradiation effects in polypropylene proceed faster if it is a constituent of PP/SBS blend; in consequence the degradation of polypropylene is then inhibited.

1. INTRODUCTION

Polypropylene is used in a very wide range of medical devices and drug packaging. In order to ensure an acceptable level of bioburdens all medical disposable materials need to be sterilized. For last decade ionizing radiation has been increasingly used to sterilize medical products either by gamma rays or by electron beams. However, conventionally stabilized polypropylene is not appropriate for exposure to radiation due to its fast degradation [1, 2, 3]. There are two stages of the process: loss of integrity during irradiation as a consequence of direct scission and post-irradiation effect results from reactions of residual radicals characterized by two kinetics – fast in amorphous phase of polypropylene and slow in crystalline one [4]. Many additives are applied to control the processes; usually these are radiation stabilizers revealing antioxidant properties. Primary antioxidants are responsible for protection of the polymer backbone whereas secondary antioxidants decompose hydroperoxides that are produced from alkyl radicals upon oxidation. Widely used hindered phenolic antioxidants [5] following irradiation are the source of discoloration of polypropylene. Therefore modern resins contain rather hindered-amine light stabilizers (HALS). Secondary and tertiary hindered amines of the piperidyl type and many other piperidyl compounds can protect various polymers against oxidation initiated by light. However, polymer chain scission induced by ionizing radiation is generally believed to proceed similar to photo-oxidation. The polypropylene might be functionalized by maleic anhydride, a compatibilizing agent capable of forming covalent or hydrogen bond with amine groups. Its role as an agent supporting influence of HALS has been studied.

There are several factors that increase radiation tolerance of polypropylene: narrow molecular-weight distribution, reduction of crystallinity, copolymerization with ethylene, etc. The other way to achieve the resistance to ionizing radiation of polypropylene might be mixing with elastomers. They are usually much more radiation tolerant than polyolefines. Special role in elastomers can play phenyl ring, which increases stability to radiation due to participation in the dissipation of energy [6]. Therefore styrene-butadiene-styrene triblock copolymer (SBS) in blend with polypropylene (PP) should induce desired properties of resulting material. Protective role of the elastomer towards polypropylene needs insight into radiation chemistry of the materials. Blends polypropylene with elastomers must comprise two phases because of their different thermodynamical properties. One can expect that the ratio of constituents determine properties of blends unless phase between two separate segments is formed.

The aim of present work is to study the effect of low dose irradiation on radical processes in the polypropylene stabilized by HALS or in blended with radiation resistant elastomer. It is well known that generation of free radicals in the materials ultimately results in changing physical and mechanical properties [7-9].

However the mechanisms of the processes, especially the possibility of paramagnetic center transfer between components of resulting material, might lead to detailed characteristics of their radiolysis. The work also deals with the analysis of the effect induced by irradiation on rheology and on phase transitions of modified polypropylene.

2. MATERIALS AND METHODS

2.1. Materials

Polypropylene Malen P J601 (isotacticity 96%) was purchased in Basell Orlen Polyolefines, stabilizers Tinuvin 622 (T622), Tinuvin 675 (T675) and Chimassorb 944 (C944) in Ciba Specialty Chemicals and maleic anhydride (MA) in Fluka. Mixing of materials was carried out using mixer and extruder (PLV-151 Brabender). The mixture was then compressed into sheets. Concentration of additives is express as the parts per hundred resin (phr). Blends were prepared from styrene-butadiene-styrene (SBS) linear copolymer (Shell Chemical Co., Cariflex 1102) and isotactic polypropylene (Petrochemia Płock S.A., Malen J 400). They contain different proportions of components that were twice mixed in a single-screw extruder at 170 ^{o}C. The samples for EPR measurements were prepared in form of rod.

2.2. Irradiation

Irradiation with 10 MeV electron beam was made using a linear accelerator LAE 13/9 in air at ambient temperature.

2.3. EPR measurements

The first EPR spectra were measured 20 min upon irradiation. Irradiated samples were inserted into EPR tubes and their signals were measured using EPR spectrometer ESP 300 with rectangular cavity TE102. The number of accumulations and amplification was always adjusted according to the intensity of the signal. Relative radical concentration and analysis of the experimental spectra were performed by comparing the spectral areas obtained by double integration using the program Apollo. Decay of radicals was monitored either for 9 days (modified polypropylene) or for 6 days (PP/elastomers blends).

2.4. Rheological properties

The Melt Flow Index (MFI) test was carried out under a load of 2.13 kg for 10 min at 230 ^{o}C. Apparent viscosity was measured with CAP 2000+ Brookfield viscosimeter at temperature indicated in figures.

2.5. Differential scanning calorimetry

For the thermal analysis of polypropylene containing stabilizers a calorimeter TA Instruments MDSC was used. The measurements were carried out at a heat rate of 10 ^{o}C/min under nitrogen gas. About 5 mg samples were placed in aluminum pan before being put in the cell. For the first run the cell was heated from ambient temperature to 200 ^{o}C and subsequently cooled to initial temperature. Then the second run was performed applying the same conditions as during the first cycle.

3. RESULTS AND DISCUSSION

The ESR spectra of neat polypropylene recorded at ambient temperature, following irradiation at the same temperature, show the presence of superimposed signals of alkyl radical, Fig.1. The most intensive pattern in form of octet represents tertiary alkyl radical $–CH_2C^{\bullet}(CH_3)CH_2–$ [10].

Weaker signals belong to much less populated radicals –CH2CH•CH2–, –CH(CH3)CH2•, –CH2CH(CH3) • and –CH2C•H(CH3). Spectra recorded 3 hours and 3 days after irradiation reveal significant difference due to oxidation of all alkyl radicals leading to production of peroxyl radicals. In isotactic polypropylene two various phases occur - ordered domains of the crystalline phase and variety of amorphous sites. Thus, there are two types of ≡COO• radicals situated in the totally different vicinity. Random orientation of macromolecules in the amorphous phase facilitates peroxyl radical mobility and involves their faster decay. Therefore the central part of spectrum C, Fig. 1, corresponded ≡COO• radical disappears just after 6 days. Signal D, Fig.1, belongs also to peroxyl radicals, but situated in the crystalline phase. Defined rigid structure delays the combination of paramagnetic species and the unpaired spin can be transferred to other sites inducing subsequent damages for months. The reactions of peroxyl radicals are responsible for generation of the polar groups in hydrocarbon polymer and for the chain scission. On a basis of EPR results it is difficult to estimate the relative contribution of primary processes and post-irradiation effects in main chain breakage. The insignificant content of –CH(CH3)CH2• and –CH2C•H(CH3) components indicate that initially, just after irradiation, the level of scission should not be high. It seems that the breakage occurs mainly via oxidation and movement of paramagnetic centers (for days in amorphous phase and for several months in crystals).

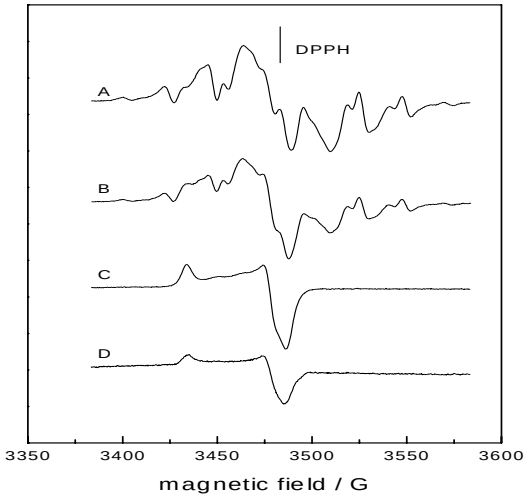

FIG. 1. EPR spectra of polypropylene irradiated at ambient temperature with a dose of 30 kGy.(A) after irradiation, (B) 3 hours, (C) 3 days, (D) 9 days upon irradiation.

Thus oxidative damage is the main reason for applying antioxidants as the radioprotective agents in polypropylene. HALSs are well known radical scavengers that both inhibit the propagation of free radicals and act as a scavenger [11]. Unexpectedly, in presence of the stabilizers the EPR spectra of modified polypropylenes do not change. Only intensities of radical signals are different. TableI presents changes in relative contribution of the intermediates for selected samples.

The amount of peroxyl radical considerably decreases in presence of modifiers, especially if there are T622 and C944 in the system. After 6 days the influence was not observed taking into account the error of the method. These results have been tentatively interpreted in terms of interaction of stabilizers with the polypropylene radicals. Decrease in population of paramagnetic intermediates in presence of HALS results from conversion of amines into nitroxide compounds following reaction with peroxyl radicals. Product subsequently binds to another radical inhibiting chain processes.

TABLE I. RELATIVE CONCENTRATION OF RADICALS IN NEAT AND MODIFIED POLYPROPYLENE IRRADIATED WITH A DOSE OF 25 KGY (NORMALISED TO THE CONTENT IN NEAT POLYPROPYLENE)

Sample	Peroxyl radical concentration [%]	
	3 hours following irradiation	6 days following irradiation
PP	100	19
MA, 0.30 phr	84	20
T622, 0.50 phr	70	24
C944, 0.50 phr	57	22

HALS stabilizers due to radical processes form nitroxyl radicals. Assuming homogenous distribution of modifiers added to polypropylene, we found unambiguously that above process undergoes predominantly in amorphous phase as in presence of hindered amines significant decrease of peroxyl radical signal characteristic for just this phase was observed. On the other hand, influence of additives on free radical processes in crystalline domains was not confirmed. Nevertheless, in the longer period of time one can not exclude analogous effect in crystalline phase since small intensity of EPR spectra precludes quantitative determination of such influence. It was found that Chimassorb 944 exhibits the highest effectiveness in termination of radical processes in random oriented, amorphous sites.

Free radical processes determine many physical properties, e.g. phase transitions. According to Yagoubi et al. [12] upon irradiation melting point in the crystalline phase of polypropylene is lower due to degradation process occurring in the crystals and growth of their imperfection. Analysis of our results leads to conclusion that relative insensitivity of measured melting points was considered as a consequence of preferential degradation in amorphous phase. In DSC results melting endothermic peaks shift slightly towards lower temperatures, Fig.2. In the second run the differences are more pronounced since for unirradiated samples the curve becomes broader whereas for irradiated one two clear peaks appear. In presence of stabilizers usually peaks are split and two or even more extremes are formed. This effect appears to indicate for more structural heterogeneity in the irradiated product. During slow cooling after melting in first cycle, the rearrangement of molecules occurs what results in better separation of different order domains. Melting peaks for samples containing HALS seam to indicate that in these cases process is more efficient.

Crystallization temperatures before and after irradiation are comprised in Tab. 2. During first and second run the maximal values are almost the same so only the average temperature is shown (variations do not exceed 0.5^{o}C). However admixture of HALS increases crystallization temperature even of 10^{o}C. The effect is very distinct for both Tinuvines, smaller or negligible for Chimassorb and maleic anhydride, depending on concentration. We conclude that Tinuvine stabilizers act as a nucleating agent facilitating formation of microcrystals. Nevertheless, the additives partly loss the nucleating properties upon ionizing radiation and crystallization temperature once more decreases. The effect is similar to that observed for benzoic acid by Ahmed et al. [13]. However for that agent the increase in concentration extends range of nucleation, contrary to HALS, Tab.2. It was found that polypropylene comprising nucleating agent is less stable upon irradiation than without such admixture. On the other hand the stabilizers acting as the antioxidants should protect polypropylene from degradation, thus the final effect depends on these two opposite tendencies. Although the enthalpies of crystallization for all studied samples are comparable and situated in the range of 77-80 J/g, the shape of crystallization peaks for irradiated samples is changing. Usually for irradiated polymers the peak is more intensive and narrower than for unirradiated samples, due to reduction of molecular weight distribution. Comparable values of enthalpy obtained for the first and second heating scans indicate that material has been enough processed and show a well balanced interface contact.

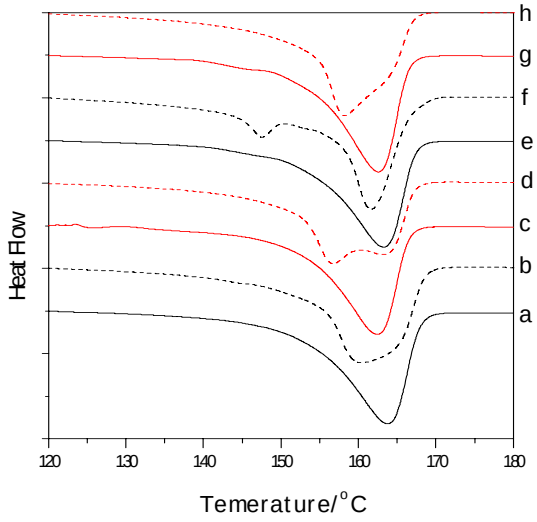

FIG. 2. Endotherms of PP (a, b, c, d) and PP+T622 (e, f, g, h) before (a, b, e, f,) and after irradiation (c, d, g, h) with a dose of 25 kGy. Full lines – first cycles, dot lines – second cycles.

TABLE II. CRYSTALLIZATION TEMPERATURES OF NEAT AND MODIFIED POLYPROPYLENE, BEFORE IRRADIATION AND 72 DAYS AFTER IRRADIATION.

Sample	Dose of irradiation [kGy]	Tc [°C]
PP	0	116.8
	25	116.4
T622, 0.50 phr	0	125.0
	25	119.7
T622, 0.75 phr	0	124,5
	25	119.8
T 765, 0.50 phr	0	126.9
	25	115.1
T 765, 0.75 phr	0	125.2
	25	115.6
C944, 0.50 phr	0	121.4
	25	115.5
C944, 0.75 phr	0	117.1
	25	114.6
MA, 0.30 phr	0	117.6
	25	115.3
MA, 0.50 phr	0	121.0
	25	114.9

MFI depends on the composition of polypropylene and on molecular weight that reduced significantly during irradiation. Its value is approximately inversely proportional to the apparent viscosity in molten state. As rheologic properties determine the flow properties, both measurements were performed to characterize degree of degradation upon irradiation. MFI values are present in Fig. 3. The studied additives diminish MFI in different degree. The most efficient radioprotector seems to be T765, the worse C944. However the results must be considered from processing point of view. T765 is liquid whereas C944 and T622 exist as the powers so their dispersion in polypropylene during mixing might be suppressed what has to influence on the observed effects.

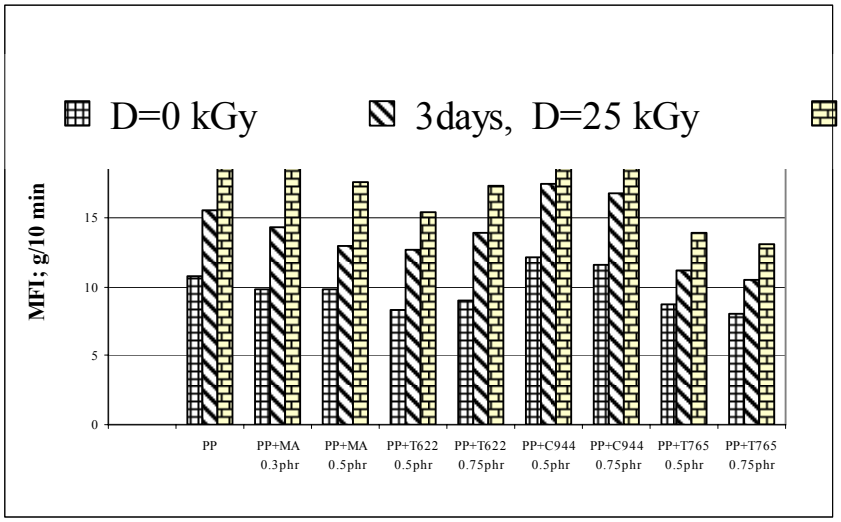

FIG. 3. MFI determined before irradiation at 230 °C and 3 and 72 days following irradiation at 180 °C.

More degraded polymer exhibits lower viscosity [14]. As seen from Fig. 4 the relationship is strong. At 200 oC, for constant shear rate equal 33 s-1, the apparent viscosity of neat polypropylene initially reaches 470 Pa•s. The addition of stabilizers usually enhances viscosity in the whole measured range of time. Only in presence of 0.5 phr MA and 0.75 phr T765 the apparent viscosity of polymer is smaller. However in both cases flow curve flatten in time indicating resistance for shearing and heating similar to neat PP, Fig 4A. The relationship viscosity - time of shearing is particularly strong at the beginning of measurement.

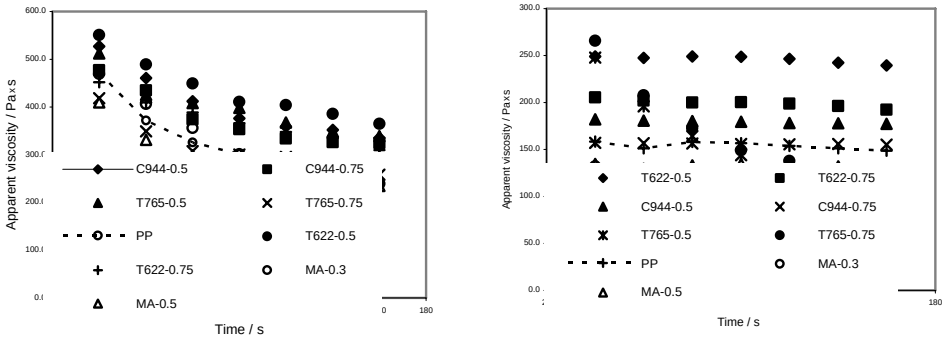

FIG. 4. Relationship between time of shearing and apparent viscosity for neat and modified polypropylene (A) before irradiation, (B) 72 days after irradiation with a dose of 25 kGy; t = 200 °C, shear rate 33 s^{-1},

Following irradiation the molten state viscosity drastically decreases. For neat polymer its value is three times diminished and in presence of 0.5 phr T622 twice. At both studied concentrations of T765 samples exhibit sensitivity towards shearing and their viscosity after 160 s decreases of 150 Pa•s. The effect can be consequence of considerable volatility and low thermal stability of T765 in comparison to other stabilizers due to its much lower molecular weight. Other irradiated samples are thermodynamically stable what results from negligible slope of function viscosity versus time.

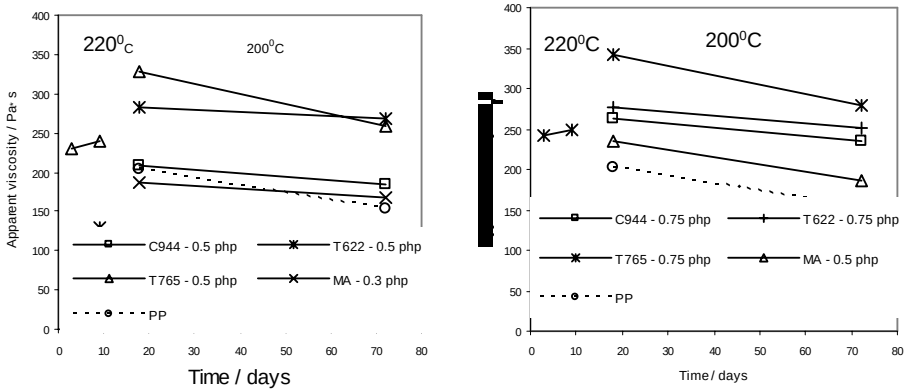

FIG. 5. Apparent viscosity of neat and modified polypropylene following irradiation with a dose of 25 kGy in function of time, shear rate 33 s^{-1}.

Correlation between elapse of time and viscosity is given in Fig. 5. Three days after irradiation viscosity is low and for the next 7 days increases. From EPR spectra we have estimated that only about 1/3 of alkyl radicals convert to peroxyl radicals. The reminded paramagnetic species form diamagnetic products and population of radicals decreases as a result of their combination. The processes initiate periodical growth of viscosity. After longer period of time bond scissions initiated by peroxyl radicals dominates over termination and the viscosity decreases. Thus the reduction results from post-irradiation degradation of polypropylene. Later decrease in viscosity caused that the next measurements had to be carried out at lower temperature (at 200 oC instead of at 220 oC).

Since polypropylene is much cheaper than thermoplastic elastomers, it can be used as economical component of thermoplastic diene elastomers. In order to evaluate the interaction between these two constituents blends of PP and SBS in various proportions were studied.

Fig. 6 shows spectra of PP/SBS blends recorded after irradiation with a dose of 30 kGy in air at room temperature. At the beginning intensities of all peaks diminish proportionally with the elapse of time and the shape of signal remains unchanged. The series of spectra for various proportions of components indicate that even for blends containing 3 times more SBS than PP only polypropylene radicals are detected. Additionally, in neat polypropylene radicals react slower than in copolymer with SBS, as seen in Fig. 6B and 6C. Conversion of alkyl radicals into peroxyl radical must proceed faster for smaller PP/SBS ratios since just after 3 hours contribution of ≡COO• considerably increases with SBS content and no alkyl radical is detected. The presence of SBS in mixture with PP creates conditions that promote easier access of oxidizing agent to alkyl radical in polypropylene. After 3 days the spectra of all samples show only the presence of peroxyl radical. The concentration of SBS radicals can not exceed a few percent otherwise their spectra would be detected easily. Thus sensitivity to ionizing radiation of SBS must be at least ten times lower than that of PP due to effective dissipation of energy by aromatic rings.

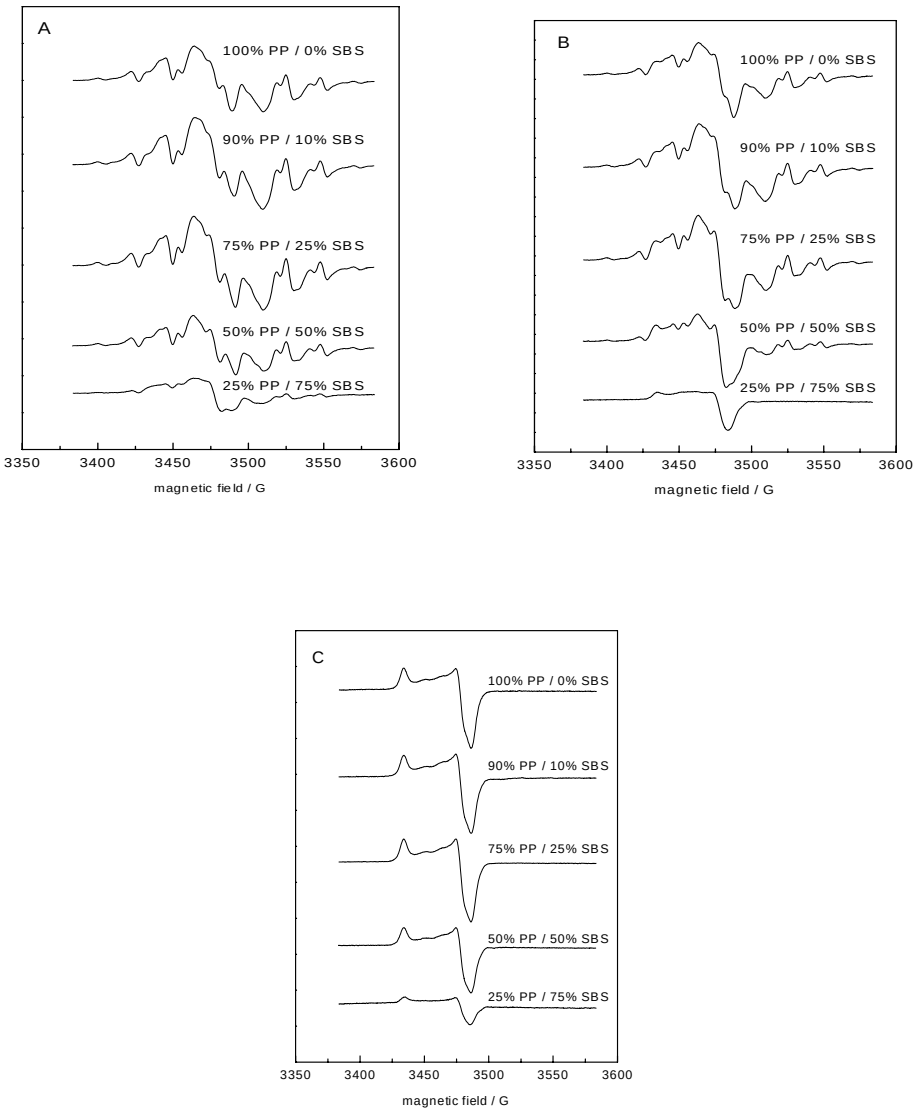

FIG. 6. EPR spectra of PP/SBS blends irradiated with a dose of 30 kGy recorded (A) after irradiation, (B) 3 hours upon irradiation, (C) 3 days upon irradiation.

4. CONCLUSIONS

Three types of HALS (Tinuvin 622, Tinuvin 765 and Chimassorb 944) cause in electron beam irradiated polypropylene:

- faster decay of radicals in amorphous phase what can result in the inhibition of radiation damage (the most significant effect was observed for C944),
- increase in apparent viscosity of molten state, particularly in presence of Tinuvins,
- increase of crystallization temperatures due to influence of the stabilizers on nucleation, degradation and exhaustion of additives.

Thus studied additives act not only as the antioxidants but as the nucleation agents as well.

If polypropylene is a component of blends with elastomer styrene-butadiene-styrene then radicals are generated predominantly in polyolefin segments and paramagnetic centers are not able to cross a border between two phases. With increasing contribution of SBS the termination of radicals proceed faster, probably as a result of amorphous phase growth in PP domines.

REFERENCES

[1] KHOYLOU, F., KATBAB, A.A., "Radiation degradation of polypropylene", Radiat. Phys. Chem. **42** (1-3) (1993) 219-222.

[2] TRIACCA, V.J., GLOOR, P.E., ZHU, S., HRYMAK, A.N., HAMIELEC, A.E., "Free radical degradation of polypropylene; random chain scission", Polym. Eng. Sci. 33 (8) (1993) 445-454.

[3] JINLIANG, Q., GENSHUAN, W., JUHONG, Z., FENGRU, Z., XUAN, H., JILAN, W., "Effect of isotacticity on radiation stability of polypropylene under lower dose irradiation", Radiat. Phys. Chem. **48** (6) (1996) 771-774.

[4] KASHIWABARA, H., SHIMADA, S., HORI, Y., "Nature of peroxyl radicals in polipropylene" Radiat. Phys. Chem. **37** (3) (1991) 511-515.

[5] HASSANPOUR, S., YOUSEFI, A., "Radiation stability of polypropylene by phenolic stabilizers", Radiat. Phys. Chem. **42** (1-3) (1993) 223-227.

[6] PRZYBYTNIAK, G.K., ZAGÓRSKI, Z.P., ŻUCHOWSKA, D., "Free radicals in electron beam irradiated blends of polyethylene and butadiene-styrene block copolymer" Radiat. Phys.Chem. 55 (1999) 655-658.

[7] STERZYNSKI, T., THOMAS, M., "Gamma radiation induced changes in the structure and properties of copolymers of polypropylene", J. Macromol. Sci.-Phys. **B34** (1,2) (1995) 119-135.

[8] ŻENKIEWICZ, M., "Investigation of tensile properties and tear resistance of polypropylene film modified irradiation", Polimery **48** (1) (2003) 66-68.

[9] STOJANOVIĆ, Z., KAČAREVIĆ-POPOVIĆ, Z., GALOVIĆ, S., MILICEVIĆ, D., SULJOVRUJIĆ, E., "Crystallinity changes and melting behavior of the uniaxially oriented iPP exposed to high doses of gamma radiation", Polym. Degrad. Stab.**87** (2005) 279-286.

[10] LACOSTE, J., VAILLANT, D., CARLSSON, D.J., "Gamma-, photo-, and thermally-initiated oxidation of isotactic polypropylene", J. Polym. Sci. Part A: Polym. Chem. **31** (1993) 715-722.

[11] BAUER, D.R., GERLOCK, J.L., "Photo-stabilization and photo-degradation of organic coatings containing a hindered amine light stabilizer: Part III- kinetics of stabilization during free radical oxidation", Polym. Degr. and Stab. **14** (1986) 97-112.

[12] YAGOUBI, N., PERON, R., LEGENDARE, B., GROSSIORD, J.L., FERRIER, D., "Gamma and electron beam radiation induced physico-chemical modifications of poly(propylene)", Nucl. Instr. and Meth. in Phys. Res B **151** (1999) 247-254.

[13] AHMED, S., BASFAR, A.A., "Influence of benzoic acid on thermal, crystallization and mechanical properties of isotactic polypropylene under irradiation", Nucl. Instr. and Meth. in Phys. Res. B, **151** (1999) 169-173.

[14] SUGIMOTO, M., MASUBUCHI, Y., TAKIMOTO, J., KOYAMA, K., "Melt rheology of polypropylene containing small amounts of high molecular weight chain. I. Shear flow", J. Polym. Sci.: Part B: Polym Phys. **39** (2001) 2692-2704.

HIGH ENERGY RADIATION PROCESSING OF EPDM IN HYDROCARBON ENVIRONMENT

T. ZAHARESCU
Advanced Research Institute for Electrical Engineering, Bucharest, Romania

Abstract

Different pressures of polypropylene (up to 1 atm), various doses (the maximum dose is 100 kGy), dose rate of 0.4 kGy/h, were applied to the EPDM dumbs and films. On the low dose range, polymer was subjected to a crosslinking process by which mechanical properties and chemical resistence are augmented. The higher dose exceeding 75 kGy brings about a decrease in thermal stability of irradiated samples due to the increase in the number of tertiary and quaternary carbon atoms. The medium pressure of propylene, around 0.7 atm, becomes the most suitable processing parameter, which is convenient for high yield of crosslinking. The mechanical measurements applied to irradiated EPDM samples emphasise the beneficial action of hydrocarbon surrounding. The ability of high energy radiation to promote structural modifications in EPDM is the lack of competition between the reactivity of free radicals with other hydrocarbon intermediates and with oxygen. The evolution in the thermal stability of EPDM specimens was determined by oxygen uptake method, which depicts the behaviour of radiation-processed elastomer under hard application condition. The kinetic parameters of thermal oxidation, oxidation induction time and oxidation rate, indicate the efficiency of low dose exposure on ethylene-propylene diene terpolymer. The consequence of the application of radiochemical method for the enlarging service duration is the decrease in the oxygen diffusion into polymer bulk and, thus, the decrease in the oxidative oxidation rate.

1. OBJECTIVE OF THE RESEARCH

This work is devoted to the improvement of the mechanical resistence of ethylene-propypene diene terpolymer by radiation exposure in reactive environment containing propylene. The gaseous surrounding contains double bond, which allows to joint neigbour macromolecules to be linked to each other. The diffusion of propylene into the polymer bulk controls the crosslinking process. The correlation between the irradiation conditions, absorbed dose and propylene pressure, is the main objective of the present work.

The stability of radiation-processed polymers in hydrocarbon environment is brought about by the involvement of monomer into the propagation of crosskinking. The initiation of hardening process is due to the radiochemical instability propylene, which generates free radicals for correction in the mechanical properties of polymer matrix.

The hydrocarbon plays the role of binder, which reacts with the ethylene-propylene diene terpolymer. The direct action of gaseous environment, in the absence of oxygen, is concretised in the improvement in mechanical behaviour and in the increased resistence against oxidative degradation. The low dose treatment is the most suitable procedure through which studied material becomes more convenient for different application under hard conditions. This work demonstrates the availability of radiation processing of polymers to promote favourable modification for longer service time.

2. INTRODUCTION

Irradiation provides a powerful method for modifying polymers. A large volume of research has been devoted to the improvement in the durability of this kind of materials. The crosslinking of polymer matrix [1-8] or the curring of composites [9-12] can create new materials, whose properties satisfy various requirements of employ.

The stability of radiation processed polymers is ensured not only by the addition of antioxidants [13-15], but also due to the compatibilization of various formulations [16-20]. The intermolecular bonds may be produced by various acrylic or vinylic compounds, which become the source of free radicals by the cleavage of double bonds [21-23].

The irradiation environment plays an important role in the high energy processing of polymers. The presence or the lack of oxygen determines the evolution of substrate. The competition between crosslinking and degradation (especially, oxidative process) will configurate the final chemical structure of material. As it is known, the diffusion of environmental gases, which is the controlling-rate stage, is involved in the start of polymer modification from the outer layers into the inner part of sample. The size of penetrating molecule influences the diffusion coefficient value, which limits the extension of changement.

In the case of hydrocarbons, the surrounding of irradiated material, the radiochemical yields the characteristic parameter for the formation of various structures indicates the direction of process development. Polypropylene that is an unsaturated compound is subjected itself to important alterations. The formation of a quantity of homopolymer on the surface or in the former macromolecular layers of sample will delay the penetration of external gas into the material bulk. In fact, the main products of hydrocarbon radiolysis, radical intermediates, transform the polymer substrate into a new material. The level of structural variation induced in high energy exposure depends on the susceptibility of material to create reactive places on macromolecular chains and on the radiation stability of irradiation environment. Ethylene-propylene diene terpolymer containing ethylidene norbornene as the third component and polypropylene contains unsaturated moieties are easy split into reactive fragments. The radiochemical stability of polymer matrix was previously studied in various environments: air [24-26], water [27], divinylbenzene[9] or methylcyclopentane [28].

The mechanisms describing the modification of polymers initiated by radiation have been reported earlier by many authors, some exemples being Chapiro [29], Dole [30], Carlsson [31], Mita and Horie [32], Zaharescu and Podină [33]. The primary events, the formation of positive ions and excited moleculed plays a significant role in the transformation of any substance, including polymers. The most ionic reaction mechanisms, which have been suggested by mass spectrometric investigations takes placed either in the condenced phase (in our case, polymer material), or in gas phase (in our experiments, propylene). As it has been previously stated, ionic species are undoubtedly present in irradiated polymers simultaneously with free radicals appeared from excited intermediates. They persist for a considerable time after irradiation [34]. However, Zaharescu and Mihalcea [35] have pointed out the interaction between diffused ions and the radiolysis intermediates of ethylene-propylene terpolymer.

Dole and Bodily [36] postulated some ion-molecule reactions occurred in irradiated polyethylene. They may be easy extended to ethylene-propylene copolymers, in which ionization and radical production are competitive processes. The probability of the mentioned reactions is high in the neighbourhood of particle tracks due to the increased concentration promoted by fast rejected electrons.

As it is indicated, ethylene-propylene copolymers may promote branching. In this case, ethylidene-norbornene would be the most reactive site on EPDM molecules. In figure 1, a mechanism through which the ethylene-propypene terpolymer subjected to ionizing radiation is presented.

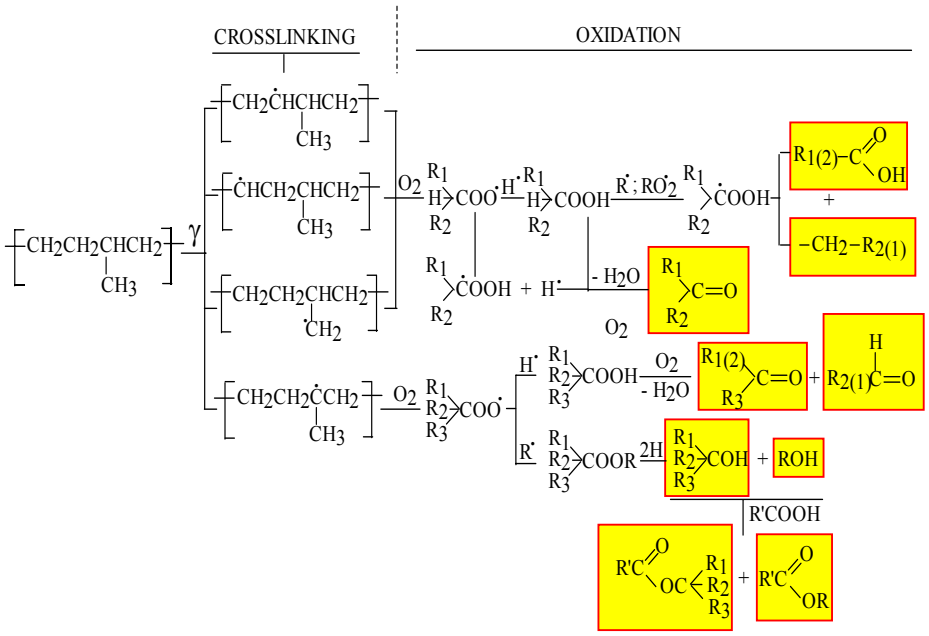

FIG. 1. A proposed mechanism for the radiochemical processing of EPDM in air [37]

The oxidation of polymer substrate can be avoided by the irradiation of material in inert atmosphere or in reactive promoting the protective behaviour of gaseous environment. Chapiro [38] and Feldman et al. [39] have reported the behaviour of hydrocarbons under the action of high energy radiation. They stated different forms of intermediates that may be produced under these conditions. It must be emphasized that both organic compounds, namely solid ethylene-propylene diene terpolymer and gaseous propylene that are under study in this work are modified in similar manner due to their structural similitude. The goal of this works is the achievement of the improvement in the resistence of polymer under special treatment by superficial or inner structural modifications.

3. MATERIALS AND METHODS

3.1. Materials

3.1.1. Ethylene-propylene diene elastomer

This polymer was provided by ARPECHIM Piteşti (Romania) as Terpit C®. Its main characteristics are presented in Table I.

TABLE I. THE MAIN CHARACTERISTICS OF EPDM

Characteristics	EPDM
Propylene content (%)	39.8
Number of CH_3 for 100 carbon atoms	0.983
Unsaturation (C=C/1000 C)	0.184
Numerical average molecular weight (Dalton)	80,800
Gravimetrc average molecular weight	155,500
Viscozimetric average molecular weight	129,300
Melting index (dl/g)	1.38
Concentration of ethylidene norbornene (%)	3.5

The distribution of molecular mass for studied elastomer is presented in *figure 2*.

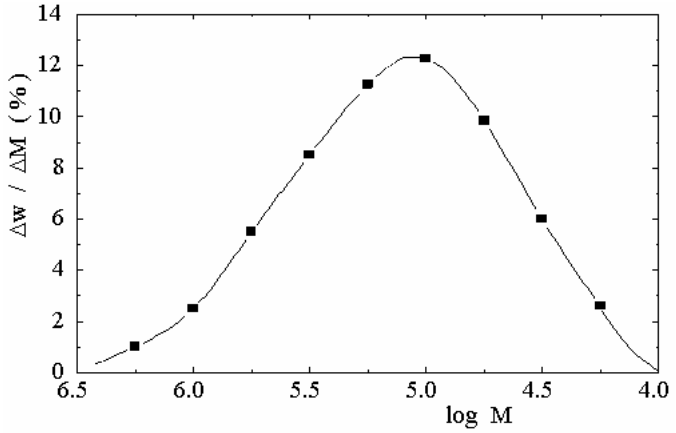

FIG. 2. Mass distribution in studied EPDM.

The elastomeric material was subjected to irradiation without any previous purification, because the industrial applications process raw materials as producer provides them. The original polymer state was distributed as block material.

3.1.2. Propylene

Gaseous propylene was provided by ROMPERTROL, Midia (Romania). The level of purity was 99.6 %

3.2. Sample preparation

Polymer sheets were prepared by pressing for 10 minures at 150 atm and 180^0C. For mechanical tests dumbs were cut before irradiation.

Spectral samples were obtained by the dissolution of polymer in cloroform and subsequent remote by natural convection at room temperature. These films were casted on steinless steel plates. Uniform thickness was obtained by the addition of solution in small volumes.

The hydrocarbon environment was obtained by remote air followed by the inleting propylene in the exposure unit (Figure 3a) by means of a glass equipment previously deaerated (Figure 3b).

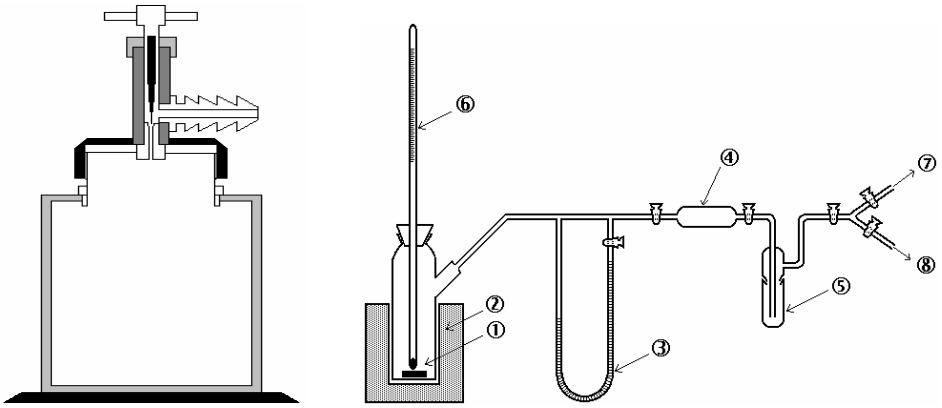

(a) (b)

FIG. 3. (a) Irradiation vessel; (b) Gas sampleing of irradiation vessel

(1) expansion vessel; (2) therostatic unit; (3) Hg manometer; (4) buffer vessel; (5) gas drier; (6) temperature controller; (7) vacuum oulet; (8) gas inlet and connection to irradiation vessel.

3.3. Irradiation

The exposure of polymer was performed in an irradiator Gammator provided with ^{137}Cs source. The dose rate was 0.4 kGy/h. Dumbs and films were placed in the irradiation vessel, tha propylene gas was allowed to surround them. This tight system was placed in the irradiation cavity on a turning plate that ensures the uniform exposure of samples. Paralel experiments with the irradiation in air were also performed in order to compare the results obtained in oxidising environment and in hydrocarbon (propylene) surrounding.

3.4. Measurements

Gel content determinations were carried out by solvent swelling and extraction of samples by refluxing *o*-xylene for 24 h. The gel content was calculated as the ratio of $(w_{gel}/w_{initial})*100\%$. Duplicate samples were processed and the average values are used. Mechanical tests were carried out on INSTRON mechanical tester according to the specifications of ASTM 620E. Five identical samples were subjected to the mechanical resistance characterization for each point. Spectral investigations were done using IR spectrophotometer Karl Zeiss (Germany). The thermal stability of studied specimens, either irradiated samples or controls, was run in the equipment presented in *Fig. 3b*. Temperature of 160^0C was selected for obtaining a nonfaster oxidation. This assessment allowed determining the important kinetic parameters of oxidation: induction period and rate of propagation.

4. RESULTS AND DISCUSSION

4.1. Gel content

The modification of gel content during the gamma exposure of EPDM specimens in propylene environment is presented in figure 4a. It can be observed that the increase in the insoluble fraction takes place faster for the former dose range. The diffusion of propylene and of other intermediates that result from radiolysis contributes to the modification of gelation state of polymer substrate.

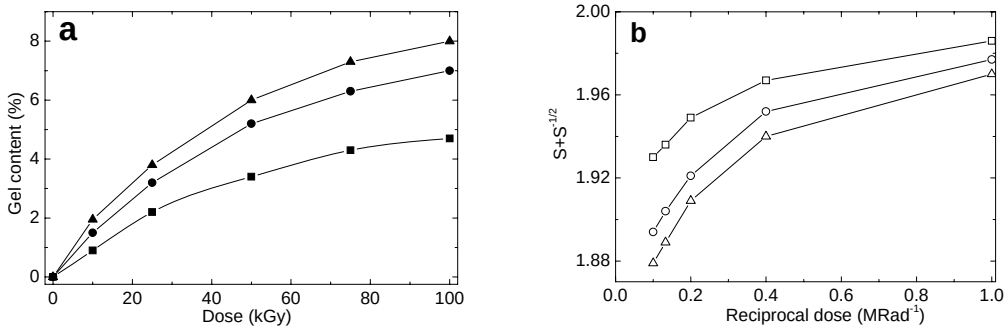

FIG. 4. The increase in gel content (a) and the Charlesby-Pinner diagram for γ-irradiated EPDM in gaseous propylene at various pressures: (■,□) 0.5 atm; (●,○) 0.7 atm; (▲,Δ) 0.9 atm.

The mechanism of propylene polymerization has demonstrated the formation of an allyl structure, CH=CH–CH_2–, which is stable under classical polymerization conditions [40]. However, the radiochemical treatment induces a slight instability of this entity and the new intermediate would react on the both ends due to the scission of double bond. The new intermolecular bridges slow the migration of radicals down. The increase in gel fraction is not proportional with the propylene pressure. The inhance in the environment pressure gets a smaller contribution to the higher pressure that at the lower one. The Charlesby Pinner representation proves that the higher selected doses, 50, 75 and 100 kGy, the linearity of graph may be considered. Their slopes are different from each other emphasizing that the ratios between the crosslinking yield and the degradation yield depend on the amount of intermediates. The higher the propylene pressure, the greater the slope. The difference in the slopes for the higher pressures would suggest that the increase in the amounts of tertiary and quaternary atoms brings about a light growth of degradation susceptibility.

4.2. Mechanical properties

The formation of intermolecular links influences the mechanical resistence of processed ethylene-propylene diene terpolymer. The elongation at break and the tensile strength of studied specimens vary with absorbed dose (figure 5).

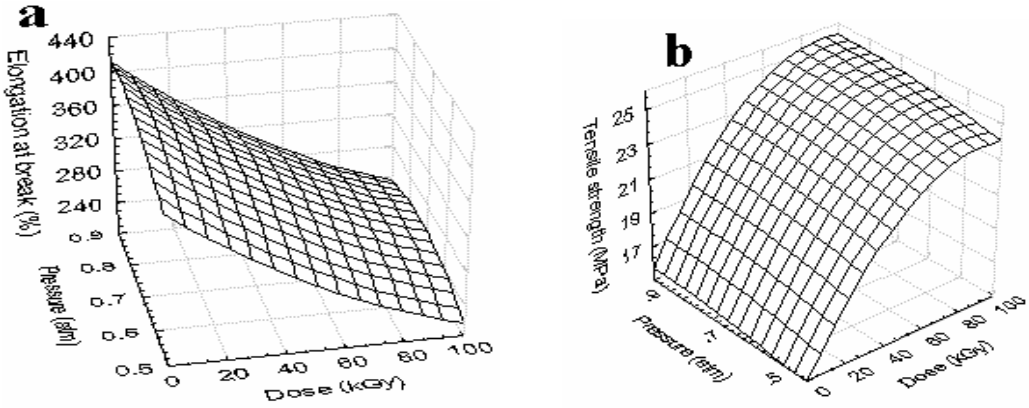

FIG. 5. (a) Elongation at break and (b) tensile strength for ethylene-propylene diene terpolymer γ-irradiated in propylene at various doses and environment pressures.

The increase in the tensile strength takes place in the irradiated EPDM by the diffusion of outer propylene. It may be supposed that at higher pressure, when the content of radicals is significant, the formation of polypropylene as homopolymer would occur. On the first stage of irradiation, the penetration of propylene into polymer bulk is easier, the interconnection of macromolecules starts and the material does not become sufficient dense for preventing the spread of intermediates. The continuous decrease in elongation at break demonstrates the capacity of material to improve its elasticity as the result of new interchain bonds. Simultaneously, the tensile strength of radiation processed EPDM increases and the direct consequence is the higher mechanical resistance under the action of stronger effort.

4.3. Oxidation resistence

The irradiation of ethylene-propylene diene terpolymer in air at room temperature induces not only an advanced crosslinking, but also a simultaneous oxidative degradation. The IR spectral study on elastomer films, which was not modified with any antioxidant, points out the formation of peculiar peaks in the regions of carbonyl and peroxyl bands. In figure 6 an IR spectrum recorded on the EPDM film subjected to □-rays is presented. The dose of 100 kGy at which EPDM was exposed explains the advanced degradation as the effect of the propagation of oxidation initiated by peroxyl radicals or hydroperoxides. The existence of molecular oxygen initially trapped in the material during manufacture does not explain the high values of absorbancy. The diffusion of oxygen from irradiation environment worsens the long term chemical resistance. The decrease in the oxidation rate of ethylene-propylene diene terpolymer follows a nonlinear dependency41. The lack of oxygen modifies the sample behaviour under radiation. The IR spectra of EPDM □-irradiated in propylene did not exhibit significant modifications, because the moieties that joint elastomer macromolecules do not differ from the host material. The absobance of methylene units is at the upper limit and any additional difference can not be detected.

The improvement of chemical resistance is demonstrated by the application of oxygen uptake method. The shape of oxidability curve, the dependency of the consumed amount of oxygen on time, differs from one sample to the other in function of absorbed dose. It can be remarked that the propagation step starts sharper at higher doses. The formation of a higher density of bridges presents an advantage on the penetration of oxygen during thermal investigations. However, this crosslinking generates more sensitive sites on hydrocarbon backbone. The grafting of short fragments of propylene molecules produces an increased number of highly substituted carbon atoms. The most instable places will be quaternary carbon atoms, whose bonds present the lowest activation energy for cleavage [42]. Figure 6 presents the IR spectrum for EPDM sample irradiated at 100 kGy in air at room temperature.

The sequence of thermal stability for the different carbon atom substitutions is presentes in the following series:

C - C (81,8 kcal/mol) < C(tertiary) - H (91kcal/mol) < C(secondary) - H (94,8kcal/mol)
< C(primary) - H (98 kcal/mol)

The advanced substitution will promote a higher sensitivity to oxidation, being pointed out by the evolution of oxygen uptake measurements. In figure 7, the oxygen consumption curves for EPDM samples irradiated in propylene environment at 0.5 atm are presented.

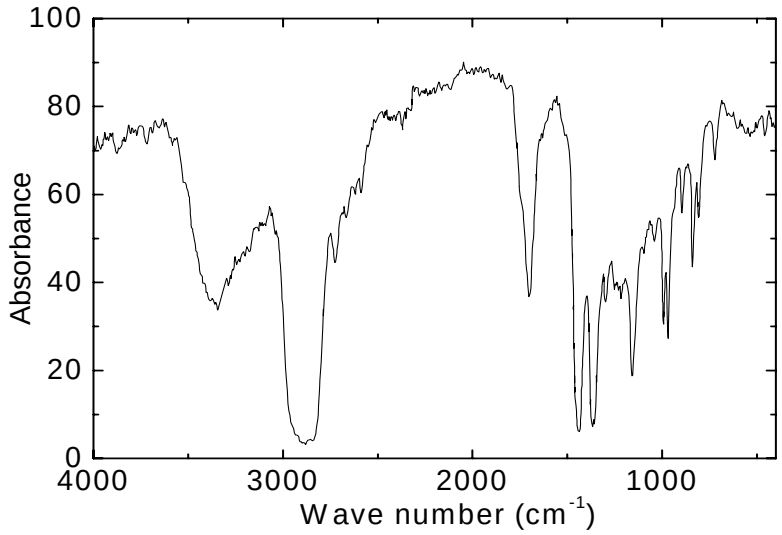

FIG. 6. IR spectrum for EPDM sample irradiated at 100 kGy in air at room temperature

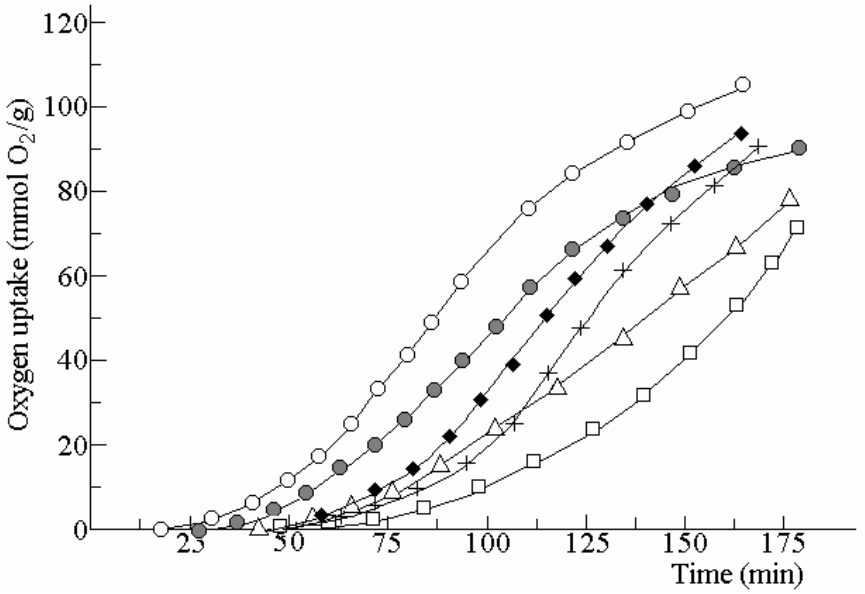

FIG. 7. Oxygen uptake dependencies on time for EPDM samples irradiated at various doses in propylene at 0.5 atm

(○) control; (●) 10 kGy; (Δ) 25 kGy; (□) 50 kGy; (+) 75 kGy; (■) 100 kGy.

The increase in the values of absorbed dose causes an improvement of oxidation resistance over the shorter exposure times. At the dose of 50 kGy, the best result was obtained. As it is listed in Table II, the both kinetic characteristics (oxidation induction time and oxidation rate) indicate an amelioration of thermal resistance of elastomer sample. If these data are correlated with the increase of gel fraction, it may be established that this dose is the convenient condition for processing. If the exposure is longer, the insoluble fraction becomes greater, but the oxidation strength decreases. The induction time is somewhat similar with the other irradiated samples at 50 and 100 kGy, but the propagation of degradation takes place faster, especially after the accumulation of oxidation promoters becomes significant. It means that the crosslinking brings not only a decrease in diffusion oxygen, but also an increase in the attack probability on a high substituted carbon atoms. The pressure of propylene brings about an increase in gel content, but the thermal stability does not follow similar ascendent behaviour.

TABLE II. KINETIC PARAMETERS FOR THERMAL OXIDATION OF IRRADIARED EPDM IN PROPYLENE ENVIRONMENT

Dose (kGy)	Induction time (min)	Oxidation rate (mmol $O_2.min^{-1}.g^{-1}$)
0	32	1.33
pressure: 0.5 atm		
10	42	1.15
25	61	0.72
50	73	0.51
75	69	1.36
100	62	1.59
pressure: 0.7 atm		
10	45	1.08
25	65	0.73
50	79	0.49
75	75	1.22
100	67	1.47
pressure: 0.9 atm		
10	46	0.98
25	68	0.69
50	83	0.50
75	80	1.20
100	70	1.35

The oxidation rate becomes on the same level or higher in comparison with the raw materials. This aspect suggests that the doses around of 100 kGy or greater are not proper for radiation processing of ethylene-propylene diene terpolymer in propylene environment. If the process is performed at moderate pressures around 0.7 atm and at the irradiation doses of 50-60 kGy, the improvement in the material quality may be considered as the important effect.

This process can be extended to the recycling of commodity wastes, where it is possible that the intermediated born during the radiolysis of propylene would act as scavengers for oxygen fragments with low molecular weights.

REFERENCES

[1] basfar, a.A., abdel-aziz, m.m., mofti, s., "Stabilization of □-radiation vulcanized EPDM against accelerated ageing", Polym. Degrad. Stabil. 66 (1999) 191–197.

[2] Zaharescu, T., Jipa, S., Setnescu, R., Setnescu, T., "Radiation processing of polyolefin blends. Part I. Crosslinking of EPDM/PP blends", J. Appl. Polym. Sci., 77 (2000) 982–987.

[3] Assink, R.A., Celina, M., GILLEN, K.T., CLOUGH, R.L., ALAM, T.M., "Morphology changes during radiation-thermal degradation of polyethylene and an EPDM copolymer by 13C NMR spectroscopy", Polym. Degrad. Stabil. 73 (2001) 355–362.

[4] Zaharescu, T., "Thermodynamic assessment of □-irradiated (NBR/Synthetic elastomers) blends", Nucl. Instrum. Meth. B185 (2001) 136-139.

[5] Zaharescu, T., Budrugeac, P., "Radiation processing of polyolefin blends", Polym. Bull. 49 (2002) 297-303.

[6] DENAC, M., MUSIL, V., ŠMIT, I., Ranogajeć, F., "Effects of talc and gamma irradiation on mechanical properties and morphology of isotactic polypropylene/talc composites", Polym. Degrad. Stabil. 82 (2003) 263-270.

[7] Gorna, K., Gogolewski, S., "The effect of gamma radiation on molecular stability and mechanical properties of biodegradable polyurethanes for medical applications", Polym. Degrad. Stabil. 79 (2003) 465-474.

[8] Grosu, E., Râpă, M., Tomescu, A., Nemeş, E., Zaharescu, T., Jipa, S., Setnescu, R., "Radiation processing of elastomer materials for medical use", Nucl. Instrum. Meth. B187 (2003) 220-224.

[9] Zaharescu, T., Feraru, E., Podină, C., "Thermal stabiliy of ethylene propylene-diene monomer/divinylbenzene systems", Polym. Degrad. Stabil. 87 (2005) 11-16.

[10] Budrugeac, P., Zaharescu, T., Mărcuță, M., Marin, G., "Accelerated electron effects on EVA based compound", J. Appl. Polym. Sci., 96 (2005) 613-617.

[11] Albano, C., Reyes, J., Ichazo, M., Gonzáles, J., Brito. M., Moronta, D., "Analysis of the mechanical, thermal and morphological behaviour of polypropylene compounds with sisal fibers and wood flour, irradiated with gamma rays", Polym. Degrad. Stabil. 76 (2002) 191-203.

[12] Zaharescu, T., Kaci, M., Hebal, G., Setnescu, R., Setnescu, T., Khima, R., Remili, C., Jipa, S., "Thermal stability of gamma irradiated low density polyethylene films containing hindered amine stabilizers", Macromol. Mater. Eng. 289 (2004) 524-530.

[13] Soebianto, Y.S., Kusuhata, I., Katsumura, Y., Ishigure, K., Kubo, J., Kudoh, H., Seguchi, T., "Degradation of polypropylene under gamma irradiation: protection of additives", Polym. Degrad. Stabil. 50 (1995) 203-210.

[14] Zaharescu, T., Giurginca, M., Jipa, S., "Radiochemical oxidation of ethylene-propylene elastomers in the presence of some phenolic antioxidants", Polym. Degrad. Stabil. 63 (1999) 245–251.

[15] Jipa, S., Zaharescu, T., Gorghiu, L.M., Dumitrescu, C., Setnescu, R., Esteves, M.A., Gigante, B., "Kinetic characterisation of radiation resistance of stabilised LDPE", J. Appl. Polym. Sci. 95 (2005) 1571-1577.

[16] Zaharescu, T., Jipa, S., Giurginca, M., "Radiochemical processing of EPDM/NB blends", J. Macromol. Sci., Pure & Appl. Chem., A35 (1998) 1093-1102.

[17] CZVIKOVSKI, T., HARTIGAI, H., "Compatibilization of recycled polymers through irradiation treatment", Radiat. Phys. Chem. 55 (1999) 727-730.

[18] BURILLO, G., Herrera-Franco, P., Vazquez, M., Adem, E., "Compatibilization of recycled and virgin PET with radiation-oxidized HDPE", Radiat. Phys. Chem. 63 (2002) 241-244.

[19] DAHLAN, H.M., KHAIRUL ZAMAN, M.D., IBRAHIM, A., "Liquid natural rubber (LNR) as a compatibilizer in NR/LLDPE blends. Part II. The effect of electron beam irradiation", Radiat. Phys. Chem., 64 (2002) 429-436.

[20] Berejka, A.J., Eberle, C., "Electron beam curing of composites in North America", Radiat. Phys. Chem., 63 (2002) 551-556.

[21] Defoort, B., Larnac, G., Coqueret, X., "Electron-beam initiation polymerization of acrylate compositions", Radiat. Phys. Chem., 62 (2001) 47-53.Nakayama, H., Kaetzu,

[22] Nakayama, H., Kaetsu, I., Uchida. K., Sakata, S., Tougou, K., Hara, T., Matsubara, I., "Radiation curing of intelligent coating for controlled release and permeation", Radiat. Phys. Chem. 63 (2002) 521-523.
[23] Palacios, O., Aliev, R., Burillo, G., "Radiation graft copolymerization of acrylic acid and N-isopropylacrylamide from binary mixtures onto polytetrafluorethylene", Polym. Bull. 51 (2003) 191-197.
[24] Meligi, G., Yoshii, F., Sasaki, T., Makuuchi, K., Rabie, A.M., Nishimoto, S., "Comparison of the degradability of irradiated polypropylene and poly(propylene-co-ethylene) in the natural environment", Polym. Degrad. Stabil. 49 (1995) 323-327.
[25] Zaharescu T., Budrugeac, P., "Radiation processing of ethylene-propylene rubber" J. Appl. Polym. Sci., 77 (2000) 293-303.
[26] Zaharescu, T., Podină, C., "Radiochemical stability of EPDM", Polym. Testing, 20 (2001) 141–149.
[27] Zaharescu, T., Jipa, S., Setnescu, R., "Degradation evaluation by radiochemical yields", Polym. Testing, 16 (1997) 491-496.
[28] Zaharescu, T., Feraru, E., Podină, C., Jipa, S., "Modifications of EPDM by gamma irradiation in hydrocarbon environment", Polym. Degrad. Stabil., 89 (2005) 373-381.
[29] Chapiro, A., "Chemical nature of the reactive species produced in polymers by ionizing radiation", in Irradiation of Polymers, editors R. L. Clough and S. Shalaby, ACS series 66, Washington DC, pp. 22-30 (1962).
[30] Dole, M, editor, "The radiation chemistry of macromolecules", Academic Press, New York, vol. I (1972), vol. II (1973).
[31] Carlsson, D.J., "Degradation and stabilization of polymers subjected to high energy radiation", in Atmospheric oxidation and antioxidants, editor G. Scott, Elsevier, New York, pp. 495-530 (1993).
[32] Mita, I, Horie, K., "Degradation and mobility of polymers", in Degradation and stabilization of polymers, editor H.H.G. Jellinek, Elsevier, New York, pp. 358-387 (1994).
[33] Zaharescu, T., Podină, C., editors, "Radiochemistry of polymers", Printing House of University, Bucharest (2003).
[34] Chapiro, A., editor, "Radiation chemistry of polymeric materials", Interscience Publishers, New York, p. 44 (1962).
[35] Zaharescu, T., Mihalcea, I., "Radiochemical behaviour of ethylene-propylene elastomers in salt solutions. Part III. Gel content investigations", Polym. Degrad. Stabil. 55 (1997) 265-268.
[36] Dole, M., Bodily, D.M., "Reactive intermediates in the radiation cemistry of polyethylene", in Irradiation of Polymers, editors R. L. Clough and S. Shalaby, ACS series 66, Washington DC, pp. 31-43 (1962).
[37] Zaharescu, T., Giurginca, M., Jipa S., "Radiochemical oxidation of ethylene-propylene elastomers in the presence of some phenolic antioxidants", Polym. Degrad. Stabil. 63 (1999) 245–251.
[38] Chapiro, A., editor, "Radiation chemistry of polymeric materials", Interscience Publishers, New York, pp. 66-120 (1962).
[39] Feldman, V.I., Sukhov, F.F., Zezin, A.A., Orlov, A.Yu., "Selectivity of radoation-induced processes in hydrocarbons, related polymers and organized polymer systems", IAEA-TECDOC-1062, pp. 41-63 (1999).
[40] Nenitzescu, C.D., "Organic chemistry", Pedagogical Printing House (VIIth Romanian edition), Bucharest, vol. I, p. 287 (1973).
[41] Zaharescu, t., Mihalcea, I., "The assessment of the oxidation resistance of ethylene-propylene elastomers", Mater. Plast. (Bucharest) 31 (l994) l39-145.

EFFECT OF IRRADIATION IN METALLOCENE POLYMERIC MATERIALS: AMORPHOUS ETHYLENE-NORBONENE COPOLYMERS AND CRYSTALLINE SYNDIOTACTIC POLYPROPYLENE

M.L. CERRADA, E. PÉREZ, A. BELLO, R. BENAVENTE, J.M. PEREÑA
Instituto de Ciencia y Tecnología de Polímeros (CSIC),Juan de la Cierva 3, Madrid, Spain

Abstract

Ethylene-norbornene copolymers and a sPP homopolymer, both synthesized with metallocene catalysts, are explored, analyzing mainly the effect of irradiation dose in the thermal behavior of the different polymers. Dynamic mechanical experiments have been performed in some of these samples

1. INTRODUCTION

The discovery of cocatalysts of the type methylaluminoxane (MAO) was an important step for the development of metallocene catalysts, more than twenty years ago [1,2]. The most important characteristics of metallocenes are their single site properties, that allow to obtain polymers (specially polyolefins) with very narrow molecular weight distributions [2,3] (polydispersity values near two). Moreover, the synthesis of a very broad range of new materials is feasible using these catalysts, thanks to the possibility of controlling the microstructure of the polymer [2,4,5]. Two of the best examples are the synthesis of cycloolefins and polypropylene with several tacticities (isotactic, atactic, syndiotactic, hemiisotactic, etc.) changing only the structure of the catalyst [6,7]. Moreover, metallocene catalysts can produce improved copolymer systems, in particular with large olefins [8-11] (1-hexene, 1-octene, etc.), due to the possibility of having a very narrow and homogeneous comonomer distribution along the chains of the polymer, and allowing to control the percentage of incorporation, maintaining the low polydispersity. These are very important properties of metallocene catalysts, compared with conventional Ziegler-Natta ones, where their multisite characteristics lead to very broad comonomer distributions, great polydispersity, and the percentage of incorporation is different for the polymer chains with different molecular weight [12].

The homopolymers of cycloolefins such as norbornene are not processable owing to the proximity of processing and degradation temperatures and their insolubility in common organic solvents. However, ethylene–norbornene copolymers do show thermoplastic behavior together with other interesting properties, such as excellent transparency and chemical, as well as solvent, resistance [13]. Due to the advances in metallocene catalysis, it is possible to control more efficiently the tacticity, molecular weight, and molecular weight distribution of the produced copolymers [14]. The nature and structure of the metallocene catalyst used [15], as well as the aluminoxane employed as a co-catalyst [16] influence the composition and microstructure of the final product.

So far, an extended variety of ethylene–norbornene copolymers has been synthesized, with the glass transition found in a wide range of temperatures, depending mainly on the content of the norbornene monomer: linear relationships are reported between the glass transition and the comonomer content [17-20], although the microstructure (the catalyst used) plays also an important role [21,22].

On the other hand, Natta and coworkers synthesized and characterized, around 1960, the syndiotactic form of polypropylene by using vanadium-based catalysts [23]. The stereospecificity reached was not high enough and, therefore, the properties exhibited were poorer than those found in its isotactic counterpart. Isotactic polypropylene, iPP, is highly crystalline with a high strength [24] while syndiotactic polypropylene, sPP, develops a lower degree of crystallinity and, consequently, is more ductile at room temperature with a greater impact strength [25].

However, sPP exhibits also a complicated polymorphism [26], which is highly dependent on crystallization conditions (such as supercooling and crystalization/annealing time) as well as on the chain stereoregularity, molecular weight, and molecular weight distribution.

In addition, the mechanical and thermal performance of sPPs show a large scatter as a function of stereo and regioregularity of their chains that governs the crystallization. Metallocene catalyzed sPP can be an elastomeric alternative to iPP for some applications, without significant differences in thermal properties required for a particular application. Moreover, sPP does have strong possibilities of being copolymerized with alpha-olefins of different lengths [27].

2. OBJECTIVE OF THE RESEARCH

Irradiation of polymers results an effective method for modification of polymers [28-33] introducing significant changes in their chemical structure that include: (i) degradation of chemical bonds and backbone structure, (ii) crosslinking of polymer chains, and (iii) an evolution of the chemical structure from the virgin polymer to a graphite-like material at high dosage. The ratio of resultant recombination, cross-linking, and chain scission will vary from polymer to polymer and to some degree from part to part based on the chemical composition and morphology of the polymer, the total radiation dose absorbed, and the rate at which the dose was deposited.That ratio is also significantly affected by the residual stress processed into the part, the environment present during irradiation (especially the presence or absence of oxygen), and the postirradiation storage environment (temperature and oxygen). Therefore, the purpose of the present investigation is to analyze the effect of the radiation on two different types of polymeric structures: amorphous norbornene-ethylene copolymers and semycrystalline syndiotactic polypropylene, evaluating the changes introduced by radiation on the macroscopic properties exhibited.

3. EXPERIMENTAL

Four ethylene-norbornene copolymers, with the comercial name TOPAS™, supplied by Ticona, with different norbornene contents were analyzed. Some of the characteristics of these copolymers are presented in Table 1. Films of each polymer were prepared by compression molding using a Collin hot press. The polymer pellets were placed between two teflon plates and heated at approximately 80ºC above their glass transition temperature, T_g, for 2 min. Throughout this initial period no pressure was applied to the polymer, allowing the polymer to melt and equilibrate at this temperature. A pressure of around 20 bar was then applied at the same temperature for further 2 min. Both the teflon plates and film were then placed between two water-cooled plates to quench the sample.

Syndiotactic polypropylene provided by Atofina was used in the present investigation. Films were obtained by compression molding in a Collin press between hot plates at 160ºC and at a pressure of 2 MPa for 4 min, and a subsequent quenching to room temperature between plates refrigerated with water.

The irradiation process was performed under two different types of radiation:

- a ^{60}Co gamma-source in CIEMAT (Centre for Energy, Environment and Technological Researches) using a Van de Graaff accelerator (2 MeV). Five different dose were applied: 20, 50, 100, 400 and 1000 kGy. Its dose rate was about 6.63 kGy/h.

- an electron source in IONMED (an industrial installation) using a 10 MeV Rhodotron accelerator. Eight doses were imposed: 30, 60, 90, 120, 150, 180, 210 and 440 kGy. Its dose rate was about 5.00 kGy/s.

The thermal properties were carried out in a Perkin-Elmer DSC-7 calorimeter connected to a cooling system and calibrated with different standards. The sample weight ranged from 6 to 8 mg. The scanning rate used was 20 ºC min^{-1}. For crystallinity determinations, a value of 196.6 J/g has been taken as the enthalpy of fusion of the perfect crystal of sPP [34]. The glass transition temperature, T_g, was determined as the temperature where the specific heat increment is the half of the total one at the transition.

Wide-angle X-ray diffraction (WAXS) patterns were recorded in the reflection mode at room temperature by using a Philips diffractometer with a Geiger counter, connected to a computer. Ni-filtered CuKα radiation was used. The diffraction scans were collected over a period of 20 minutes in the range of 2θ values from 3 to 43 degrees, using a sampling rate of 1 Hz. The goniometer was calibrated with a silicon standard.

Viscoelastic properties were measured with a Polymer Laboratories MK II and a Rheometrics V dynamic mechanical thermal analyzers, working in tensile and single cantilever modes, respectively. The temperature dependence of the storage modulus, E′, loss modulus, E″, and loss tangent, tan δ, was measured at several frequencies over a temperature range from –150 to 250 ºC at a heating rate of 1.5 ºC min^{-1}. The specimens used were rectangular strips 2.2 mm wide, around 0.7 mm thick and over 10 mm long.

4. RESULTS AND DISCUSSION

4.1.Norbornene-ethylene copolymers

Ethylene-norbornene copolymers offer several technical properties that make them useful in a variety of food, pharmaceutical, and medical device applications. In particular, the moisture barrier properties of the polymers are very attactive in food and pharmaceutical flexible packaging, and in certain rigid packaging applications (e.g. containers formed from thermoforming of sheets). The polymers also offer good clarity, and a high heat deflection temperature. The latter is of importance in applications involving steam autoclave treatment of the product. Since some of the applications may require the sterilization of the material, the study of the irradiation influence is pretty interesting in these materials. These copolymers analyzed in the present investigation have middle and high norbornene contents (Table 1), and, therefore, they are completely amorphous, as depicted in Figure 1.

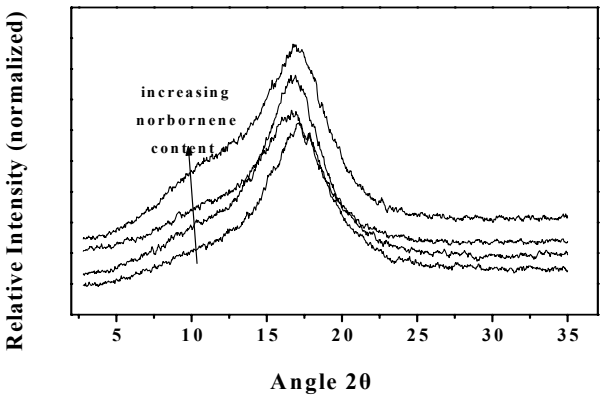

FIG. 1. X ray patterns for the different EN copolymers: EN8007, EN6013, EN6015 and EN6017 from bottom to top.

Accordingly, they exclusively exhibit one thermal transition related to the cooperative motions of long chain segments, *i. e*., the glass transition temperature. Figure 2a shows that application of gamma radiation has a strong influence on the location of this thermal transition in the EN6017 copolymer even at the smallest applied dose. A progressive shift of T_g to lower temperatures is observed as dose content increases. This latest feature is common for all of the copolymers independently of the norbornene molar fraction, as depicted in Figure 2b, though the irradiation effect is considerably smoother. The glass transition temperature is moved, as expected, at higher temperature as norbonene content is raised in the copolymer (Table 1). Additionally, the shift to lower temperature with dose is more pronounced in EN6017 copolymer, due to the degradative ease of norbornene compared to that found in ethylene where the crosslinking is favored at relatively low dose. In these copolymers, there is not a clear evidence of such a chemical crosslinks because an increase in T_g is not observed, though a practically T_g constance is obtained for EN8007, EN6013 and EN6015 at the two lowest doses, 20 and 50 kGy.

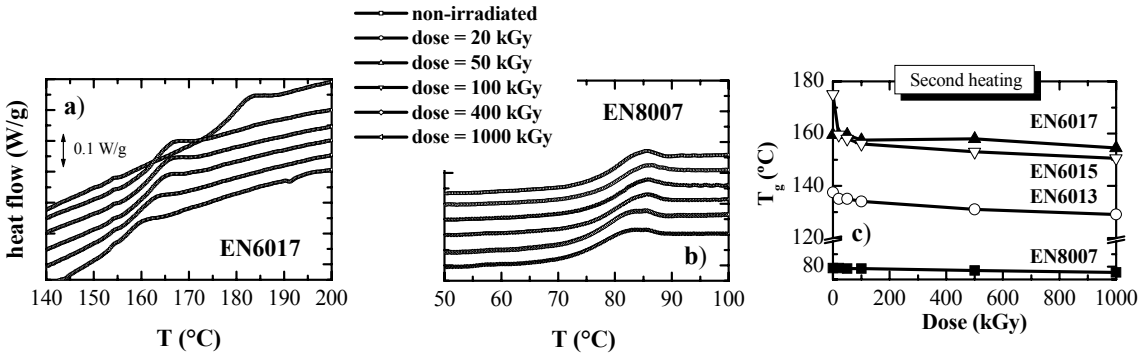

FIG. 2. Glass transition region of: a) EN6017 and b) EN8007. From top to bottom: non-irradiated, 20 kGy, 50 kGy, 100 kGy, 400 kGy and 1000 kGy specimens; c) Glass transition temperatures for the different ethylene-norbornene copolymers as a function of dose (kGy).

TABLE I. MOLECULAR CHARACTERISTICS AND RESULTS FROM DSC AND DMTA MEASUREMENTS FOR THE DIFFERENT ETHYLENE-NORBORNENE COPOLYMERS

Sample	%Nb[1]	MVR[2] (ml/min)	T_g (°C) DSC	T_g (°C) DMTA[3]
EN8007	36	30	78.0	101
EN6013	51	13	137.5	163
EN6015	56	4	159.5	189
EN6017	60	1	175.0	204

[1] Norbornene content calculated by a T_g vs mol %Nb graph, supplied by Ticona
[2] Melting Volume Flow Rate , measured by ISO 1133 test method, supplied by Ticona
[3] Values calculated by DMTA in a bending mode

This reduction in the T_g is accompanied by a yellowing discoloration of the samples, this yellow color being more intense as norbornene content increases in the copolymer. This fact points out to the occurrence of a degradative process that is also evidenced by a higher fragility of specimens when they are manipulated. Consequently, it is rather difficult to obtain appropriate strips to perform a reliable mechanical characterization because some cracks are created in the process of cutting.

These EN copolymers present three different relaxation processes, labeled as γ, β and α in order of increasing temperatures, as seen in Figure 3a. The intensity of the secondary mechanisms strongly depends on the comonomer content, mainly that related with the γ relaxation that appears at temperatures around −120ºC and is related to the movement of the methylene units in the polymer chain. Therefore, the intensity of this relaxation decreases as norbornene conted is raised. At the proximity of 50ºC, a very weak process though with a very broad relaxation time distribution is observed, that might be associated with restricted motions of the lateral links of norbornene with the backbone. This relaxation is more clearly observed as comonomer content increases because it overlaps at low contents with that associated with the glass transition.

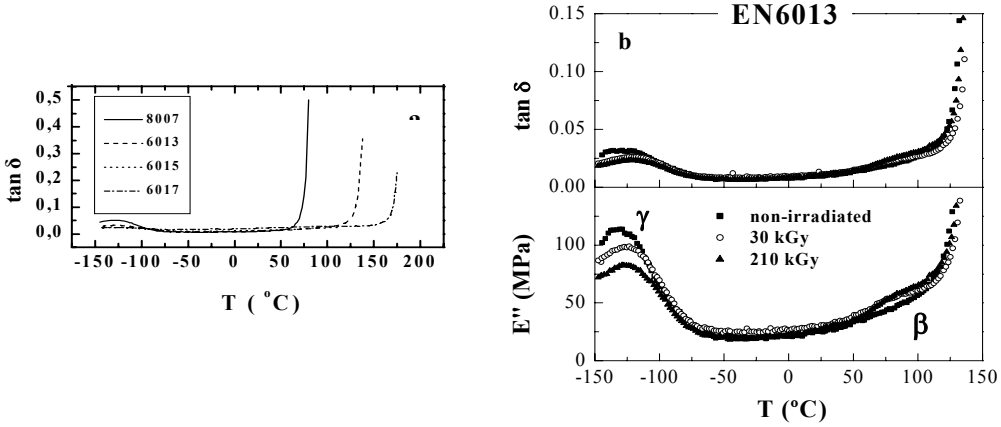

FIG. 3. a) Relaxation processes in EN copolymers under tensile deformation mode. b) Effect of radiation in EN6013 on the secondary processes.

The influence of the electron radiation in the secondary relaxation is seen in Figure 3b for tan δ and E″. The intensity of γ process diminishes indicating that probably the number of methylenic units has been reduced. However, the β relaxation becomes more evident. Since tensile deformation mode is used, the mechanism related to cooperative motions cannot be measured because EN copolymers become so soft due to their amorphous nature that start to elongate. For this reason, measurements under single cantilever mode were performed to observe glass transition region for EN8007 and EN6017 at 0.5 Hz irradiated with 20, 100 and 1000 kGy (Fig.4). In general, a diminishment of bending storage modulus is observed as well as a the shift to lower temperatures of the location of the relaxation associated with cooperative motions. These features are more noticeable again in EN6017.

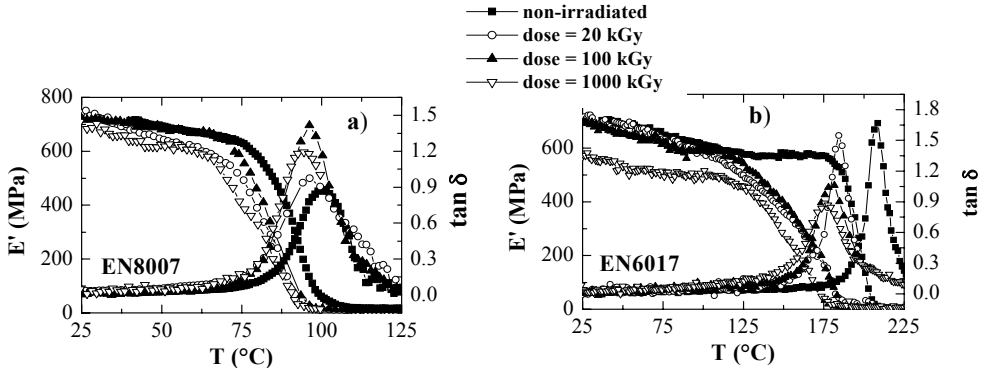

FIG. 4. Glass transition region of: a) EN8007 and b) EN6017.

4.2.Syndiotactic polypropylene

Figure 5a shows the DSC curves corresponding to the sPP under study. The initial melting (upper curve) presents a clear glass transition at around 9 ºC and the main melting endotherm at 126 ºC. This rather low melting temperature is due to the relatively low syndiotactic content and causes the sample to have a tail at the low temperature side of the melting curve that extends down to room temperature. Additionally, the appearance of a small endotherm is observed at 50 ºC (see upper curve of Figure 5a). This feature might arise from the annealing process related to keeping of the sample at room temperature, as occurs in other olefinic materials [35-37] where the annealing peak appears at a temperature around 15-20 degrees higher than the annealing temperature (room temperature in most cases). Alternatively, considering the complicated polymorphic behavior of sPP aforementioned, this endotherm could be also associated with a transformation (or simply melting) from a polymorph different than the major crystalline structure that melts at 117ºC. This second possibility seems to be unlikely from some preliminary real-time variable temperature WAXS experiments.

A total enthalpy of melting of 36 J/g is deduced from the melting curve, that corresponds to a crystallinity degree of around 18%, this value being also rather low because of the moderately low syndiotactic content. The middle curve in Figure 5a represents the cooling of the sPP sample from the melt. It shows a crystallization exotherm, centered at 61 ºC, with an enthalpy of 34 J/g. However, this crystallization peak is characterized by a considerable broadness owing to the slow crystallization rate exhibited by sPP, contrarily to that observed in its stereoisomer iPP. This fact is due to the low stereoregularity and to the alternation of methyl groups that confers on sPP a more flexible backbone and leads to a higher density of molecular entanglements within the molten state [38]. Below that crystallization exotherm, the glass transition is observed at around –9 ºC. The subsequent melting (lower curve of Figure 5a) first shows the glass transition, at around 1 ºC. A shift to lower temperatures and a slightly higher specific heat increment are observed compared to that shown during the first melting, due to the small difference in crystallinity degree developed by the specimen while cooling. Finally, a main melting endotherm, with a maximum at 127 ºC, is observed.

The crystalline structure developed under the used processing conditions is the disordered Form I that consists of an orthorhombic lattice with antichiral t_2g_2 conformation, as represented in Figure 5b. Thus, four diffractions are observed in the 2θ representation at around 12.2, 15.8, 20.8 and 24.5 degrees, corresponding to the (200), (010), (111) and (400) reflections, respectively [39,40].

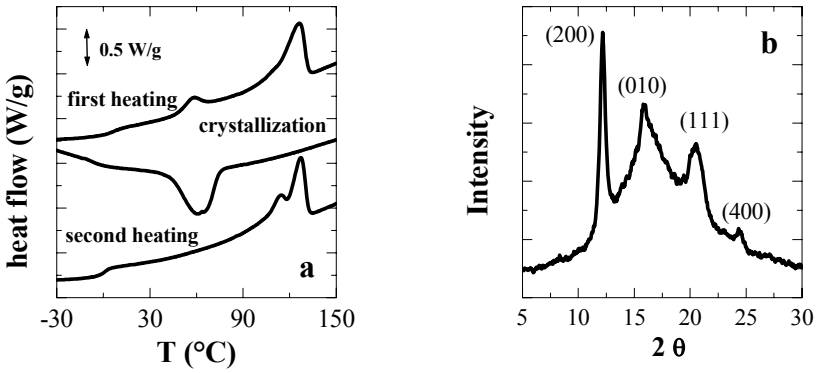

FIG. 5. a) DSC traces for sPP: first melting, crystallization and second melting from upper, middle and bottom curves, respectively. b) X ray diffractogram of sPP under studied.

The effect of irradiation on the thermal behavior can be seen in Figure 6. At first approximation, it seems that there is not effect of irradition on sPP for dose lower than 210 kGy. At the highest dose (440 kGy), a significant decrease in T_g and T_m are observed. Much more noticeable changes are evidenced during further crystallization and second melting. (Figure 6).

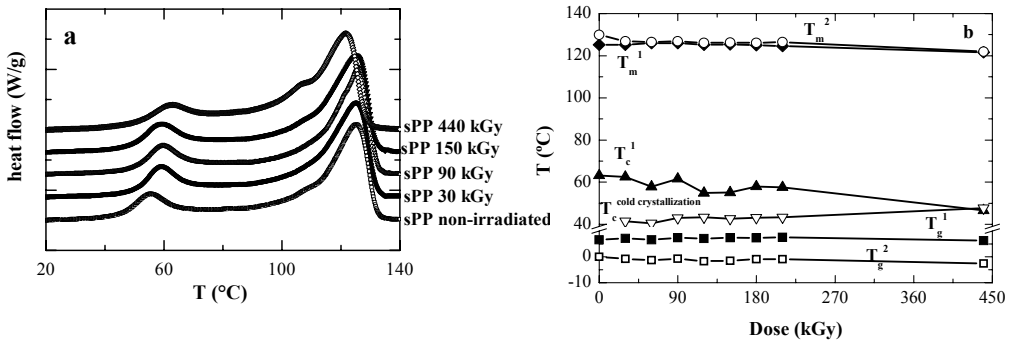

FIG. 6. a) First melting of non-irradiated and some of irradiated metallocenic sPP specimens. b) Summary of characteristic temperatures for non-irradiated and irradiated sPP samples.

The low crystallization rate in sPP has been already mentioned and, sometimes, if the syndiotacticity degree is not very high (around 80%), then the crystallization process is not fully accomplished during a typical cooling process at 20ºC/min. This feature is not observed in the non-irradiated sample of sPP here studied. However, the crystallization process is slowed down by the effect of irradiation: thus the higher the applied dose is the slower the process of crystalline ordering is, as seen in Figure 7a, since the intensity of the crystallization peak diminishes, being very small in the sample irradiated with 440kGy but there is a cold crystallization process during the second heating (Figure 7b) attaining a final crystallinity rather similar in all of the specimens.

In relation to the glass transition, the lower values observed during the second melting concern to the reduction in the crystallinity degree during the cooling process found in the different samples more than the influence of irradiation.

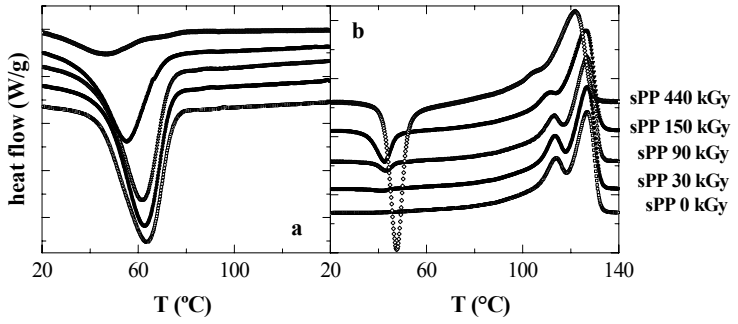

FIG. 7. a) Crystallization and b) second heating of non-irradiated and some of irradiated metallocenic sPP specimens.

5. CONCLUSIONS

Irradiation considerably affect the structure of either amorphous and semicrystalline mettallocenic polymers. In the former ones, the glass transition, the unique existing characteristic transition, is moved to lower temperatures independently of the norbornerne content, although the greater effect has been found for the copolymer with the highest norbornene incorporation. The thermal transitions in sPP vary a little during the first heating up to a dose of 210 kGy. However, the irradiation effect is striking for the subsequent crystallization and second melting. The crystallization rate of sPP is significantly slowed down, decreasing the already little dimentional stability of this polymer. Determination of mechanical parameters are quite difficult in irradiated specimens because they become more fragile and the preparation of suitable strips are really complicated.

REFERENCES

[1] H. Sinn, W. Kaminsky, H. J. Vollmer, R. Woldt. *Angew. Chem.* **1980**, *19*, 390.
[2] W. Kaminsky, A. Laban. *Appl. Catalysis A: General* **2001**, *222*, 47.
[3] J. Huang, G. L. Rempel. *Prog. Polym. Sci*. **1995**, *20*, 459.
[4] J. Kukral, P. Lehmus, T. Feifel, C. Troll, B. Rieger. *Organometallics* **2000**, *19*, 3767.
[5] H. Schumann, M. Glanz, E. Rosenthal, H. Z. Hemling. *Anorg. Allg. Chem.* **1996**, *622*, 1865.
[6] J. A. Ewen, R. L. Jones, A. Razavi, J. D. Ferrara. *J. Am. Chem. Soc.* **1988**, *110*, 6255.
[7] H. H. Brintzinger, D. Fischer, R. Mulhaupt, B. Rieger, R. M. Waymouth. *Angew. Chem.* **1995**, *107*, 1255; *Angew. Chem. Int. Ed. Engl.* **1995**, *34*, 1143.
[8] S. Jungling, S. Koltzenburg, R. Mulhaupt. *J. Polym. Chem.* **1997**, *35*, 1.
[9] N. Naga, T. Shiono, T. Ikeda. *Macromolecules* **1999**, *32*, 1348.
[10] R. Quijada, J. Retuert, J. L. Guevara, R. Rojas, M. Valle, P. Saavedra, H. Palza, G. B. Galland. *Macromol. Symp.* **2002**, *189*, 111.
[11] R. Quijada, R. Rojas, G. Bazan, Z. J. A. Komon, R. S. Mauler, G. B. Galland. *Macromolecules* **2001**, *34*, 2411.
[12] R. A. Bubeck. *Materials Sci. Eng.* **2002**, *39*, 1.
[13] W. Kaminsky, M. Arndt-Rosenau. In "Metallocene-based Polyolefins: Preparation, Properties and Technologies"; Scheirs, J; Kamisky, W., Eds.; Wiley: New York, **2000**; Vol. 2, Chapter 5.
[14] W. Kaminsky. *Macromol. Chem. Phys* .**1996**, *197*, 3907.
[15] D. Ruchatz, G. Fink. *Macromolecules* **1998**, *31*, 4669.
[16] Q. Wang, J. Weng, Z. Fan, L. Feng. *Macromol. Rapid Commun.* **1997**, *18*, 1101.
[17] E. Brauer, C. Wild, H.Wlegleb. *Polym. Bull.* **1987**, *18*, 73.
[18] O. Henschke, F. Köller, M. Arnold. *Macromol. Rapid Commun.* **1997**, *18*, 617.
[19] M. Arndt, I. Beulich. *Macromol Chem Phys* **1998**, *199*, 1221.
[20] D. Ruchatz, G. Fink. *Macromolecules* **1998**, *31*, 4681.
[21] J. Forsyth, T. Scrivani, R. Benavente, C. Marestin, J. M. Pereña. *J. Appl. Polym. Sci.* **2001**, *82*, 2159.
[22] J. Forsyth, J. M. Pereña, R. Benavente, E. Pérez, I. Tritto, L. Boggioni, H.-H. Brintzinger. *Macromol. Chem. Phys.* **2001**, *202*, 614.
[23] G. Natta, I. Pasquon, A. Zambelli. *J. Am. Chem. Soc.* **1962**, *84*, 1488.
[24] V. K. Gupta. In "Handbook of Engineering Polymeric Materials". N. P Cheremisinoff, editor. New York: Marcel; Dekker Inc. **1997**. Page 115 .
[25] K. B. Sinclair. *Proc Int Conf Polyolefins VIII* **1993**, Soc Plast Eng. Houston (USA).
[26] C. De Rosa, F. Auriemma, P. Corradini. *Macromolecules **1996***, *29,* 7452.
[27] J. Arranz-Andrés, J. L. Guevara, T. Velilla, R.Quijada, R. Benavente, E. Pérez, M. L. Cerrada. Submitted to Polymer.
[28] O. N. Tretinnikov, S. Fujita, S. Ogata, Y. Ikada. *J. Polym. Sci.: Polym. Phys.* **1999**, *37*, 1503.
[29] A. Keller, G. Ungar. *Radiat. Phys. Chem.* **1983**, *22*, 155.
[30] E. Pérez, D.L. VanderHart. *J. Polym. Sci.: Polym. Phys.* **1988**, *26*, 1979.
[31] M. Misheva, M. Mihailova, N.Djourelov, M. Kresteva, V. Krestev, E. Nedkov. *Radiat. Phys. Chem.* **2000**, *58*, 39.
[32] "Radiation-Resistant Polymers", in "Encyclopedia of Polymer Science and Engineering", Vol. 13, p. 667. Wiley, New York, **1988**.
[33] A. Rivaton, D. Lalande, J. L. Gardette. *Nucl. Instr.and Methods in Phys. Research* **2004**, *000*.
[34] S. Haftka, K. Könnecke. *J. Macromol. Sci. Phys.* **1991**, *B30*, 319
[35] A. Alizadeh, L. Richardson, J. Xu, S. McCartney, H. Marand, Y. W. Cheung, S. Chum. *Macromolecules* **1999**, *32*, 6221.
[36] M. L. Cerrada, R. Benavente, E. Pérez. *J. Mater. Res.* **2001**, *16*, 1103.
[37] M. L. Cerrada, R. Benavente, E. Pérez. *Macromol. Chem. Phys.* **2002**, *203*, 718.
[38] W. R. Wheat. *SPE ANTEC'97 Conference Proceedings* **1997**, 1968.
[39] J. Rodriguez-Arnold, Z. Bu, S. Z. D. Cheng. *J. Macromol. Sci.-Reviews in Macromol. Chem. Phys.* **1995**, *C35*, 117.
[40] P. Supaphol. *J. Appl. Polym. Sci.* **2001**, *82*,1083.

USE OF RADIATION-INDUCED DEGRADATION IN CONTROLLING MOLECULAR WEIGHTS OF POLYSACCHARIDES AND CONDUCTIVITY OF POLYANILINE BLENDS

O. GÜVEN
Department of Chemistry, Hacettepe University, Ankara, Turkey

Abstract

Better understanding of chemistry of radiation-induced degradation is becoming of increasing importance on account of the utilization of polymeric materials in a variety of radaition environments as well as beneficial uses of degraded polymers. In this report degrading effects of radiation have been considered from the point of views of controlling the molecular weights of kappa- and iota-carrageenans and alginates on one hand and controlling the conductivity of polyaniline blends by doping via radiation-induced HCl released from poly(vinyl chloride) on the other.

1. INTRODUCTION

Among various techniques used for the modification of polymer properties the use of ionizing radiation either in photonic (gamma rays, X rays) or particulate forms (accelerated electrons, ion beams) has proven to be a very convenient technique. Since the ultimate properties of polymers are generally controlled by their molecular weights, the control of molecular weight and its distribution are of great importance in determining the technical specifications required for a particular end-use. The polymers find their wide utilization in everyday life due to their light weights, relative ease of fabrication in the final form and unequalled mechanical properties based on performance vs. weight. The improvement in the mechanical properties is mostly achieved by increased molecular weights and/or crosslinking of polymer chains. The increased resistance to heat, deformation and mechanical stresses obtained through radiation-induced crosslinking has long been the main reason for the use of high energy radiations in polymer processing.

The opposite effect of radiation, in other words chain scissoring or degradation of polymers has not found great industrial interest until recently. The degradation effects of ionizing radiation has been generally connected with the chemical structure of polymer chains, presence or absence of some additives and irradiation atmosphere, presence of oxygen or air leading mostly to radiation-induced oxidation. It has been amply shown that polymers carrying quaternary carbon atoms in the main chain suffer from chain scission. Poly(methyl methacrylate), polyisobutylene, poly(α-methyl styrene) are typical degrading type of polymers. Most of the natural and synthetic polymers carrying oxygen atom in their main chains also degrade upon irradiation. Poly(oxyethylene), cellulose and other polysaccharides are examples with repeating -C-O- groups on their backbones undergoing main chain scissoring.

A different interpretation of structure vs. chain scissioning sensitivity is based on the heat of polymerization of monomers. Polymers showing relatively low heats of polymerization tend mostly to degrade upon irradiation. Although polymers can be categorized into two groups according to their ultimate response to high energy radiation as crosslinking and degrading types, exceptions to this classification can always be found. Poly(tetrafluoro ethylene) is one such example showing exclusively degradation upon irradiation at ambient temperature. In order to compare quantitatively the radiation response of polymers the amount of chemical changes should be related to the radiation energy absorbed. The efficiency of radiation-induced events is expressed by the so-called G-value. The G-value is equal to the number of events per 100 eV of energy absorbed has been customarily used to measure radiation chemical yield, but μmol/J is now recommended (1 μmol/J=10G).

Scission and crosslinking decrease or increase, respectively the molecular weights of the polymer molecules. Therefore measurement of the changes in molecular weight averages or distribution with dose can quantify these processes. Viscometric measurements in solution to give [η] indicate whether crosslinking or scission predominates. [η] values then will give M_v, provided that K and a for the Mark-Houwink relation are known. If the molecular weight distribution is known then M_n can be derived from M_v which can further be used to calculate the scission yield G(S). Molecular weights obtained from [η] values can be misleading if the initial molecular weight distribution is different from the most probable. An initially broad distribution will become narrow and turn into the most probable distribution with irradiation dose if there is only scission and G(S) will be overestimated from M_v values. Crosslinking reduces the ratio of hydrodynamic volume to molecular weight compared to linear molecules and [η] values will then lead to underestimation of the molecular weight. Gel Permeation Chromatography (GPC) is used widely to determine the average molecular weights and distribution of polymers. GPC suffers from the same hydrodynamic volume problem when crosslinking occurs, but this is generally ignored.

Polymers in which crosslinking predominates over scission, as determined by G(S)<4G(X), become incompletely soluble above the gel dose, D_g and it is possible to derive values of G(S) and G(X) from measurements of the soluble or insoluble(gel) fraction of the polymer as a function of dose. A.Charlesby was the first in analysing quantitatively radiation response of polymers, a short account of his approach is given below [1].

2. CALCULATION OF G(S) AND G(X) FROM MOLECULAR WEIGHTS

The relationship between average molecular weights and G(S) and G(X) are given in the equations below:

$$1/M_{nD} = 1/M_{n0} + 1.04x10^{-10} [G(S) – G(X)] D \quad (1)$$

$$1/M_{wD} = 1/M_{w0} + 5.18x10^{-11} [G(S) – 4G(X)] D \quad (2)$$

where the dose D is given in Gy and subscripts D and 0 denote irradiated and unirradiated cases. Equation 1 applies to all initial molecular weight distributions. Equation 2 is the relationship between M_w and dose for an initial most probable molecular weight distribution. If scission only occurs then either equation 1 or 2 alone can be used to calculate G(S). When both crosslinking and scission occur G(S) and G(X) can be obtained from the combination of two equations provided that initial molecular weight distribution is the most probable.

If scission is the only mode of action of radiation then the radiation-chemical yield of degradation (scission) G(S) is determined from the Alexander-Charlesby-Ross equation:

$$G(S) = [1/M_{nD}-1/M_{n0}]0.965x10^5/D \quad (3)$$

Where the absorbed dose D is in kGy and M_{nD} and M_{n0} are the number average molecular weights of the polymer before and after irradiation.

3. CALCULATION OF G(S) AND G(X) FROM SOLUBLE FRACTIONS

The values of G(S) and G(X) for the irradiation of a polymer when G(S)<4G(X) are usually calculated from the Charlesby-Pinner equation which predicts a linear relationship between $s+s^{0.5}$ and 1/D :

$$s+s^{0.5} = G(S)/2G(X) + [4.82x10^9] / [G(X) M_{n0} D] \quad (4)$$

This equation is based on the assumption that (1) the unirradiated polymer has a most probable molecular weight distribution, (2) crosslinking occurs by a H-link mechanism, (3) crosslinking and scission occur with random spatial distributions in the polymer without any clustering.

In the present report radiation-induced degradation of some polysaccharides namely carrageenans and alginates will be investigated in detail by a careful Gel Permeation Chromatographic analysis of their respective molecular weights before and after irradiation and above mentioned equations will be used in determining their radiation-chemical yields. Furthermore the degrading effect of radiation on poly(vinyl chloride) will be shown for beneficial use to initiate and enhance conductivity in polyaniline blends

4. EXPERIMENTAL

Commercially available kappa-carrageenan (KC) and iota-carrageenan (IC) and sodium alginate (NaAlg) were obtained from Sigma-Aldrich and used as received.

In order to irradiate the polysaccharides mentioned above under controlled humidity conditions, saturated aqueous salt solutions were prepared from NaCl, NaNO3 and MgCl2 . In the Table given below relative humidity of atmosphere above respective salt solutions are listed. The polymer samples in powder form first dried in a vacuum oven at 40oC and then placed in baskets suspended over the saturated salt solutions kept in closed containers. The powders kept for three days in various constant relative humidities absorbed corresponding amounts of water by reaching equilibrium, all at room temperature. Water uptake of polymers corresponding to different humidity levels are also indicated in the same Table I below.

TABLE I. WATER UPTAKE OF POLYMERS CORRESPONDING TO DIFFERENT HUMIDITY LEVELS

Saturated solution (30° C)	Incubation period (Day)	Atm. humidity (%)	Absorbed water for KC (%)	Absorbed water for IC (%)	Absorbed water for SA (%)
$MgCl_2$	3	50	5	2	5
NaCl	3	75	21	17	18
KNO_3	3	90	40	31	37
Water	3	100	230	150	196

The polymer samples equilibrated with different humidity of surrounding atmospheres were placed in tightly closed containers and irradiated to required doses (2.5, 5, 10, 20, 50 and 100 kGy) in a Gammacell 220 type ^{60}Co – gamma irradiator at room temperature in air.

Irradiated and unirradiated samples were analysed in a Waters Breeze model Gel Permeation Chromatograph. 0.1 M $NaNO_3$ was used as the eluting solvent. Waters hydrogel columns were used to provide separation within a molecular weight range of 20,000 – 600,000. Universal calibration was constructed by using narrow molecular weight (20600-553000) standard samples of poly(ethylene oxide). The Mark-Houwink parameters used for PEO were $K = 6.4 \times 10^{-5}$ dL/g and $a = 0.82$. Corresponding constants for carrageenans and sodium alginate were taken as $K= 5.98 \times 10^{-5}$, $a= 0.90$ and $K= 7.3 \times 10^{-5}$, $a= 0.92$ respectively.

5. RESULTS AND DISCUSSION

5.1. Controlling of molecular weight of polysaccharides

It is very well known that polysaccharides in dry form or in solution degrade when exposed to ionizing radiation [2,3]. The results reported so far on the radiation-induced degradation of polysaccharides indicated that chain scission yield strongly depends on the relative concentration of polymer. In dilute aqueous solutions with polymer concentration less than 4% (w/v) the dominating effect is chain scission. The same applies to solid state irradiated polysaccharides. G(S) values reported for kappa-, iota- and lambda-carrageenans irradiated in solid form are within 1 to 1.3 range whereas for 4% solution G(S) values change from 8 to 12 and 13 respectively for the three carrageenans mentioned above [4]. Alginates have been found to be more sensitive to degradation by irradiation and while in solid state irradiation G(S) was found to be similar to that of carrageenans, 1.9, in 4% aqueous solutions chain scission yield increases to 18 [5]. When the concentration of polysaccharide is increased beyond viscous solution to paste-like condition, crosslinking effect starts to dominate and typically chain scissioning polymers turn into crosslinking type [6].

It is very well known that the difference observed in the effect of radiation on polymers irradiated in dry or solution form is due to indirect effect of radiation. In irradiations carried out in the presence of water the radiolysis products of water play the major role. In the above mentioned studies, an order of magnitude increase in G(S) values obtained for irradiations carried out in aqueous solutions is simply because of the secondary reactions between the polysaccharides and radiolysis products of water, mainly OH radicals. The strong effect of the presence of water on the overall effect of irradiation of polysaccharides has lead us to consider the effect of humidity on the radiation chemistry of polysaccharides. We therefore decided to irradiate the carrageenan and alginate samples under different but well-defined humidities. For this purpose saturated solutions of certain salt solutions were prepared whose equilibrium humidity levels are very well known as reported in Table I.

Figure 1 shows the normalized GPC chromatograms of dry KC irradiated to doses indicated on the figure, from 2.5 to 100 kGy.

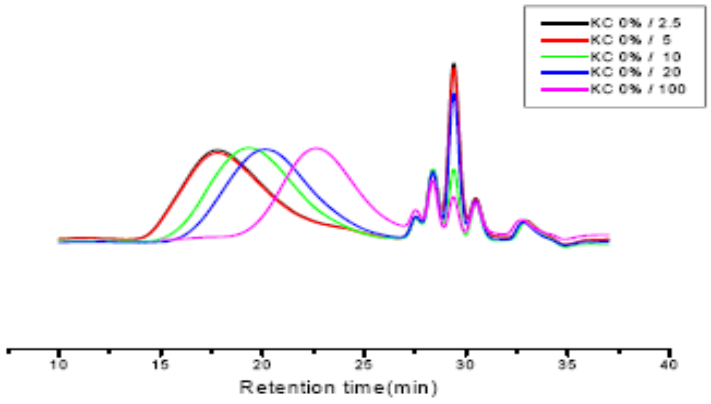

FIG. 1. Normalized GPC chromatograms of KC irradiated in dry form to indicated doses.

The degradation effect of radiation is clearly seen from the shifting of chromatograms to lower molecular weight ranges with increasing dose. The small multiple after-peaks are due to some anions and cations present in KC and they act like internal standards [7]. When KC kept at different humidity conditions was irradiated the chromatograms obtained were observed to shift depending on the dose. The sample chromatograms shown below in Figure 2 are for KCs irradiated to 50 kGy at different humidities.

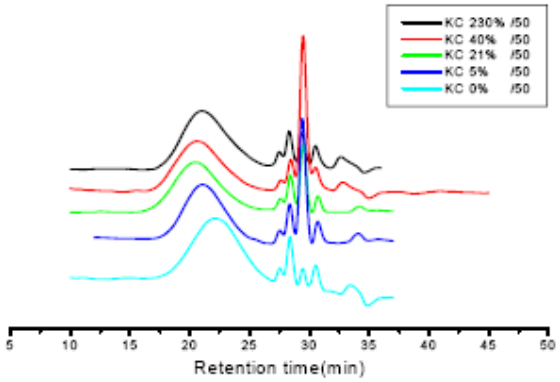

FIG. 2. The changes in molecular weight distributions of KC irradiated to 50 kGy dose at different levels of water uptake.

The effect of presence of small amounts of water in the solid form of KC brings a big difference to the radiation-induced chain scission. This can be more easily seen from Figure 3 where M_n values of irradiated KCs are plotted against dose as a function of actual water content of polymers.

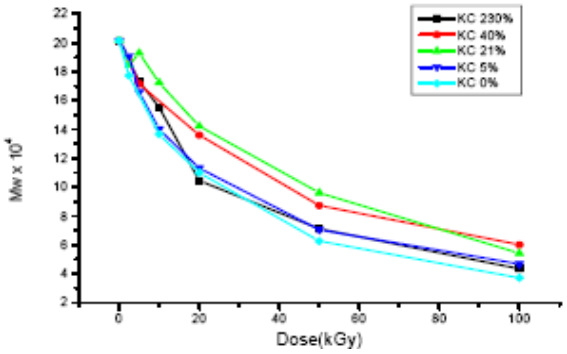

FIG. 3. The change of number-average molecular weight of KC irradiated with different water contents as a function of dose.

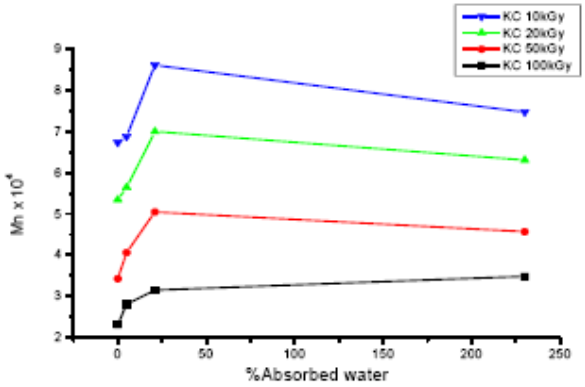

FIG. 4. The change in number-average molecular weight of KC samples irradiated to 10-100 kGy doses at different water contents.

The information given in Figure 3 can be better seen from Figure 4 where the effect of small changes in the water contents cause significant differences in radiation response of KC in terms of M_n values. As can be seen from Figure 4, a KC sample irradiated to 20 kGy dose at 75% humidity shows equal M_n for the same KC irradiated to 10 kGy at 50% humidity.

As it has been indicated in the Introduction section, in order to obtain quantitative information on chain scission yields, $1/M_n$ vs. dose diagrams must be constructed according to eqn.1. When this is done Figure 5 is obtained. Although it may be possible to calculate a value for G(S) from the overall slope of the linear parts of the curves in this Figure, we have preferred to calculate individual values of G(S) values by using eqn. 3. The results thus obtained are collected in the Table below.

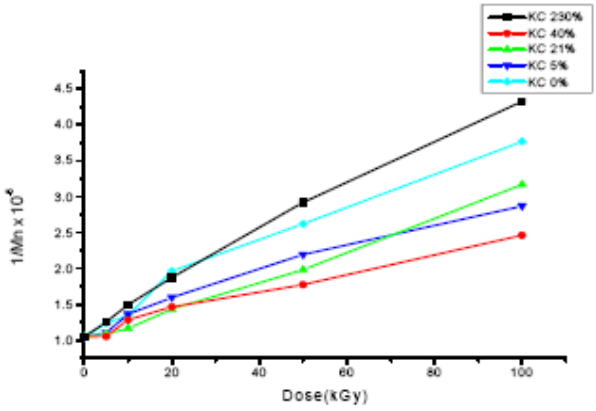

FIG. 5. $1/M_n$ vs. dose plot to determine G(S) values.

TABLE II. CHANGE OF G(S) WITH HUMIDITY FOR KC AS A FUNCTION OF DOSE

Absorbed water	2.5	5	10	20	50
0%	0.73	0.65	0.29	0.44	0.30
5%	0.23	0.62	0.22	0.25	0.28
21%	0.16	0.08	0.20	0.19	0.18
40%	0.32	0.46	0.40	0.20	0.21
230%	0.30	0.40	0.43	0.40	0.36

The effect of low level of water present in the solid form of KC on radiation-induced degradation is clearly seen from the G(S) values given in this Table. Degradation yield is the highest for dry irradiated samples and with water taken up from surrounding humidity degradation becomes less pronounced and G(S) values show a decrease. At very high water contents degradation effect again becomes more effective. This polymer and other polysaccharides degrade upon irradiation in aqueous solutions and in dry form. The polysaccharides samples appearing dry may contain a certain amount of water which will be directly related to the humidity of surrounding atmosphere. One therefore has to be very careful when irradiating polysaccharides in appearently dry form and their actual water contents should be determined before every irradiation. Otherwise as shown in this report inconsistent values of molecular weights and/or scission yields might be reported for the same sample irradiated to the same dose if the humidity conditions are different.

Results very similar to those given for KC were obtained for IC and SA. In Figure 6, below one can see the similar trend in changing molecular weight distribution of IC irradiated to 50 kGy dose at varying humidity conditions.

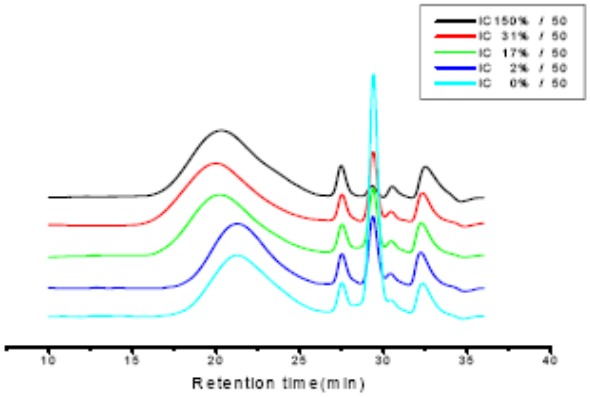

FIG. 6. GPC chromatograms of IC with various water contents irradiated to 50 kGy.

The radiation response of sodium alginate is no different from carrageenans which means that small amounts of water present in solid polysaccharide structures reduce the degrading effect of radiation, yielding lower G(S) values.

When polysaccharides are irradiated in very dry form, the radicals generated on the main chains do not benefit from the segmental mobility of chains to encounter with each other to form crosslinks but separate from each other with the formation of fractures. In dilute solutions however although chains are fully mobile, the probablity of two radicalic sites on two separate chains to meet each other to reestablish a covalent bond is very small due to large distances involved between the polymer coils in the solution. The additional indirect effect of water radiolysis even enhances the radical attacks on the chains with eventual reorganization to form chain ends. The G(S) values obtained from aqueous solution irradiations are therefore much higher than those observed for solid state irradiations. When there is small amount of water in the polysaccharide structure, due to very low amount of water in the polymer+water system, it is unlikely to expect an indirect effect. The water located in between the polymer chains however can give enough mobility to chains, plastifying effect, which may enhance the radical-radical combinations thus lowering the rate of degradation hence reducing G(S) values.

5.2.Controlling the conductivity of polyaniline blends

Polyaniline has three different oxidation states which are called leucomeraldine, pernigraniline and emeraldine. Only emeraldine polymer exhibits conductivity. If emeraldine base polymer is treated with acidic solution (either organic or inorganic protonic acids) with pH lower than 4, it is converted to emeraldine salt form which is the conducting form of the emeraldine polymer [8].

Poly(vinyl chloride) (PVC), is a degrading type of polymer and known to undergo extensive dehydrochlorination (resulting mainly loss of HCl) when exposed to energetic radiations like gamma rays, accelerated electrons, etc. Similar effect has been observed for poly(vinyl acetate) (PVAc), when it is irradiated with ionizing radiations causing the release of acetic acid. These radiolytic products can be captured by the neighboring PANI molecules in their respective blends thus enhancing the electrical conductivity of PANI moieties. The electrical conductivity of poly(aniline-base) is known to increase when exposed to strong acids like HCl.

Therefore onset and further enhancement of conductivity in the films prepared from PANI base and PVC was observed when they are irradiated with ionizing radiations [9]. Since, poly(vinylidene chloride), (PVDC) undergoes a high degree of side chain degradation when exposed to ionizing radiation (resulting mainly loss of HCl) as in the case of PVC, it has also been considered as a source of HCl for the doping of PANI-base. Due to the highly crystalline nature of PVDC thus difficulty in dissolution, its copolymer with vinyl acetate was prepared and used in PANI blend formation.

The polymer, polyaniline obtained by Focke's chemical oxidation method [10] in this work is conductive polyaniline and called as emeraldine-salt (PANI-salt). It is deprotonated before preparing PANI based blend films. For the casting of PANI/PVC and PANI/P(VDC-co-VAC) films, PANI base and PVC and P(VDC-co-VAc) copolymer were pairwise dissolved in N-methyl pyrrolidone/Tertahydrofurane (NMP-THF). Homogeneous solutions of these polymer mixtures were transferred into petri dishes to obtain smooth films. The films were irradiated in a Gammacell 220 type of ^{60}Co – gamma irradiator at room temperature in air.

Conductivity of pure PANI and PANI blends were measured before and after irradiation by using standard four-probe method under DC current. A Keithley 2410 sourcemeter was used as voltage and current source. Measured current values were plotted versus voltage values and resistivity of samples was calculated from the slope of the I–V plots. In the scheme given below the release of HCl from PVC or other similar polymers upon irradiation and its capture by the neibouring PANI-base is shown. Radiation induced conductivity of the PANI/ PVC and PANI/PVDC copolymer blends involves therefore the removal of HCl from PVC and PVDC chains as radiolysis products and subsequent addition onto PANI structure. In this way we manage to use degradation effect of radiation for initiating and enhancing conductivity in PANI-base blends.

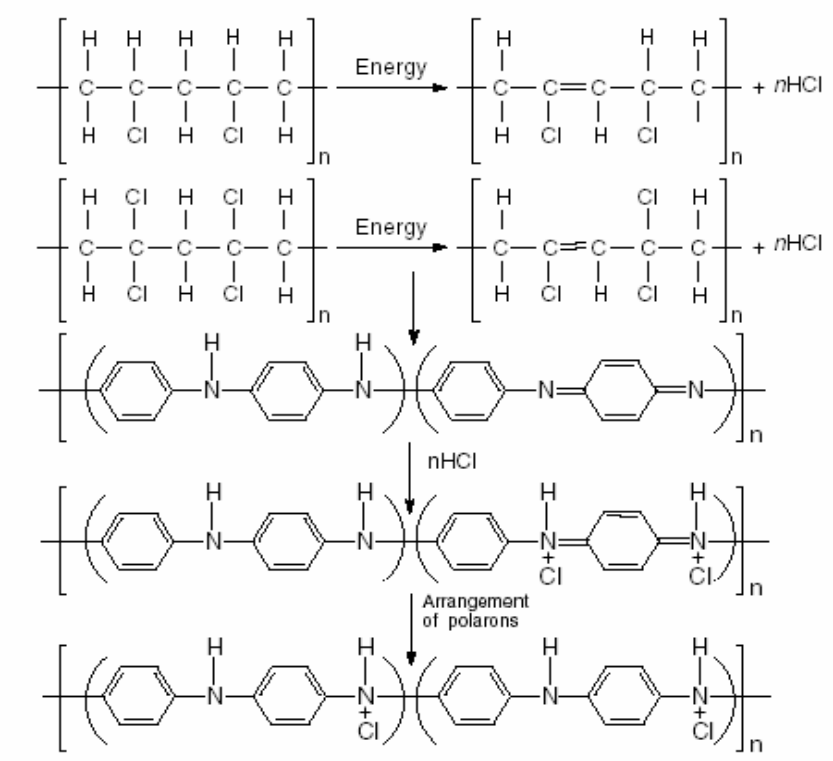

Scheme 1. The radiation-induced mechanism of HCl release from PVC and subsequent doping of polyaniline.

Figure 7 shows the changes in the conductivities of PVC/PANI blends as a function of radiation dose for 0.3, 0.4, 0.5, 0.7, 1.0, 2.0, 3.0 PVC/PANI mole ratios (on a repeating unit basis). A maximum value of 10^{-4} S/cm was reached indicating a saturation point for doping. Increasing the content of PVC in PVC/PANI blend results with an initially steep increase followed by a decrease in the conductivity beyond a certain composition as shown in Figure 8.

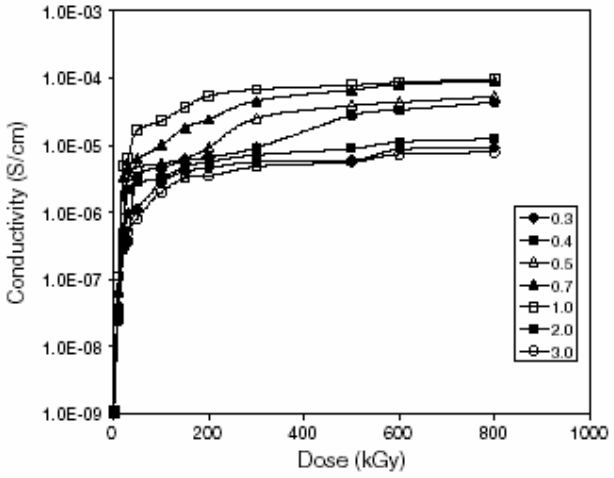

FIG. 7. The change in conductivities of PANI/PVC blends as a function of irradiation dose for 0.3, 0.4, 0.5, 0.7, 1.0, 2.0, 3.0 PVC/PANI mole ratios

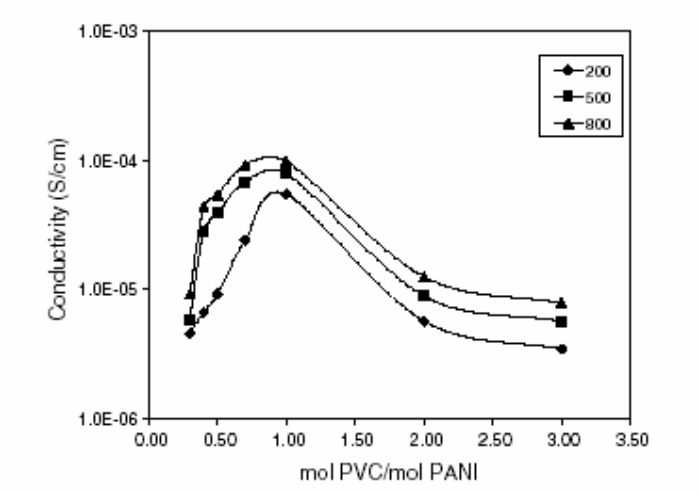

FIG. 8. Conductivities of PANI/PVC blends as a function of blend composition for 200, 500, 800 kGy doses.

In order to prepare PANI blends showing better response to radiation-induced conductivity new films composed of PANI/P(VDC-co-VAc) and PANI/P(VDC-co-VC) pairs in various compositions were prepared. Composition of these blends were tried to be kept similar to those for PANI/PVC blends. Irradiations were carried out at ambient conditions covering a wide dose range up to 800 kGy. The conductivity versus composition of blends for selected doses were constructed which were very similar in appearance to Fig. 8 [11]. The main difference being significantly higher conductivities were obtained with maxima at different PANI/PVDC copolymer ratios.

Table below shows collectively the results pertaining to maximum conductivities obtained for blend systems studied in this work in comparison to conductivities of unirradiated blends and their physical appearance.

TABLE III. MAXIMUM RADIATION INDUCED CONDUCTIVITIES REACHED IN PANI BLENDS

Sample	Irradiation dose (kGy)	Host polymer/PANI ratio in blend	Conductivity before irradiation (S/cm)	Conductivity after irradiation (S/cm)	Remarks on the appearance of the films
P(VDC-co-VAc)	500	0.5	1.0×10^{-09}	3.7×10^{-02}	Smooth, flexible, most strong
P(VDC-co-VC)	500	0.4	1.0×10^{-10}	9.7×10^{-03}	Smooth, slightly brittle
PVC	800	1.0	1.0×10^{-09}	7.8×10^{-05}	Smooth, most flexible, strong
PANI-base	800	–	1.0×10^{-11}	6.7×10^{-09}	–
PANI-salt	800	–	2×10	6.0×10^{-02}	–

The results presented in this part of this report clearly show that ionizing radiation is an effective means to induce conductivity in the blends of PANI with chlorine carrying polymers.The main mechanism behind this radiation-induced conductivity is in-situ doping of PANI-base with HCl released from partner polymers by the degrading effect of radiation.

REFERENCES

[1] CHARLESBY, A., "Atomic Radiation and Polymers" Pergamon Pres, New York 1960.
[2] CHOI, W-S., AHN, K.-J., LEE, D.-W., BYUN,M.W., PARK, H.J., Polym. Deg. Stab., 78(2002)533-538.
[3] WASIKIEWICZ, J.M., YOSHII, F., NAGASAWA, N., WACH, R.A., MITOMO, H., Rad. Phys. Chem., 73(2005)287-295.
[4] RELLEVE, L., NAGASAWA, N., LUAN, L.Q., YAGI, T., ARANILLA, C., ABAD, L., KUME, T., YOSHII, F. DELA ROSA, A., Polym. Deg. Stab., 87(2005)403-410.
[5] NAGASAWA, N., MITOMO, H., YOSHII, F., KUME, T., Polym. Deg. Stab., 69(2000)279-285.
[6] YOSHII, F., ZHAO, L., WACH, R.A., NAGASAWA, N., MITOMO, H., KUME, T., Nuclear Inst. Met. Phys. Res.B, 208(2003)320-324.
[7] ALTUNTAS, E., SEN, M., GÜVEN, O., to be published (2006).
[8] CHIANG, C.K., MacDIARMID, A.G., Synthetic Metals, 13(1986)193-198.
[9] BODUGOZ, H., SEVIL, U.A., GÜVEN, O., Macromol. Symposia, 169(1998) 89-94.
[10] FOCKE, W.W., WNEK, G.E., WEI, Y., J. Phys. Chem., 91(1987)5813-5817.
[11] BODUGOZ, H., GÜVEN, O., Nuclear Inst. Met. Phys. Res.B, in publication (2005).

SELECTIVE ^{13}C LABELING AS A TECHNIQUE TO UNDERSTAND RADIATION-OXIDATION DEGRADATION IN POLYPROPYLENE

D. M. MOWERY, R. A. ASSINK, R. BERNSTEIN, D. K. DERZON, S. B. KLAMO†, R. L. CLOUGH
Organic Materials Department, Sandia National Laboratories, Albuquerque, USA
†Arnold and Mabel Beckman Laboratories of Chemical Synthesis
California Institute of Technology, Pasadena, USA

Abstract

Polypropylene (PP) samples with selective ^{13}C isotopic labeling at different positions along the macromolecular chain have been used to gain insight into the radiation-oxidation chemistry of this polymer. Unstabilized thin films of these materials were subjected to γ-irradiation in air and under inert atmosphere, and to post-irradiation treatment in air. The oxidation products were quantified as a function of time and temperature using solid-state ^{13}C nuclear magnetic resonance (NMR) spectroscopy. Dramatic differences were found in the type and distribution of oxidation products originating from the three carbon atom sites within the PP macromolecule (tertiary carbon, secondary carbon, and methyl side group). Most of the oxidation products that formed on the polymer chain originated through chemical reactions at the PP tertiary carbons. Under all of the aging conditions examined, tertiary peroxides (from the PP tertiary site) were the most abundant functional group produced, with tertiary alcohols second in abundance. Important differences in product ratios were found as a function of temperature, including large differences in the amount of methyl ketones, which are associated with chain scission. Radiation-oxidation results for PP are compared and contrasted under varying experimental conditions, and are discussed in light of NMR-based radiation-oxidation results obtained recently for polyethylene.

1. INTRODUCTION

Many important polymer processing applications, some commercialized and others still under development, involve the use of ionizing radiation [1]. The control of degradation (macromolecular chain scission leading to a reduction in molecular weight) is critical in essentially all of these applications, which can be considered in two categories when discussing degradation control. In the first category, degradation is simply an undesirable side reaction, and the goal is to find ways to minimize it to the greatest extent possible. Important examples of technologies in this category include numerous crosslinking and curing applications, as well as radiation-sterilization of items for medical, pharmaceutical, or food applications. In the second category, the partial degradation of the macromolecular material is desired outcome of the radiation treatment. For instance, the alteration of the molecular weight distribution to improve processing, melt-flow, and miscibility properties is an important commercial application for polymers such as poly(tetrafluoroethylene) and polypropylene. Other examples in which controlled polymer degradation is of interest for existing or potential industrial use include: surface modification for enhanced adhesion, treatment of cellulose for production of viscose in the rayon industry, the processing of polysaccharides into useful agricultural products, recycling of plastics and rubbers, production of ion-track membranes, and X-ray or e-beam microlithography.

Some types of polymers undergo intrinsic chain cleavage upon irradiation. For many cases of polymer irradiation, extrinsic factors (i.e., variable environmental conditions, additives, and irradiation parameters) can have a major influence on the extent of degradation. Understanding and controlling these factors thus offers a means of controlling the nature and extent of degradation in radiation processing.

One of the most widely encountered factors in the radiation-degradation of polymers is the influence of atmospheric oxygen. Depending upon specific experimental conditions, polymers of the intrinsically-crosslinking type can be made to undergo predominantly chain scission when oxygen is present.

This paper focuses on gaining a better fundamental understanding of radiation-oxidation, and in particular introduces a promising new method for obtaining a more detailed molecular-level understanding of the complex mixture of oxidation products and chemical reaction pathways that underlie radiation-oxidation chemistry in polymeric materials. In addition to improving the ability to control degradation in the radiation processing of polymers, progress in radiation-oxidation studies should have an impact in two other technological areas: 1) better understanding of the chemistries underlying the "peroxidation" method of radiation-grafting processes, and 2) understanding of the aging processes in materials used in the construction of radiation-producing facilities (nuclear power plants, high-energy particle-physics facilities, etc.).

Polypropylene, on which this study has focused, is a widely used synthetic polymer that is highly susceptible to oxidative degradation induced by irradiation, as well as by thermal and photo-initiated processes. Polypropylene is extensively used in the world-wide manufacture of disposable medical items such as syringes, for which treatment using γ-irradiation or e-beam accounts for a large and increasingly important means of sterilization. Additionally, as mentioned above, the irradiation of polypropylene to modify its molecular weight distribution is an industrial process of growing importance.

Due to its commercial importance, much work has been published on the oxidation of polypropylene, including useful reviews [23]. Although many of the oxidation products in polypropylene have been identified, others remain in question or have yet to be recognized, and the detailed chemical reaction pathways leading to the various products require more thorough exploration. Quantification of oxidation products (or indeed of the reaction products of any chemical modification of macromolecular materials) is difficult due to their low concentrations. In chemical reactions conducted on small organic molecules, each reaction product can be isolated by chromatography or similar means, and each product's structure can be precisely determined by various spectroscopic techniques. However, in the case of macromolecular materials, the various chromophores and structures resulting from chemical reactions are not readily separated, and are correspondingly more difficult to study.

Nuclear magnetic resonance (NMR) spectroscopy is a powerful tool in the elucidation of polymer chain structure and dynamics [4, 5]. NMR has proven very useful in studying both oxidative degradation and radiation-induced changes in polyolefin thermoplastics such as polyethylene [6-10], polypropylene [11,12], and ethylene copolymers [13, 14], as well as other common industrial polymers [15-20]. Due to the relatively wide range of isotropic chemical shifts, 13C NMR offers good spectroscopic resolution and effective identification of resonance peaks originating from the different oxidation products. Typically, 13C NMR analyses of oxidation-induced functional groups in polymers have been conducted on samples in liquid solution at high temperatures (>100oC). However, such measurement conditions can induce further chemical reactions that could significantly alter the structure and concentration of the oxidation products. Recently, our laboratories have employed [10] solid-state 13C NMR to analyze oxidation products formed by γ-irradiation in polyethylene samples that were 99% 13C enriched. The use of 13C enriched polymer samples provides a much needed increase in detection sensitivity, of nearly 2 orders of magnitude. Used together with magic-angle spinning (MAS) NMR, isotopic enrichment eliminates the necessity for dissolving or swelling the material at high temperatures.

In order to provide more direct insight into the complex chemical reaction pathways by which polymers undergo oxidative degradation, we are now beginning to use selective isotopic labeling of macromolecules, combined with solid-state NMR analyses of the materials following exposure to radiation environments [21]. The samples utilized in this study were prepared from unstabilized polypropylene powders that were enriched with selective 13C labeling of the three different main-chain sites (see scheme below). By selectively labeling polypropylene with the 13C nucleus, we are able to unambiguously identify the origin of the various oxidative products and their relative concentrations with consideration to mechanisms of their formation.

13C resonances could be assigned to various oxidation-induced functional groups, and the distribution and time-dependent accumulation of these oxidation products were then obtained for various irradiation and post-irradiation experiments. Main-chain carbon sites in the polypropylene macromolecule is given below:

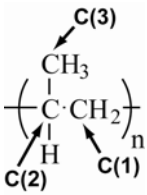

2. EXPERIMENTAL

2.1. ^{13}C labeled polypropylene materials

Three polypropylene (PP) samples with different ^{13}C labeling schemes were employed in this study. They are referred to as C(1), C(1,3), and C(2) labeled samples (refer to the scheme above). All of the polypropylene materials were predominantly isotactic based on high-temperature (130^{o}C) solution ^{13}C NMR results, and the samples exhibited a semi-crystalline morphology. Material properties for each of the labeled PP samples are summarized in Table I. The C(1,3) and C(2) labeled samples were purchased (Isotec) in powder form. For these samples, the ^{13}C labeled monomers were polymerized using triisobutylaluminum and $TiCl_4$ in an anhydrous xylene/toluene solution. In the C(2) labeled material, the tertiary (or methine) carbons were enriched with ~99% ^{13}C. In C(1,3) labeled samples, the secondary (or methylene) and primary (or methyl) carbons were enriched with ~68% and ~31% ^{13}C, respectively. The distribution of labeled carbons in the C(1,3) sample was the result of scrambling during the polymerization of 1-^{13}C-propylene.

The C(1) labeled polypropylene was prepared in our laboratory (Pasadena, CA). All air and/or moisture sensitive compounds were manipulated using standard high vacuum line or Schlenk techniques, or in a glove box under a nitrogen atmosphere, as described previously [22]. Toluene (EM Science) was dried by the method of Grubbs [23] and stored under vacuum over sodium benzophenone ketyl. Prior to experiments, toluene was collected at -78°C by vacuum transfer and stored in a glove box under a nitrogen atmosphere. Aqueous hydrochloric acid (36.5-38%, EM Science), methanol (EM Science), and *rac*-ethylene-*bis*-indenylzirconium dichloride (Strem) were purchased and used as received. Methylaluminoxane was purchased (Albemarle) and prepared by removing toluene and free trimethylaluminum *in vacuo;* the white MAO solid was dried at 25°C for 48 hours at high vacuum. 1-^{13}C-propylene (99.2 atom % ^{13}C, 99% chemical purity) was purchased (CDN Isotopes), purified by passage through a column of MnO on vermiculite and activated molecular sieves, transferred into a thick walled glass vessel at -196°C, and stored under vacuum at -78°C. *CAUTION: Extreme care should be taken with the storage of propylene in a closed container as its vapor pressure at room temperature exceeds 12 atm.*

Polymerizations of the 1-^{13}C-propylene yielding the C(1) labeled polypropylene were carried out in 1:1 (v/v) toluene / 1-^{13}C-propylene at 0°C in a thick-walled glass vessel (V ≈ 70 mL) sealed with an 8-mm Kontes needle valve. A ground glass joint was also present for connection to a vacuum line. The monomer was first distilled through a dry ice / acetone cooled trap into a calibrated cone for volume measurement, and then distilled into the liquid nitrogen cooled reaction vessel. Polymerization experiments were conducted using the following procedure. In an inert atmosphere glove box, a polymerization vessel equipped with a stir bar was charged with MAO (80 mg, ≈ 2200 equiv), toluene (1 mL), and *rac*-ethylene-*bis*-indenylzirconium dichloride (0.26 mL of a 2.4 mM solution in toluene) to give a yellow-orange solution.

The vessel was then cooled in liquid nitrogen and evacuated on a high vacuum line. 1-^{13}C-propylene (1 mL at -78°C, ≈ 20,000 equiv) was added by vacuum transfer. In the fume hood behind a blast shield, the reaction was warmed to 0°C in a sodium chloride / ice water bath. The polymerization was allowed to proceed for 10 min with rapid stirring. The vessel was then transferred to a dry ice / acetone bath and residual monomer was recovered via vacuum transfer on a high vacuum line. The polymerization was quenched with a 4:1 (v/v) mixture of methanol and dilute aqueous HCl (50 mL). The contents of the vessel were transferred to a flask with additional methanol (150 mL) and toluene (4 mL), and allowed to stir overnight. The polymer precipitated from this solution as a white solid; this powder was removed by filtration, washed with methanol, and dried *in vacuo* at 25°C for 24 h. Approximately 300–400 mg of the C(1) labeled polymer was typically isolated.

TABLE I. MATERIAL PROPERTIES OF SELECTIVELY ^{13}C LABELED POLYPROPYLENES

PP material	Relative ^{13}C abundance of main-chain carbons[a]			M_w[b] (g/mol)	M_w/M_n[b]	ΔH_f[c] (J/g)
	CH	CH_2	CH_3			
C(1)	1.0 ± 0.2	96.7 ± 0.5	2.3 ± 0.3	159,000 ± 27,000	1.9 ± 0.6	81 ± 3
C(1,3)	0.9 ± 0.1	68.3 ± 0.7	30.8 ± 0.6	255,000 ± 10,200	3.2 ± 0.5	83 ± 7
C(2)	98.5 ± 0.3	0.8 ± 0.1	0.8 ± 0.1	207,000 ± 4,400	2.5 ± 0.2	91 ± 15

[a]Determined with high-temperature, solution ^{13}C NMR spectroscopy. Samples of the PP powder were dissolved in 1,2,4-trichlorobenzene at 130°C.
[b]Molecular weight parameters determined with PP powder samples using high-temperature size exclusion chromatography calibrated with polystyrene standards.
[c]Heats of fusion ΔH_f of the melt-pressed thin films were measured with differential scanning calorimetry (DSC) calibrated with indium and zinc, and using a heating rate of 10°C/min.

2.2. Film samples

Thin, melt-pressed films were prepared from the unstabilized powders in our laboratory (Albuquerque, NM). Before pressing, the C(1,3) labeled polypropylene was ground using a Spex 6700 freezer/mill for about 1.3 min resulting in particles that were ≤ 1 mm in size. The C(1) and C(2) labeled materials were pressed as received. Using a Carver laboratory press, 0.62 g of powder was pressed for 60 s between two polished aluminum plates at a temperature of 180°C and a pressure of 1.4 MPa. Films were then quenched in room-temperature (24°C) water. The average thickness of the films was 100–150 μm. Film samples were kept in a commercial refrigerator at -25°C to inhibit oxidation.

2.3. γ-Irradiation

The pressed films were cut into pieces about 2–3 cm in size for γ-radiation exposure. For irradiation in air, the film pieces were placed into open 20-mL glass vials. For irradiation in an inert (argon) environment, the film pieces were placed into sealed steel containers backfilled with ~100 torr argon. γ-Irradiation was conducted at the Low Intensity Cobalt Array (LICA) facility (Albuquerque, NM), which has been previously described in detail.[24] For irradiation in air, samples were subjected to γ-irradiation under flowing air at room temperature (24°C) and at 80°C.

Samples sealed in argon-filled containers were irradiated in a static air environment surrounding the containers at 24°C. For all experiments the γ-radiation was generated with a ^{60}Co source at a dose rate of 70–90 krad/h. Following irradiation, samples were kept in a commercial refrigerator until they were analyzed with solid-state ^{13}C NMR.

2. 4. Thermal aging

For post-irradiation thermal aging experiments, the irradiated films were cut into pieces about 1–3 mm in size and packed into 4-mm outer diameter zirconia rotors used for NMR MAS experiments. (It should be noted that the highly degraded air-irradiated samples readily crumbled and were packed directly into the MAS rotors without cutting.) Approximately 50–60 mg of material was packed into each rotor. Leaving one end of each rotor open to the environment, the packed rotors were placed into air-circulating, commercial aging ovens under ambient atmospheric conditions (~630 mm Hg in Albuquerque, NM). The temperatures of the ovens used were at 80°C, 95°C, and 109°C, with a temperature control of ±2°C. After a selected period of time in the aging ovens, the packed rotors were removed, allowed to cool to room temperature, and analyzed with ^{13}C solid-state NMR. The packed rotors were then placed back into the oven for continued thermal aging, or were stored in a commercial refrigerator during periods of intentional inactivity.

2.5. NMR parameters

Solid-state NMR experiments were conducted at room temperature (21°C) in a Bruker Avance NMR spectrometer operating at a ^{13}C resonance frequency of 100.6 MHz. Samples were analyzed under magic-angle spinning (MAS) conditions using 4-mm zirconia rotors with Kel-F caps at a spinning frequency of typically 10 kHz. This spinning speed is optimal for the detection and characterization of common oxidation-induced functional groups in polyolefins, as the resulting spinning sidebands do not overlap with any significant resonances attributed to these degradation products [10]. In this study, ^{13}C direct polarization (DP) spectra were acquired with a 60-s recycle delay and a ^{13}C excitation pulse length of 4 μs. High-power ^{1}H decoupling at $\gamma B_1/2\pi$ = 63 kHz utilizing the two-pulse phase modulation (TPPM) decoupling scheme[25] was applied. ^{13}C isotropic chemical shifts were calibrated with an external glycine standard. Unless a specific reference is given, the isotropic chemical shifts of ^{13}C resonances observed in this study were identified with distinct chemical moieties based on simulations carried out using the ACD/CNMR software package (Advanced Chemistry Development, Toronto, Canada).

3. RESULTS AND DISCUSSION

3.1. ^{13}C resonance identification.

Examples of solid-state ^{13}C DP/MAS NMR spectra of C(2), C(1,3), and C(1) labeled polypropylene samples exposed to γ-radiation in room-temperature air are shown in Fig. 1. The selective ^{13}C isotopic labeling is clearly visible in the NMR spectra, based on the three main-chain resonances (peaks 1–3 in figure 1, refer to the PP scheme above). Spectra at maximum intensity and 25× are given for each sample. Major ^{13}C resonances are identified. Main-chain resonances: (1) secondary or methylene (CH_2) carbon; (2) tertiary or methine (CH) carbon; (3) primary or methyl (CH_3) carbon. Functional group resonances: (a) tertiary hydroperoxides and/or dialkyl peroxides; (b) tertiary alcohols; (c) methyl ketones; (d) esters and/or peresters on the C(2) carbon; (e) esters and/or peresters on the C(1) carbon; (f) ketals. Spinning sidebands of the main-chain resonances due to MAS at 10 kHz are designated with 'SSB'.

A minor resonance near 0.9 ppm in the C(2) spectrum was present in the unaged polymer and did not increase or decrease with oxidative aging. Due to scaling, relative peak heights cannot be compared between the various samples in this figure.

Solid-state ^{13}C MAS NMR spectra of neat isotactic polypropylene exhibit three distinct resonances, each resonance corresponding to the three different carbon sites on the PP chain [26,27]. The dominant resonance in the C(2) spectrum at 25.9 ppm is attributed to the methine or tertiary (CH) carbon. The two main resonances in the C(1,3) spectrum at 43.5 and 21.4 ppm are identified with the methylene or secondary carbon (CH_2) and the methyl or primary carbon (CH_3), respectively. The dominant resonance in the C(1) spectrum at 43.5 ppm corresponds to the methylene carbon. First-order spinning sidebands of the labeled main-chain resonances due to MAS at 10 kHz are found at 125.4 ppm for the C(2) sample, 143.3 and 120.9 ppm for the C(1,3) sample, and 143.3 ppm for the C(1) sample. A very small, narrow peak near 0.9 ppm in the C(2) spectrum was present in some of the unirradiated C(2) labeled PP material and did not increase or decrease with subsequent oxidation. This resonance near 0.9 ppm is consistent with a methyl carbon bonded to a siloxane group, present as an impurity.

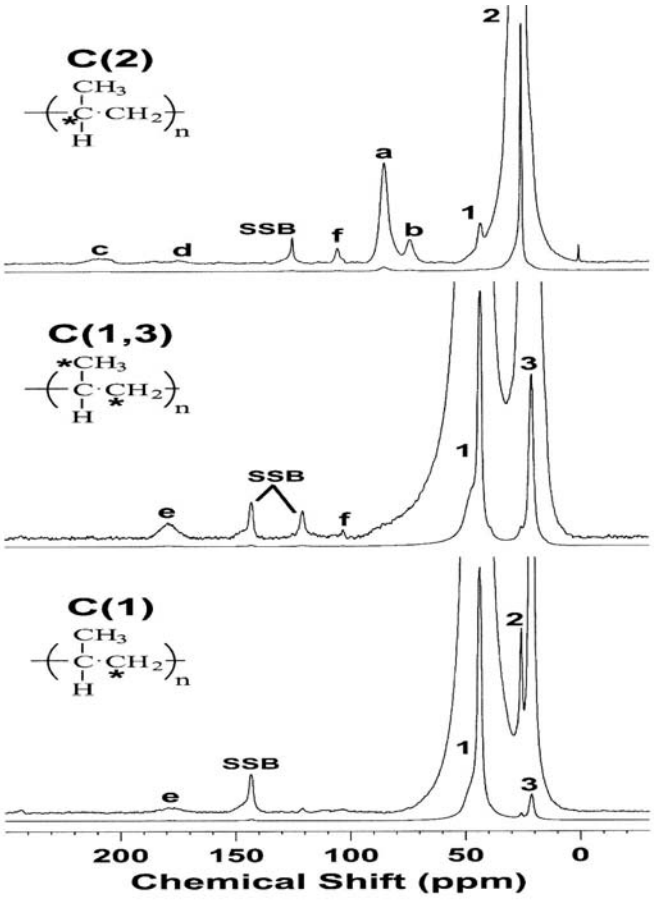

FIG. 1. 60-s ^{13}C DP/MAS spectra of C(2) and C(1,3) labeled polypropylene samples exposed to γ-radiation in 24°C air to a dose of 23 Mrad and of a C(1) labeled polypropylene sample exposed to γ-radiation in 24°C air to a dose of 9 Mrad.

γ-Initiated oxidation yielded functional groups on the polypropylene chains that showed distinct ^{13}C resonances in all of the labeled sample NMR spectra. The resonances were subsequently identified with various functional groups based on their isotropic chemical shifts. A summary of these observed resonances and their corresponding identifications are listed in Table II.

The specific position of origin on the PP chain (i.e. the C(1), C(2), or C(3) carbon, refer to the PP scheme above) and the aging conditions in which the functional group is experimentally observed are given as well. It is apparent from the list of resonances in Table II that the majority of oxidation-induced functional group types formed on the PP chain originate from the tertiary carbon (the C(2) site on the unaged polymer chain). The tertiary carbon site is in fact expected to be most susceptible to free-radical-mediated hydrogen abstraction during oxidation.

3.2. C(2) sample resonances.

The largest NMR peak attributed to oxidation was consistently observed near 85.3 ppm in the C(2) labeled sample spectra, regardless of the aging conditions. This resonance is identified with hydroperoxides and/or dialkyl peroxides (peak a in Fig. 1). In the solid-state ^{13}C NMR analysis of γ-irradiated, ^{13}C enriched polyethylene films, performed previously in our laboratories[10] we observed a similar resonance at ~85 ppm, which was attributed to secondary hydroperoxides. Likewise, a resonance in the range 83–85 ppm was observed by other workers in high-temperature, solution-state ^{13}C NMR analyses of aged polyethylene[8] and polypropylene[12], and these were also identified as hydroperoxide groups. The carbons in dialkyl peroxide linkages would also resonate near 85 ppm and cannot be readily distinguished from the hydroperoxide carbons. If present, the dialkyl peroxides could also be expected to form exclusively between tertiary carbons. A standard oxidation scheme[2,3] leading to hydroperoxides (POOH) and dialkyl peroxides (POOP) is shown below, in Eq. 1.

$$P^{\bullet} + O_2 \longrightarrow POO^{\bullet} \quad (1a)$$

$$POO^{\bullet} + PH \longrightarrow POOH + P^{\bullet} \quad (1b)$$

$$POO^{\bullet} + P^{\bullet} \longrightarrow POOP \quad (1c)$$

$$POO^{\bullet} + POO^{\bullet} \longrightarrow POOOOP \longrightarrow POOP + O_2 \quad (1d)$$

In the PP samples examined in this work, the 85.3-ppm resonance is only detected in the C(2) labeled sample spectra, indicating the exclusive formation of tertiary hydroperoxides, with no primary or secondary hydroperoxides detected in either the C(1) or C(1,3) labeled sample spectra.

Two other ^{13}C resonances were observed in the C(2) labeled sample spectra near 74 and 207 ppm. Like the resonance attributed to peroxides, the ^{13}C resonance at 74.2 ppm due to alcohol groups (peak b in Fig. 1) was only observed in the C(2) sample spectra. 3-Methyl-3-pentanol, a representative small-molecule tertiary alcohol, exhibited an alcohol resonance at 73.0 ppm in ^{13}C NMR spectra, when dissolved in chloroform [28]. Primary and secondary alcohol groups gave smaller isotropic chemical shifts. Thus, the observed chemical shift, along with its origin from the C(2) tertiary carbon, indicates the 74.2-ppm peak to be due to tertiary alcohol groups. Alcohol groups can be produced when alkoxy radicals formed from the degradation of peroxides abstract hydrogen atoms from the same or a nearby polymer chain (Eq. 2). Hence, the tertiary alcohols detected in the C(2) labeled samples most likely originated from the decomposition of tertiary peroxides. It should be noted here that although secondary and primary peroxide and alcohol groups were not experimentally detected in this study, they still might be present during the course of PP oxidation.

$$POOH \longrightarrow PO^{\bullet} + {}^{\bullet}OH \quad (2a)$$

$$PH + PO^{\bullet} \longrightarrow P^{\bullet} + POH \quad (2b)$$

The broad resonance at ~207 ppm is identified with methyl ketones (peak c in Fig. 1), which would occur at the ends of PP chains, thus implying chain scission reactions.

The IR absorbance peaks of methyl and in-chain ketones overlap, and these two species were first distinguished experimentally in oxidized polypropylene with high-temperature solution-state ^{13}C NMR [12]. Methyl ketones are formed by the β-scission of an alkoxy radical, which results in the formation of a primary alkyl radical and a corresponding reduction in molecular weight (Eq. 3) [29, 30]. According to this mechanism, the carbonyl carbon in the methyl ketone group would originally have been a tertiary carbon (C(2) site) on the pre-oxidized chain backbone, as observed here.

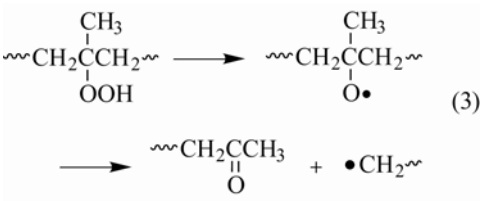

TABLE II. ^{13}C RESONANCES OF OXIDATION-INDUCED FUNCTIONAL GROUPS OBSERVED IN SOLID-STATE NMR SPECTRA OF SELECTIVELY LABELED POLYPROPYLENE SAMPLES

^{13}C chemical shift (ppm)	Functional group		PP position of origin	Aging conditions observed*
~215 (broad)	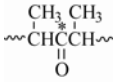	in-chain ketone	C(1)	γ (80°C) γ' (109°C)
~207 (broad)	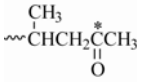	methyl (chain-end) ketone	C(2)	γ (24°C, 80°C) γ' (22°C – 109°C)
~185 (broad)	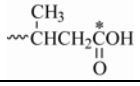	carboxylic acid	C(2)	γ (24°C) γ' (22°C)
~179 (broad)	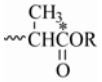	ester	C(1)	γ (24°C, 80°C) γ' (22°C, 109°C)
170–175 (broad)	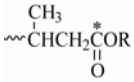	ester	C(2)	γ (24°C, 80°C) γ' (22°C – 109°C)
	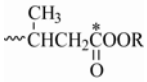	perester		
100–117 (several peaks)		ketal	C(1) C(2)	γ (24°C, 80°C) γ' (22°C – 109°C)
85.3	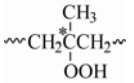	tertiary hydroperoxide	C(2)	γ (24°C, 80°C) γ' (22°C – 109°C)
	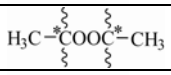	dialkyl peroxide		
74.2	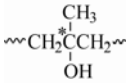	tertiary alcohol	C(2)	γ (24°C, 80°C) γ' (22°C – 109°C)

*γ = exposure to γ-radiation in air; γ' = exposure to γ-radiation in 24°C argon followed by post-irradiation thermal aging in air

Carboxylic acids and esters have ^{13}C chemical shifts ranging from 170–185 ppm. In the C(2) labeled material, resonances were observed at either 170–174 ppm or ~175 ppm, and at ~185 ppm.

The 185-ppm peak is identified with the carboxyl carbon of a carboxylic acid. Carboxylic acid groups detected in the C(2) labeled material could have formed from further oxidation of the chain-end ketones (Eq. 4a) [31]. The broad resonance at either 170–174 ppm or ~175 ppm in C(2) labeled samples is identified with the carboxyl carbon of ester and/or perester groups (peak d in Fig. 1). The 175-ppm peak was observed for materials irradiated at 24°C in air, whereas the resonance is shifted slightly upfield from ~175 ppm to 170–174 ppm for samples irradiated at 80°C in air.

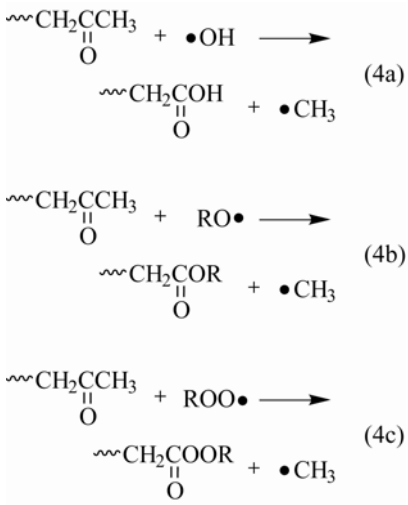

Similar to the oxidation of ketones to carboxylic acids, esters might be produced when a ketone is attacked by an alkoxy radical (Eq. 4b) [31]. Likewise, a perester can form when an alkyl peroxy radical attacks the ketone group[31], as shown in Eq. 4c. Previous workers [32] have inferred that peresters may be present in oxidized polypropylene, based on chemical techniques including iodometry. The carboxyl carbon of a peracid would also resonate from 170–175 ppm. Evidence of peracids in oxidized polypropylene using IR analysis has been obtained [33-35], but also disputed [36].

Two small, reasonably narrow resonances were observed at 105.7 ppm and 114.1 ppm in the C(2) labeled sample spectra (peak f in Fig. 1). The peak at 114.1 ppm was not detected in the sample γ-irradiated at 24°C in air, and therefore does not appear in the C(2) spectrum in Fig. 1. A distribution of relatively smaller intensity was generally found between the two peaks. In previous high-temperature solution-state ^{13}C NMR studies of oxidatively degraded polypropylene [11,12], a resonance at 111.5 ppm was observed and identified with the vinylidene carbon. However, the corresponding resonance of the second unsaturated carbon in the double bond, which should appear in the range 135–155 ppm, was not seen in the solution-state NMR spectra. Overlap with the strong solvent peaks in the same spectral region was cited as the reason for the lack of detection of this second peak.

In the current work, no resonance in the range of 135–155 ppm was observed in the C(2), C(1,3), or C(1) labeled sample spectra. The spinning frequency was adjusted to 5 kHz and 7 kHz, and spectra of the C(2), C(1,3), and C(1) samples were recorded at each of these spinning speeds so that the spectral region of interest was free of spinning sidebands. No additional peaks in the 135–155 ppm region were found, thus ruling out vinylidene and other unsaturated structures. We therefore attribute the resonances observed from 100–110 ppm in the C(2) labeled sample spectra to carbons in alkyl O–C–O (unprotonated ketal and protonated acetal) groups. Acetals have been detected in thermo-oxidized poly(ethylene oxide) using solution-state ^{13}C NMR [19, 20]. We have employed a solid-state NMR technique utilizing ^{13}C CSA dephasing[37] in the characterization of the selectively labeled PP samples in this study, confirming these resonances at 100–110 ppm to be associated with alkyl sp^3-hybridized carbon sites.

In this same study, C-H dipolar dephasing experiments showed these resonances to be unprotonated ketal groups. This work will be reported in detail elsewhere.[38] Unprotonated ketal groups could also include hemiketal structures.

3.3. C(1) and C(1,3) sample resonances

A large, broad resonance at ~179 ppm in the C(1) and C(1,3) labeled samples can be identified with the carboxyl carbon of a carboxylic acid or an ester. It may also be identified with the carboxyl carbon of a γ-lactone [39] (which incorporates an ester group). IR evidence for γ-lactones has been reported in the literature [40, 41]. Recent advanced solid-state ^{13}C NMR experiments [38] have confirmed this resonance to be attributed to an ester functional group, which would not exclude γ-lactones or peresters. Another ^{13}C resonance observed in the C(1) and C(1,3) labeled sample spectra was found at ~215 ppm for material irradiated at 80°C or subjected to post-irradiation treatment at elevated temperatures. This chemical shift is identified with in-chain (or internal) ketones [12]. These ketones are most likely to form on the methylene carbons (C(1) site).

As with the C(2) spectra, resonances in the range of 100–117 ppm were detected in the C(1) and C(1,3) spectra (resonance labeled 'f' in the C(1,3) sample spectrum of Fig. 1). As with the C(2) labeled sample spectra, these resonances are identified with ketal groups. Potentially, these could be present in some type of cyclic peroxidic structure, which have been proposed in the literature [42]. In the C(1,3) sample spectra, two small peaks were seen near 30 ppm (Fig. 2), following γ-irradiation at 80°C. One sample was unirradiated, and the other sample was exposed to γ-radiation (8 Mrad) in 80°C air. Spectra are presented at 5× the maximum intensity. The two small resonances near 30 ppm in the irradiated sample (identified with an arrow) are attributed to methyl groups in the methyl ketone structure and the tertiary alcohol structure.

The peaks were not detected in any C(1) spectra, indicating that they originate from the methyl C(3) carbon. These two resonances are attributed to methyl groups in the methyl ketone structure and the tertiary alcohol structure, which form through oxidation at the C(2) carbon site. The chemical shifts of methyl groups in PP methyl ketones and tertiary alcohols were calculated to be 28.3 ppm and 29.1 ppm, respectively, based on simulations. Representative small-molecule compounds showed similar ^{13}C chemical shifts for these specific methyl groups [28]. The methyl group in the methyl ketone structure of 4-methyl-2-pentanone and 3-methyl-3-pentanol (both dissolved in chloroform) was found to resonate at 30.3 ppm and 33.7 ppm, respectively. The methyl group in a tertiary peroxide structure would resonate further upfield, near 24 ppm, which would be masked by the large C(3) main-chain resonance. A comparison of C(1) and C(1,3) samples subjected to radiation-oxidation under similar conditions indicates that there is no evidence for any significant amount of oxidative product that originates through chemical reaction at the methyl side chain (the C(3) carbon site).

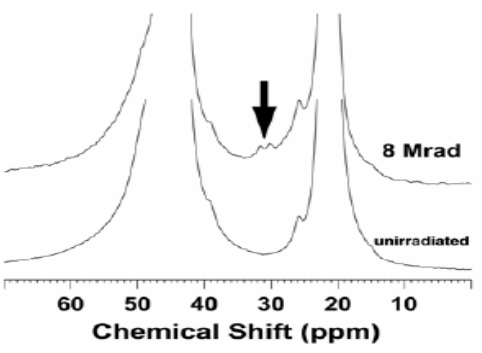

FIG. 2. 60-s ^{13}C DP/MAS spectra (aliphatic region) of two C(1,3) labeled polypropylene samples γ-irradiated in air to different amounts

3.4. Distribution and kinetic accumulation of oxidation products

Solid-state ^{13}C NMR can provide a direct, quantitative measurement of all the oxidation products formed in the polypropylene materials, provided that a suitable recycle delay is chosen so that the magnetization of all ^{13}C sites is sufficiently relaxed. This is a significant advantage over many other common spectroscopic techniques, such as IR spectroscopy. We have determined that a 60-s recycle delay allows for sufficient relaxation of the ^{13}C magnetization in all the detected resonances for the various selectively labeled samples [21].

Solid-state ^{13}C DP/MAS spectra of the C(2), C(1,3), and C(1) labeled polypropylene samples were acquired at different γ-radiation doses or post-irradiation thermal aging times. An example is given in Fig. 3, in which 60-s spectra are presented for a C(2) labeled PP sample exposed to γ-radiation in room-temperature argon followed by post-irradiation thermal aging at 109°C in the presence of air. The accumulation of oxidation products due to post-irradiation thermal aging is clearly seen in this example.

Using the resonance identifications detailed in the previous section (Table II), the kinetic accumulation of these functional groups was analyzed for each specific aging condition. The effects of time and temperature on the distribution and build-up of oxidation products can thus be investigated and compared to available results obtained by IR measurements [32, 43, 44].

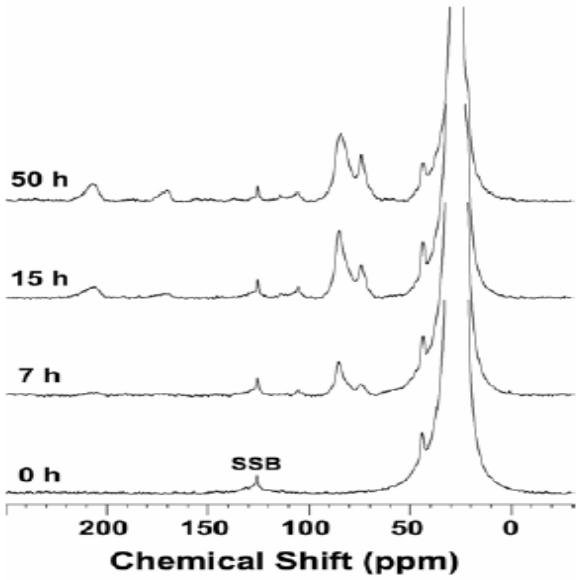

FIG. 3. 60-s ^{13}C DP/MAS spectra of a C(2) labeled polypropylene sample exposed to γ-radiation (24 Mrad) in room temperature (24°C) argon and then subjected to post-irradiation thermal aging in 109°C air for varying times, as indicated in the figure. Spectra are presented at 25× the maximum intensity. The spinning sideband is denoted with 'SSB' in the freshly irradiated (0 h) sample.

3.5. γ-irradiation in air, at two different temperatures: 24°C and 80°C.

The kinetic accumulation of functional groups in solid polypropylene samples due to oxidation by γ-irradiation in either 24°C or 80°C air (using a dose rate of 80-90 krad/h) is shown in Fig. 4 and 5, respectively. Overall product distributions estimated for the polypropylenes γ-irradiated in air are shown in Table III.

The peroxides (tertiary hydroperoxides and/or dialkyl peroxides) are the most abundant oxidation product, which agrees with the results of previous studies [32, 43, 44] at dose rates ranging from 28 to 700 krad/h. Increasing the irradiation temperature from 24°C to 80°C accelerates the rate of oxidation and increases the total product formation (Fig. 4 and 5), which was also observed by Decker and Mayo [43] using IR analysis. For irradiation at 24°C, the tertiary peroxides (58.5%) and the esters/peresters (11.1%) are significantly higher than for the material irradiated at 80°C (Table III). The samples irradiated at 80°C show increased concentrations of alcohols, methyl ketones and carboxylic acids/esters, compared with the lower temperature irradiation.

This is consistent with enhanced decomposition of peroxidic species to form secondary oxidation products at the higher irradiation temperature. The large decrease in the ester/perester resonance (peak d in Fig. 1) at higher temperatures is consistent with a significant component of a peroxidic species in this peak in the case of the 24°C irradiation. The temperature dependence of the product yields seen in the irradiated polypropylene may be contrasted to the results we have obtained in corresponding thermal oxidation experiments[21] on these labeled polypropylene samples in the absence of radiation; for the thermal-only aging experiments, the product distributions were essentially independent of aging temperature over the range included in the study (50°C to 110°C).

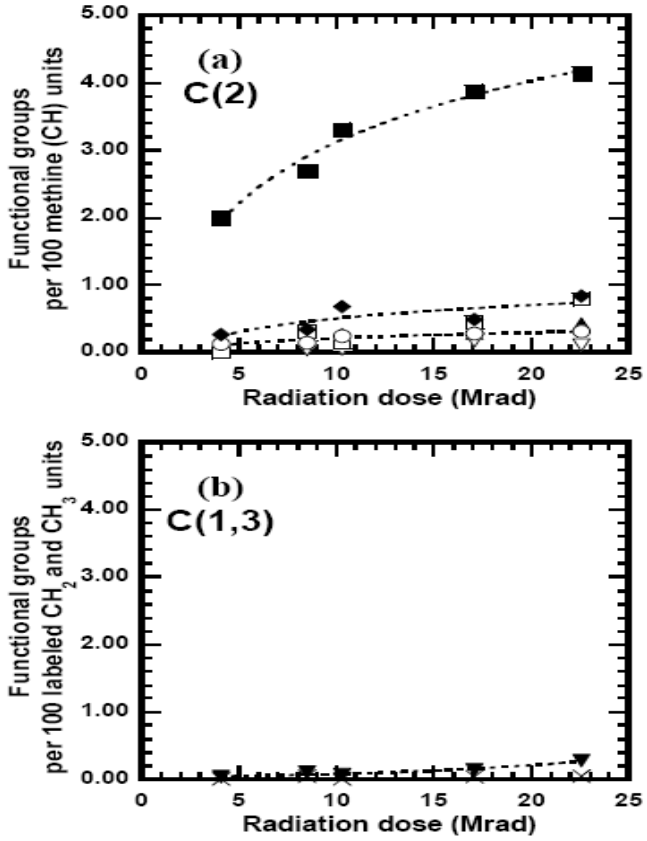

FIG. 4. Kinetic accumulation of oxidation products in solid polypropylene samples exposed to γ-radiation in 24°C air. (a) C(2) labeled sample; (b) C(1,3) labeled sample. Symbols for functional groups (Fig. 4–8,11): (■) tertiary hydroperoxides and/or dialkyl peroxides; (♦) tertiary alcohols; (▲) methyl ketones; (Δ) in-chain ketones; (▽) carboxylic acids on C(2) carbon; (□) esters and/or peresters on C(2) carbon; (▼) esters and/or peresters on C(1) carbon; (◊) ketals on C(2) carbon (114.1 ppm); (○) ketals on C(2) carbon (105.7 ppm); (×) ketals on C(1) carbon (100–117 ppm). Dotted lines are guides to the eye.

Indeed, comparison of the oxidation product distributions in Table III for PP material highly irradiated (17 Mrad) at 80°C versus material highly oxidized (~175 h past the induction period) at 80°C in the absence of any radiation shows some significant differences. For instance, irradiated PP material shows an increased proportion of methyl ketones, whereas material that underwent thermal-only oxidation exhibits larger concentrations of alcohols and ketals.

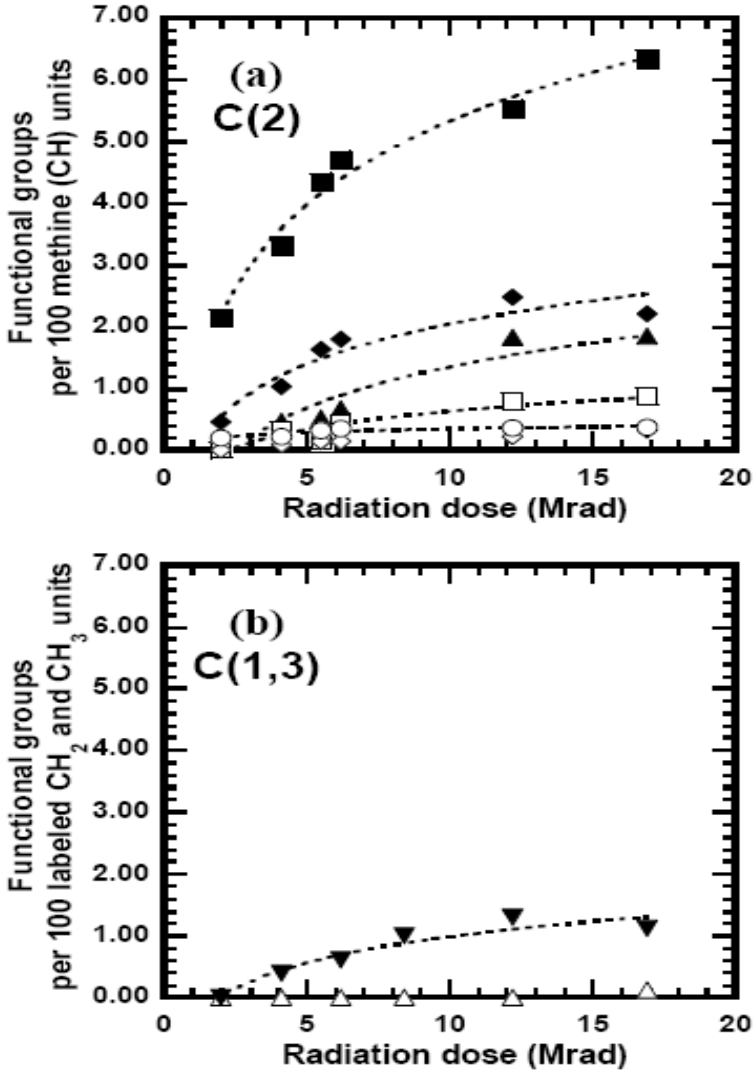

FIG. 5. Kinetic accumulation of oxidation products in solid polypropylene samples exposed to γ-radiation in 80°C air. (a) C(2) labeled sample; (b) C(1,3) labeled sample. Symbols for functional groups as in Fig. 4. Dotted lines are guides to the eye.

TABLE III. DISTRIBUTION OF OXIDATION-INDUCED FUNTIONAL GROUPS OBSERVED IN POLYPROPYLENE SAMPLES EXPOSED TO Γ-RADIATION OR THERMAL AGING IN AIR

Functional group	Aging temperature and radiation dose / thermal aging time after induction period					
	24°C, 23 Mrad irradiation		80°C, 17 Mrad irradiation		80°C, ~175 h no irradiation	
	C(2)[b]	C(1,3)[c]	C(2)[b]	C(1,3)[c]	C(2)[b]	C(1,3)[c]
Tertiary hydroperoxides/ dialkyl peroxides	58.5	—	46.0	—	42.7	—
Tertiary alcohols	11.7	—	16.0	—	21.6	—
Methyl ketones	5.9	—	13.5	—	8.0	—
Carboxylic acids on C(2) carbon	1.6	—	—	—	—	—
Esters/peresters on C(2) carbon	11.1	—	6.3	—	5.6	—
Esters/peresters on C(1) carbon	—	5.8	—	11.9	—	13.8
In-chain ketones	—	—	—	1.3	—	1.3
Ketals on C(2) carbon (114.1 ppm)	—	—	2.3	—	2.2	—
Ketals on C(2) carbon (105.7 ppm)	4.4	—	2.7	—	4.1	—
Ketals on C(1) carbon	—	1.0	—	—	—	0.7

[a]Values presented are the mole percents of the total oxidation products on the PP chain with each aging temperature.
[b]Values derived from the C(2) labeled sample NMR spectra are relative to values from the C(1,3) labeled sample spectra.
[c]Integral fractions from the C(1,3) NMR spectra were normalized by 0.68, based on the assumption these products originate exclusively from the C(1) carbon.

The occurrence of a greatly-enhanced methyl ketone signal in the 80°C irradiated C(2) labeled sample spectra, compared with the 24°C irradiated C(2) spectra, is significant. Interestingly, the methyl ketone signal in the 80°C irradiated material is in fact much larger than that found in any of our previous thermal aging experiments, while the tertiary alcohol signal is smaller compared with these thermal-only experiments. When a tertiary peroxide decomposes, the two main reaction paths lead either: 1) to a methyl ketone, which also results in cleavage of the macromolecular chain (Eq. 3), or else 2) to a tertiary alcohol, which does not involve chain cleavage (Eq. 2). These facts can be considered in light of the long-standing observation by Clough and Gillen [45], as well as others, that for many common polymers, the simultaneous application of radiation and elevated temperature often leads to a much larger decrease in mechanical properties, compared with radiation exposure at room temperature. This observation has been described previously in terms of a "synergism" between the environmental effects of radiation and temperature.

3.6. γ-irradiation under inert atmosphere, followed by exposure to air

Fig. 6 shows the time-dependent formation of post-irradiation oxidation products in thin films of C(2) and C(1,3) labeled polypropylene samples that were exposed to γ-radiation in argon to a dose of approximately 24 Mrad, and were subsequently held in room-temperature (22°C) air for a period of more than 1 year. These conditions are relevant to the situation of radiation-sterilization of polypropylene by e-beam irradiation, where the high dose rate will consume the dissolved oxygen more rapidly than it can be replenished by diffusion into the material from the surrounding atmosphere. It is seen that the products formed through reactions involving the C(2) carbon are dominant. Peroxides, which are again the major product, are seen to rise in an essentially linear fashion throughout the time period studied. Fig. 7 and 8 show post-irradiation results for polypropylene samples that were similarly exposed to γ-radiation under inert atmosphere, and were then exposed to a variety of elevated temperatures in air. In all cases, the peroxides dominate and increase approximately linearly during the early aging times. After very extensive oxidation, the product concentrations enter a plateau region.

Table IV shows the relative concentrations of degradation products in highly oxidized C(2) labeled PP samples from post-irradiation experiments conducted at varying temperatures. Some trends are apparent. The overall yield of peroxides is highest in the irradiated samples that were subsequently exposed at room temperature, and they account for nearly 70% of the products. The relative fraction of peroxides decreases as progressively higher temperatures are utilized for the post-irradiation exposures. At the highest temperature studied (109°C), peroxides comprise about 54% of the overall products. The two oxidative functional groups which arise from reaction of peroxidic species at the tertiary C(2) carbon (methyl ketones from chain cleavage, and tertiary alcohols from hydrogen abstraction by an alkoxy radical) both increase with increasing post-irradiation temperature. The methyl ketones more than double over the temperature range studied, and the tertiary alcohols increase by about 75%. These temperature-dependent trends in the chemistry are in the same direction as those observed for materials irradiated in air at 24°C versus 80°C, as discussed in the previous section.

TABLE IV. DISTRIBUTION[A] OF OXIDATION-INDUCED FUNCTIONAL GROUPS OBSERVED ON THE C(2) CARBON IN POLYPROPYLENE SAMPLES Γ-IRRADIATED IN ARGON FOLLOWED BY POST-IRRADIATION THERMAL AGING IN AIR

Functional group	Post-irradiation aging temperature			
	22°C	80°C	95°C	109°C
Tertiary hydroperoxides/ dialkyl peroxides	69.2	56.9	57.3	54.3
Tertiary alcohols	12.2	20.0	20.6	21.7
Methyl ketones	5.7	8.8	11.3	12.7
Carboxylic acids	0.3	0.5	—	—
Esters/peresters	2.7	6.2	4.4	5.7
Ketals (114.1 ppm)	2.1	2.2	1.7	2.1
Ketals (05.7 ppm)	7.7	5.4	4.7	3.6

[a]Values presented are the mole percents of the total oxidation products on the PP C(2) main-chain carbon with each post-irradiation aging temperature.

In Fig. 6–8 it is clearly observed that the accumulation of tertiary peroxides in the C(2) labeled PP samples is linear with post-irradiation time during early aging times. The accumulation rates of tertiary peroxides at these early times can be derived from a linear regression. The Arrhenius plot of linear accumulation rates for tertiary peroxidic products at post-irradiation aging temperatures ranging from 22°C to 109°C is shown in Fig. 9. From this plot, an apparent activation energy of 68 kJ/mol (16 kcal/mol) is obtained for tertiary peroxide accumulation at early post-irradiation aging times.

The onset of formation of oxidation products in pre-irradiated polypropylene, which begins immediately when the samples are exposed to air, can be contrasted with the result when unirradiated polypropylene is similarly subjected to air at elevated temperature. In the latter instance, there is a significant, initial time period during which no oxidation chemistry detectable by solid-state NMR takes place (an "induction" period). Once the oxidation gets underway, the rate of peroxide formation is essentially the same as for the pre-irradiated samples. This can be readily seen by comparing the peroxide accumulation curves shown in Fig. 10 for C(2) labeled material held at 80°C and 109°C, both with and without pre-irradiation treatment.

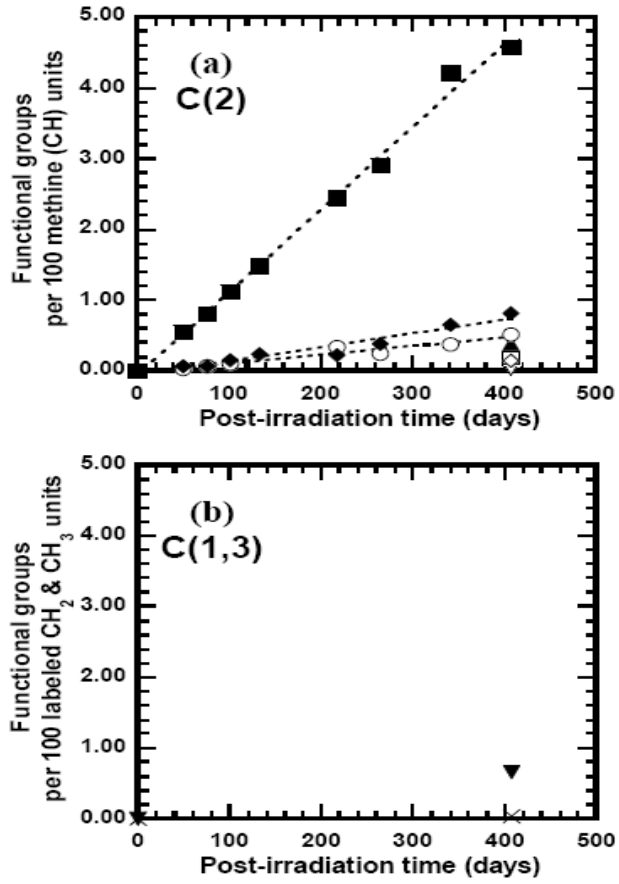

FIG. 6. Kinetic accumulation of oxidation products in solid polypropylene samples exposed to γ-radiation (24 Mrad) in 24°C argon followed by post-irradiation thermal aging in 22°C air. (a) C(2) labeled sample; (b) C(1,3) labeled sample. Symbols for functional groups as in Fig. 4. Dotted lines are guides to the eye.

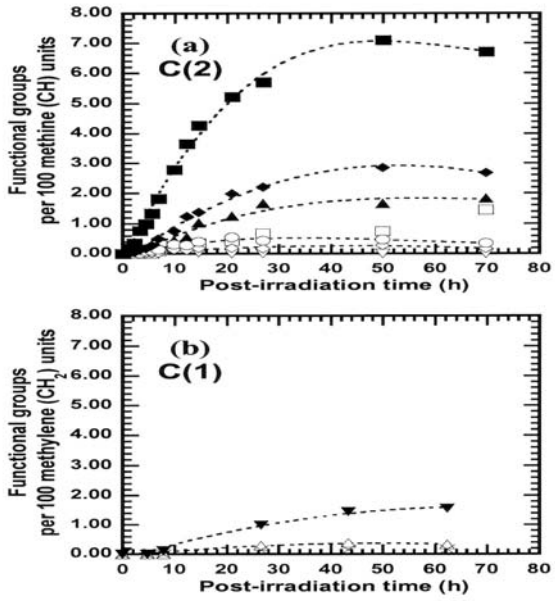

FIG. 7. Kinetic accumulation of oxidation products in solid polypropylene samples exposed to γ-radiation (24 Mrad) in 24°C argon followed by post-irradiation thermal aging in 109°C air. (a) C(2) labeled sample; (b) C(1) labeled sample. Dotted lines are guides to the eye.

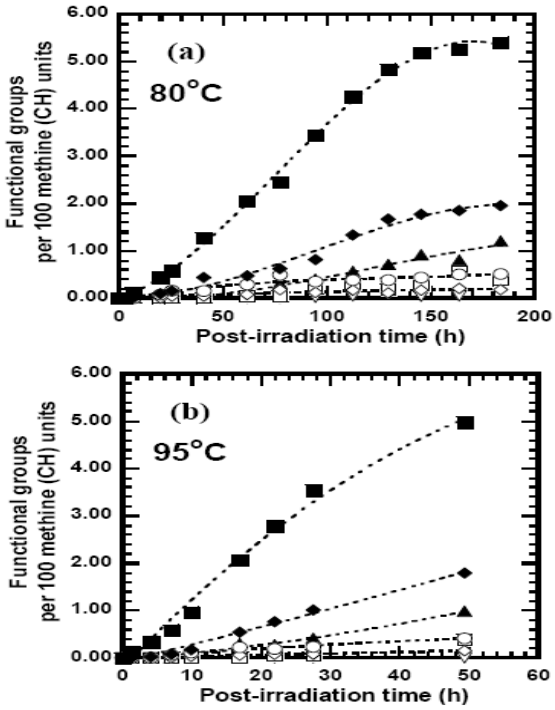

FIG. 8. Kinetic accumulation of oxidation products in solid C(2) labeled polypropylene samples exposed to γ-radiation (24 Mrad) in 24°C argon followed by post-irradiation thermal aging in air at different temperatures. (a) C(2) sample thermally aged at 80°C; (b) C(2) sample thermally aged at 95°C. Dotted lines are guides to the eye.

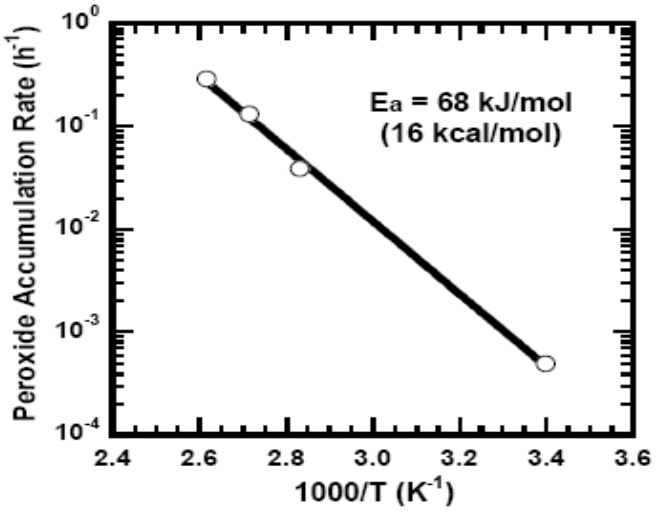

FIG. 9. Arrhenius plot of the tertiary peroxide linear accumulation rate for solid C(2) labeled polypropylene samples exposed to γ-radiation (24 Mrad) in 24°C argon followed by post-irradiation thermal aging in air. The apparent activation energy for tertiary peroxide accumulation during early post-irradiation aging times is 68 kJ/mol (16 kcal/mol).

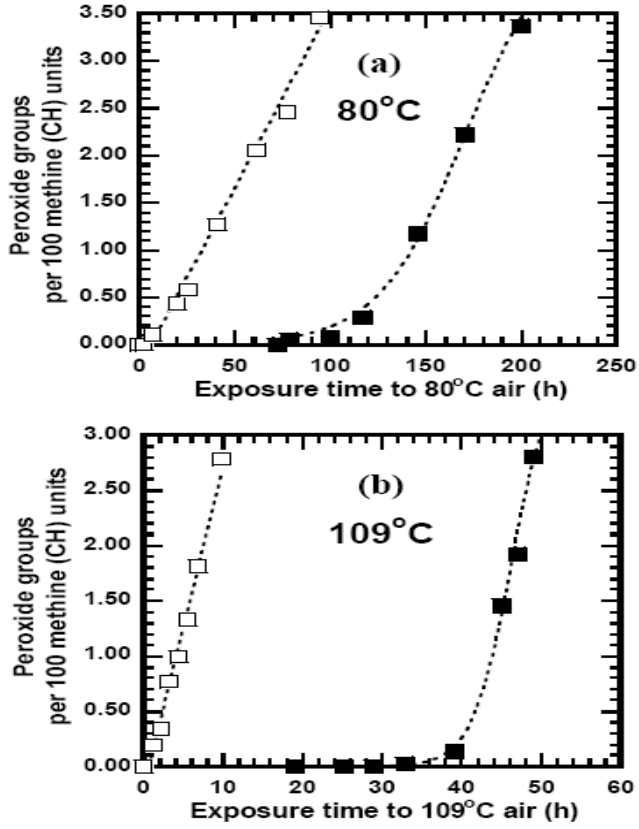

FIG. 10. Comparison of the kinetic accumulation of tertiary peroxide groups in solid C(2) labeled polypropylene samples exposed to γ-radiation (24 Mrad) in 24°C argon followed by post-irradiation thermal aging in air (□) versus unirradiated samples thermally aged air (■), at two different aging temperatures, (a) 80°C and (b) 109°C.

The one temperature-dependent trend that is very different in the post-irradiation experiments is in the formation of esters/peresters on the C(2) carbon (peak d in Fig. 1). In the samples γ-irradiated in air at 24°C (Table 3), this peak accounts for about 11% of the total products, whereas for the material irradiated in air at 80°C, this product has decreased to about 6% of the total. In contrast, for the post-irradiation experiment at 22°C, this peak accounts for only about 2% of the total products, while this percentage rises to as much as 6% at higher temperatures (Table 4). This difference may be explained by the fact that the peaks in this region represent two species that cannot be easily resolved by NMR. It is quite possible that irradiation in air at 24°C results in the formation of a large amount of the peroxidic product (perester), whereas irradiation at 80°C gives little if any of this product, which may likely be thermally unstable. If the chemistry leading to the perester were functioning only when oxygen is present *during* irradiation, then the results of the post-irradiation experiments could be understood in terms of no contribution from a perester component. The post-irradiation results would then indicate an increase in ester formation at higher temperatures, similar to the increase observed in the alcohols and methyl ketones.

There are two NMR peaks associated with ketal products. The larger of these two peaks (105.7 ppm) shows a temperature dependence in the post-irradiation experiments (Table 4), with the relative amount of product formed in the room temperature exposure being approximately twice the amount found at high temperature. Ketals are products of modest stability, and are subject to decomposition – particularly through hydrolytic chemistry, which could explain their presence in lower amount with increasing temperature. A temperature dependence of the 105.7-ppm ketal peak also seems to occur in the irradiation experiments at 24°C versus 80°C in air (Table 3).

3.7. γ-irradiation in air, followed by elevated temperature exposure

Fig. 11 shows time-dependent post-irradiation oxidation data for experiments in which C(2) labeled polypropylene was γ-irradiated in air at a dose rate of ~70 krad/h to a total dose of approximately 34 Mrad, after which the samples were placed in an environment of elevated temperature in the presence of air. At each of the three post-irradiation aging temperatures studied (80°C, 95°C, and 109°C), the NMR peaks representing the initial amounts of tertiary alcohol, methyl ketone, and ester/perester (formed during the course of air irradiation), are seen to increase significantly at relatively short aging times. The amount of growth in these secondary reaction products may be somewhat dependent on the temperature, and is not precisely measurable due to scatter in the data, but in very approximate terms, the tertiary alcohols increase by a factor of roughly 2, the methyl ketones increase by a factor of roughly 1.5 to 2, and the ester/perester peak rises by a factor of roughly 2 or 3. The peroxide peak exhibits little or no change within the experimental scatter. At longer aging times, all of the oxidation product concentrations appear to reach a plateau value, beyond which further changes are relatively small, if they occur at all.

3.8. Comparison with radiation-oxidation of polyethylene

Our research group has previously reported detailed studies on the radiation-oxidation of polyethylene that was isotopically labeled at 99% (^{13}C at all positions along the chain) with data obtained using solid-state ^{13}C NMR spectroscopy [10]. The differences in radiation-oxidation chemistry of polypropylene, versus the radiation-oxidation chemistry of polyethylene, are substantial. In stark contrast to the polypropylene findings in the present study, in which peroxides dominate the products under all conditions, the peroxides in polyethylene are of low stability and have been difficult to study. In the case of irradiation at 25°C, ^{13}C NMR of isotopically labeled polyethylene allowed the detection of peroxides, which were observed to reach a maximum at relatively low doses, after which their concentration then decreased steadily to very low levels upon further irradiation, while other oxidation products grew to dominate the NMR spectrum.

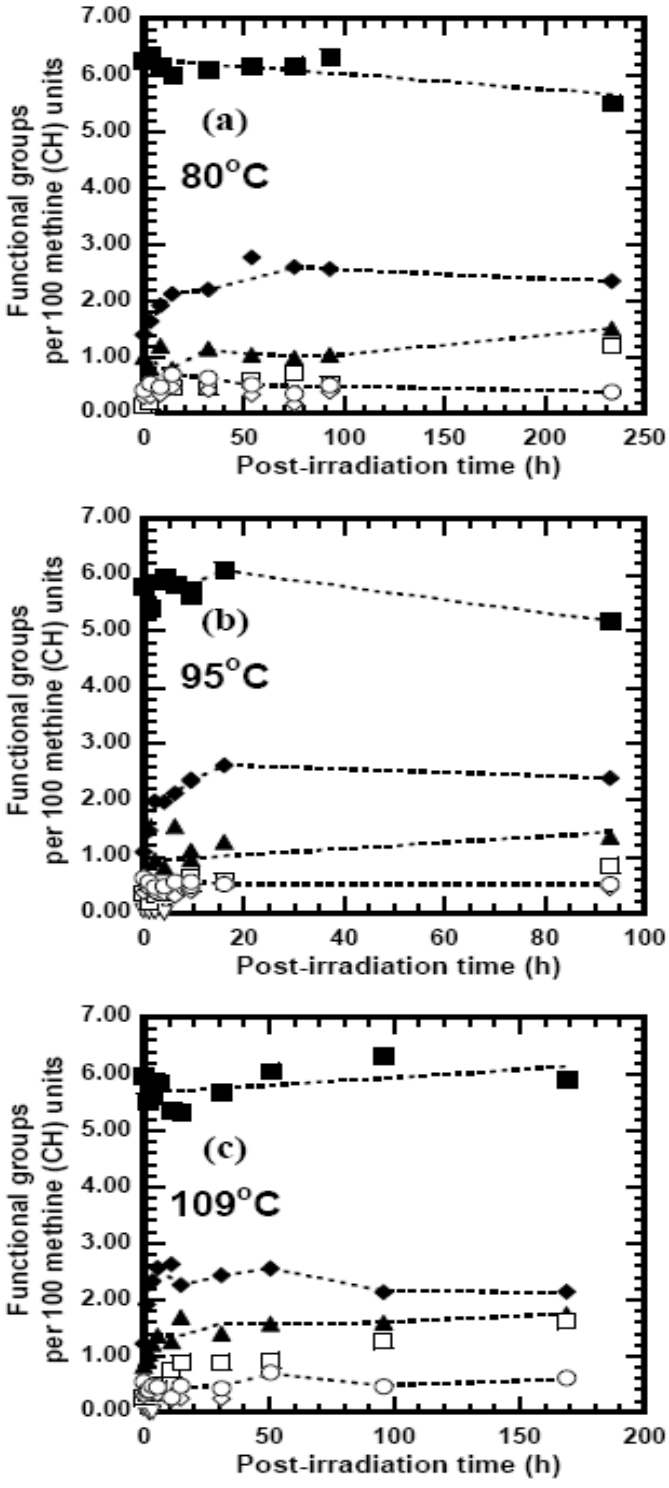

FIG. 11. Kinetic plots of oxidation products in solid C(2) labeled polypropylene samples exposed to γ-radiation (34 Mrad) in 24°C air followed by post-irradiation thermal aging in air at different temperatures. (a) C(2) sample thermally aged at 80°C; (b) C(2) sample thermally aged at 95°C; (c) C(2) sample thermally aged at 109°C. Dotted lines are guides to the eye.

When samples of polyethylene that had been pre-irradiated in air at 25°C were subjected to elevated temperature environments ranging from 22°C to 110°C, in the presence of air, the peroxides that had formed during the irradiation were seen to decrease quite rapidly, and then to disappear entirely, while secondary oxidation products of ketones, alcohols and acids increased. For example, at 110°C, the complete disappearance of the peroxides in polyethylene took place during the course of about 2 h. When the polyethylene was irradiated in the presence of air at 80°C, no peroxide was ever observed, due to its apparently low concentration resulting from its thermal instability, whereas the other oxidation products were readily measured throughout the course of the experiment.

The nature of the oxidation products is quite different in polypropylene and polyethylene. In the case of polypropylene, as can be seen by reviewing the figures presented above, the rank ordering of the concentrations of different oxidation products basically always remains unchanged throughout the course of the degradation process. For polyethylene this is not the case, and the relative ratios of various oxidation products can change significantly as oxidation progresses. As can be seen from the data throughout this paper, under all conditions studied, the oxidation products in highest concentration in polypropylene are tertiary peroxides, and the products second highest in concentration are the tertiary alcohols. In contrast, for polyethylene, the largest oxidation products are acids/esters (most dominant at high extents of degradation) and ketones (more dominant at lower extents of degradation).

4. CONCLUSIONS

Polypropylene samples were prepared in which chains were isotopically labeled at specific positions with ^{13}C. Unstabilized thin films of these materials were subjected to γ-irradiation and to post-irradiation thermal oxidation, and were analyzed with solid-state ^{13}C NMR spectroscopy. It was found that the vast majority of oxidation-induced functional groups formed either during irradiation or upon post-irradiation treatment occurred on the tertiary (CH) carbons of the polypropylene. Of these products, tertiary hydroperoxides and/or dialkyl peroxides, which share the same ^{13}C resonance, were the most abundant, with tertiary alcohols as the second most abundant product. We detected no peroxides or alcohols originating from the secondary (CH_2) or the methyl positions of the PP; indeed we found no evidence of any chemistry occurring at the methyl side chain carbon. Carboxylate products were observed from both the secondary and tertiary carbon atoms (likely a mixture of acids, esters, and peresters). Other oxidation products included methyl ketones (for which the carbonyl carbon originated from the tertiary PP carbon), in-chain ketones (from the secondary PP carbon), and ketals (from both the tertiary and secondary PP carbons).

Oxidation product distributions for irradiated materials were substantially different for room temperature versus elevated temperature exposure. Samples irradiated at 24°C in air exhibited exceptionally high concentrations of peroxidic species, whereas irradiation at 80°C gave rise to higher yields of oxidation products attributable to the decomposition of peroxides, such as tertiary alcohols and carboxylic acids, and particularly large amounts of methyl ketones, indicative of a high yield of chain scission for a combined environment of radiation and temperature. Overall similar temperature-dependent trends were found in the case of samples exposed to irradiation under inert atmosphere, followed by exposure to air at varying temperatures. For example, in pre-irradiated samples exposed to air at room temperature for over a year, peroxides accounted for about 70% of the total oxidation products. This ratio decreased when higher temperature post-irradiation exposures were used, for example amounting to about 54% peroxides when 109°C was chosen for the post-irradiation treatment. With increasing post-irradiation temperature, the proportion of products attributable to peroxide decomposition increased, with methyl ketones more than doubling and alcohols rising by about 75% upon going from room temperature to 109°C. For samples irradiated in air, and then exposed to elevated temperature in air, important products such as ketones and alcohols that had formed during the irradiation were seen to further increase in concentration at first, and then reach a plateau, while peroxide concentrations changed little throughout the post-irradiation exposure.

The results gained in this study allow polypropylene to be compared to polyethylene, which we have studied recently using a fully isotopically-labeled sample, together with NMR analysis. Quite different radiation-oxidation chemistry trends are apparent. The relative rank ordering of oxidation product yields in polypropylene tends to remain the same throughout a given irradiation or post-irradiation exposure. As described above, peroxides dominate the products, and show remarkable thermal stability. In polyethylene, the peroxides are of low stability, and disappear rapidly when irradiated samples are subjected to elevated temperature. The dominant products in polyethylene are also different (either acids/esters, or ketones, dependent upon the extent of degradation).

ACKNOWLEDGMENTS

Sandia is a multiprogram laboratory operated by Sandia Corporation, a Lockheed Martin Company, for the United States Department of Energy's National Nuclear Security Administration under contract DE-AC04-94AL8500. The authors are grateful to Mat Celina for offering valuable comments, to Prof. John Bercaw for cooperation in providing the C(1) labeled PP sample, to Michelle Shedd for DSC measurements, and to Sean Winters, Don Berry, Don Hanson, and Zane Lawson for assistance in irradiating samples. Impact Analytical (Midland, MI) is acknowledged for acquiring the molecular weight data.

REFERENCES

[1] CLOUGH, R.L., "High-energy radiation and polymers: A review of commercial processes and emerging applications", Nuclear Instruments and Methods in Physics Research B **185** (2001) 8-33.

[2] CARLSSON, D.J., WILES, D.M., "The Photooxidative Degradation of Polypropylene. Part 1. Photooxidation and Photoinitiation Processes", Journal of Macromolecular Science -- Reviews in Macromolecular Chemistry **C14**(1) (1976) 65-106.

[3] GEORGE, G.A., CELINA, M., "Homogeneous and Heterogeneous Oxidation of Polypropylene", in: Handbook of Polymer Degradation (HAMID, S.H., Ed.) Second Edition, Marcel Dekker, Inc., New York 2000, 277-313.

[4] BOVEY, F.A., JELINSKI, L., MIRAU, P.A., Nuclear Magnetic Resonance Spectroscopy, Second Edition, Academic Press, San Diego 1988.

[5] SCHMIDT-ROHR, K., SPIESS, H.W., Multidimensional Solid-State NMR and Polymers, Academic Press, San Diego 1994.

[6] CHENG, H.N., SCHILLING, F.C., BOVEY, F.A., "13C Nuclear Magnetic Resonance Observation of the Oxidation of Polyethylene", Macromolecules **9**(2) (1976) 363-365.

[7] RANDALL, J.C., ZOEPFL, F.J., SILVERMAN, J., "High-Resolution Solution Carbon 13 NMR Measurements of Irradiated Polyethylene", Radiation Physics and Chemistry **22**(1/2) (1983) 183-192.

[8] JELINSKI, L.W., DUMAIS, J.J., LUONGO, J.P., CHOLLI, A.L., "Thermal Oxidation and Its Analysis at Low Levels in Polyethylene", Macromolecules **17**(9) (1984) 1650-1655.

[9] HORII, F., ZHU, Q., KITAMARU, R., YAMAOKA, H., "13C NMR Study of Radiation-Induced Cross-Linking of Linear Polyethylene", Macromolecules **23** (1990) 977-981.

[10] ASSINK, R.A., CELINA, M., DUNBAR, T.D., ALAM, T.M., CLOUGH, R.L., GILLEN, K.T., "Analysis of Hydroperoxides in Solid Polyethylene by MAS ^{13}C NMR and EPR", Macromolecules **33**(11) (2000) 4023-4029.

[11] BUSFIELD, W.K., HANNA, J.V., "A ^{13}C NMR Study of End Groups and Stereoregularity Changes Induced by γ Irradiation of Molten Polypropylenes", Polymer Journal **23**(10) (1991) 1253-1263.

[12] VAILLANT, D., LACOSTE, J., DAUPHIN, G., "The oxidation mechanism of polypropylene: contribution of ^{13}C-NMR spectroscopy", Polymer Degradation and Stability **45** (1994) 355-360.

[13] O'DONNELL, J.H., WHITTAKER, A.K., "Observation by ^{13}C n.m.r. of H-crosslinks and methyl end groups due to main-chain scission in ethylene-propylene copolymers after γ-irradiation", Polymer **33**(1) (1992) 62-67.

[14] O'DONNELL, J.H., WHITTAKER, A.K., "Radiation Degradation of Linear Low-Density Polyethylene -- Determination of Lamallae Thickness, Crystallinity and Cross-Linking by Solid-State C-13 NMR and DSC", Radiation Physics and Chemistry **39**(2) (1992) 209-214.
[15] HILL, D.J.T., O'DONNELL, J.H., PERERA, M.C.S., POMERY, P.J., "Determination of New Chain-End Groups in Irradiated Polyisobutylene by NMR Spectroscopy", in: Irradiation of Polymers: Fundamentals and Technological Applications (CLOUGH, R.L., SHALABY, S.W., Eds.) Volume 620, ACS Symposium Series, American Chemical Society, Washington, DC 1996, 139-150.
[16] YANG, L., HEATLEY, F., BLEASE, T.G., THOMPSON, R.I.G., "A Study of the Mechanism of the Oxidative Thermal Degradation of Poly(ethylene oxide) and Poly(propylene oxide) Using ^{1}H- and ^{13}C-NMR", European Polymer Journal **32**(5) (1996) 535-547.
[17] ALAM, T.M., CELINA, M., ASSINK, R.A., CLOUGH, R.L., GILLEN, K.T., WHEELER, D.R., "Investigation of Oxidative Degradation in Polymers Using ^{17}O NMR Spectroscopy", Macromolecules **33**(4) (2000) 1181-1190.
[18] ALAM, T.M., CELINA, M., ASSINK, R.A., CLOUGH, R.L., GILLEN, K.T., "^{17}O NMR investigation of oxidative degradation in polymers under γ-irradiation", Radiation Physics and Chemistry **60** (2001) 121-127.
[19] MKHATRESH, O.A., HEATLEY, F., "A ^{13}C NMR Study of the Products and Mechanism of the Thermal Oxidative Degradation of Poly(ethylene oxide)", Macromolecular Chemistry and Physics **203**(16) (2002) 2273-2280.
[20] MKHATRESH, O.A., HEATLEY, F., "A study of the products and mechanism of the thermal oxidative degradation of poly(ethylene oxide) using ^{1}H and ^{13}C 1-D and 2-D NMR", Polymer International **53** (2004) 1336-1342.
[21] MOWERY, D.M., ASSINK, R.A., DERZON, D.K., KLAMO, S.B., CLOUGH, R.L., BERNSTEIN, R., "Solid-State ^{13}C NMR Investigation of the Oxidative Degradation of Selectively Labeled Polypropylene by Thermal Aging and γ-Irradiation", Macromolecules **38**(12) (2005) 5035-5046.
[22] BURGER, B.J., BERCAW, J.E., New Developments in the Synthesis, Manipulation, and Characterization of Organometallic Compounds, Volume 357, ACS Symposium Series, American Chemical Society, Washington, DC 1987.
[23] PANGBORN, A.B., GIARDELLO, M.A., GRUBBS, R.H., ROSEN, R.K., TIMMERS, F.J., "Safe and Convenient Procedure for Solvent Purification", Organometallics **15** (1996) 1518-1520.
[24] GILLEN, K.T., CLOUGH, R.L., JONES, L.H., "Investigation of cable deterioration in the containment building of the Savannah River reactor", Sandia Labs Report SAND81-2613 (1982).
[25] BENNETT, A.E., RIENSTRA, C.M., AUGER, M., LAKSHMI, K.V., GRIFFIN, R.G., "Heteronuclear decoupling in rotating solids", Journal of Chemical Physics **103**(16) (1995) 6951-6958.
[26] BUNN, A., CUDBY, M.E.A., HARRIS, R.K., PACKER, K.J., SAY, B.J., "High resolution ^{13}C n.m.r. spectra of solid isotactic polypropylene", Polymer **23** (1982) 694-698.
[27] GOMEZ, M.A., TANAKA, H., TONELLI, A.E., "High-resolution solid-state ^{13}C nuclear magnetic resonance study of isotactic polypropylene polymorphs", Polymer **28** (1987) 2227-2232.
[28] POUCHERT, C.J., BEHNKE, J., Eds. The Aldrich Library of ^{13}C and ^{1}H FT NMR Spectra, First Edition, Volume 1, Aldrich Chemical Company 1993.
[29] CARLSSON, D.J., WILES, D.M., "The Photodegradation of Polypropylene Films. II. Photolysis of Ketonic Oxidation Products", Macromolecules **2**(6) (1969) 587-597.
[30] MILL, T., RICHARDSON, H., MAYO, F.R., "Aging and Degradation of Polyolefins. IV. Thermal and Photodecompositions of Model Peroxides", Journal of Polymer Science: Polymer Chemistry Edition **11** (1973) 2899-2907.
[31] GEUSKENS, G., KABAMBA, M.S., "Photo-oxidation of Polymers -- Part V: A New Chain Scission Mechanism in Polyolefins", Polymer Degradation and Stability **4** (1982) 69-76.

[32] LACOSTE, J., VAILLANT, D., CARLSSON, D.J., "Gamma-, Photo-, and Thermally-Initiated Oxidation of Isotactic Polypropylene", Journal of Polymer Science: Part A: Polymer Chemistry **31** (1993) 715-722.
[33] ZAHRADNÍCKOVÁ, A., SEDLÁR, J., DASTYCH, D., "Peroxy Acids in Photo-oxidized Polypropylene", Polymer Degradation and Stability **32** (1991) 155-176.
[34] GIJSMAN, P., HENNEKENS, J., VINCENT, J., "The mechanism of the low-temperature oxidation of polypropylene", Polymer Degradation and Stability **42** (1993) 95-105.
[35] GIJSMAN, P., KROON, M., OORSCHOT, M.V., "The role of peroxides in the thermooxidative degradation of polypropylene", Polymer Degradation and Stability **51** (1996) 3-13.
[36] FALICKI, S., CARLSSON, D.J., GOSCINIAK, D.J., COOKE, J.M., "Reactions of dimethyl sulfide with oxidized polypropylene", Polymer Degradation and Stability **41** (1993) 205-210.
[37] MAO, J.-D., SCHMIDT-ROHR, K., "Separation of aromatic-carbon ^{13}C NMR signals from di-oxygenated alkyl bands by a chemical-shift-anisotropy filter", Solid State Nuclear Magnetic Resonance **26** (2004) 36-45.
[38] MOWERY, D.M., CLOUGH, R.L., BERNSTEIN, R., ASSINK, R.A., in preparation.
[39] IRING, M., TÜDÖS, F., "Thermal Oxidation of Polyethylene and Polypropylene: Effects of Chemical Structure and Reaction Conditions on the Oxidation Process", Progress in Polymer Science **15** (1990) 217-262.
[40] ADAMS, J.H., "Analysis of the Nonvolatile Oxidation Products of Polypropylene I. Thermal Oxidation", Journal of Polymer Science: Part A-1 **8** (1970) 1077-1090.
[41] GEORGE, G.A., CELINA, M., VASSALLO, A.M., COLE-CLARKE, P.A., "Real-time analysis of the thermal oxidation of polyolefins by FT-IR emission", Polymer Degradation and Stability **48** (1995) 199-210.
[42] GUGUMUS, F., "Re-examination of the thermal oxidation reactions of polymers 1. New views of an old reaction", Polymer Degradation and Stability **74** (2001) 327-339.
[43] DECKER, C., MAYO, F.R., "Aging and Degradation of Polyolefins. II. γ-Initiated Oxidations of Atactic Polypropylene", Journal of Polymer Science: Polymer Chemistry Edition **11** (1973) 2847-2877.
[44] TIDJANI, A., WATANABE, Y., "Study of the Effect of γ-Dose Rate on the Oxidation of Polypropylene", Journal of Applied Polymer Science **60** (1996) 1839-1845.
[45] CLOUGH, R.L., GILLEN, K.T., "Combined Environment Aging Effects: Radiation-Thermal Degradation of Polyvinylchloride and Polyethylene", Journal of Polymer Science: Polymer Chemistry Edition **19** (1981) 2041-2051.

COMBINED TREATMENT USING CHEMICAL OXIDATION AND RADIATION FOR ENHANCEMENT DEGRADATION OF CHITOSAN

TRUONG THI HANH, NGUYEN QUOC HIEN, TRAN TICH CANH
Research and Development Centre for Radiation Technology
Vietnam Atomic Energy Commission

Abstract

Combined treatment using chemical oxidation and radiation has been considered for enhancement of chitosan degradation. The oxidative reagent was chosen to be hydrogen peroxide from heterogeneous reaction. Optimal conditions of concentration, temperature, pH were also determined. Characteristics of chitosan products were investigated by measurements of proton nuclear magnetic resonance spectroscopy (^{1}HNMR), infrared spectroscopy (IR), viscosity average molecular weight (MW), ultraviolet spectrophotometry (UV), thermogravimetry analysis (TGA) and X-ray diffraction (XRD).

1. INTRODUCTION

Chitin, poly-β-(1→4)-N-acetyl-D glucosamine, is one of the second most abundant polysaccharides in nature after cellulose. It is commonly found in the shell of crustaceans and in cell walls of insects [1]. Chitosan, poly-β-(1→4)-D glucosamine, is the deacetylated derivative of chitin and the degree of deacetylation (DD) of this product is an important chemical characteristic which could determine by IR and ^{1}HNMR spectroscopy [2]. Chitin and chitosan have been used in variety of applications such as in food processing, water treament, cosmetics, medicine, agriculture…[3]. However, in some fields, the application of this polysaccharide is limited by its high molecular weight (MW) so that the degradation of chitosan to prepare low MW chitosan or oligochitosan has been considered.

At present, three methods for degradation of chitosan including chemical treament, enzymatic hydrolysis and radiation technology can be applied. Enzymatic hydrolysis involves mild process conditions and lead to the production of low MW with high yields but the enzymes are too expensive to be commercialized. Besides, several oxidative reagents have been studied for degradation of chitosan to obtain low MW but most of them are toxic reagents that are not desirable for application in cosmetics, pharmaceutics and food. Nevertheless, some reagents were used for degradation such as sodium nitrite ($NaNO_2$), sodium hypochlorite (NaClO) and hydrogen peroxide (H_2O_2). Especially, hydrogen peroxide has been chosen in this work because the productions of chitosan achieve preselected size, low cost of production, simple procedure and capability of being a nontoxic reagent [4]. Exceptionally, further degradation by H_2O_2 led to ring-opening oxidation, the formation of carboxyl groups and deamination [1]. For those reasons, radiation and oxidative reagent were combined to enhance the scission of chitosan. Recently, radiation was used as a tool for degradation of different polymers, namely, natural polymers such as alginate, chitosan, carrageenan, cellulose, pectin have been investigated for recycling these bioresources and reducing the environmental pollution [5].

An understanding of chemical structure and molecular weight of resulting product is essential to the successful application. Therefore, we investigated features of the modified chitosan by H_2O_2 combined with radiation treatment.

2. MATERIALS AND METHODS

2.1. Materials

Chitosan used in this work were made from shrimp shell which was supplied by the seafood export company. All chemicals and solvents were used as analytical reagent grade.

2.2. Methods

2.2.1. Preparation of Chitin/Chitosan and characterization

2.2.1.1. Production of Chitin/Chitosan:

The deproteinization from shrimp shells was treated by 3% sodium hydroxide at 100°C for 3 hour and retained for 24 hours at ambient temperature, then washing shells with deionized water until neutral. The deproteinized shrimp shells were soaked in 3% HCl solution for 48 hours in order to remove the mineral, then shells were washed in the same way as after deproteinization. The yield of dry chitin was found to be about 6% of wet raw material shrimp shells.

Deacetylation of chitin to prepare chitosan was carried out by 50 % sodium hydroxide at 100°C for 1,2,3 and 5 hours. The liquid was seperated from the reaction mixture and the deacetylated chitin flakes were washed with water until neutral and dried at 60°C. The yield of chitosan from chitin was 70 to 80% on a dry basis. The scheme of process for Chitin/Chitosan (Fig. 1) production was shown as follows:

Shrimp Shell → Deproteinization (3% NaOH, 100^0C,3h) → Wash with water → Decalcification (3% HCl, 30^0C, 48h) → Wash with water → Chitin → Deacetylation (50% NaOH, 100^0C,1-5h) → Chitosan.

2.2.1.2. Determination of the degree of deacetylation of Chitin by IR and ^{1}H-NRM spectra:

IR spectroscopy of chitosan powder in the form of KBr pellet was obtained using IR-Bruker-IFS 48* Carlo Erba GC 6130 instrument with a frequency range of 4000-500cm^{-1}. Chitosan was dried at 80°C for 24 hours and dissolved by D_2O and CF_3COOD solutions for 24 hours at 70-80°C. ^{1}HNMR was carried out on Bruker Advance instrument with a frequency 500 mHz at 353°K.

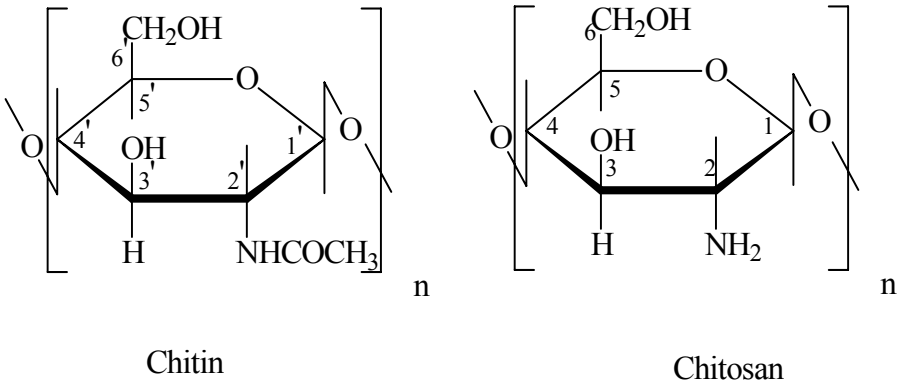

FIG. 1. The structure of chitin and chitosan

2.2.2. Degradation of chitosan:

2.2.2.1. Oxidation degradation:

Oxidation degradation of chitosan was carried out in heterogeneous medium by oxidative reagents such as sodium nitrite, sodium hypochlorite, or hydrogen peroxide. An amount of 100g chitosan flake was added into 500 ml of oxidative reagent solution with concentration 0.6 M. The mixture was stirred for 1 hour to 5 hours under mild conditions (pH 7, 30°C), then oxidized chitosan was washed with deionized water and finally was collected by drying at 60°C.

2.2.2.2. Effects of concentration and temperature on degradation of chitosan by H_2O_2:

Concentration of H_2O_2 was used for oxidation of chitosan in the range of 0.15 M to 1.2 M at 30 ^oC. Reaction temperatures of oxidation chitosan by 0.6 M of H_2O_2 were carried out at 30 ^oC, 60^oC, 90^oC in neutral medium (pH 7).

2.2.2.3. Radiation degradation:

The oxidized chitosan was sealed in a polyethylene bags and irradiated by a Co-60 gamma source in the range of 5 to 30 kGy at a dose rate 1.6 kGy/h.

2.2.3. Analytical procedures:

Viscosity average molecular weights (MW) of chitosan were measured by a capillary Ubbelode type viscometer at temperature 25 ^oC. MW was calculated by equation:

$$[\eta] = kMW$$

where k= 1.81 10^{-3} cm^3/g, α= 0.93 [6]

UV-Visible spectroscopy of chitosan solution was carried out on UV-2401 instrument in the range 200-300nm at 0.25% chitosan concentration. The viscosity of chitosan solution (3%) was determined by Brookfield model DV-II+. Thermogravimetric analysis (TGA) of sample (8mg) were performed by a differential thermal analyzer model DTG-60 (Shimadzu, Japan) under a nitrogen atmosphere from 25^oC-400^oC at a heating rate of 10 ^oC/min. X-ray diffraction patterns of degraded chitosan were measured by diffractrometer of VIMLUKI.

3. RESULTS AND DISCUSSION

3.1.The deacetylation degree of Chitin/Chitosan by IR and 1H-NRM spectra

^{1}HNRM spectroscopy is one of the most useful methods for studying the structure of carbohydrates. Degree of deacetylation of chitin was determined from the interaction of protons in D-glucosamine and N-acetyl D- glucosamine of chitosan. ^{1}HNRM spectroscopy of deacetylation chitosan for 3 hours is shown in Fig.2. The signals at the chemical shifts of δ= 5.2 ppm and δ= 2.4 ppm assigned to proton of H_1 when interaction with H_2 and proton of –$COCH_3$ group respectively.

The degree of acetylation was calculated from integral intensities of protons in –$COCH_3$ group (I_{COCH3}= 0.446) and proton of H_1 (I_{H1}=1) about 15%, resultant of deacetylation degree to be 85%.

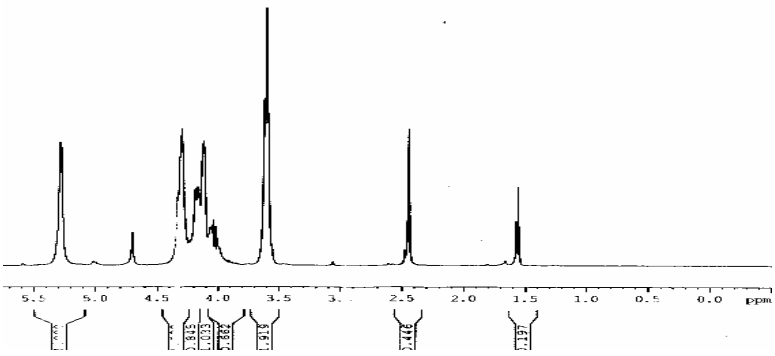

FIG. 2. HNRM spectrum of deacetylated chitosan for 3 hours.

TABLE I. CHARACTERISTIC FUNCTIONAL GROUPS OF CHITOSAN FROM IR SPECTRA

Frequency (cm^{-1})	Functional groups
3400	O-H stretch
2880	C-H stretch
1660	C=O stretch and N-H bend
1420	C-H bend (CH_3)
1322	C-O-H bend

Infrared spectral absorbance of chitosan is shown in Fig.3. Major peaks are presented in table I. In the IR spectroscopic method, some authors estimated DD based on the absorbance intensity of the hydroxyl group at frequency $3400cm^{-1}$ and the amide I band at $1650cm^{-1}$. However, from structural units investigation and especially an important absorbance at $1650cm^{-1}$ exists in both glucosamine and N-acetyl glucosamine. Another equation was proposed by Brugnerotto [2]:

$$A_{1320}/A_{1420} = 0.3822 + 0.03133 \times DA$$

Where A_{1320} and A_{1420} were the absorbance of C-O-H and C-H (CH_3) bending, DA was the degree of acetylation.

Table II showed the values of deacetylation degree of chitosan for deacetylation time of 1,2 3,5 hours. The DD of sample for 3 hours obtained to be 87%, it was good agreement with result based on ^{1}HNRM. When the deacetylation time was longer than 3 hours, DA increased slightly so that chitosan sample deacetylated for 3 hours was chosen for further study.

TABLE II. DEACETYL DEGREE FROM IR SPECTRA

Deacetylation Time, h	A_{1320}	A_{1420}	DA	DD
1h	1.00	1.05	18.19	81.81
2h	1.00	1.10	16.81	83.19
3h	0.70	0.90	12.63	87.37
5h	0.80	1.05	12.12	87.88

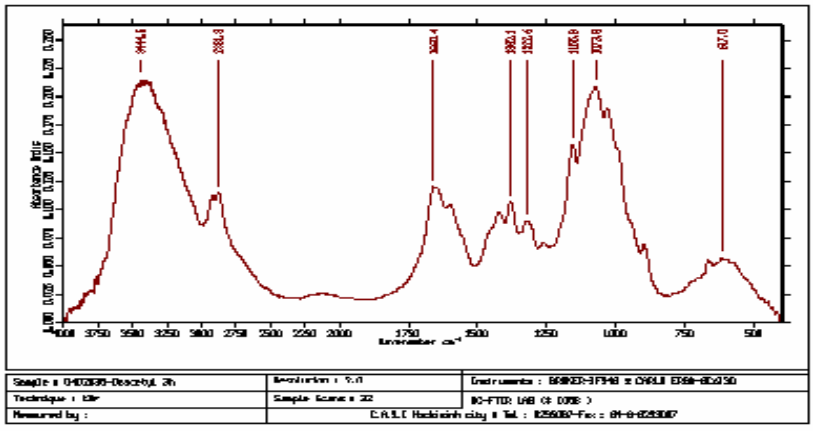

FIG. 3. IR spectrum of deacetylated chitosan for 3 hours

3.2. The characterization of chitosan with combined treatment using the oxidative reagent and radiation

3.2.1. Selection of oxidative reagents:

Effects of the oxidative reagent and radiation were estimated from the changes of molecular weight and structure of chitosan. The relationship between MW of chitosan and oxidative time was presented in Fig.4. The results showed that MW of oxidized chitosan in the same concentration of 0.6 M of reagents including sodium nitrite, sodium hypochlorite decreased slightly, especially, MW of chitosan oxidized by H_2O_2 decreased rapidly. It was a good agreement with the data of viscosity of chitosan solution (3%) at 30^oC in Table III. Therefore, hydrogen peroxide was selected for further experiments.

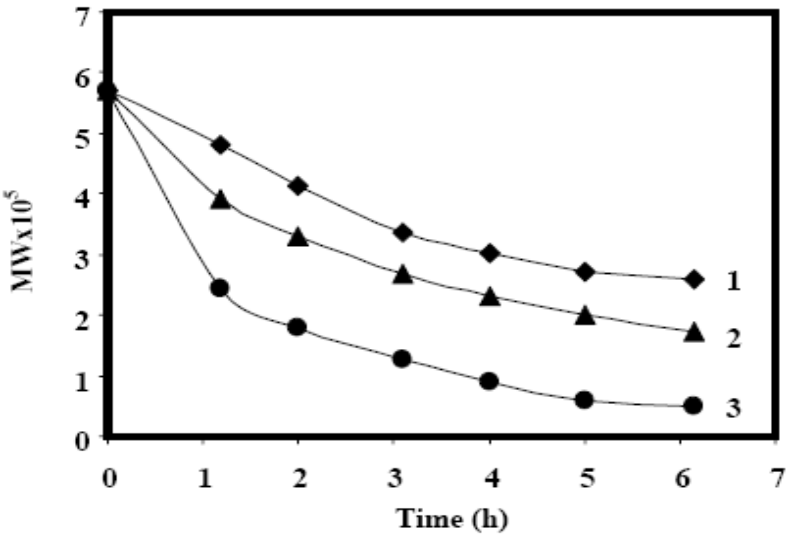

FIG. 4. The relationship between MW of oxidized chitosan and oxidation time1. $NaNO_2$ 2. NaClO 3. H_2O_2

TABLE III. VISCOSITY OF CHITOSAN SOLUTION (3%) BY DIFFERENT REAGENTS FOR 4 HOURS

Reagents	Viscosity (cps)
H_2O_2	3860
NaClO	6380
$NaNO_2$	7030

3.2.2. Oxidation of chitosan by hydrogen peroxide combined with radiation:

Effect of concentration of H_2O_2 on degradation was determined via results of the change of MW of chitosan as the time and the hydrogen peroxide concentration increased. In Fig.5, a steep reduction of MW was observed up to 4 hours, then gradually leveled off as the oxidation time increased further. It is known that, the degradation occurring in the first stage is mainly assigned to that in amorphous regions and slow degradation is assigned to that in crystalline regions. Besides, concentration of hydrogen peroxide considerably affects the ability of chitosan degradation. Thus, the use of low concentration of peroxide (0.15M) leads to the decrease of MW being unremarkable.

The reduction of MW proved that H_2O_2 caused the scission of chitosan chain. Based on suggestions of Qin et al. [1] scheme of degradation mechanism for carbohydrates by H_2O_2 was as follows:

$$H_2O_2 \rightarrow H^+ + HOO^-$$
$$H_2O_2 + HOO^- \rightarrow HO^\bullet + O_2 + H_2O$$
$$RH + HO^\bullet \rightarrow R^\bullet + H_2O$$
$$R^\bullet \rightarrow F^\bullet_1 + F_2 \quad \text{(scission)}$$

The decrease in stability of H_2O_2 is caused by the unstability of the perhydroxyl anion $HCOO^-$This anion reacts with H_2O_2 to form the highly reactive hydroxyl radical ($HO^\bullet$) that abstracting a C-bonded H atom of carbohydrates. $R^\bullet$ is a carbohydrate macroradical and $F^\bullet_1$, F_2 are fragments of main chain after scission.

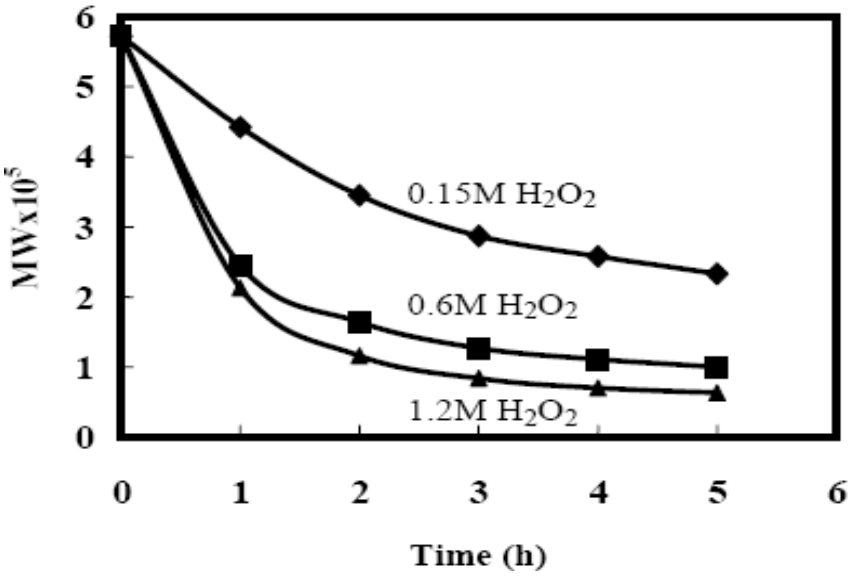

FIG. 5. Effect of concentration of H_2O_2 on MW of chitosan

Degradation of chitosan by H_2O_2 combined with radiation can be estimated by calculating the radiation degradation yields (Gd) [7]. As shown in Table IV, Gd values of chitosan and oxidized chitosan by 0.6 M H_2O_2 and 1.2 M H_2O_2 for 4 hours are 1.04, 5.10 and 7.22 respectively when chitosan were irradiated in the dose range of 5 to 30 kGy. Hence, it is concluded that the oxidative chitosan was found to be more susceptible to radiation than the non-oxidative one. This is a method to reduce absorbed dose for degradation of chitosan. Kume et al. reported that to induce pisatin in soybean, chitosan was irradiated to 1000 kGy [8], in this case, if oxidized chitosan is used, radiation dose will be much decreased.

TABLE IV. GD VALUE OF IRRADIATED CHITOSAN

Sample	Gd
Control	1.04
0.6M H_2O_2	5.10
1.2M H_2O_2	7.22

The UV spectra of oxidized chitosan (Fig.6) were shown an new absorbance peak at around 217 nm and the peak intensity increases with increasing the oxidative time as well as the absorbed dose (Fig.7). It can be assigned to double bonds formed due to main chain scission of chitosan and hydrogen abstraction reaction by oxidative reagent and irradiation.

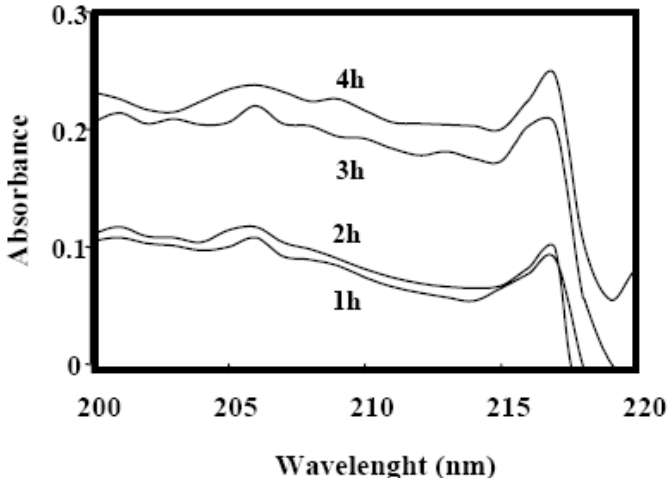

FIG. 6. UV spectra of oxidized chitosan

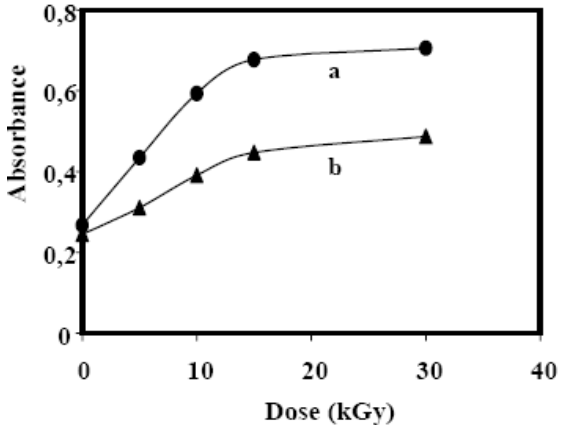

FIG. 7. Absorbance at 217 as a function of dose at different oxidation time a.1.2 M H_2O_2 b. 0.6 M H_2O_2

The results of thermogravimetry analysis (TGA) are recorded in the temperature range of 50-400^oC. From the Fig.8, it can be seen that, the oxidized chitosan at concentration 0.6 M H_2O_2, there is a systematic decrease in the decomposition temperature when the samples were irradiated in the range of 5 to 30 kGy. The weight loss was remarkable from 260 ^oC to 298 ^oC. Curves of a (control), b (5 kGy) and c (15 kGy) were different from curve of d which showed the least thermal stability of irradiated chitosan at dose 30 kGy, starting to decompose from 140^oC and there was no obvious peak of the greatest weight loss. Reason for this could be the difference in their structures and molecular weight. When chitosan was treated with H_2O_2 and radiation, the thermostability decreased because degradation led to the disintegration of intramolecular interaction and partial breaking of the molecular structure.

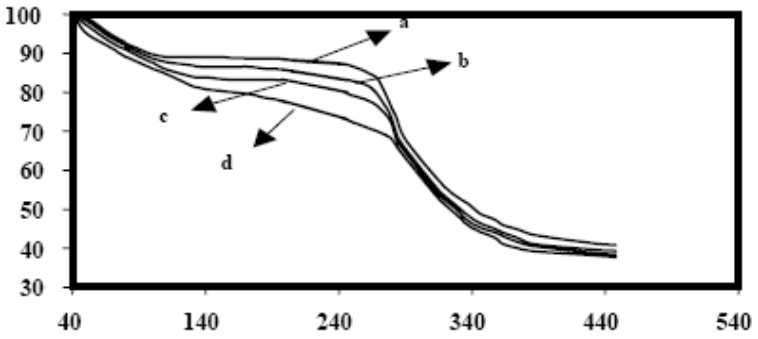

FIG. 8. TGA of chitosan at different radiation doses a. Control b. 5 kGy c. 15 kGy d. 30 kGy

Fig.9 shows X-ray diffraction patterns of main fraction of chitosan resulting from the degradation in 0.6M H2O2. The initial chitosan (Chi-I) exhibited two characteristic peaks at 2θ = 9.7o and 2θ = 19.8o which coincided with the pattern of shrimp chitosan reported by some authors [1]. For oxidized chitosan (Chi-O) the pattern had three peaks, a peak at 2θ = 9.7o rose and the peak at 19.8o also increased, a new peak at 2θ = 22o. The rise in crystallinity of Chi-O showed the preferential degradation of amorphous parts of chitosan whereas the crystalline was preserved. However, with deeper degradation by oxidative reagents, the crystalline structure was destroyed and the crystallinity decreased. Thus, it was assumed that the degradation occurred first in the amorphous region and then proceeded to the inside of the crystalline. Surprisingly, the degradation by radiation does not affect the crystalline structure of chitosan significantly.

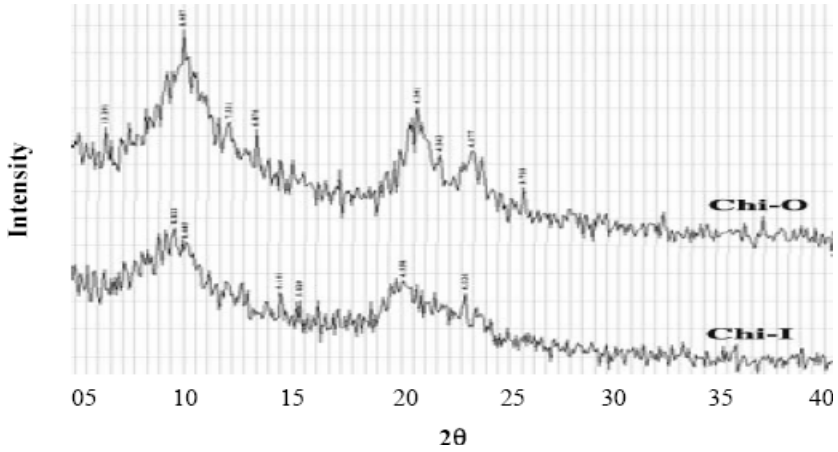

FIG. 9. X-ray diffraction patterns of initial chitosan and oxidized chitosan

Temperature also significantly affects on degradation of chitosan, this can be explained that the unstability of H_2O_2 leading to the rapid formation of $^{\bullet}OH$ radicals at high temperature so that the scission of chitosan chain may be advantageous. This result was also demonstrated by IR spectra in Fig.10, the intensity of the carbonyl (C=O) and hydroxyl (OH) groups related bands at 1653 cm^{-1} and 3400 cm^{-1} of oxidized chitosan at 90^{o}C and 60^{o}C for 30 minutes are higher than that of oxidized chitosan at 30 ^{o}C in the same oxidation time. However, it is difficult to obtain the products which have desirable properties with oxidized chitosan was treated at high temperarure.

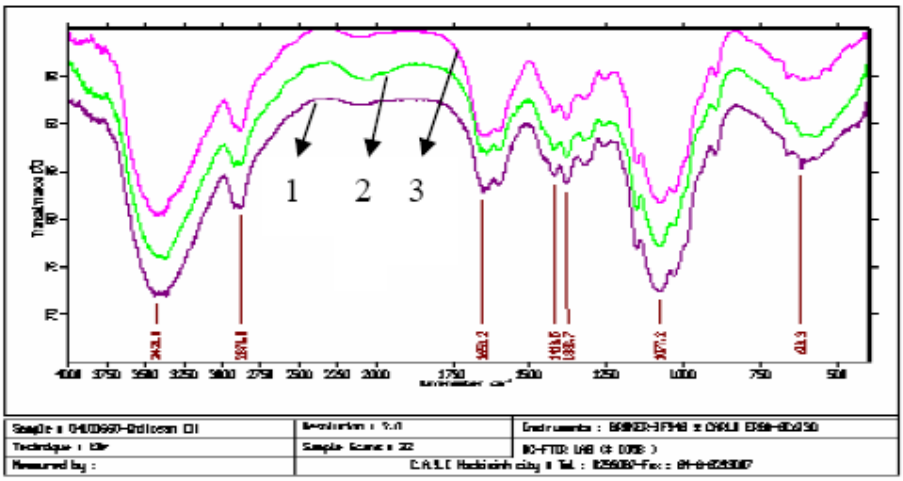

FIG. 10. IR spectra of oxidized chitosan at different temperature 1. 90°C 2. 30°C 3. 60°C

4. CONCLUSIONS

Chitosan could be degraded by oxidative reagents such as sodium nitrite, sodium hypochloride, hydrogen peroxide to produce the low MW chitosans. Degradation occurred most rapidly by H_2O_2 which may cause the change of MW and chemical structure such as formation of chromophore groups, decreasing thermostability and the change in the crystalline region of chitosan. These changes were confirmed by the analytical results of IR, UV spectral, TGA, X ray diffraction.

Degradation of chitosan by oxidative reagent to MW smaller than $5x10^4$ had lost amino groups as well as ring – opening oxidation [1]. Thus, in this work, the oxidation stopped with MW of chitosan above $6.0x10^4$ with concentration of H_2O_2 at 0.6M for 4 hours at 30°C and in neutral pH. Afterward, chitosan was treated by radiation for further degradation.

REFERENCES

[1] C.Q. QIN, Y.M. DU, L. XIAO, Polymer Degradation and Stability **76** (2002), 211-218.
[2] J. BRUGNEROTTO et al., Polymer **42** (2001), 3569-3580.
[3] L.Y. LIM et al., J. Biomed. Mater. Res. (Appl. Biomater.) **43** (1998), 282-290.
[4] C.Q. QIN et al., Journal of Applied Polymer Science **86** (2002), 1724-1730.
[5] W. S. CHOI, Polymer Degradation and Stability **78** (2002), 533-538.
[6] G.A.F. ROBERTS AND J.D. DOMSZY, Int. J. Biol. Macromol. **4** (1982), 374-377.
[7] A.CHARLESBY, Atomic Radiation and Polymers, England Pergamon Press (1960), 20 pp.
[8] T. KUME et al., Radiation Physics and Chemistry **63** (2003), 625-627.

LIST OF PARTICIPANTS

Mr. Leonardo SILVA
Instituto de Pesquisas Energeticas e Nucleares – IPEN
Centro de Tecnologia das Radiacoes – CTR
Av. Prof. Lineu Prestes, 2242, Cidade Universitaria
05508-000 Sao Paulo, SP, BRAZIL
Tel: +55-11-3816-9268, Fax: +55-11-3816-9186
E-mail: lgasilva@baitaca.ipen.br

Ms. Marijka A. MISHEVA
Faculty of Physics, Sofia University
5 J. Bourchier Blvd
1164 Sofia, BULGARIA
Tel: +359-2-962-5276, Fax. +359-2-974-4978
E-mail: misheva@phys.uni-sofia.bg

Ms. Hanna BOLDYRYEVA
Nuclear Physics Institute of
Academy of Sciences of the Czech Republic
Rez near Prague, 250 65, CZECH REPUBLIC
Tel: +42-02-661-72102, Fax: +42-02-209-40141
E-mail: boldyryeva@ujf.cas.cz

Mr. El-Sayed A. HEGAZY
Industrial Irradiation Division
National Center for Radiation Research and Technology
3 Ahmed El-Zomor Street, POB 29, Nasr City
Cairo, EGYPT
Tel: +20-2-274-7413, Fax: +20-2-274-9298
E-mail: hegazy_ea@hotmail.com

Mr. Tariq YASIN
Polymer Processing and Radiation Technology Lab.
ACD, PINSTECH, PO Nilore
Islamabad, PAKISTAN
Tel: +92-51-220-7371, Fax: +92-51-929-0275
E-mail: yasintariq@gmail.com

Ms. Grażyna PRZYBYTNIAK
Department of Radiation Chemistry and Technology
Institute of Nuclear Chemistry and Technology
Dorodna Str. 16, 03-195 Warsaw
POLAND
Tel: +48-22-811-2347, Fax: +48-22-811-1532
E-mail: przybyt@orange.ichtj.waw.pl

Mr. Traian ZAHARESCU
Advanced Research Institute for Electrical Engineering
313 Splaiul Unirii, POB 87
Bucharest 74204, ROMANIA
Tel: +40-21-346-7231, Fax: +40-21-346-8299
E-mail: traian_zaharescu@yahoo.com

Mr. Young-Chang NHO

Korea Atomic Energy Research Institute (KAERI)
Radiation Application Dpt.
POB 105, Yusong, Daejon 305-600
REPUBLIC OF KOREA
Tel: +82-42-868-8054, Fax: +82-42-862-8188
E-mail: ycnho@kaeri.re.kr

Mr. Ernesto PEREZ
Instituto de Ciencia y Tecnologia de Polimeros (CSIC)
Juan de la Cierva 3
28006 Madrid, SPAIN
Tel: +34-91-562-2900 ext. 266, Fax: +34-91-564-4853
E-mail: ernestop@ictp.csic.es

Mr. Olgun GUEVEN
Dpt. of Chemistry, Hacettepe University, Beytepe
06532 Ankara, TURKEY
Tel: +90-312-297-7977, Fax: +90-312-297-7977
E-mail: guven@hacettepe.edu.tr

Mr. Roger CLOUGH
Sandia National Labs, M.S. 0888
Albuquerque, N.M., 87185
USA
Tel.: +1-505-844-3492, Fax: +1-505-844-9624
E-mail: rlcloug@sandia.gov

Ms. Thi Hanh TRUONG
Research and Development Center for Radiation Technology (VINAGAMMA)
Truong Tre St., Linh Xuan Ward, Thu Duc Distr.
Ho Chi Minh City, VIETNAM
Tel: +84-8-897-5922, Fax: +84-8-897-5921
E-mail: vinagamma@hcm.vnn.vn

José Ignacio MARTIN GALAN
Electron Service Line; S. L.
Av. Menéndez Pelayo, 2 3°D
21009 Madrid, SPAIN
Tel.: +34 91 781 1244, Fax: +34 91 781 1469
Email: jimg@eserline.com

Andrzej G. CHMIELEWSKI
(Scientific Secretary)
Ind. Appl. & Chem. Section/Division of Physical and Chemical Sciences of IAEA
Wagramer Strasse 5, P.O. Box 100,
1400 Vienna, AUSTRIA
Tel: +43-1-2600-21744 or 21747, Fax: +43-1-2600-7-21744
Email: A.Chmielewski@iaea.org